

**CLINCH RIVER
BREEDER REACTOR PROJECT**

**PRELIMINARY
SAFETY ANALYSIS
REPORT**

VOLUME 21

PROJECT MANAGEMENT CORPORATION

TABLE OF CONTENTS

<u>Section</u>		<u>Page</u>
1.0	<u>INTRODUCTION AND GENERAL DESCRIPTION OF THE PLANT</u>	1.1-1
1.1	<u>INTRODUCTION</u>	1.1-1
1.1.1	General Information	1.1-2
1.1.2	Overview of Safety Design Approach	1.1-3
1.1.3	Applicability of Regulatory Guides	1.1-5
1.2	<u>GENERAL PLANT DESCRIPTION</u>	1.2-1
1.2.1	Site	1.2-1
1.2.2	Engineered Safety Features	1.2-2
1.2.3	Reactor, Heat Transport and Related Systems	1.2-2
1.2.4	Steam Generator - Turbine and Related Systems	1.2-3
1.2.5	Offsite and Onsite Power	1.2-5
1.2.6	Instrumentation, Control and Protection	1.2-6
1.2.7	Auxiliary Systems	1.2-7
1.2.8	Refueling System	1.2-8
1.2.9	Radwaste Disposal System	1.2-9
1.2.10	Reactor Confinement/Containment System	1.2-9
1.2.11	Major Structures	1.2-10
1.3	<u>COMPARISON TABLES</u>	1.3-1
1.3.1	Comparisons with Similar Designs	1.3-1
1.3.2	Detailed Comparison with Fast Flux Test Facility	1.3-2
1.4	<u>IDENTIFICATION OF PROJECT PARTICIPANTS</u>	1.4-1
1.4.1	Functions, Responsibilities and Authorities of Project Participants	1.4-2
1.4.2	Description of Organizations	1.4-3
1.4.3	Interrelationships with Contractors and Suppliers	1.4-21a
1.4.4	General Qualification Requirement of CRBRP Project Participants	1.4-22
1.5	<u>REQUIREMENTS FOR FURTHER TECHNICAL INFORMATION</u>	1.5-1
1.5.1	Information Concerning the Adequacy of a New Design	1.5-2
1.5.2	Information Concerning Margin of Conservatism of Proven Design	1.5-28
1.5.3	References	1.5-47

TABLE OF CONTENTS (Cont'd.)

<u>Section</u>		<u>Page</u>
1.6	<u>MATERIAL INCORPORATED BY REFERENCE</u>	1.6-1
1.6.1	Introduction	1.6-1
1.6.2	References	1.6-1
	Appendix 1-A Flow Diagram Symbols	1.A-1
2.0	<u>SITE CHARACTERISTICS</u>	2.1-1
2.1	<u>GEOGRAPHY AND DEMOGRAPHY</u>	2.1-1
2.1.1	Site Location and Layout	2.1-1
2.1.2	Site Description	2.1-2
2.1.3	Population and Population Distribution	2.1-4
2.1.4	Uses of Adjacent Lands and Waters	2.1-8
2.2	<u>NEARBY INDUSTRIAL, TRANSPORTATION AND MILITARY FACILITIES</u>	2.2-1
2.2.1	Locations, Routes, and Descriptions	2.2-1
2.2.2	Evaluations	2.2-3
2.2.3	New Facility/Land Use Requirements	2.2-4c
2.3	<u>METEOROLOGY</u>	2.3-1
2.3.1	Regional Climatology	2.3-1
2.3.2	Local Meteorology	2.3-4
2.3.3	On-site Meteorological Monitoring Program	2.3-9
2.3.4	Short-Term (Accident) Diffusion Estimates	2.3-9
2.3.5	Long-Term (Average) Diffusion Estimates	2.3-13
2.4	<u>HYDROLOGIC ENGINEERING</u>	2.4-1
2.4.1	Hydrologic Description	2.4-1
2.4.2	Floods	2.4-6
2.4.3	Probable Maximum Flood (PMF) on Streams and Rivers	2.4-10
2.4.4	Potential Dam Failures (Seismically and Otherwise Induced)	2.4-21
2.4.7	Ice Flooding	2.4-31
2.4.8	Cooling Water Canals and Reservoirs	2.4-31a
2.4.9	Channel Diversions	2.4-32
2.4.10	Flooding Protection Requirements	2.4-32
2.4.11	Low Water Considerations	2.4-33
2.4.12	Environmental Acceptance of Effluents	2.4-42
2.4.13	Groundwater	2.4-44
2.4.14	Technical Specification and Emergency Operation Requirement	2.4-55

TABLE OF CONTENTS (Cont'd.)

<u>Section</u>		<u>Page</u>
2.5	<u>GEOLOGY AND SEISMOLOGY</u>	2.5-1
2.5.1	Basic Geologic and Seismic Information	2.5-1
2.5.2	Vibratory Ground Motion	2.5-20
2.5.3	Surface Faulting	2.5-27
2.5.4	Stability of Subsurface Materials	2.5-32
2.5.5	Slope Stability	2.5-48a
	Appendix 2-A Field Investigative Procedures	2A-1
	Appendix 2-B Laboratory Test Procedures	2B-1
	Appendix 2-C Report of Test Grouting Program	2C-1
	Appendix 2-D Report of Engineering Properties for Crushed Stone Materials from Commercial Suppliers	2D-1
	Appendix 2-E Extracts from U.S. Atomic Energy Commission AEC Manual	2E-1
	Supplement 1 to Chapter 2 Deleted	
	Supplement 2 to Chapter 2 Question and Responses Related to Chapter Two Information and Critical For NRC Docketing of CRBRP Environmental Report	1
3.0	<u>DESIGN CRITERIA - STRUCTURES, COMPONENTS EQUIPMENT AND SYSTEMS</u>	3.1-1
3.1	<u>CONFORMANCE WITH GENERAL DESIGN CRITERIA</u>	3.1-1
3.1.1	Introduction and Scope	3.1-1
3.1.2	Definitions and Explanations	3.1-2
3.1.3	Conformance with CRBRP General Design Criteria	3.1-8
3.2	<u>CLASSIFICATIONS OF STRUCTURES, SYSTEMS, AND COMPONENTS</u>	3.2-1
3.2.1	Seismic Classifications	3.2-1
3.2.2	Safety Classifications	3.2-2
3.3	<u>WIND AND TORNADO LOADINGS</u>	3.3-1
3.3.1	Wind Loadings	3.3-1
3.3.2	Tornado Loadings	3.3-2
3.4	<u>WATER LEVEL (FLOOD) DESIGN</u>	3.4-1
3.4.1	Flood Protection	3.4-1
3.4.2	Analysis Procedures	3.4-1a

TABLE OF CONTENTS (Cont'd.)

<u>Section</u>		<u>Page</u>
3.5	<u>MISSILE PROTECTION</u>	3.5-1
3.5.1	Missile Barrier and Loadings	3.5-4
3.5.2	Missile Selection	3.5-4a
3.5.3	Selected Missiles	3.5-7
3.5.4	Barrier Design Procedures	3.5-10
3.5.5	Missile Barrier Features	3.5-13c
3.6	<u>PROTECTION AGAINST DYNAMIC EFFECTS ASSOCIATED WITH THE POSTULATED RUPTURE OF PIPING</u>	3.6-1
3.6.1	Systems In Which Pipe Breaks are Postulated	3.6-1
3.6.2	Pipe Break Criteria	3.6-2
3.6.3	Design Loading Combinations	3.6-2
3.6.4	Dynamic Analysis	3.6-3
3.6.5	Protective Measures	3.6-8
3.7	<u>SEISMIC DESIGN</u>	3.7-1
3.7.1	Seismic Input	3.7-1
3.7.2	Seismic System Analysis	3.7-4a
3.7.3	Seismic Subsystem Analysis	3.7-11
3.7.4	Seismic Instrumentation Program	3.7-16
3.7.5	Seismic Design Control	3.7-20
	Appendix to Section 3.7 Seismic Design Criteria	3.7-A.1
3.8	<u>DESIGN OF CATEGORY I STRUCTURES</u>	3.8-1
3.8.1	Concrete Containment (Not Applicable)	3.8-1
3.8.2	Steel Containment System	3.8-1
3.8.3	Concrete and Structural Steel Internal Structures of Steel Containment	3.8-8
3.8.4	Other Seismic Category I Structures	3.8-22a
3.8.5	Foundation and Concrete Supports	3.8-35
	Appendix 3.8A Buckling Stress Criteria	3.8A-1
	Appendix 3.8-B Cell Liner Design Criteria	3.8-B.1
	Appendix 3.8-C Catch Pan and Fire Suppression Deck Design Criteria	3.8-C.1
3.9	<u>MECHANICAL SYSTEMS AND COMPONENTS</u>	3.9-1
3.9.1	Dynamic System Analysis and Testing	3.9-1
3.9.2	ASME Code Class 2 and 3 Components	3.9-3a
3.9.3	Components Not Covered by ASME Code	3.9-5
3.10	<u>SEISMIC DESIGN OF CATEGORY I INSTRUMENTATION AND ELECTRICAL EQUIPMENT</u>	3.10-1
3.10.1	Seismic Design Criteria	3.10-1

TABLE OF CONTENTS (Cont'd.)

<u>Section</u>		<u>Page</u>
3.10.2	Analysis, Testing Procedures and Restraint Measures	3.10-3
3.11	<u>ENVIRONMENTAL DESIGN OF MECHANICAL AND ELECTRICAL EQUIPMENT</u>	3.11-1
3.11.1	Equipment Identification	3.11-1
3.11.2	Qualification Test and Analysis	3.11-1
3.11.3	Qualification Test Results	3.11-1
3.11.4	Loss of Ventilation	3.11-2
3.11.5	Special Considerations	3.11-2
3A.0	<u>SUPPLEMENTARY INFORMATION ON SEISMIC CATEGORY I STRUCTURES</u>	3A.1-1
3A.1	Inner Cell System	3A.1-1
3A.2	Head Access Area	3A.2-1
3A.3	Control Building	3A.3-1
3A.4	Reactor Service Building (RSB)	3A.4-1
3A.5	Steam Generator Building	3A.5-1
3A.6	Diesel Generator Building	3A.6-1
3A.7	Deleted	
3A.8	Cell Liner Systems	3A.8-1
4.0	<u>REACTOR</u>	4.1-1
4.1	<u>SUMMARY DESCRIPTION</u>	4.1-1
4.1.1	Lower Internals	4.1-1
4.1.2	Upper Internals	4.1-3
4.1.3	Core Restraint	4.1-4
4.1.4	Fuel Blanket and Removable Radial Shield Regions	4.1-4
4.1.5	Design and Performance Characteristics	4.1-9
4.1.6	Loading Conditions and Analysis Techniques	4.1-9
4.1.7	Computer Codes	4.1-10
4.2	<u>MECHANICAL DESIGN</u>	4.2-1
4.2.1	Fuel and Blanket Design	4.2-1
4.2.2	Reactor Vessels Internals	4.2-118
4.2.3	Reactivity Control Systems	4.2-228
4.3	<u>NUCLEAR DESIGN</u>	4.3-1
4.3.1	Design Bases	4.3-1
4.3.2	Description	4.3-3
4.3.3	Analytical Methods	4.3-69
4.3.4	Changes	

TABLE OF CONTENTS (Cont'd.)

<u>Section</u>		<u>Page</u>
4.4	<u>THERMAL AND HYDRAULIC DESIGN</u>	4.4-1
4.4.1	Design Bases	4.4-1
4.4.2	Description	4.4-4
4.4.3	Evaluation	4.4-45
4.4.4	Testing and Verification	4.4-75
4.4.5	Core Instrumentation	4.4-80
5.0	<u>HEAT TRANSPORT AND CONNECTED SYSTEMS</u>	5.1-1
5.1	<u>SUMMARY DESCRIPTION</u>	5.1-1a
5.1.1	Reactor Vessel, Closure Head, and Guard Vessel	5.1-1a
5.1.2	Primary Heat Transport System	5.1-2
5.1.3	Intermediate Heat Transport System	5.1-5
5.1.4	Steam Generator System	5.1-7
5.1.5	Residual Heat Removal System	5.1-8
5.1.6	Auxiliary Liquid Metal System	5.1-9
5.1.7	Features for Heat Transport System Safety	5.1-10
5.1.8	Physical Arrangement	5.1-11
5.2	<u>REACTOR VESSEL, CLOSURE HEAD, AND GUARD VESSEL</u>	5.2-1
5.2.1	Design Basis	5.2-1
5.2.2	Design Parameters	5.2-4b
5.2.3	Special Processes for Fabrication and Inspection	5.2-7
5.2.4	Features for Improved Reliability	5.2-8
5.2.5	Quality Assurance Surveillance	5.2-10d
5.2.6	Materials and Inspections	5.2-11
5.2.7	Packing, Packaging, and Storage	5.2-11a
	Appendix 5.2.A Modifications to the High Temperature Design Rules for Austenitic Stainless Steel	5.2A-1
5.3	<u>PRIMARY HEAT TRANSPORT SYSTEM (PHTS)</u>	5.3-1
5.3.1	Design Bases	5.3-1
5.3.2	Design Description	5.3-9
5.3.3	Design Evaluation	5.3-33
5.3.4	Tests and Inspections	5.3-72
5.4	<u>INTERMEDIATE HEAT TRANSPORT SYSTEM (IHTS)</u>	5.4-1
5.4.1	Design Basis	5.4-1
5.4.2	Design Description	5.4-6
5.4.3	Design Evaluation	5.4-12

TABLE OF CONTENTS (Cont'd.)

<u>Section</u>		<u>Page</u>
5.5	<u>STEAM GENERATOR SYSTEM (SGS)</u>	5.5-1
5.5.1	Design Bases	5.5-1
5.5.2	Design Description	5.5-5
5.5.3	Design Evaluation	5.5-17
5.6	<u>RESIDUAL HEAT REMOVAL SYSTEMS</u>	5.6-1
5.6.1	Steam Generator Auxiliary Heat Removal System (SGAHR)	5.6-1b
5.6.2	Direct Heat Removal Service (DHRS)	5.6-20
5.7	<u>OVERALL HEAT TRANSPORT SYSTEM EVALUATION</u>	5.7-1
5.7.1	Startup and Shutdown	5.7-1
5.7.2	Load Following Characteristics	5.7-2
5.7.3	Transient Effects	5.7-2a
5.7.4	Evaluation of Thermal Hydraulic Characteristics and Plant Design Heat Transport System Design Transient Summary	5.7-6
6.0	<u>ENGINEERED SAFETY FEATURES</u>	6.1-1
6.1	<u>GENERAL</u>	6.1-1
6.2	<u>CONTAINMENT SYSTEMS</u>	6.2-1
6.2.1	Confinement/Containment Functional Design	6.2-1
6.2.2	Containment Heat Removal	6.2-9
6.2.3	Containment Air Purification and Cleanup System	6.2-9
6.2.4	Containment Isolation Systems	6.2-10
6.2.5	Annulus Filtration System	6.2-14
6.2.6	Reactor Service Building (RSB) Filtration System	6.2-16
6.2.7	Steam Generator Building Aerosol Release Mitigation System Functional Design	6.2-17
6.3	<u>HABITABILITY SYSTEMS</u>	6.3-1
6.3.1	Habitability System Functional Design	6.3-1
6.4	<u>CELL LINER SYSTEM</u>	6.4-1
6.4.1	Design Base	6.4-1
6.4.2	System Design	6.4-1
6.4.3	Design Evaluation	6.4-1
6.4.4	Tests and Inspections	6.4-1
6.4.5	Instrumentation Requirements	6.4-1

TABLE OF CONTENTS (Cont'd.)

<u>Section</u>		<u>Page</u>
6.5	<u>CATCH PAN</u>	6.5-1
6.5.1	Design Base	6.5-1
6.5.2	System Design Description and Evaluation	6.5-1
6.5.3	Tests and Inspections	6.5-1
6.5.4	Instrumentation Requirements	6.5-1
7.0	<u>INSTRUMENTATION AND CONTROLS</u>	7.1-1
7.1	<u>INTRODUCTION</u>	7.1-1
7.1.1	Identification of Safety Related Instrumentation and Control Systems	7.1-1
7.1.2	Identification of Safety Criteria	7.1-1
7.2	<u>REACTOR SHUTDOWN SYSTEM</u>	7.2-1
7.2.1	Description	7.2-1
7.2.2	Analysis	7.2-13
7.3	<u>ENGINEERED SAFETY FEATURE INSTRUMENTATION AND CONTROL</u>	7.3-1
7.3.1	Containment Isolation System	7.3-1
7.3.2	Analysis	7.3-3
7.4	<u>INSTRUMENTATION AND CONTROL SYSTEMS REQUIRED FOR SAFE SHUTDOWN</u>	7.4-1
7.4.1	Steam Generator Auxilliary Heat Removal Instrumentation and Control Systems	7.4-1
7.4.2	Outlet Steam Isolation Instrumentation and Control System	7.4-6
7.4.3	Remote Shutdown System	7.4-8a
7.5	<u>INSTRUMENTATION AND MONITORING SYSTEM</u>	7.5-1
7.5.1	Flux Monitoring System	7.5-1
7.5.2	Heat Transport Instrumentation System	7.5-5
7.5.3	Reactor and Vessel Instrumentation	7.5-13
7.5.4	Fuel Failure Monitoring System	7.5-14
7.5.5	Leak Detection Systems	7.5-18
7.5.6	Sodium-Water Reaction Pressure Relief System (SWRPRS) Instrumentation and Controls	7.5-30
7.5.7	Containment Hydrogen Monitoring	7.5-33b
7.5.8	Containment Vessel Temperature Monitoring	7.5-33b
7.5.9	Containment Pressure Monitoring	7.5-33b
7.5.10	Containment Atmosphere Temperature	7.5-33c
7.5.11	Post Accident Monitoring	7.5-33c

TABLE OF CONTENTS (Cont'd.)

<u>Section</u>		<u>Page</u>
7.6	<u>OTHER INSTRUMENTATION AND CONTROL SYSTEMS REQUIRED FOR SAFETY</u>	7.6-1
7.6.1	Plant Service Water and Chilled Water Instrumentation and Control Systems	7.6-1
7.6.2	Deleted	
7.6.3	Direct Heat Removal Service (DHRS) Instrumentation and Control System	7.6-3
7.6.4	Heating, Ventilating, and Air Conditioning Instrumentation and Control System	7.6-3e
7.6.5	SGB Flooding Protection Subsystem	7.6-3f
7.7	<u>INSTRUMENTATION AND CONTROL SYSTEMS NOT REQUIRED FOR SAFETY</u>	7.7-1
7.7.1	Plant Control System Description	7.7-1
7.7.2	Design Analysis	7.7-16
7.8	<u>PLANT DATA HANDLING AND DISPLAY SYSTEM</u>	7.8-1
7.8.1	Design Description	7.8-1
7.8.2	Design Analysis	7.8-2
7.9	<u>OPERATING CONTROL STATIONS</u>	7.9-1
7.9.1	Design Basis	7.9-1
7.9.2	Control Room	7.9-1
7.9.3	Local Control Stations	7.9-6
7.9.4	Communications	7.9-6
7.9.5	Design Evaluation	7.9-6
8.0	<u>ELECTRIC POWER</u>	8.1-1
8.1	<u>INTRODUCTION</u>	8.1-1
8.1.1	Utility Grid and Interconnections	8.1-1
8.1.2	Plant Electrical Power System	8.1-1
8.1.3	Criteria and Standards	8.1-3
8.2	<u>OFFSITE POWER SYSTEM</u>	8.2-1
8.2.1	Description	8.2-1
8.2.2	Analysis	8.2-4
8.3	<u>ON-SITE POWER SYSTEMS</u>	8.3-1
8.3.1	AC Power Systems	8.3-1
8.3.2	DC Power System	8.3-44

TABLE OF CONTENTS (Cont'd.)

<u>Section</u>		<u>Page</u>
9.0	<u>AUXILIARY SYSTEMS</u>	9.1-1
9.1	<u>FUEL STORAGE AND HANDLING</u>	9.1-1
9.1.1	New Fuel Storage	9.1-3
9.1.2	Spent Fuel Storage	9.1-5
9.1.3	Spent Fuel Cooling and Cleanup System	9.1-20
9.1.4	Fuel Handling System	9.1-33
9.2	<u>NUCLEAR ISLAND GENERAL PURPOSE MAINTENANCE SYSTEM</u>	9.2-1
9.2.1	Design Basis	9.2-1
9.2.2	System Description	9.2-1
9.2.3	Safety Evaluation	9.2-3
9.2-4	Tests and Inspections	9.2-3
9.2-5	Instrumentation Applications	9.2-4
9.3	<u>AUXILIARY LIQUID METAL SYSTEM</u>	9.3-1
9.3.1	Sodium and NaK Receiving System	9.3-1a
9.3.2	Primary Na Storage and Processing	9.3-2
9.3.3	EVS Sodium Processing	9.3-9a
9.3.4	Primary Cold Trap NaK Cooling System	9.3-10
9.3.5	Intermediate Na Processing System	9.3-12
9.4	<u>PIPING AND EQUIPMENT ELECTRICAL HEATING</u>	9.4-1
9.4.1	Design Bases	9.4-1
9.4.2	Systems Description	9.4-2
9.4.3	Safety Evaluation	9.4-3
9.4.4	Tests and Inspections	9.4-3b
9.4.5	Instrumentation Application	9.4-3b
9.5	<u>INERT GAS RECEIVING AND PROCESSING SYSTEM</u>	9.5-1
9.5.1	Argon Distribution Subsystem	9.5-2
9.5.2	Nitrogen Distribution System	9.5-6
9.5.3	Safety Evaluation	9.5-10
9.5.4	Tests and Inspections	9.5-12
9.5.5	Instrumentation Requirements	9.5-12
9.6	<u>HEATING, VENTILATING AND AIR CONDITIONING SYSTEM</u>	9.6-1
9.6.1	Control Building HVAC System	9.6-1
9.6.2	Reactor Containment Building	9.6-12
9.6.3	Reactor Service Building HVAC System	9.6-25
9.6.4	Turbine Generator Building HVAC System	9.6-37
9.6.5	Diesel Generator Building HVAC System	9.6-40
9.6.6	Steam Generator Building HVAC System	9.6-45

TABLE OF CONTENTS (Cont'd.)

<u>Section</u>		<u>Page</u>
9.7	<u>CHILLED WATER SYSTEMS</u>	9.7-1
9.7.1	Normal Chilled Water System	9.7-1
9.7.2	Emergency Chilled Water System	9.7-4
9.7.3	Prevention of Sodium or NaK/Water Interactions	9.7-9
9.7.4	Secondary Coolant Loops (SCL)	9.7-12
9.8	<u>IMPURITY MONITORING AND ANALYSIS SYSTEM</u>	9.8-1
9.8.1	Design Basis	9.8-1
9.8.2	Design Description	9.8-2
9.8.3	Design Evaluation	9.8-5
9.8.4	Tests and Inspection	9.8-7
9.8.5	Instrumentation Requirements	9.8-8
9.9	<u>SERVICE WATER SYSTEMS</u>	9.9-1
9.9.1	Normal Plant Service Water System	9.9-1
9.9.2	Emergency Plant Service Water System	9.9-2
9.9.3	Secondary Service Closed Cooling Water System	9.9-4
9.9.5	River Water Service	9.9-11
9.10	<u>COMPRESSED GAS SYSTEM</u>	9.10-1
9.10.1	Service Air and Instrument Air Systems	9.10-1
9.10.2	Hydrogen System	9.10-3a
9.10.3	Carbon Dioxide System	9.10-4
9.11	<u>COMMUNICATIONS SYSTEM</u>	9.11-1
9.11.1	Design Bases	9.11-1
9.11.2	Description	9.11-3
9.12	<u>LIGHTING SYSTEMS</u>	9.12-1
9.12.1	Normal Lighting System	9.12-1
9.12.2	Standby Lighting Systems	9.12-2
9.12.3	Emergency Lighting System	9.12-3
9.12.4	Design Evaluation	9.12-4
9.13	<u>PLANT FIRE PROTECTION SYSTEM</u>	9.13-1
9.13.1	Non-Sodium Fire Protection System	9.13-1
9.13.2	Sodium Fire Protection System (SFPS)	9.13-13
9.13A	Overall Fire Protection Requirements -- CRBRP Design Compared with APCSB 9.5-1 & ASB 9.5-1	9.13A-1
9.14	<u>DIESEL GENERATOR AUXILIARY SYSTEM</u>	9.14-1
9.14.1	Fuel Oil Storage and Transfer System	9.14-1

TABLE OF CONTENTS (Cont'd.)

<u>Section</u>		<u>Page</u>
9.14.2	Cooling Water System	9.14-2
9.14.3	Starting Air Systems	9.14-4
9.14.4	Lubrication System	9.14-5
9.15	<u>EQUIPMENT AND FLOOR DRAINAGE SYSTEM</u>	9.15-1
9.15.1	Design Bases	9.15-1
9.15.2	System Description	9.15-1
9.15.3	Safety Evaluation	9.15-2
9.15.4	Tests and Inspections	9.15-2
9.15.5	Instrumentation Application	9.15-2
9.16	<u>RECIRCULATION GAS COOLING SYSTEM</u>	9.16-1
9.16.1	Design Basis	9.16-1
9.16.2	System Description	9.16-1
9.16.3	Safety Evaluation	9.16-6
9.16.4	Tests and Inspection	9.16-7
9.16.5	Instrumentation and Control	9.16-7
10.0	<u>STEAM AND POWER CONVERSION SYSTEM</u>	10.1-1
10.1	<u>SUMMARY DESCRIPTION</u>	10.1-1
10.2	<u>TURBINE GENERATOR</u>	10.2-1
10.2.1	Design Bases	10.2-1
10.2.2	Description	10.2-1a
10.2.3	Turbine Missiles	10.2-5
10.2.4	Evaluation	10.2-9
10.3	<u>MAIN STEAM SUPPLY SYSTEM</u>	10.3-1
10.3.1	Design Bases	10.3-1
10.3.2	Description	10.3-1
10.3.3	Evaluation	10.3-2
10.3.4	Inspection and Testing Requirements	10.3-2
10.3.5	Water Chemistry	10.3-3
10.4	<u>OTHER FEATURES OF STEAM AND POWER CONVERSION SYSTEM</u>	10.4-1
10.4.1	Condenser	10.4-1
10.4.2	Condenser Air Removal System	10.4-2
10.4.3	Turbine Gland Sealing System	10.4.3
10.4.4	Turbine Bypass System	10.4-4
10.4.5	Circulating Water System	10.4-5
10.4.6	Condensate Cleanup System	10.4-7

TABLE OF CONTENTS (Cont'd.)

<u>Section</u>		<u>Page</u>
10.4.7	Condensate and Feedwater Systems	10.4-9
10.4.8	Steam Generator Blowdown System	10.4-14
11.0	<u>RADIOACTIVE WASTE MANAGEMENT</u>	11.1-1
11.1	<u>SOURCE TERMS</u>	11.1-1
11.1.1	Modes of Radioactive Waste Production	11.1-1
11.1.2	Activation Product Source Strength Models	11.1-2
11.1.3	Fission Product and Plutonium Release Models	11.1-5
11.1.4	Tritium Production Sources	11.1-7
11.1.5	Summary of Design Bases for Deposition of Radioactivity In Primary Sodium on Reactor and Primary Heat Transfer Surfaces and Within Reactor Auxiliary Systems	11.1-7
11.1.6	Leakage Rates	11.1-10
11.2	<u>LIQUID WASTE SYSTEM</u>	11.2-1
11.2.1	Design Objectives	11.2-1
11.2.2	System Description	11.2-2
11.2.3	System Design	11.2-4
11.2.4	Operating Procedures and Performance Tests	11.2-5
11.2.5	Estimated Releases	11.2-6
11.2.6	Release Points	11.2-6
11.2.7	Dilution Factors	11.2-7
11.2.8	Estimated Doses	11.2-8
	Appendix 11.2A Dose Models: Liquid Effluents	11.2A-1
11.3	<u>GASEOUS WASTE SYSTEM</u>	11.3-1
11.3.1	Design Base	11.3-1
11.3.2	System Description	11.3-1
11.3.3	System Design	11.3-10
11.3.4	Operating Procedures and Performance Tests	11.3-11a
11.3.5	Estimated Releases	11.3-14
11.3.6	Release Points	11.3-15
11.3.7	Dilution Factors	11.3-17
11.3.8	Dose Estimates	11.3-17
	Appendix 11.3A Dose Models: Gaseous Effluents	11.3A-1
11.4	<u>PROCESS AND EFFLUENT RADIOLOGICAL MONITORING SYSTEM</u>	11.4-1
11.4.1	Design Objectives	11.4-1
11.4.2	Continuous Monitoring/Sampling	11.4-2
11.4.3	Sampling	11.4-3

TABLE OF CONTENTS (Cont'd.)

<u>Section</u>		<u>Page</u>
11.5	<u>SOLID WASTE SYSTEM</u>	11.5-1
11.5.1	Design Objectives	11.5-1
11.5.2	System Inputs	11.5-1
11.5.3	Equipment Description	11.5-1
11.5.4	Expected Volumes	11.5-3
11.5.5	Packaging	11.5-4
11.5.6	Storage Facilities	11.5-4
11.5.7	Shipment	11.5-4
11.6	<u>OFFSITE RADIOLOGICAL MONITORING PROGRAM</u>	11.6-1
11.6.1	Expected Background	11.6-1
11.6.2	Critical Pathways to Man	11.6-2
11.6.3	Sampling Media, Locations and Frequencies	11.6-4
11.6.4	Analytical Sensitivity	11.6-4
11.6.5	Data Analysis and Presentation	11.6-4
11.6.6	Program Statistical Sensitivity	11.6-5
12.0	<u>RADIATION PROTECTION</u>	12.1-1
12.1	<u>SHIELDING</u>	12.1-1
12.1.1	Design Objectives	12.1-1
12.1.2	Design Description	12.1-3
12.1.3	Source Terms	12.1-13
12.1.4	Area Radiation Monitoring	12.1-23
12.1.5	Estimates of Exposure	12.1-24
	Appendix to Section 12.1	12.1A-1
12.2	<u>VENTILATION</u>	12.2-1
12.2.1	Design Objectives	12.2-1
12.2.2	Design Description	12.2-1
12.2.3	Source Terms	12.2-3
12.2.4	Airborne Radioactivity Monitoring	12.2-3
12.2.5	Inhalation Doses	12.2-5
12.3	<u>HEALTH PHYSICS PROGRAM</u>	12.3-1
12.3.1	Program Objectives	12.3-1
12.3.2	Facilities and Equipment	12.3-3
12.3.3	Personnel Dosimetry	12.3-6
12.3.4	Estimated Occupancy Times	12.3-7
	Appendix 12A - Information Related to ALARA for Occupational Radiation Exposures	12A-1

TABLE OF CONTENTS (Cont'd.)

<u>Section</u>		<u>Page</u>
13.0	<u>CONDUCT OF OPERATIONS</u>	13.1-1
13.1	<u>ORGANIZATIONAL STRUCTURE OF THE APPLICANT</u>	13.1-1
13.1.1	Project Organization	13.1-1
13.1.2	Operating Organization	13.1-5
13.1.3	Qualification Requirements for Nuclear Plant Personnel	13.1-12
13.2	<u>TRAINING PROGRAM</u>	13.2-1
13.2.1	Program Description	13.2-1
13.2.2	Retraining Program	13.2-6
13.2.3	Replacement Training	13.2-6
13.2.4	Records	13.2-6
13.3	<u>EMERGENCY PLANNING</u>	13.3-1
13.3.1	General	13.3-1
13.3.2	Emergency Organization	13.3-2
13.3.3	Coordination with Offsite Groups	13.3-5
13.3.4	Emergency Action Levels	13.3-6
13.3.5	Protective Measures	13.3-7
13.3.6	Review and Updating	13.3-7
13.3.7	Medical Support	13.3-7
13.3.8	Exercises and Drills	13.3-8
13.3.9	Training	13.3-8
13.3.10	Recovery and Reentry	13.3-9
13.3.11	Implementation	13.3-9
	Appendix 13.3A	13.3A-1
13.4	<u>REVIEW AND AUDIT</u>	13.4-1
13.4.1	Review and Audit - Construction	13.4-1
13.4.2	Review and Audit - Test and Operation	13.4-1
13.5	<u>PLANT PROCEDURES</u>	13.5-1
13.5.1	General	13.5-1
13.5.2	Normal Operating Instructions	13.5-1
13.5.3	Abnormal Operating Instructions	13.5-2
13.5.4	Emergency Operating Instructions	13.5-2
13.5.5	Maintenance Instructions	13.5-3

Amend. 68
May 1982

TABLE OF CONTENTS (Cont'd.)

<u>Section</u>		<u>Page</u>
13.5.6	Surveillance Instructions	13.5-4
13.5.7	Technical Instructions	13.5-4
13.5.8	Sections Instruction Letters	13.5-4
13.5.9	Site Emergency Plans	13.5-4
13.5.10	Radiation Control Instructions	13.5-4
13.6	<u>PLANT RECORDS</u>	13.6-1
13.6.1	Plant History	13.6-1
13.6.2	Operating Records	13.6-1
13.6.3	Event Records	13.6-1
13.7	<u>RADIOLOGICAL SECURITY</u>	13.7-1
13.7.1	Organization and Personnel	13.7-1
13.7.2	Plant Design	13.7-3
13.7.3	Security Plan	13.7-6
14.0	<u>INITIAL TESTS AND OPERATION</u>	14.1-1
14.1	<u>DESCRIPTION OF TEST PROGRAMS</u>	14.1-1
14.1.1	Preoperational Test Programs	14.1-2
14.1.2	Startup Test Program	14.1-2
14.1.3	Administration of Test Program	14.1-3
14.1.4	Test Objectives of First-of-a-Kind Principal Design Features	14.1-6
14.2	<u>AUGMENTATION OF OPERATOR'S STAFF FOR INITIAL TESTS AND OPERATION</u>	14.2-1
15.0	<u>ACCIDENT ANALYSES</u>	15.1-1
15.1	<u>INTRODUCTION</u>	15.1-1
15.1.1	Design Approach to Safety	15.1-1
15.1.2	Requirements and Criteria for Assessment of Fuel and Blanket Rod Transient Performance	15.1-50
15.1.3	Control Rod Shutdown Rate and Plant Protection System Trip Settings	15.1-93
15.1.4	Effect of Design Changes on Analyses of Accident Events	15.1-105
15.2	<u>REACTIVITY INSERTION DESIGN EVENTS - INTRODUCTION</u>	15.2-1
15.2.1	Anticipated Events	15.2-5
15.2.2	Unlikely Events	15.2-34
15.2.3	Extremely Unlikely Events	15.2-51

TABLE OF CONTENTS (Cont'd.)

<u>Section</u>		<u>Page</u>
15.3	<u>UNDERCOOLING DESIGN EVENTS - INTRODUCTION</u>	15.3-1
15.3.1	Anticipated Events	15.3-6
15.3.2	Unlikely Events	15.3-29
15.3.3	Extremely Unlikely Events	15.3-38
15.4	<u>LOCAL FAILURE EVENTS - INTRODUCTION</u>	15.4-1
15.4.1	Fuel Assembly	15.4-2
15.4.2	Control Assemblies	15.4-42
15.4.3	Radial Blanket Assembly	15.4-51
15.5	<u>FUEL HANDLING AND STORAGE EVENTS - INTRODUCTION</u>	15.5-1
15.5.1	Anticipated Events (None)	15.5-4
15.5.2	Unlikely Events	15.5-4
15.5.3	Extremely Unlikely Events	15.5-23
15.6	<u>SODIUM SPILLS - INTRODUCTION</u>	15.6-1
15.6.1	Extremely Unlikely Events	15.6-4
15.7	<u>OTHER EVENTS - INTRODUCTION</u>	15.7-1
15.7.1	Anticipated Events	15.7-3
15.7.2	Unlikely Events	15.7-9
15.7.3	Extremely Unlikely Events	15.7-18
15.A	Appendix 15.A - Radiological Source Term for Assessment of Site Suitability	15.A-1
16.0	<u>TECHNICAL SPECIFICATIONS</u>	16.1-1
16.1	<u>DEFINITIONS</u>	16.1-1
16.1.1	Reactor Operating Condition	16.1-1
16.1.2	Reactor Core	16.1-2
16.1.3	Plant Protection System Instrumentation	16.1-3
16.1.4	Safety Limit	16.1-5
16.1.5	Limiting Safety System Setting (LSSS)	16.1-5
16.1.6	Limiting Conditions for Operation (LCO)	16.1-6
16.1.7	Surveillance Requirements	16.1-6
16.1.8	Containment Integrity	16.1-6
16.1.9	Abnormal Occurrence	16.1-6

TABLE OF CONTENTS (Cont'd.)

<u>Section</u>		<u>Page</u>
16.2	<u>SAFETY LIMITS AND LIMITING SAFETY SYSTEM SETTINGS</u>	16.2-1
16.2.1	Safety Limit, Reactor Core	16.2-1
16.2.2	Limiting Safety System Settings	16.2-1
16.3	<u>LIMITING CONDITIONS FOR OPERATION</u>	16.3-1
16.3.1	Reactor Operating Conditions	16.3-1
16.3.2	Primary Heat Transport System (PHTS)	16.3-2
16.3.3	Intermediate Heat Transport Coolant System	16.3-6
16.3.4	Steam Generation System (SGS)	16.3-7
16.3.5	Auxiliary Liquid Metal System	16.3-12
16.3.6	Inert Gas System Cover Gas Purification System	16.3-13
16.3.7	Auxiliary Cooling System	16.3-14
16.3.8	Containment Integrity	16.3-21
16.3.9	Auxiliary Electrical System	16.3-21
16.3.10	Refueling	16.3-24
16.3.11	Effluent Release	16.3-27
16.3.12	Reactivity and Control Rod Limits	16.3-31
16.3.13	Plant Protection System	16.3-34
16.4	<u>SURVEILLANCE REQUIREMENTS</u>	16.4-1
16.4.1	Operational Safety Review	16.4-1
16.4.2	Reactor Coolant System Surveillance	16.4-1
16.4.3	Containment Tests	16.4-3
16.4.4	HVAC and Radioactive Effluents	16.4-6
16.4.5	Emergency Power System Periodic Tests	16.4-10
16.4.6	Inert Gas System	16.4-13
16.4.7	Reactivity Anomalies	16.4-13
16.4.8	Pressure and Leakage Rate Test of RAPS Cold Box Cell	16.4-15
16.4.9	Pressure and Leakage Rate Test of RAPS Noble Gas Storage Vessel Cell	16.4-15a
16.5	<u>DESIGN FEATURES</u>	16.5-1
16.5.1	Site	16.5-1
16.5.2	Confinement/Containment	16.5-1
16.5.3	Reactor	16.5-2
16.5.4	Heat Transport System	16.5-5
16.5.5	Fuel Storage	16.5-7
16.6	<u>ADMINISTRATIVE CONTROLS</u>	16.6-1
16.6.1	Organization	16.6-1
16.6.2	Review and Audit	16.6-1
16.6.3	Instructions	16.6-4
16.6.4	Actions to be Taken in the Event of Reportable Occurrence in Plant Operation	16.6-6

TABLE OF CONTENTS (Cont'd.)

<u>Section</u>		<u>Page</u>
16.6.5	Action to be Taken In the Event a Safety Limit Is Exceeded	16.6-6
16.6.6	Station Operating Records	16.6-6
16.6.7	Reporting Requirements	16.6-7
16.6.8	Minimum Staffing	16.6-8
17.0	<u>QUALITY ASSURANCE - INTRODUCTION</u>	17.0-1
17.0.1	Scope	17.0-1
17.0.2	Quality Philosophy	17.0-1
17.0.3	Participants	17.0-2
17.0.4	Project Phase Approach	17.0-3
17.0.5	Applicability	17.0-3
17.1	<u>QUALITY ASSURANCE DURING DESIGN AND CONSTRUCTION</u>	17.1-1
17.1.1	Organization	17.1-1
17.1.2	Quality Assurance Program	17.1-2
17.1.3	References Referred to In the Text	17.1-6
17.1.4	Acronyms Used In Chapter 17 Text and Appendices	17.1-6a

TABLE OF CONTENTS (Cont'd.)

<u>Section</u>		<u>Page</u>
Appendix 17A	A Description of the Owner Quality Assurance Program	17A-1
Appendix 17B	A Description of the Fuel Supplier Quality Assurance Program	17B-1
Appendix 17C	A Description of the Balance of Plant Supply Quality Assurance Program	17C-1
Appendix 17D	A Description of the ARD Lead Reactor Manufacturer Quality Assurance Program	17D-1
Appendix 17E	A Description of the Architect-Engineer Quality Assurance Program	17E-1
Appendix 17F	A Description of the Constructor Quality Assurance Program	17F-1
Appendix 17G	RDT Standard F2-2, 1973, Quality Assurance Program Requirements	17G-1
Appendix 17H	A Description of the ARD Reactor Manufacturer Quality Assurance Program	17H-1
Appendix 17I	A Description of the GE-ARSD-RM Quality Assurance Program	17I-1
Appendix 17J	A Description of the ESG-RM Quality Assurance Program	17J-1
Appendix A	Computer Codes	A-1
Appendix B	General Plant Transient Data	B-1
Appendix C	Safety Related Reliability Program	C.1-1
Appendix D	Deleted	
Appendix E	Deleted	
Appendix F	Deleted	
Appendix G	Plan for Inservice and Preservice Inspections	G-1
Appendix H	Post TMI Requirements	H-1

Question 241.1 (3.7.3.15)

Seismic analysis of fuel assemblies described in section 3.7.3.15 as well as in 3.7.2.1.2 are too general and the level of detail is not sufficient to comment on their adequacy. Even though the final results may be presented in the FSAR we need the following information at the PSAR stage:

- (1) A detailed description of the mathematical model including schematics showing all the pertinent components of the fuel assembly such as ducts, control rods, fuel rods, etc. Specify how many masses and springs will represent a fuel assembly and other components and how many assemblies will actually be analyzed as representative of the whole core.
- (2) Equations and description of the mathematical model and a discussion of their solution.
- (3) A verification of the analysis
- (4) A list of important input values for the analysis and a discussion of how they will be obtained. Describe component test programs when used as input to the analysis.
- (5) Discuss how the seismic response will be combined with other applicable accidents.
- (6) Present the fuel rod and assembly mechanical design limits in terms of stresses, and/or deflections. Provide the bases for the limits.

You may supply this information in a topical report.

Response:

(1) (2) (3) (4)

The description of the seismic analyses and mathematical models presented in Sections 3.7.3.15 and 3.7.2.1.2 of the PSAR are given to demonstrate overall conservatism in the methods used to derive the seismic response. A more detailed description of the seismic loading development and structural analysis of fuel assemblies has been provided in the response to NRC request No. 9 of Reference Q241.1-1. This description explains the six computer finite element models to be used in the analyses, and the derivation of the seismic input excitation. Other detailed seismic and structural analysis techniques and detailed mathematical models on individual parts of the overall system will be developed consistent with the finalization of detailed component design. These details will be supplied in the FSAR. 140

(5)

The design bases for the fuel assemblies are described in Section 4.2. The criteria and performance requirements for the fuel to meet these design bases is provided in Sections 4.2.1.1.2.2 and 15.1. Sections 15.2, 15.3, and 15.4 demonstrate the ability of the fuel to meet the design bases. In particular, Section 15.2.3.3 provides a description of the additional accident loads assumed to occur concurrently with the seismic loads associated with the SSE in the fuel assembly design.

(6)

For the fuel rods, the strain criteria and stress limits are given in Section 4.2.1.1.2.2 as modified in response to question 241.48.

REFERENCES

- Q241.1 (1) NRC Letter, Themis P. Speis (NRC) to Peter Van Nort (PMC) "Request for Additional CRBRP Information", dated October 6, 1975.

| 25

Question 241.2 (4.1.4.1)

Part 1

Section 4.1.4.1 states that the fuel rod plenum is "sized to allow the design fuel burnup to be reached without the buildup of excessive internal gas pressure". This implies that gas in the annular space between the fuel pellets and cladding will communicate freely with the plenum gas. Demonstrate that this is true over the whole life of the fuel rod.

Part 2

What would be the consequences of normal operation if this were not true?

Response:

Part 1

The basis for the assumptions relating to fission gas release is provided in new Section 4.2.1.1.3.9.

Part 2

Part two of the subject question requires making the assumption that the gas does not communicate with the plenum. Under these assumed conditions, the fission gas pressure within the fuel column would be significantly higher than used in design calculations and the probability of cladding breaches occurring would increase. The consequences of such cladding breaches would be similar to those for stochastic core fuel rod failures. As discussed in revised Section 15.4.1.1 of the PSAR, such failures would be easily accommodated.

Question 241.3 (4.1.4.1)

On Page 4.1-5, reference is made to "the desired bowed configuration of the fuel assemblies". What are the estimated dimensions of this effect? What is the magnitude of the reactivity effects caused by this bowing as a function of burnup? What is the effect on flow area? Is this effect accounted for in hot channel factors? If not, why is it acceptable to ignore this effect? Describe, or give a reference describing the pads discussed on page 4.1-5. What are the acceptable limits on this bowing? What effect causes these limitations?

Response:

The above question consists of five separate parts. The following response addresses each of these parts in the sequence they are presented.

Numerical estimates of fuel assembly bowing patterns are provided in Figure 4.2-88 through 4.2-92 of the PSAR. The analytical bases and methods for these results are presented in Section 4.2.2.4.1.8. Figure 4.2-85 provides arrangement information on the results presented in Figures 4.2-88 through 4.2-92.

The magnitude of bowing reactivity change due to fuel assembly burnup was not separately or explicitly calculated for inclusion in the PSAR because the core restraint model described in paragraph 4.2.2.4.1.8.3 was considered to be of limited value in predicting integrated core effects. Some of these limitations are touched on in paragraphs 4.2.2.4.1.8.1 and 4.2.2.4.1.8.3. If, however, the bowing pattern changes indicated by a comparison of Figure 4.2-88 and 4.2-89 are combined with beginning of first cycle reactivity worths for radial motion from Table 4.3-12, a reactivity increase of approximately 8¢ over the first cycle is estimated. This result should be treated as a scoping estimate. Fuel assembly bowing patterns are a function of the thermal and nuclear environment at each assembly location, interaction with adjacent assemblies at the load plane elevations, the assumed form of the irradiation creep and swelling correlations as well as the assembly burnup status. Core restraint models capable of better representing the above factors are being developed for use in the final stage of the core restraint system design (see Section 1.5.2.5). Therefore, improved estimates of burnup related bowing reactivity and uncertainties associated with this effect will be included in the PSAR.

The effect of fuel assembly bowing on flow area is small relative to other effects that can influence this parameter. This effect was accounted for in estimating hot channel factors. The subject of flow area effects on hot channel factors is addressed as "subchannel flow area" in Table 4.4.-2 of the PSAR, and a brief discussion of the rationale leading to their selection is contained in paragraph 2.1.11 of Reference 15 of Section 4.4. A description of the load pads can be found in revised Section 4.1.4.1.

The acceptable limits for bowing are defined by the requirement to prevent general condition of duct to duct contact in the active core region. This requirement and its basis are discussed in paragraph 4.2.2.1.2.8h of the PSAR. Analysis has shown that both assembly bowing and duct dilation are the important effects which influence the portion for duct to duct contact. Paragraph 4.2.2.4.1.8.3 of the PSAR summarized the results of analysis of the combined effect of assembly bowing and duct dilation as it relates to duct to duct contact.

Question 241.4 (4.1.4.2)

What is the peak internal pressure expected in the radial blanket rods?

Response:

The maximum steady state pressure in blanket rods due to gases (fission, fill and residual) is reported in Section 4.4.3.3.4. Conservatism adopted in the evaluation of plenum gas pressure is discussed in Section 4.4.3.2.4.

The peak transient internal pressure considered for mechanical design purposes in the radial blanket rods is determined by applying the temperature increment for the umbrella emergency transient of Table 4.2-59 to the steady state pressure in the hot rod of radial blanket assembly 201 (Figure 4.2-10B) at the end of 4 cycles. A peak transient pressure of approximately 360 psi was determined using this method and applied in the cladding transient evaluations described in Section 4.2.1.3.

51

Question 241.5 (4.2.1.1)

- a) Define thermal creep by presenting the explicit creep equation used in fuel design. Define and discuss how one can distinguish thermal from irradiation creep in the Dounreay Fast Reactor or any other data on Figure 4.2.1. Discuss why only thermal creep and not irradiation creep is considered in the cladding analysis.
- b) Discuss why only 2 to 1 stress biaxiality ratio is considered in the criteria for strain during steady state operation. What do you do when the stress ratio is other than 2 to 1. Is it right to assume that circumferential to axial stress ratio is 2 to 1 or the other way around?
- c) Define circumferential strain. Is it D/D , or does the circumferential strain vary across the thickness? Relate calculated strain to measured strain.
- d) Discuss why post irradiation test data (for example; the data in Figure 4.2-1) represent the in-reactor environment.
- e) Design requirement 4 of Page 4.2-6 on deformation should give specific values.
- f) Design requirements 5 and 6 were set to be less than or equal to one. Discuss explicitly how much of a safety factor is in this limit.
- g) In design requirement 7, define by means of specific values, what you mean by "extended period of time" and "short duration".
- h&j) Discuss why cladding melting is the only design limit used for the faulted conditions. If stress, strain, or deflection exceed their design limits, show how you maintain the coolable geometry of the fuel rod (pg. 4.2-8).

Limit 5 on page 4.2-9 discusses coolable geometry. Define in precise terms what is meant by "coolable geometry".

- i) Clarify, or explain which design limits apply to the fuel, and which to the fuel assembly (Pg. 4.2-81).
- k) The following should be provided in terms of specific values:
 - (1) Design limit for the wire wraps;
 - (2) Design limit for the duct;
 - (3) Design limit for fuel rod bowing;
 - (4) Design limit for fuel rod vibration and fretting.

- l) The design limits 1 through 6 (Pg. 4.2-8 - 4.2-9) are too general. They should be given in terms of specific values. The statement that "the design limit...shall be patterned after...Section III of the ASME" is not specific enough for the PSAR.
- m) The design limits on fuel rods (Pg. 4.2-5 - 4.2-8) do not consider failures due to stresses, or instability, such as buckling. Please justify this omission. Even though the operational mode or the design is such that stress may not be the main cause of failure we think a complete design limit should address all possible failure modes.
- n) Provide a specific numerical value for the deformation limit 4, Page 4.2-6.

Response:

- a) The requested creep equation is presented in Table 4.2-52, which has been added to the PSAR. The remaining information requested is found in amended PSAR Sections 4.2.1.1.2.2, 4.2.1.1.3.1, and 4.2.1.1.3.2.
- b) Stress biaxiality ratios other than 2 to 1 are considered in the criteria for fuel rod component strains during steady state operation, as described in amended PSAR Section 4.2.1.1.2.2.
- c) As indicated in Section 4.2.1.1.2.2, the circumferential strain does not vary across the cladding thickness, and is approximately by $\Delta D/D$.
- d) Revised Section 4.2.1.1.3 discusses the applicability of post irradiation test data.
- e&n) A quantitative discussion of deformation limits is provided in revised Section 4.2.1.1.2.2.
- f) A discussion of safety factors is provided in revised Section 4.2.1.1.2.2.
- g) As indicated in revised Section 4.2.1.1.2.2, "short duration" is a time interval on the order of seconds. An "extended period of time" is a time interval on the order of minutes.
- h&j) The design limit in fuel rod criteria 8 of Section 4.2.1.1.2.2 should be interpreted as "...maintaining the sodium temperature below its boiling point,..." rather than cladding melting. Cladding melting is the failure mechanism which is precluded by this design limit. The section has been amended to clarify this requirement.
- i) The Section 4.2.1 has been amended to identify which design limits apply to the fuel, and which apply to the fuel assembly.

- k) (1) The design limits for the wire wrap are the same as those given for the fuel rod in Section 4.2.1.1.2.2. The pertinent stress, strain, and CDF limits are explicitly defined in that section.
- (2) The design limits for the duct (as part of the fuel assembly) are discussed in Section 4.2.1.1.2.2.2.
- (3) Deformation limits are discussed in amended item 4 of Section 4.2.1.1.2.2.
- (4) As evaluated in Section 4.2.1.3.1.1, Subsection 4, fuel rod vibration is limited such that insignificant fatigue damage is generated in the cladding or wire wrap. In other words, the alternating stress amplitude due to flow induced vibration must be below the fatigue endurance limit.

Fretting wear of the cladding which may result from fuel rod vibration must not exceed the design basis wastage allowance of 2 mils given in Section 4.2.1.1.3.4.

- l) Revised Section 4.2.1.1.2.2.2 addresses the applicability of the ASME Code to the fuel assemblies.

- m) It was the intent of Section 4.2.1.1.2.2 to present all potential failure modes identified to date in the LMFBR Base Technology and FFTF Development Programs. To incorporate any pertinent data which might be developed any additional failure modes identified during future testing will be evaluated against the appropriate limits.

With regard to stress limits, item 3 of Section 4.2.1.1.2.2 requires that the primary equivalent stresses during steady state operation remain below the proportional elastic limit. Both cladding damage mechanisms during steady state operation, thermal creep rate in ductility limited strain and time to rupture in CDF, are highly sensitive to stress state as well as temperature. For transient conditions, each damage mechanism is such that the limiting value of strain or CDF would be achieved when the cladding stress reached the ultimate tensile strength. This is shown in Figures 15.1.2-3, and 15.1.2-39 for CDF and strain respectively. Justification for not specifying limits on buckling is provided in revised Section 4.2.1.1.2.2.2.

Question 241.6 (4.2.1.1.2.1)

Describe the tests mentioned in Section 4.2.1.1.2.1 which measured shipping and handling loads. Mention especially those features which are prototypical and non-prototypical in the tests.

Response:

The response to this question is provided in revised Section 4.2.1.1.2.1.

Question 241.7 (4.2.1.1.2.1)

Justify a drop height of 3 inches for a fuel assembly which is correctly located, and 1 inch for a fuel assembly which is incorrectly located. Define what is meant by incorrectly located.

Response

An incorrectly located fuel or radial blanket assembly is an assembly that is located in a position where it does not mate with the receptacle discriminator. This occurs when an assembly (fuel, blanket or control) is positioned over the incorrect zone or location. Since the discriminator post length is 2 inches, an incorrectly located assembly fully inserted, would be located 2 inches above the position of a fully inserted, correctly located assembly.

At the time the PSAR was written, there existed a possibility of releasing an assembly 3 inches above its fully inserted position, i.e., the tolerance on the release height was 3 inches. This tolerance was needed to allow for:

- a) length manufacturing tolerances of the various components;
- b) switch hysteresis
- c) switch setting tolerance; and
- d) fuel assembly growth due to irradiation.

Thus, a correctly located assembly could be dropped 3 inches into its fully seated position. Also, since the discriminators post length is only 2 inches, an incorrectly located assembly could be dropped (3 inches - 2 inches) or one inch into its fully inserted position due to interference with the discriminator.

These drop heights were based on the values of items a) through d) at the time of PSAR submittal. Since that time, improved calibration procedures have reduced the allowable assembly release height to less than 1.5 inches above the fully inserted position. Thus, an incorrectly located assembly cannot be released, and the maximum drop height for a correctly located assembly is less than 1.5 inches.

This information has been incorporated into PSAR Sections 4.2.1.1.2.1, 9.1.4.4.2 and 16.3.10.3.2.

Question 241.8 (4.2.1.1.2.2, Section 4.4.1)

- a) Explain how the minimum power for incipient fuel melting is determined. If done by experimental data, cite the source of the data, provide the reference document to the staff, tabulate the data used and discuss the uncertainties in the data and the prototypicality of the data.
- b) If done by calculation, cite the computer program used, if any, provide a reference document to the staff, and discuss in detail how the fuel rod was modeled for this calculation, e.g., was a center void region assumed? What assumptions were made as to pellet thermal conductivity and its change with restructuring?
- c) What temperature is used as the melting temperature of the fuel? Show the change in melting temperature with burnup. Discuss the uncertainties in this temperature.
- d) Item 5 of Section 4.4.1 speaks of design uncertainties considered in calculating that no fuel centerline melting has occurred. List these design uncertainties and give their magnitude.
- e) In the Table in Section 4.4.2.1, the maximum fuel temperature at overpower is 5000°F. Why is no effect of diminution of melting point with burnup accounted for?
- f) What is the expected decrease in solidus temperature due to redistribution of actinides?

Response:

Since the above question is composed of six different questions, they will be answered individually, in the same order as formulated.

- a) The minimum power for incipient fuel melting was determined on the basis of the P-19 experiments conducted by HEDL (Reference 12 of the PSAR Section 4.4). The empirical equation correlating the experimental data is reported in PSAR Section 4.4.2.6.14 (Equation 4.4.2.6-13) together with the uncertainty band. The P-19 data were prototypical of FFTF (and CRBRP) fuel pins: rod diameter and fuel density were reproduced; the cold gap size was investigated parametrically (the range included CRBRP cold gap); the cladding ID temperature (1060°F) reproduced FFTF conditions. The correction in power-to-melt due to different ID temperatures in CRBRP fuel pins is reported in PSAR Section 4.4.2.6.14.
- b) As discussed in (a), the minimum power-to-melt was determined on the basis of experimental data, rather than by calculation. Confirmatory "back-calculation" of fuel temperature, as discussed in response to PSAR Question 241.42, for the P-19 predicted incipient melting conditions, yielded a value very close to the melting temperature of 5000°F. The adopted equation for the pellet thermal conductivity is

Q241.8-1

Amend. 16
Apr. 1976

reported in PSAR Section 4.4.2.6.7 (Equation 4.4.2.6-8). The adopted restructuring parameters (1910°C restructuring temperature; 98% density in restructured zone) were those recommended by HEDL on the basis of the P-19 tests.

- c) The assumed melting temperatures and the associated uncertainties are discussed in revised PSAR section 4.4.2.6.12.
- d) Design uncertainties considered in the evaluation of the minimum power-to-melt are those uncertainties affecting the heat flux as reported in Table I of Topical Report WARD-D-0050, Reference 15 of PSAR Chapter 4.4 and provided in response to question 241.37. A detailed discussion on how the design uncertainties on one side and the experimental uncertainties on the other side are accounted for in assessing the margin-to-melting was provided in response to question 001.46.
- e) Assumptions regarding melting temperature at overpower conditions are discussed in revised PSAR section 4.4.2.6.12.
- f) The effect of actinide redistribution on solidus temperature is discussed in revised PSAR section 4.4.2.6.12.

Question 241.9 (4.2.1.1.2.2)

Explain the selection of the 15% overpower for the fuel melting criterion.

Response:

The discussion requested is provided in revised section 4.2.1.1.2.2.

25

Question 241.10 (4.2.1.1.2.3)

Cite data to demonstrate the design limit for fretting and wear is acceptable. Discuss prototypicality of data. What features are incorporated in the design to minimize fretting and wear?

Response:

The information requested is provided in revised PSAR Section 4.2.1.1.3.4.

Question 241.11 (4.2.1.1.2.3)

List all places in the fuel assembly where there are dissimilar materials in contact or potentially in contact during the in-core lifetime of the fuel bundle. At what locations is there a potential for galling or self-welding? What type of hard coating is used to protect these surfaces?

Response:

Revised Section 4.2.1.2.1 provides the information requested.

| 25

Question 241.12 (4.2.1.1.2.3)

What tests and calculations have been done or will be done before the manufacture of the fuel for CRBRP to show that the fuel column holddown spring is adequately designed.

What material is used for the holddown spring?

Response:

The information requested is provided in revised Section 4.2.1.2.1.

25

Q241.12-1

Amend. 25
Aug. 1976

Question 241.13 (4.2.1.1.3.4)

Provide assurance that the corrosion and clad wastage allowance in the Clinch River fuel is adequate. Provide the data base for the values used.

Response:

The data base for the fretting wear allowances used in the CRBRP fuel rod design are given in the response to NRC Question 241.10. The cladding wastage data utilized in the CDF analysis of the CRBRP fuel rod are given in Chapter III, Section B, of the report "The Development and Application of a Cumulative Mechanical Damage Function for Fuel-Pin Failure Analysis in LMFBR Systems", by D. C. Jacobs (see Reference 3, Section 1.6) which was provided under separate cover in June, 1976. The data base and correlations used for cladding wastage in the strain-limit analysis of the CRBRP fuel rods are discussed in the report WARD-D-0147 "Internal/External Cladding Degradation", by M. L. Travis. This document was provided under separate cover in August, 1977. 42 42 42

The data base supporting the clad wastage allowance is discussed in revised Section 4.2.1.1.3.4. As discussed in the responses to NRC Questions 001.284, 241.15 and 241.57, more tests are planned or in progress to further assure the adequacy of the parameters used in the fuel rod performance models, including the cladding wastage allowance. 22

Question 241.14 (4.2.1.3)

- a. Clarify which fuel rod code will be used for what purpose. CYGRO-F, MINIGRO, and LIFE are mentioned.
- b. Provide the calculational method used to predict wire wrap stresses and strains. Discuss how the method is verified.
- c. Provide the calculational method used to predict duct interactions and deflections as well as its consequences to duct, fuel assembly, and rods. Discuss how the method is verified. Discuss the observations in EBR-II.
- d. Describe how one calculates fuel rod cladding ductility limited strain. Include a sample problem. Identify sources of input data of the transient. Justify the validity of the method.

Response:

- a. The response to this question is contained in amended PSAR Sections 4.2.1.3.1.1 and A.18.
- b. The response to this question is contained in amended PSAR Sections 4.2.1.3.1.1, 4.2.1.3.2.2.4, and A.99.b.
- c. The response to this question has been incorporated into amended PSAR Sections 4.2.1.3.1.1, 4.2.1.3.1.2 and a new figure identified as Figure 4.2-26a.
- d. The method for calculating fuel rod cladding ductility limited strain is given in the response to NRC Question 001.278.

For a sample problem, the cladding ductility limited strain accumulated over a 2-day time interval will be calculated. This time interval is chosen to be sufficiently short so that the cladding steady state temperature and fuel rod dimension changes during the interval are negligible, i.e., less than $\sim 0.02\%$. That this change is indeed negligible has been verified by calculation. For fuel rods, this time interval is $\sim 1-2$ days.

We assume the following conditions for the sample calculation:

- a) T_m = cladding midwall temperature during time interval = $1190^\circ\text{F} = 916^\circ\text{K}$
- b) P = rod plenum pressure during time interval = 1000 psi
- c) τ = cladding thickness during time interval = 0.011 in.
- d) d = rod inner diameter during time interval = 0.201 in.

Cladding stresses during time interval:

- a) Tangential (loop) stress = $\sigma_t = Pd_i/2\tau = 9136$ psi

- b) Axial stress = $\sigma_a = \sigma_t/2 = 4568$ psi
- c) Radial stress = $\sigma_r = -P/2 = -500$ psi
- d) Equivalent stress = $\sigma = \frac{1}{\sqrt{2}} [(\sigma_t - \sigma_r)^2 + (\sigma_a - \sigma_r)^2 + (\sigma_t - \sigma_a)^2]^{1/2}$
 $= 8349$ psi

The equation for the cladding thermal creep is given in Table 4.2-52. In this equation, the term $\epsilon_t[1 - \exp(-rt)]$ represents the primary thermal creep. The contribution of the primary thermal creep strain to the total ductility limited strain of the cladding is quite small for typical fuel rod environments, so for this calculation we will assume $\epsilon_c =$ total thermal creep over specified time interval.
 $\Delta t \approx \dot{\epsilon}_m \Delta t$.

Substituting the above values for σ , T , and Δt into the equations of Table 4.2-52, we find:

$$\begin{aligned} \epsilon_m &= \text{equivalent secondary thermal creep rate} = 8.229 \times 10^{-6} \text{ \%/hr.} \\ \epsilon_c &= \dot{\epsilon}_m t = (8.229 \times 10^{-6}) (2 \text{ days}) (24 \text{ hr/day}) = 3.95 \times 10^{-4} \% \\ &= \text{the cladding equivalent ductility limited strain accumulated over the 2 day period.} \end{aligned}$$

The cladding ductility limited hoop strain, ϵ_H , accumulated over the 2 day period is:

$$\begin{aligned} \epsilon_H &= \frac{\epsilon_c}{\sigma} [\sigma_t - 0.5(\sigma_a + \sigma_r)] = \frac{3.95 \times 10^{-4}}{8349} [9136 - 0.5(4568 - 500)] \\ &= 3.36 \times 10^{-4} \% \end{aligned}$$

For the fuel rod cladding strain analysis, the above steps are performed by a computer code (FRS), which sums the strains calculated over the short time intervals to give the total cladding strain accumulated over the fuel rod lifetime.

The sources of thermal-hydraulic input data for the transients are given in Sections 15.2 and 15.3 of the PSAR. The sources of cladding materials properties data used in the transient analyses are given in Sections 4.2.1.1.3 and 15.1 of the PSAR.

The validity of the method for calculating cladding ductility limited strain is justified by direct comparison between thermal creep strains calculated with the equations of Table 4.2-52 and experimental thermal creep data. Further verification of the strain limit method is given in the response to NRC Questions 241.48 and 241.13.

Question 241.15 (4.2.1.3.1.3)

Figure 4.2-27 illustrates the number and schedules of tests which have been, or are being conducted in various development areas. Provide the following additional information on these tests:

- 1) a more detailed description of these tests and the test results obtained,
- 2) references for test programs and test data,
- 3) the role that the results of these tests play in providing verification of the adequacy of the CRBRP fuel design.

Describe the FFTF fuel performance verification program and the transient tests on prototypic fuel rods being planned. Discuss the applicability of those to the CRBRP.

In figure 4.2-28, the number of stainless-steel clad mixed oxide fuel rods irradiated to greater than the FFTF/CRBRP initial peak fuel burnup goal of 80,000 MWD/MTD, is shown to be in excess of 500 fuel rods. Conclusions regarding sodium corrosion, dimensional stability, fuel densification and thermal performance capability of the fuel rods compared to the CRBRP current design are given. The following additional information regarding the performance of these rods should be given.

- 1) references for the data cited,
- 2) the differences between the fuel rods tested and the test conditions compared to the CRBRP fuel rod design and operating conditions,
- 3) a discussion of the results of the foreign programs and comparisons with CRBRP.

Provide more specific information on the LMFBR transient testing programs being conducted at HEDL including:

- 1) The test matrix for both the transient overpower and engineering proof tests,
- 2) The results of the test program should be stated in specific terms and comparisons given instead of statements such as "design limits for the FFTF fuel rods were only distantly approached" as given in the PSAR,
- 3) Applicability of the test matrix as established for both the engineering proof and transient overpower tests to CRBRP,
- 4) A more detailed discussion of the test results and the conclusions inferred from these results,
- 5) References for tests and test programs.

Discuss any plans or test programs to evaluate the potential for fuel failure propagation and its consequences.

Provide references and describe in more detail the results of foreign experience to high burnups (100,000 MWD/MTU) and operation with failures for periods up to 2 1/2 years without significant mechanical effects that this section alludes to. Discuss the applicability of this data to the evaluation of the CRBRP fuel performance.

Response:

The details requested on the steady-state tests and foreign experience are provided in revised PSAR Section 4.2.1.3.1.3. Transient tests, their applicability and impact on CRBRP design are discussed in response to questions 001.282, 001.283 and 001.284.

Question 241.16 (4.2.1.1.3.8)

It is stated that fuel failures that exhibit only fission gas release (assembly detectable during operation) will not be removed, but failures having gross fuel losses or excess sodium exposure will be removed on a priority basis. What kind of surveillance program is planned? How frequent will inspections be performed to look for such fuel?

Response:

See revised Section 4.2.1.1.3.8 for the information requested.

25

Q241.16-1

Amend. 25
Aug. 1976

Question 241.17 (4.2.1.2.3)

Eight styles of discriminatory systems are defined for the different fuel types. In addition, there are two types of control assemblies. Describe the discrimination details for the control assemblies.

Response:

The response to this question is in amended PSAR Section 4.2.3.2.1.3 under the title "Assembly Discrimination".

Question 241.18 (4.2.1.3)

The following questions address the fuel assembly.

- (1) Expand and justify the statement in page 4.2-47 "duct secondary stresses due to differential swelling across the duct wall were found to be relaxed by non-damaging irradiation creep. Therefore, these stresses were not specifically evaluated in PSAR".
- (2) Provide a reference from which the values in Table 4.2-7 are obtained.
- (3) Discuss and justify how one can only evaluate stresses and conclude that the design is satisfactory. How about creep and accumulated damage.
- (4) Identify all the computer codes specifically used for the fuel assembly (including duct) evaluation.

Response:

The requested information on fuel assemblies is provided in revised Section 4.2.1.3.1.2.

25

Question 241.19 (4.2.1.3)

Part 1: On page 4.2-56 it is stated that "If necessary, a vibration test will be performed..." Please clarify the term "if necessary" by means of specific engineering criteria.

Part 2: The calculational technique and verification of cladding-spacer wire interaction analysis should be provided.

Response:

Part 1: The response to this part of the question is found in amended PSAR Section 4.2.1.3.2.1.4.

Part 2: The response to Part 2 is given in the response to Part b of Question 241.14.

Question 241.20 (4.2.1.4.2)

The list of typical inspections under Fabrication Examination should be complete. Notably absent are the following: fuel chemical impurity analysis, cladding metallurgical state, wire wrap analysis, fuel and tag gas analysis, and fuel densification tests.

Will 100% radiography distinguish between blanket and fuel pellets with the same fuel rod?

For on-site acceptance tests, describe the procedures or tests which will assure that the fuel, blanket, and absorber pellet columns are in their proper location within the cladding.

Response:

In Section 4.2.1.5.2 (Tables 4.2-59A and 4.2-59B) a reasonably complete but not exhaustive listing of the characteristics of the Quality Conformance inspection plan for fuel assembly components is given. All of the characteristics listed are included in the characteristics of the inspection plan with the exception of fuel densification testing. Analysis has shown that densification is not a problem in CRBRP (see CRBRP-ARD-0168 provided in response to NRC Question 3, Reference Q241.20-1).

It will be possible to distinguish between fuel and axial blanket pellets within a fuel rod using 100% autoradiography.

After manufacture, all fuel and control rods are 100% inspected to insure that all pellet columns are properly located within the cladding. As indicated in the response to NRC Question 241.12, the standard analysis techniques utilized to evaluate the pellet column holddown springs insure that these springs will maintain column position during shipping and handling loads up to 6g. CRBR core assembly shipping casks will have acceleration indicators which will trip when shipping and handling loads exceed the 6g limit. These indicators will be checked on site to insure that the core assemblies have not been subjected to loads above this limit. A tripped indicator will be cause for rejection; the assembly would then be returned to the fabricator for more detailed evaluation.

Reference Q241.20-1: Letter, T. P. Speir to P. S. Van Nort, dtd. Oct. 6, 1975

Question 241.21 (4.2.1.4.2)

The fuel quality assurance program should include measurement of a pellet characteristic (such as thermal resintering) that will indicate the fuels densification behavior. Information is available from the NRC on such methods being developed for a Regulatory Guide.

Response:

A commitment to consider all available Regulatory Guides is noted in revised PSAR Section 4.2.1.4.2.

Q241.21-1

Amend. 15
April 1976

Question 241.22 (4.2.3)

In regard to the answer to Question 120.6, do any of the planned EBR-II irradiation tests of B_4C include transient cycling of absorber rods, typical of their real application?

Response:

A discussion of cycling tests of B_4C is included in revised PSAR Section 4.2.3.3.1.5.

Question 241.23 (4.2.3)

Provide a description or reference of the analytical codes used in the absorber rod design. For example, SIEX-B and PECT-IC are used for the FFTF program. In addition, provide an axial temperature profile for the absorber rod similar to Figure 4.4-1 for the inserted (at highest absorber temperatures) and withdrawn positions.

Response:

The response to the question on analytical codes is provided in amended PSAR Section 4.2.3. Discussions regarding the use of these as well as other codes in PCA analysis are provided in the revised PSAR Section 4.4.3.4 prepared in response to NRC PSAR question 001.49. The requested temperature profiles are provided in Figures 4.4-40 and 4.4-41, and referenced in amended PSAR Section 4.4.3.3.4.

Question 241.24

Provide a table similar to Table 4.2-42 for the Primary Control Assembly dimensions.

Response:

The requested table is provided and incorporated in the PSAR as Table 4.2-42a.

Q241.24-1

Amend. 14
Mar. 1976

Question 241.25 (4.2.3.3.2.3)

Explain how the peak centerline and hot spot temperature for the primary and secondary absorber rods can be identical when the secondary pellet is higher in enrichment by a factor of 1.5 and the diameter is larger by a factor of 1.15.

Response:

There was no intent to imply that the peak centerline and hot spot temperature for the primary and secondary absorber rods were identical.

PSAR Section 4.2.3.3.2.3 is a subsection of 4.2.3.3.2 entitled, "Secondary System Evaluation", and was intended to convey the information that the peak centerline and hot spot temperature for the secondary system was 2870⁰F for the hot spot and 2260⁰F for nominal conditions.

PSAR Section 4.2.3.3.1.5 and Table 4.2-46 provides thermal data for the Primary control assembly.

Question 241.26 (4.2.3.4.4)

The acceptance tests for the control assemblies and absorber pellets should be complete. Notably absent from the present description are: stoichiometry, chemical impurities, fill and tag gas analysis, and cladding metallurgical state. This section should be patterned after the revised 4.2.1.4.2 section.

Response:

The response to this question is supplied in amended PSAR Section 4.2.3.4.4.

Question 241.27 (4.4.1)

What is the cold plenum volume of the fuel rod, blanket rod, and control rod?

Response:

The difference between the total plenum volume and the material volume of the rod components which are located in the plenum region is the effective plenum volume. This effective plenum volume represents the region available for fission and/or reaction product gases. The cold effective plenum volume of the fuel rod is given in Table 4.2-4, while the cold effective plenum volume of the radial blanket rod is given in Table 4.2-5. These rods have fission gas plena located above the fuel pellet stack only. Tables 4.2-4 and 4.2-5 have been revised to clarify that these are cold available volumes.

The primary control rods have plenum spaces both above and below the absorber pellet stack. At room temperature the primary control rod upper effective plenum volume is 4.021 in^3 , while the primary control rod lower plenum has an effective volume of 2.349 in^3 . The total primary control rod plenum effective volume is therefore $4.021 \text{ in}^3 + 2.349 \text{ in}^3 = 6.370 \text{ in}^3$.

Question 241.28 (4.4.2.4.2)

Show power generation as a function of time for: a) the peak power fuel rod; b) the average power fuel rod; c) the peak power radial blanket rod; and d) the average power radial blanket rod.

Response:

New Table 4.3-7A, figure 4.3-8A and revised Section 4.3.2.2 contains the requested information.

25

Question 241.29 (4.4.2.6.3)

Is the correlation for the thermal conductivity of 316 SS based on irradiated data? Cite the data used for the correlation.

In calculating the thermal conductance of the cladding wall, explain how changes in cladding structure due to corrosion, wastage and irradiation are handled.

Response:

Revised Section 4.4.2.6.3 provides the requested information.

Question 241.30 (4.4.2.6.5)

For the peak power fuel rod and the average power fuel rod using the power histories described in Question 241.28, give the following values as a function of time for several positions along the axial length (where applicable):

- (a) burnup
- (b) hot gap
- (c) change in fuel pellet diameter due to thermal expansion
- (d) change in fuel pellet diameter due to relocation
- (e) change in fuel pellet diameter due to densification
- (f) change in fuel pellet diameter due to swelling
- (g) change in cladding diameter due to thermal expansion
- (h) change in cladding diameter due to swelling
- (i) change in cladding diameter due to corrosion
- (j) change in cladding diameter due to wastage
- (k) diameter of central void
- (l) diameter of equiaxed grain growth region
- (m) diameter of columnar grain growth region
- (n) fission gas release fraction
- (o) fission gas distribution in pellet
- (p) hot pellet diameter
- (q) hot cladding diameter
- (r) internal gas pressure
- (s) gas thermal conductivity
- (t) axial fuel length
- (u) gap conductance

Response:

Not all of the parameters listed in this question were determined explicitly in the PSAR analysis. Those that were determined are included in PSAR Sections 4.3 and 4.4.

In its final form, the LIFE code will be capable of calculating all of the parameters listed in this question. However, at this time, the LIFE code is undergoing checkout and calibration against experimental data. This code will be available for evaluation of these parameters for the FSAR.

Question 241.31 (4.4.2.6)

Equation (4.4.2.6-6) does not include a term for the thermal conductivity of the gas. Explain how this is treated in fuel temperature calculations.

Response:

The gap conductance is generally related to thermal conductivity. This is explained in Revised Section 4.4.2.6.5.

25

Question 241.32 (4.4.2.6.5)

Equation (4.4.2.6-6) is stated to be valid only in the range of 2 to 7 mils. How is the gap conductance of smaller hot gaps calculated?

Response:

As stated in PSAR Section 4.4.2.6.5, the HEDL P-19 data, from which equation (4.4.2.6-6) is derived, were conducted at beginning-of-life conditions. Therefore, hot gaps smaller than 2 mils were not observed, hence, the stated range of validity. As regards adoption of the P-19 correlation for other times in life than beginning-of-life conditions, this is discussed at length in Section 4.4.2.6.5.

Question 241.33 (4.4.2.6.5)

Explain how the various uncertainties involved in the calculation of the gap conductance uncertainty factor are statistically combined.

Justify neglecting the uncertainties of other factors which also effect gap conductance such as fuel density.

Response:

This information is provided in revised PSAR Section 4.4.2.6.5.

Question 241.34 (4.4.2.6.5)

The gap conductance equation (4.4.2.6-6) is given in terms of hot gap. Explain how these hot gaps were obtained from the experimental data. If computer calculations were used to obtain the hot gap, why are the uncertainties in the computer calculations not included in the estimate of uncertainty in the correlation?

Response:

The response to this question is contained in amended PSAR Section 4.4.2.6.5.

Question 241.35

What is the correlation coefficient of equation (4.4.2.6-6)? What is the prediction interval of equation (4.4.2.6-6)?

Response:

It is not clear what is meant by the term "correlation coefficient" in the question. If this question relates to the numerical values of equation (4.4.2.6-6), they are merely empirical coefficients determined through analytical backfitting of the P-19 experimental data.

As stated in the PSAR text, equation (4.4.2.6-6) is valid for hot gap in the range of 2 to 7 mils and FFTF/CRBRP typical fuel rod design parameters as prototypically tested in the P-19 experiment; by substituting in the equation, the nominal gap conductance is in the range of 900 to 3200 Btu/hr-ft²-°F.

Question 241.36 (4.4.2.6.6)

Explain in detail how the hot gap size of the control rod is obtained. Include a complete description of the procedure and all material property data used. If possible, a report may be referenced.

Response:

The response to this question is in amended PSAR Section 4.4.2.6.6.

Q241.36-1

Amend. 15
Apr. 1976

Question 241.37

Provide the following references: Section 4.4: Reference 5, Reference 7, Reference 13, Reference 15, Reference 16, and Reference 17.

Response:

As requested, the following references are provided under separate cover.

5. R. D. Leggett, "Interim Status Report on Thermal Performance of LMFBF Mixed Oxide Fuel (HEDL P-19)", HEDL-TME-71-92.
7. "Recommendations of Thermal Performance Models for LIFE-II", W/FFTF 732091, Letter, R. J. Jackson to L. Bernath, Westinghouse Hanford Engineering Development Laboratory, Richland, Washington, March 9, 1973.
13. "Review of the Influence of Burnup on the Linear Heat Rating to Incipient Fuel Melting for Mixed Oxide Fuel", Letter, W. R. Roake to Project Director, Reactor Division Project Office, USAEC, Richland, Washington, W/FFTF 740486, January 30, 1974, Westinghouse Hanford Engineering Development Laboratory, Richland, Washington.
15. M. D. Carelli and D. R. Spencer, "CRBRP Assemblies Hot Channel Factors Preliminary Analysis", Westinghouse Advanced Reactors Division, Madison, Pennsylvania, WARD-D-0050, October, 1974.
16. M. D. Carelli and others, "Predicted Thermal Hydraulic Performance of CRBRP Fuel and Blanket Assemblies", Westinghouse Advanced Reactors Division, Madison, Pennsylvania, WARD-D-0054, December, 1975.
- (*) 17. D. Y. Nee, "Preliminary Thermal and Hydraulic Evaluations in the Development of the CRBRP Primary Control System Design", Westinghouse Advanced Reactors Division, Madison, Pennsylvania, WARD-D-0033, April, 1974.

(*) Early report to support Control Assembly design decision.

Question 241.38 (4.4.2.6.7)

Provide an estimate of the uncertainty in equation (4.4.2.6-8), which gives the fuel thermal conductivity as a function of porosity and temperature.

Response:

The uncertainty in calculated values of fuel thermal conductivity is +10% as stated in PSAR Tables 4.4.2 and 4.4.5, the response to Question 00T.46, and in Reference Q241.38-1.

Reference:

Q241.38-1 M.D. Carelli, D. R. Spencer, "CRBRP Assemblies Hot Channel Factors Preliminary Analysis", WARD-D-0050, October, 1974.

Question 241.39 (4.4.2.6.8)

Provide an estimate of the uncertainty in equation (4.4.2.6-9), which gives the thermal conductivity of B₄C as a function of temperature and porosity.

Response:

Equation 4.4.2.6-9 has been corrected for typographical errors. It is valid between 440°F and 1800°F and at burnup levels greater than 5×10^{20} captures/cc. A discussion of the uncertainty in equation 4.4.2.6-9 is provided in revised Section 4.4.2.6.8.

Question 241.40 (4.4.2.6.15)

Two fuel restructuring models are presented: one in LIFE and one based on P-19 test data. List the different phenomena (e.g., gap conductance, fission gas release, etc.) that each of these models is used to calculate.

Response:

The PSAR used only one restructuring model, that based on the P-19 data, for all fuel thermal analyses. The gap conductance model was also based on the P-19 data and thus, it is internally consistent with the restructuring model. They have been discussed in detail in response to questions: 241.8, 241.31, 241.32, 241.33, 241.34. Discussion of fuel temperature calculations were provided in response to questions: 241.38, 241.42, 241.61. The fission gas release model is discussed in response to questions: 241.41, 241.60.

The LIFE code model was referred to in the PSAR only to note that more detailed models were under development which would be used as a basis for future (FSAR) analysis.

Question 241.41 (4.4.2.6.16)

In Section 4.4.2.6.16 it is stated that the fission gas yield was 0.274. Substantiate the basis for this number. What is the uncertainty of this number? Show the difference in the end-of-life fuel rod pressure if the fission yield were assumed to be $0.274 + U$, where U is the uncertainty.

Response:

The response to this question is included in revised PSAR section 4.4.2.6.16.

Question 241.42

Describe in detail how the fuel ΔT hot channel factor is combined statistically with the gap ΔT .

Response:

As mentioned in PSAR Section 4.4.3.2 the rationale for statistically combining fuel and gap hot spot factors is that the combined effect of the gap and the fuel thermal characteristics determines the overall fuel behavior as experimentally investigated (Reference 4.4-5). The section has been expanded to discuss the statistical combination in more detail.

17

Question 241.43 (4.4.3.2)

In Table 4.4.2, explain or show calculations for all the hot channel factors in the Table; e.g., what data was analyzed to derive such factors as the 'pellet cladding eccentricity' or the 'gap conductance'?

For 'direct' variables, what reactor experience was used to select these values?

What, if any, computer calculations were used to select these values for the hot channel factors?

Show how each of these hot channel factors is applied to the calculation of fuel temperature.

Response:

A comprehensive discussion covering all the questions raised can be found in the following document:

M. D. Carelli and D. R. Spencer, "CRBRP Assemblies Hot Channel Factors Preliminary Analysis", WARD-D-0050, October, 1974.

The above document is cited as Reference 15 in Section 4.4 of the PSAR and is being sent to you separately as indicated in the response to question 241.37.

Question 241.44 (15.5.2.1.1)

Provide a schematic drawing of a tubular housing and grapple and the interlock system between them.

Response:

An updated, more detailed schematic of the IVTM, is provided as revised Figure 9.1-16. New Figure 9.1-16A gives a cross section of grapple and core assembly handling socket, depicting the grapple fingers discussed in their extended and retracted configurations. The interlock system in Section 15.5.2.1 is schematically shown in new Figure 9.1-16B. The safety assurance diagram, PSAR Figure 15.5.2.1.1-1, has been modified and is also attached to this response. The interlocks shown in Figure 15.5.2.1.1-1 have the same designations as those shown in Figure 9.1-16B.

Question 241.45 (D.4.2.3)

In Section D.4.2.4, equations are given for the isotherms for columnar and equiaxed grain growth. What data were used to derive these correlations? Give an estimate of the uncertainty in these temperatures. How would this uncertainty affect the various analysis done with the SAS code if they were included?

Response: *

1. The restructuring isotherms were interim models which were considered for, but not incorporated into, the LIFE-2 computer code. These correlations, which were based on testing done in EBR-II (Ref. Q241.45-2), have been superceded. However, as noted in parts 2 and 3, they are consistent with the correlations used in the HEDL SIEX code, Ref. Q241.45-1.
2. The uncertainties for these correlations have not been characterized. However, SAS code restructuring predictions follow the same pattern as those of the SIEX code (see the following section for the comparison of SAS and SIEX), and the error in the grain growth radius calculated by the SIEX code is approximately $\pm 1\%$ (Ref. Q241.45-1). The error in the SAS code correlation would be expected to be similar. (See discussion in last paragraph)
3. Uncertainties in the restructuring isotherm correlation will affect the temperature at which restructuring is predicted to occur. If the calculated restructuring temperature is too high, too little restructuring will be predicted, and conversely, if the calculated restructuring temperature is too low, too much restructuring will be predicted.

Two studies have been made in which fuel restructuring was one of the parameters considered. The first was a comparison of a high gap conductivity SAS3A model with that used in the CRBRP HCDA analysis (see response 160 to Q001.451); the second was a comparison of the experimentally correlated SIEX code and the SAS3A code (see the response to Q001.469). The restructuring patterns from these studies are shown in Figures Q241.45-1 and 2. It can be seen from these figures that the SAS3A model used in the Project's HCDA analysis predicts the greatest amount of restructuring. However, as noted in the response to Q001.469, the comparison of SAS3A results and the results from SIEX, COBRA-3M and damage parameter analyses indicate the steady state uncertainties will not significantly affect the overall accident scenario or energetics. 160

*Note that Appendix D has been withdrawn in Amendment #24. 160

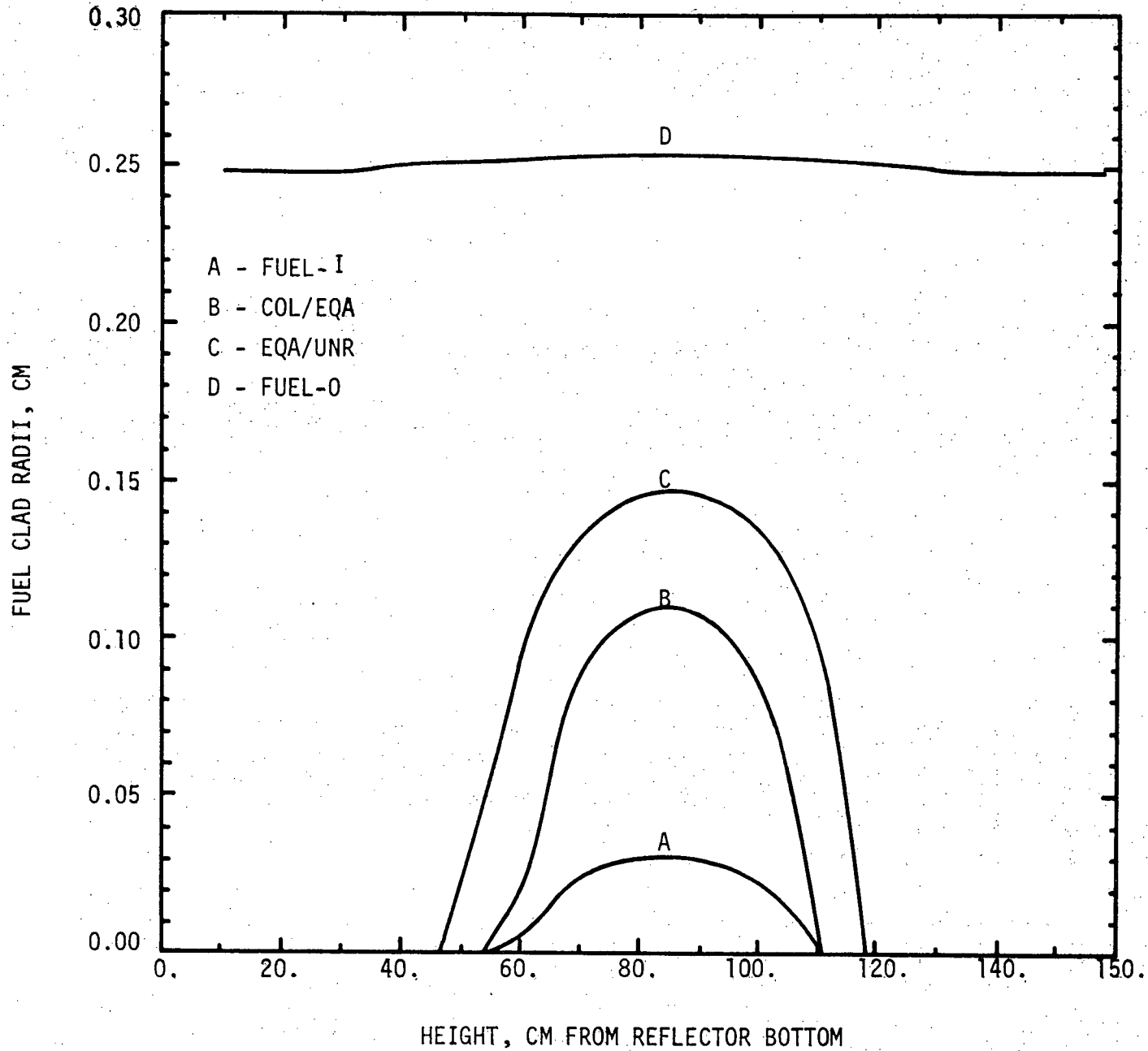
References

- Q241.45-1. Dutt, D.S. and Baker, R.B., HEDL-TME 74-55, SIEX, "A Correlated Code for the Prediction of Liquid Metal Fast Breeder Reactor (LMFBR) Fuel Thermal Performance", pp. 58-59, June 1975.
- Q241.45-2. Dutt, D.S., Baker, R.B., Jackson, R.J., "Interim Fuel Thermal Performance Models for LIFE-2, W/FFTF 73518," January 15, 1973.

Q241.45-2

Amend. 27
Oct. 1976

STEADY STATE CRBRP HIGH GAP CONDUCTANCE



Q241.45-3

Amend. 27
Oct. 1976

FIGURE Q241.45-1

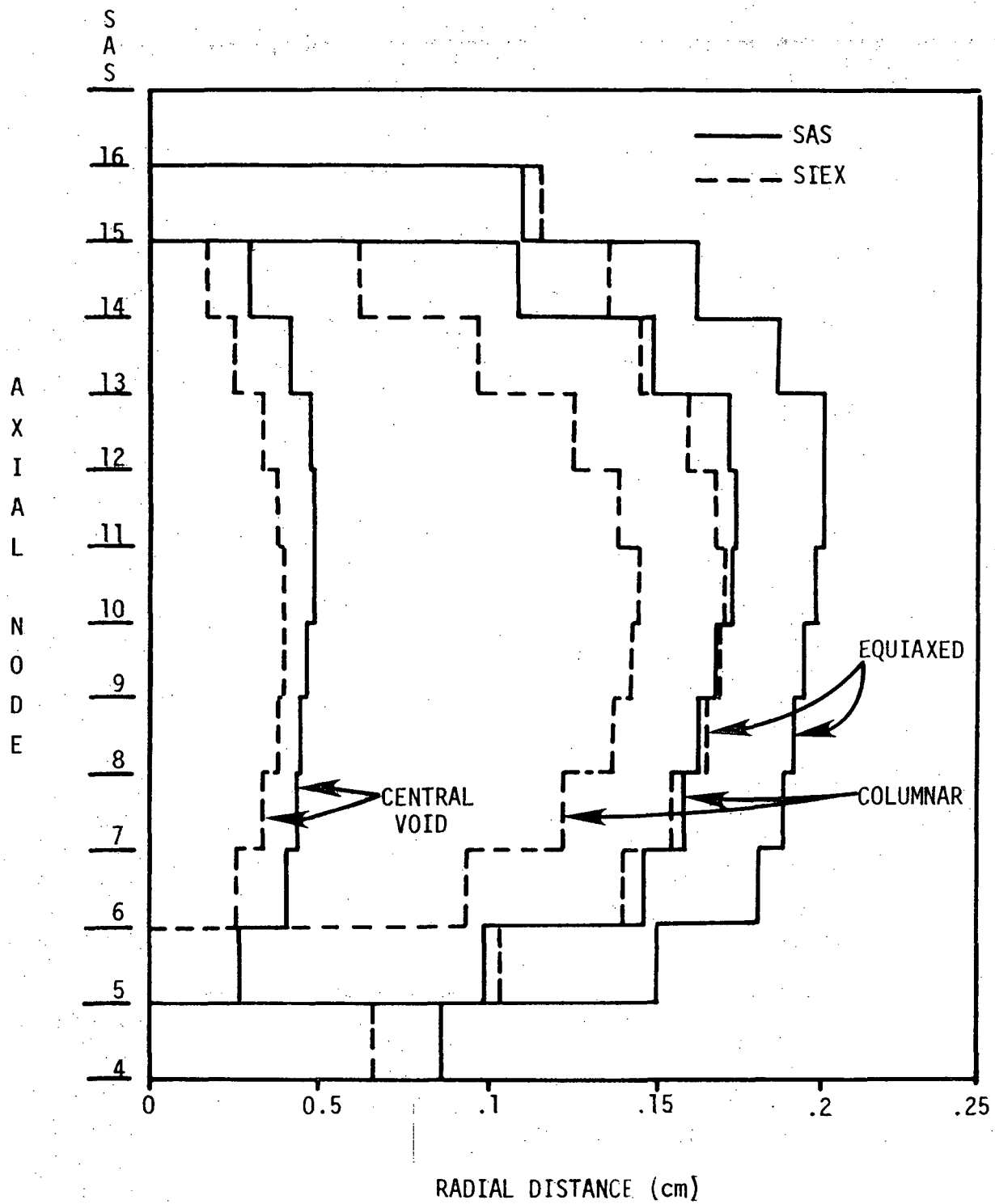


Figure Q241.45-2 Fuel Restructuring Patterns (Channel 2)

Question 241.46 (D.4.2.3)

In Section D.4.2.3, an equation is given for the gap conductance which is used in SAS. What data were used to derive this correlation? Give an estimate of the uncertainty in these data. What is the range of conditions (gap size, burnup, etc.) for which this correlation is valid?

Response:

This question requests clarification of information which is no longer a part of the current documentation. The Project has since consolidated all considerations given Hypothetical Core Disruptive Accidents into report CRBRP-3 (References 10a and 10b, PSAR Section 1.6) and its associated references; consequently, PSAR Appendices D and F have been withdrawn in Amendments 24 and 60 respectively.

The fuel-clad gap heat transfer coefficient correlation was obtained from the LIFE-II computer code and is based on data contained in Reference Q241.46-1. The correlation for the gas thermal conductivity used in the heat transfer coefficient correlation fits the data of Reference Q241.46-2.

No statistical analysis of the data is available. However, as shown in Reference Q241.46-1, the spread in the data is within approximately +50% of the mean value for data obtained near the CRBRP operating temperature.

References:

- Q241.46-1 V. Z. Jankus and R. W. Weeks, "Analysis of Fast Reactor Fuel Element Behavior", Nuclear Engineering and Design, Vol. 18, p 83, 1972.
- Q241.46-2 H. Von Ubisch, et.al., "Thermal Conductivity of Rare Gas Mixtures", 2nd International Conference on the Peaceful Uses of Atomic Energy, 1958, Volume 7, Paper 143, pages 697 through 700.

60

Question 241.47 (D4)

In Table D4-20, to which references do the reference numbers refer ?

Response:

This question requests clarification of information which is no longer a part of the current documentation. The Project has since consolidated all considerations given Hypothetical Core Disruptive Accidents into report CRBRP-3 (References 10a and 10b, PSAR Section 1.6) and its associated references; consequently, PSAR Appendices D and F have been withdrawn in Amendments 24 and 60 respectively.

60

Question 241.48 (4.2.1.1.2.2)

Provide the basis for the steady state thermal creep strain criterion (0.2% hoop strain at a 2 to 1 stress biaxiality ratio). All references must include a direct identification of the empirical evidence allowing its full characterization. The inclusion of evidence exhibiting a typical characteristics (e.g., alloy, temperature, fluence) must be justified. Any normalizations of parameters must be justified (e.g. using a uniform hoop strain definition to report a total strain measured by incremental diametral increases).

Response:

As described in revised Section 4.2.1.1.2.2 and Figure 4.2-1, extrapolation of the trend line of the four data points to prototypic FFTF/CRBRP lifetime gives a rupture hoop strain of 0.7%. However, the steady state strain limit is only 0.2%. As indicated in Section 4.2.1.1.3.4, Item 4, this design factor of 3.5 was applied to account for the degradation of material strength due to additional irradiation and depletion effects from sodium exposure. Further revisions to Section 4.2.1.1.2.2 show this margin to be conservative.

Q241.48-1

Amend. 15
April 1976

Question 241.49 (4.2.1.1.2.2 and 15.1.2.2)

Provide a justification for excluding a total creep strain plus plastic strain limit which depends upon the state of stress in fuel and radial blanket rods. This dependency has been recognized elsewhere by CRBR (Paragraph 4.2.2.1.1.9.C) and by FFTF (Figure A-1.1, FCF-213).

Response:

A total creep plus plastic strain limit which depends on the state of stress in the fuel and radial blanket rods has not been excluded from the criteria. The first paragraph of Design Requirement 1 in Section 4.2.1.1.2.2 states: "During steady state operation, the primary and secondary thermal creep strain in the circumferential (hoop) direction shall be less than 0.2% at a 2 to 1 stress biaxiality ratio. This criterion applies primarily to fuel rod cladding and with appropriate stress biaxiality corrections for other rod components."

Question 241.50 (4.2.1.1.2.2 and 15.1.2.1)

Provide a more definitive discussion of the uncertainties in the CDF (Σ_k) and in the residual strength (Σ_σ) and their stated dependence upon operational histories, phenomenological synergisms and material properties. Include some examples of the methods used to determine the magnitudes of these uncertainties.

Response:

The response to this question is provided in revised Section 15.1.2.1.

Question 241.51 (15.1.2.1)

Provide the means whereby the vector quantity stress rate ($\dot{\sigma}$) is combined with scalar quantities temperature rate (\dot{T}), flux (\dot{F}) and the rate of change in composition (\dot{C}) to give equation 8, page 15.1-52.

Response:

The quantity σ in equation 8 on page 15.1-53 is not a vector quantity. Rather, it is the scalar magnitude of a (positive) stress vector.

Although the distinction between scalar vs. vector is not explicitly made, it is implied by usage, for example, the familiar interchange of vector velocity and scalar speed. The vector stress is that computed from the operational loads on the clad, e.g., gas pressure and fuel-clad mechanical interaction (see response to question 241.55). On the other hand, the scalar magnitude appears (along with other scalar quantities) in those functions which define a specific characteristic of the clad. In these cases it is (along with the other scalars) a quasi-state variable.

When acting as a quasi-state variable the stress magnitude is not "combined" with the other variables in the sense that they have first order mutual dependence. These parameters merely functionally define the current characteristics of the clad in terms of phenomena believed to affect these characteristics in nature.

Amend. 14
Mar. 1976

Q241.51-1

Question 241.52 (4.2.1.1.2.2 and 15.1.2.1)

Provide a justification for the exclusion of the fatigue damage from the CDF. Include a discussion of the potential for fatigue-creep interaction.

Response:

A discussion of fatigue relative to the CDF is provided in the revised Section 15.1.2.1.

Q241.52-1

Amend. 16
April 1976

Question 241.53 (15.1.2.1)

Provide a more definitive discussion of the third "obvious" restriction on L_T (page 15.1-54). Include a discussion of the possible combinations which are affected by the magnitude of the rate of change of stress (e.g., no change in the stress level, σ_e , and a fluence dependent change in the PEL, σ_p).

Response:

The revised Section 15.1.2.1 for discussion.

25

Q241.53-1

Amend. 25
Aug. 1976

Question 241.54 (4.2.1.1.2.2)

Provide a discussion which compares the CDF to conventional design limits such as total inelastic strain, generalized stress, and engineering toughness. The discussion should include the methods for normalizing between the CDF and other design limits (e.g., a total engineering toughness limit for component failure - stress times strain - and a cumulative inelastic strain - number of times about the PEL).

Response:

In general, the CDF technique described in PSAR Section 15.1.2.1 calculates loss of structural integrity due to two failure modes. When the CDF equals 1, then:

1. The equivalent stress exceeds the material residual strength, and/or
2. The maximum principal stress for a given period of time exceeds the creep strength for the same period of time.

These two limits are directly comparable to time independent and time dependent "generalized stress" limits, respectively, such as those given in the ASME high temperature code cases. However, the CDF is based on a numerical evaluation of test data, and provides a better correlation between environment and performance for a specific material than do the more universal stress limits of the ASME code. More importantly, the CDF correlates the interdependence of the ductile rupture and creep rupture failure mechanisms, whereas simple generalized stress limits do not.

The inelastic strain criteria as given in Section 15.1.2.2 of the PSAR essentially guard against the same failure modes as the CDF; the difference being that the limits are expressed in terms of strain. In other words, a "strain CDF" could also be defined as follows:

$$CDF^S = \sum \frac{\Delta \epsilon_C}{\epsilon_{lim}} + \sum \frac{\Delta \epsilon_P}{\epsilon_{lim}} \leq 1.0$$

where:

- $\Delta \epsilon_C$ = creep strain increment
- $\Delta \epsilon_P$ = plastic strain increment
- ϵ_{lim} = 0.3% strain limit

This "inelastic strain" criteria would also predict loss of integrity, i.e., $CDF^S = 1.0$, for either of conditions 1 or 2 above. It should be noted that the plastic damage term of the CDF, L_p , accumulates damage for stress excursions beyond the proportional elastic limit. This is also true of the plastic strain term in the "strain CDF".

The 0.3% strain limit was selected to be conservative, and provides generally a lower limit on the failure strain.

The CDF does not include a damage correlation based upon "engineering toughness", and no attempt has been made to correlate data using this failure model. However, as discussed in the responses to NRC Questions 241.48, 241.13, and 001.36, available experimental data show that the fuel rod performance is adequately predicted by those criteria presented in PSAR Section 4.2.1.1.2.2.

Q241.54-2

Amend. 62
Nov. 1981

Question 241.55 (15.1.2.1)

Provide or reference the working definition of stress employed in the CDF.

Response:

A definition and additional data on stress is provided in revised Section 15.1.2.1.

25

Q241.55-1

Amend. 25
Aug. 1976

Question 241.56 (1.5 and 15.1.2.1)

Specifically identify those data which must be obtained in support of the empirical correlations employed by the CDF. The programs to provide these data must be identified and summarized.

Response:

The verification plans requested are discussed in revised PSAR Section 15.1.2.1.

Q241.56-1

Amend. 19
May 1976

Question 241.57 (4.2.1.1.2.2)

Provide a description of the program to be employed for verification of the CDF.

Response:

Revised Section 15.1.2.1 provides the information requested.

19

Question 241.58 (4.2.1.1.2.2)

Provide specific design requirements for the fuel and radial blanket assembly structural components. Include the interpretations for phrases such as: "design limits...shall be patterned after the applicable portions of Section III of the ASME...code", "appropriate limits on primary membrane and bending stresses shall be imposed", "... deformation limits... shall be designed so that distortion...does not produce gross interference...", "...components...deformation and failure shall not interfere with reactor shutdown or emergency cooling of the fuel rods".

Response:

The information requested has been provided in PSAR Section 4.2.1.1.2.2 as revised in response to Question 241.48.

Q241.58-1

Amend. 16
Apr. 1976

Question 241.59 (4.2.1.3.1.1)

Provide a description of the "selective assembly of the bundle and duct" referred to on page 4.2-39.

Response

The requested discussion is provided in revised PSAR Section 4.2.1.2.1.

15

Question 241.60 (4.2.6.16)

The fission gas release correlation gives F_N , the fractional gas release from non-restructured fuel, in terms of burnup and local linear power. Explain how this relationship was obtained from data, and how it is used in calculations. Define precisely the local power and show how this quantity is calculated.

Response:

The response to this question is provided in revised Section 4.4.2.6.16.

Question 241.61:

Describe the overall method used to calculate fuel temperatures, and show how all the different correlations and hot channel factors discussed are used. A flow chart should be supplied.

Response:

It is believed that the point-by-point procedure description provided in revised PSAR Section 4.4.3.3 answers this question, thus making a flow chart unnecessary, since it would be a mere graphical transposition of the discussion.

Q241.61-1

Amend. 17
Apr. 1976

Question 241.62

No discussion is made of the correlation for fuel relocation used in calculating fuel temperatures. If this correlation is used, please give the equation and empirical constants used, a discussion of the statistics of the correlation (correlation coefficient, prediction interval, etc.) and provide a complete listing of all data used in the correlation".

Response:

Two mechanisms can be considered under the classification of "fuel relocation": migration of uranium and plutonium and fuel restructuring. As regards the former mechanism, no significant migration will occur for the stoichiometric ratio of CRBRP fuel, as discussed in detail in response to part f) of question 241.8. Fuel restructuring has been accounted for in fuel thermal analyses: the restructuring model was based on the results of the HEDL P-19 tests as discussed in part b) of question 241.8.

Question 241.63 (1.3.2)

Table 1.3-3, (PSAR p. 1.3-13, Amend. 8, Dec. 1975) provides comparative data for CRBRP & FFTF. The FFTF linear heat rates do not correspond to the published FFTF data. Please cite a reference for the FFTF heat rates in the PSAR or provide a corrected comparison along with appropriate changes in the PSAR.

Response

A clarification provided by NRC for this question identified HEDL-TME 75-48 as the source for information that differed from FFTF data listed in the PSAR. This HEDL document was provided to NRC as information derived from the base technology conducted by ERDA. The operating conditions quoted in this document represent expected conditions, for which the testing program will provide confirmatory data. This is not a primary document for the specification of FFTF parameters; however, the peak heat rate quoted is 12.6 KW/ft., which is essentially the same as the 12.7 KW/ft. value quoted in the CRBRP PSAR. The value of 14.5 KW/ft. given in the NRC clarification cannot be identified, unless it was found in an earlier version of the HEDL-TME 75-48 than the one transmitted by CRBRP.

Inquiries made to the FFTF Engineering Dept. at HEDL verified the accuracy of both the peak and maximum (peak x hot channel factors at 115% power) linear powers quoted in the CRBRP PSAR. The primary source for information of this nature is given in the FFTF FSAR, Chapter 4, Reference 74. (G. J. Calamai, et.al, Steady State Thermal and Hydraulic Characteristics of the FFTF Fuel Assemblies, ARD-FRT-1582, June 1974.)

| 31

Question 241.64 (1.3.2)

On PSAR page 1.3-13, state if core fluxes are average or peak. What is the resultant fluence-to-burnup ratio and in-core residence time (at power)? The data on page 1.3-17 (Table 1.3-13) are insufficient and nonspecific (e.g., "core residence time = 3 years," last item).

Response:

Amended Table 1.3-13 provides updated nuclear design data in the specific areas related to peak core fluxes and peak-fast-fluence-to-peak-burnup ratio.

Question 241.65 (4.2.1.1)

On page 4.2-2 of the CRBRP PSAR it is stated that the fuel assembly design life of 411 full power days, corresponding to a peak fuel pellet burnup of 80,000 MWD/T, has been shown by FFTF Technology and EBR-II irradiation experience to be achievable in CRBRP with "conservative levels of safety and reliability". With the use of specific examples, please indicate which EBR-II irradiation test data and which aspects of FFTF technology have demonstrated that the designated design life will be conservatively achieved in CRBRP with respect to safety and reliability. In this regard it would, for example, be helpful to have a list of the pertinent EBR-II test data, together with a short description of the test rods and conditions. How many rods were prototypic of the current CRBRP design? Where the rods deviated from current design parameters, how did this affect the test results? Provide a quantitative estimate of the degree of conservatism in safety and reliability which have resulted from the application of the EBR-II irradiation experience and FFTF technology to the design and design life of the current CRBRP fuel.

Response:

The referenced portion of the PSAR was intended as a general summation of the information contained in later sections, i.e., 4.2.1.3 Design Evaluation, 4.2.1.3.1.3 Irradiation Experience, and 4.2.1.4 Testing and Inspection Plans. As a summation, the details of the statement are not presented at the referenced page (page 4.2-2) but in later sections and amendments since made to the PSAR. A specific example of the use of FFTF technology has previously been given (Amendment 15) in a preliminary indication that the 0.2% thermal creep strain limit used in conjunction with the CRBRP strain calculation procedure is conservative relative to design fuel rod lifetime. The results of this example utilize specific EBR-II irradiation data presented in Ref. 4.2-75 and in summary table 4.2-B. The design limits given in Table 15.1.2-1 have been chosen to preclude failure. However, even if the cladding breaches, this does not necessarily mean that safety is compromised. In fact, failures have been reported in Ref. 4.2-101 in fuel rod bundles with no discernable deleterious effects on adjacent rods. In addition, it is expected that further operation with breached (Ref. Q241.65-1) rods is safe.

Pertinent EBR-II steady state test data together with a description of the test rods and conditions are given in Ref. 4.2-162, Table A-1. Figures A-1 and A-2 of that reference list the relevant steady state program requirements which each of the individual subassemblies are designed to address. In addition, preliminary planning for use of EBR-II test results has been provided previously in Section 4.2.1.3.1.3.

EBR-II assemblies which are considered as being key to the CRBRP are listed in Tables Q241.65-1, 2, and 3. These assemblies contain ~1200 rods. As noted in an earlier response (Amendment 20, Section 4.2.1.3.1.3), the major differences between these rods and CRBRP rods are the fluence/burnup ratio, axial power distribution and coolant velocity-temperature combinations. This response also noted that FFTF fuel performance verification and CRBRP surveillance can provide more data to verify the applicability of the EBR-II data base, the analytical methods and the CRBRP fuel design.

It is not possible to provide a quantitative estimate of the degree of conservatism in safety and reliability directly from the application of EBR-II experience and FFTF technology. Therefore, the reference to the conservatism has been deleted from Section 4.2.1.1 of the PSAR.

Reference:

Q241.65-1 Letter S:L:1628, "Additional Information on Subassembly Faults", A. R. Buhl to R. S. Boyd, September 20, 1976 (Enclosure 2, "Operation with Failed Fuel").

TABLE Q241.65-1

KEY EBR-II SUBASSEMBLIES FOR STEADY STATE IRRADIATION PERFORMANCE

TEST	SUBASSEMBLY	CLADDING TYPE	PEAK POWER KW/ft	PEAK CLAD (TEMP (°F))	GOAL BURNUP (@/%)	PROVIDES DATA FOR TABLE 4.2-62						
						I	II	III	IV	V	VI	VII
XX02	PNL-17	20% CW 316SS	11.1	1050	3.8					•		
XX04	PNL-17A	20% CW 316SS	12.3	1110	0.4					•		
X051	PNL-3	Annealed 304SS	5.5	855	6.9	•						
X054	PNL-5	Annealed 304SS	14.2	1010	5.9	•						•
X059	PNL-4	Annealed 304SS	9.7	905	10.1	•						
X062	GE-F9B	Annealed 304, 316, 321SS	12.1	1055	15.0	•						
X069	PNL-7	Annealed 316SS	9.6	1000	10.9	•						
X073	PNL-6	Annealed 316SS	6.8	1010	8.0					•		
X074	PNL-8	Annealed 316SS	13.2	1080	9.6		•					
X076	WSA-2/WSA-5	Annealed 20% CW 316SS	7.1 - 11.5	1075 - 1270	13.0	•			•			•
X087	PNL-9	20% CW 316SS	5.9	915	5.6						•	
X088	WSA-1/WSA-5	Annealed 20% CW 316SS	6.7 - 7.8	1040 - 1140	14.0	•			•			•
X093	PNL-10	20% CW 316SS	9.6	1080	6.0						•	
X096	NUMEC-E	20% CW 316SS	13.1	1215	2.7							•
X097	NUMEC-F	20% CW 316SS	12.2	1115	5.0							•
X107	PNL-11	20% CW 316SS	12.6	1075	5.3			•			•	
X108	P-19	20% CW 316SS	19.4	1080	5.3					•		
X114	PNL-5A	Annealed 304SS	13.5	1030	14.1		•	•				
X115	WSA-3	20% CW 316SS	10.5	1125	13.5				•		•	•
X116	PNL-5B	Annealed 304SS	14.3	1040	16.1	•	•	•				
X117	GE-F8B	Annealed 304, 316SS, INC-800	5.9	950	13.0	•						
X118	GE-F8B	Annealed 304SS, 20% CW 316SS, Annealed INC-800	6.6	960	12.7	•						

Q241.65-3

Amend. 32
Dec. 1976

TABLE 241.65-1 (Cont.)

KEY EBR-II SUBASSEMBLIES FOR STEADY STATE IRRADIATION PERFORMANCE

TEST	SUBASSEMBLY	CLADDING TYPE	PEAK POWER KW/ft	PEAK CLAD (TEMP (°F))	GOAL BURNUP (0/%)	PROVIDES DATA FOR TABLE 4.2-62						
						I	II	III	IV	V	VI	VII
X121	GE-F10A	Annealed 304SS, 20-30% CW, C.A., Annealed 316 SS, 20-30% CW	15.8	1285	11.0				•			
X122	GE-F10B	304, 321, 347SS, INC- 800 Annealed, 316H SS Annealed, 20% CW, C.A.	15.5	1305	5.8				•			
X138	P-23A	20% CW 316SS	12.8	1400	9.3		•	•	•			•
X141	GE-F11A	304, 316SS Annealed, 20% CW, C.A., 321, 347SS Annealed	14.9	1360	5.6				•			•
X143	GE-F9A/C	Annealed 304SS/ Annealed 316HSS	12/7/12.8	940/1055	13.3			•				
X144	GE-F9A/C	Annealed 316, 321SS/ Annealed 316HSS	13.2/13.0	955/1090	13.0			•				
X145	GE-F9E	Annealed 316SS	15.0	1135	12.7						•	
X150	P-1ZA	10, 20, 30% CW 316SS	11.9	1400	7.9				•			•
X151	GE-E1/F5	304, 321, 347SS, INC- 800 Annealed	13.7	1130	9.5				•			
X154	WSA-4	20% CW 316SS	6.8	1230	15.0		•		•		•	•
X155	GE-F9F	20% CW 316SS	13.2	1240	10.6						•	•
X159	ANL-4	20% CW 316SS	11.2	1170	10.5				•			
X160	ANL-5	20% CW 316SS	15.1	1115	12.1				•			
X161	ANL-4A	20% CW 316SS	11.1	1155	0.1			•				
X162	ANL-5A	20% CW 316SS	15.9	1140	0.1			•				
X169	P-20	20% CW 316SS	15.2	1125	7.8					•		
X181	P-23B	20% CW 316SS	12.2	1350	7.0		•	•	•			•

Q241.65-4

Amend. 32
Dec. 1976

TABLE Q241.65-1 (Cont.)

KEY EBR-II SUBASSEMBLIES FOR STEADY STATE IRRADIATION PERFORMANCE

TEST	SUBASSEMBLY	CLADDING TYPE	PEAK POWER KW/ft	PEAK CLAD TEMP (°F)	GOAL BURNUP (0/%)	PROVIDES DATA FOR TABLE 4.2-62						
						I	II	III	IV	V	VI	VII
X186	P-12A	10, 20, 30% CW 316SS	11.4	1410	4.1				•			•
X190	GE-F20	316SS Annealed, 20% CW	17.8	1255	10.0			•		•		
X191	NUMEC-E	20% CW 316SS	12.8	1190	4.6						•	•
X192	PNL-9	20% CW 316SS	6.2	1095	9.8				•			•
X193	PNL-10	20% CW 316SS	8.8	1085	6.8						•	
X194	PNL-11	20% CW 316SS	11.8	1125	11.8				•			•
X199	WSA-8	316SS, 321SS, 316+T1SS, 20% CW	12.4	1420	7.3				•		•	•
X202	P-E/F	20% CW 316SS	11.1	1060	6.5				•		•	•
X203	P-23C	316SS and 316+TI, 20% CW	12.4	1550	6.0		•	•	•			•
X204	GE-F9D	Annealed 316HSS	10.3	1100	14.0	•						
X206	ANL-08	20% CW 316SS	13.1	1240	9.5				•			
X213	P-12A	10, 20, 30% CW 316SS	11.5	1375	8.2				•			•
X215	P-15	20% CW 316SS	6.1	1135	1.5	•		•				
X229	P-13	20% CW 316SS	14.5	1080	5.5						•	
X230	P-14	20% CW 316SS	13.2	1182	8.0						•	
X231	P-14A	20% CW 316SS	8.3	1142	8.0						•	

Q241.65-5

Amend. 32
Dec. 1976

TABLE Q241.65-2

TASK B. RUN-TO-CLADDING-BREACH SUBASSEMBLIES

Test Subassembly	Cladding Type	Nominal Peak Power, kW/ft	Nominal Peak Cladding Temp, °F (outer surface)	Cladding Breach EBR-II Run
X084 NUMEC-D	SA-316L	15	1180	62
X114 PNL-5A	SA-304	14	950	66C
X115 WSA-3*	20% CW-316	10	1050	(1)
X116 PNL-5B	SA-304	14	1050	74F
X138 P-23A	20% CW-316	12	1365	(1)
X141 F11A	SA-304, SA-316 SA-347, SA-321 CW-304, CW-316	14	1350	76A
X155 F9F*	20% CW-316	14	1250	(1)
X181 P-23B	20% CW-316	12	1300	76A
X181 P-23B	20% CW-316	12	1300	(1)
X186 P-12AA	30% CW-316	12	1200	67A
X191 NUMEC-E	20% CW-316	13	1200	67B
X193 PNL-10	20% CW-316	9	1025	68C
X194 PNL-11	20% CW-316	13	1025	75H
X199 WSA-8*	20% CW-316 CW-321, CW-316 +Ti	13	1200	(1)
X202 P-E/F	20% CW-316	12	1100	76F
X203 P-23C	20% CW-316 20% CW-316+Ti	12	1250	(1)
X213 P-12AB	20% CW-316	11	1260	75B
X229 P-13	20% CW-316	14	1050	(1)
X230 P-14	20% CW-316	14	1075	(1)
X231 P-14A	20% CW-316	9	1100	(1)

* Grid-spaced subassemblies. All others are wire-wrap spaced.

(1) At end of Run 80B cladding breach in the test pins had not yet occurred.

TABLE Q241.65-3

SUBASSEMBLIES FOR RUN-BEYOND-CLADDING-BREACH TESTING

S/A	Peak Burnup at End of Run 81 Mwd/MTM	S/A Status	Goal Burnup Mwd/MTM	Hot Na Exposure at Goal Burnup (hours)	No. of Pins at Peak Burnup	Peak Cladding Temp, °F (EOL)	Peak Power kW/ft
P-23A(X138)	93,000	RTCB	RTCB	10,000*	22	1260	13
P-23B(X181)	70,000	RTCB Run 83	RTCB	7,600*	18	1320	12.5
P-23C(X203)	75,000	In Reactor for Runs 83 & 84	RTCB	9,300*	11	1220	12.5
P-13(X229)	45,000	Reinsert Run 83	80,000	9,100	61-37	1150	13-14
P-14(X230)	50,000	In Reactor	80,000	8,200	61-37	1150	13-14

*Exposure at beginning of RTCB irradiation.

Q241.65-7

Amend. 32
Dec. 1976

Question 241.66 (4.2.1.1)

For equilibrium cycle conditions the fuel assembly burnup is given as 150,000 MWD/T peak and 100,000 MWD/T average, although it is acknowledged in the PSAR that these burnups cannot be conservatively demonstrated at this time. It is stated that "future test data could show that equilibrium cycle burnups are achievable". Please outline the portions of the current test program that are designed to confirm the conservatisms of the equilibrium cycle peak burnup. Include test scope and schedule as part of the requested outline.

Response:

The response to this question is provided in amended PSAR Section 4.2.1.1.2.1.

Question 241.67 (4.2.1.1)

For normal and upset conditions, fuel and radial blanket assembly component temperatures are said to be based upon maximum expected plant operating conditions and upper 2σ level semistatistical hot channel factors, which result in a 97.5% probability that the corresponding temperatures will not be exceeded. It is further stated that "this is conservative since the long term damage associated with these temperature levels is expected to more closely correspond to that associated with time averaged nominal temperatures." Some clarification of the above relationships is needed as follows:

- (a) Provide a list of the expected and/or design values for the fuel and radial blanket assembly component temperatures for normal and upset conditions.
- (b) Provide a list of the maximum expected plant operating conditions and upper 2σ level "semistatistical" hot channel factors.
- (c) Show how the maximum expected plant operating conditions and upper 2σ level semistatistical hot channel factors result in the 97.5% probability that the component temperatures will not be exceeded.
- (d) Explain in greater detail why the 97.5% probability value is considered conservative if the long term damage associated with these temperature levels is expected to more closely correspond to that associated with time averaged nominal temperatures. Provide quantitative values for the damage estimates.

Response:

The response to this question is provided by revision of the referenced statement in PSAR Section 4.2.1.1.2.1.

Question 241.68 (4.2.1.1)

The discussion of fuel rod load mechanisms (PSAR pages 4.2-3, -4, and -5) groups the loading mechanisms into six general categories, and states that "as shown in Table 4.2-52 and the exemplary references cited therein, the above loading conditions are supported by FFTF fuel assembly design evaluation and EBR-II reactor operating experience and information from the U.S. and foreign LMFBR programs. Therefore, as a minimum, these loadings shall be required for evaluation of the design adequacy of the fuel and radial blanket assembly fuel rods".

- (a) The above statements imply that the design adequacy of the fuel and radial blanket assembly fuel rods has not yet been assessed by the CRBRP staff. Please provide a schedule for this assessment.
- (b) The applicant should provide or reference a comprehensive analysis and discussion of the relationships between the FFTF fuel assembly design evaluation, EBR-II reactor operating experience, information from the U.S. and foreign LMFBR programs, and the postulated loading conditions in CRBRP.

Response

- (a) The subject statement, which appears in Section 4.2.1.1.2, gives design requirements. It is not intended to imply that the design adequacy of the fuel rods has not yet been assessed. Indeed, the requested assessment has been provided in PSAR Section 4.2.1.3, Design Evaluation.
- (b) The references cited in Table 4.2-52 were provided only as examples to indicate the types of loadings to be considered. They were not intended to provide the absolute magnitude of these loadings. Therefore, the requested discussion given below concentrates on the applicability of the cited references to the postulated loading conditions in CRBRP. Table 241.68-1 gives a summary of the nominal design and operating conditions cited in the exemplary references. As shown in the following subsections, the conclusion is that the cited references do indeed support the postulated CRBRP fuel rod loading conditions.

FFTF Fuel Assembly Design Evaluation

Since the fuel and cladding design differences between FFTF and CRBRP are minimal and the FFTF operating conditions envelope CRBRP, the loadings given on pages 2.1 and 2.2 of Reference 4.2-59 and page 1 of Reference 4.2-60 were considered directly applicable to CRBRP.

EBR-II Reference Fuel Irradiation Experiments

On page 185 of Reference 4.2-61, it is stated that: "At least three-quarters

of the gas produced by fission was released to the plenums. Thus, it appears that conservative fuel element design cannot rely on any substantial retention of gas in the ceramic". This finding was considered valid. Other findings relative to the unimportance of fuel-cladding differential expansion and high loading due to wire-wrap cladding interaction were discounted because as stated on page 185: "Substantially more cladding swelling was observed with Type 304L than with Type 316 stainless steel".

Reference 4.2-62 states on page 98: "The potential for cladding deformation due to fuel-cladding mechanical interaction should be considered in LMFBR fuel rod design". This guideline, based upon 316 solution annealed clad fuel rods irradiated in EBR-II, was considered valid for the reason stated on page 97: "Consequently, although the fluence-to-burnup ratio for the experimental rods was less than will be experienced by the near-term LMFBR fuel rods, the ratio of cladding swelling to burnup in the experimental rods with annealed cladding may be of the same order as that anticipated with the cold-worked cladding in near-term LMFBR's".

Reference 4.2-63 was evaluated for results pertinent to wire wrapped 316 solution annealed fuel rods because of the applicability of the swelling to burnup ratio as discussed above. From page 317 of this reference: "Total fission gas release was similar, 70% in Rod F9D-10 (coprecipitated fuel) and 66% in Rod F9D-15 (physically mixed fuel)". And from page 316: "In agreement with calculations, the channel (referred to as duct in CRBRP design) could not be moved relative to the rod bundle with a reasonable pull force limit . . . Profilometry indicated significant local rod deformation at wire pinch planes". These results, which are indicative of loading by support system and duct interaction, were considered overly conservative even for the 304 SS wire wrap and duct. The reason is as stated on page 316: "An unirradiated channel was placed on the F9A test assembly after interim examination at 6.5% burnup. During further irradiation to 9 atom % average burnup, there was a significant growth of the bundle but little growth of the channel because of the exponential fluence dependence of metal swelling". Since this type of loading may occur in the CRBRP assembly because the duct operates at lower temperatures than the wire wrapped rod bundle, it was considered as a loading mechanism.

U.S. LMFBR Program

Reference 4.2-64 is a study of loading mechanisms in a general LMFBR with 720°F inlet and 1000°F mixed mean outlet temperature. Analyses of FFTF type fuel rods were performed at core midplane (highest power) and core outlet (highest cladding temperature) for a typical hot rod, peak power rod, average rod and minimum power rod. Because of the similarity to CRBRP design and operating conditions, the following loadings were judged to be appropriate: Page 26 - "Stresses which are due to fission gas, thermal strains and the differential swelling strains". Page 33 - "Stresses due to fuel-cladding interaction. Page 48-49 - "Wire-Wrap to Cladding and Bundle-Duct Interaction".

Reference 4.2-65 is a synopsis of LMFBR reference fuel pin transient behavior

based upon the experimental data (referenced but not reported) at that time (late 1972). The loading mechanisms identified were all considered generic for CRBRP since there was insufficient data to prove otherwise. Page 628 states: "Several experimentally identified mechanisms may act individually or collectively to produce cladding strain under transient conditions. These include: a) differential fuel-cladding thermal expansion, b) intergranular fission gas induced fuel swelling, and c) transient release of the intergranular fission gases". A more recent summary (January, 1975) of the reference fuel transient irradiation program identifies the same loading mechanisms. (See page 50 of Reference 4.2-56). Page 632 of Reference 4.2-65 identified post-failure loading mechanisms as molten fuel and fission gas ejection.

Reference 4.2-66 is a general discussion of fuel rod vibrations in an LMFBR. Since the sample calculation given on pages 416 to 421 used parameters similar to those of the CRBRP wire wrapped rod bundle, fuel rod vibration was considered a CRBRP fuel rod loading mechanism.

Foreign LMFBR Programs

The references cited in this area are not very detailed regarding design and operational parameters. Therefore, a large number of the entries in Table 241.68-1 are NS (not specified). These details for PFR, the initial SNR-300 core and Phenix, as taken from Table IIa of Reference 241.68-1, are indicated in parenthesis after the NS entry.

Reference 4.2-67 describes the theoretical and experimental studies (out-of-pile and DFR irradiation) to support the U.K. LMFBR program. As noted in Table 241.68-1, the design and operating conditions are not significantly different from CRBRP. Therefore, the following loadings from page 331 of this reference were considered relevant:

- "(a) The steady mechanical interaction between fuel and cladding after lengthy operation of the reactor at steady power.
- (b) The transient fuel/clad interaction pressure during a rapid power increase after lengthy operation at reduced power.
- (c) Cladding stresses caused by the pressure of released fission gases
- (d) The transient fuel/clad interaction stresses during a regular sequence of power cycles.
- (e) Self-stressing of the cladding due to differential thermal expansion and differential voidage swelling".

The PFR initial core will use grid spacers with wire wrap as the backup support system. In the design evaluation described in the reference, page 337, thermal bowing due to differential thermal and irradiation induced expansion and pin vibration were considered for both support systems.

Reference 4.2-68 describes the design procedure of an experimental sub-assembly (MOL-7B) in support of SNR. Of particular interest, a computer code developed to analyze SNR fuel pin cladding was used to evaluate the MOL-7B fuel pin designs. As stated on page 173 of the reference: "The following loads, variable with time, are considered:

- (a) Outer coolant pressure;
- (b) Inner gas pressure due to filling gas and the release of gaseous fission products;
- (c) Axial force associated with the inner and outer pressures considered above;
- (d) Contact pressure and axial force due to fuel swelling;
- (e) Temperature gradient caused by heat generation in the fuel itself and the gamma heating in the cladding".

As demonstrated by the reference, these general LMFBR fuel rod loadings are not keyed to any specific set of design and operating parameters. Therefore, they were considered appropriate for CRBRP.

Reference 4.2-69 reports on a thermal reactor irradiation of an LMFBR (Phenix) type fuel pin. The purpose of the study was to determine the effect of cladding breach on the fuel, fuel rod and sodium circuit. As stated in the Abstract, page 261, the results of the testing indicated that the primary loadings were gas release and sodium-fuel interaction. These results agree with the transient loading mechanisms reported by the U.S. LMFBR program (Reference 4.2-65), and are considered applicable to CRBRP.

Reference

241.68-1 - K. Kummerer, "General Characteristics of a Fast Reactor Fuel Pin", Nuclear Energy Maturity, Proceedings of the European Nuclear Conference, Paris, 21-25, April, 1975, Vol. 3, Part 1, page 446, Pergamon Press, 1976.

TABLE Q241.68-1

Summary of Design and Operating Conditions for CRBRP Fuel Rod Loading References

Exemplary Reference, 4.2 -		PSAR	59,60	61	62	63	64	66	67	68	69
Reactor/Subassemblies		CRBRP Fuel	FFTF Driver Fuel	EBR-11 F3A	EBR-11 F2,F3,F5,F9	EBR-11 F9	LMFBR Fuel	LMFBR Fuel	DFR & PFR Fuel	SNR-300 BOR/MOL 7-B	Phenix Fuel
Fuel Design											
Pu in (U,Pu) _x		18.7, 27.1	19.8, 24.2	25	20 - 25.4	25	NS, Implied	NS	30 & 25	NS	NS
Oxygen to Metal Ratio	---	1.94 - 1.97	1.94 - 1.97	1.98, 2.00	1.98, 2.00	2.0	Same as	NS	2	2	2
Pellet Form	Note 1	SP	SP, CP, MM	SP & AP, CP	SP & AP	SP & AP, CP, MM	FFTF	NS	SP & VC	SP, VC	NS (SP)
Pellet Density	% Theor.	91.3	90.4	84 - 95	89 - 96	79 - 98	↓	90.4	NS	NS (86.5)	NS (85)
Pellet Diameters	Inch	0.1935	0.1945	0.245	.206 - .218	NS ⁽³⁾		NS	NS	NS (.200)	NS (.2165)
Smear Density	% Theor.	85.5	85.5	81.1 - 88.4	82 - 93	NS		85.5	NS (80)	NS (80.0)	NS
Cladding											
SS Material Type	---	316	316	304L, 316	321, 316	316, 304, 321	316	300 Series	M 316, FV548, PE16	WN 4970, 4988	NS (316L)
Cold Work	*	20	20	.0	0 & 50	0	20	NS	NS	0	NS
Outside Diameter	Inch	.230	0.230	0.290	0.250	0.250	.230	.230	.230	NS (.236)	NS (.258)
Wall Thickness	Inch	.015	0.015	0.020	0.015	0.015	.015	.015	NS (.015)	NS (.015)	NS (.0177)
Nominal Conditions											
Max. Cladding MW Temp.	°F	1230 ⁽⁴⁾	1118 - 1310 ⁽⁴⁾	981 - 1180	815 - 1180	986 - 1058	980 - 1372	1000	1292	1292	-1110
Peak Fuel Burnup	% Atom	80 MWD/Kg ⁽²⁾	80 MWD/Kg ⁽²⁾	5.56	3.7 - 11.1	6.8 - 15.4	NS (13,150 hrs)	NS	7.5	64-80 MWD/Kg ⁽²⁾	NS (60 MWD/Kg)
Peak Linear Power	Kw/Ft	6.6 - 11.1	7.1 - 12.4	15 - 17	12.6 - 14.2	9.7 - 13.6	NS, Implied Same as FFTF	NS	15.75	11.8 - 14.8	18.0

Notes: (1) SP = Solid Pellet, AP = Annular Pellet, VC = Vibro Compacted, CP = Coprecipitated, MM = Mechanically Mixed

(2) 1 Atom % Burnup Corresponds to 9.5 MWD/Kg in FFTF or CRBRP.

(3) NS = Not Specified in Cited Reference.

(4) Design (Hotspot) Value at 80 MWD/Kg Peak Burnup.

Q241.68-5

Amend. 32
Dec. 1976

Question 241.69 (4.2.1.1)

Please provide further discussion and documentation in support of the contention that irradiation induced creep and swelling are super-plastic phenomena and thus not ductility limited.

Response:

The response to this question is provided in amended PSAR Section 4.2.1.1.2.2.

Question 241.70 (4.2.1.1)

The treatment of fatigue effects in the PSAR requires amplification because it is not sufficient to state that "the appropriate fatigue component will be added to the CDF" (PSAR page 4.2-8). Please add specificity by listing exemplary fatigue components and values together with estimates of corresponding reductions in fuel design life or operation. Also show how the fatigue component would be added to the CDF.

Response:

A discussion of fuel rod cladding fatigue damage is provided in revised PSAR Section 4.2.1.3.1.1 and the methodology for including fatigue effects in the CDF procedure is discussed in PSAR Section 4.2.1.1.2.2.

Q241.70-1

Amend. 29
Oct. 1976

Question 241.71 (4.2.1.1)

In the discussion of maximum cladding midwall temperature (item 7, page 4.2-8) the term "design guideline" is used. Please explain the significance of this terminology. How is a "guidleing" different from a "limit"? Present and discuss the "recent data on irradiated prototypic cladding" which indicates "short-term failure at temperatures much higher than 1600°F", as suggested on PSAR page 4.2-8.

Respose:

The response to this question is provided in the response to Question 241.85.

Question 241.72 (4.2.1.1)

CRBRP section 4.2.1.1.2.3, Requirements for Design Features, provides a useful focus on specific design features to be incorporated into the fuel and radial blanket assembly designs. Nowhere in the PSAR, however, is discussion provided of the means by which these design feature requirements would be met. While it is understood that much of the LMFBR base technology is still under development, the PSAR should contain this discussion, to the fullest extent possible within the present state of the art. The applicant should also make a commitment to submit topical reports, which will resolve any outstanding items in this general area, before the submittal of the FSAR.

Response

For a discussion of the design features that satisfy the requirements given in PSAR Section 4.2.1.1.2.3 and itemized below, see the indicated PSAR Section and/or question referenced:

|30

1. Features incorporated into the fuel assembly design to minimize flow induced vibration and the potential for fretting and wear are specified in PSAR Sections 4.2.1.1.3.4 and 4.2.1.2.1. An explanation of why vibration of the radial blanket rods is not expected to occur is given in PSAR Section 4.2.1.3.2.1.4.
2. Fuel and radial blanket assembly component materials are specified in PSAR Section 4.2.1.2. Tests to verify that galling or self-welding do not occur at the hard coated surfaces are detailed in PSAR Section 4.2.1.2.1.
3. As specified in PSAR Section 4.2.1.2.1 the fuel pellet column is retained in position during preirradiation shipping and handling by a preloaded helical compression spring. Design calculations for the preliminary fuel column holddown spring were performed following standard, industry accepted analysis techniques. References for spring design calculations and the requirements satisfied are given in PSAR Section 4.2.1.2.1.

Q241.72-1

Amend. 30
Nov. 1976

4. Explanation of the assembly external support system and thermal expansion provisions are given in the response to PSAR Question 241.80. Unlikely events to cause loss of hydraulic balance, the precautions taken to preclude these events and analysis of the effects and consequences of assembly movement are discussed in PSAR Section 15.2.2.1.

Within the assembly the initial cold gaps provided for differential axial growth between the duct and fuel or radial blanket rods are shown on the fuel and radial blanket assembly schematics (Figures 4.2-11 and 4.2-14, respectively). Presently, for the fuel assembly this gap is 2.1 inches (Table 4.2-4) and 1.6 inches for the radial blanket assembly.

5. As shown in schematics of the fuel and radial blanket assembly (Figures 4.2-11 and 4.2-14, respectively) multiple radial inlet slots or holes are provided in the inlet nozzles. According to standard techniques of hydraulic analysis (Reference Q241.72-1) complete blockage of one of the six inlet slots in the fuel assembly would increase the inlet nozzle pressure drop from the values given in Figure 4.2-2 by 4.5 psi. This would correspond to a design flow rate decrease to approximately 97.5% in the highest flow assembly. The inlet plenum feature model test initial results, reported in Reference Q241.72-2, verifies that an assembly with two partially blocked inlet slots typically has about 2% less flow than a full flow assembly (see Figure 15.4.1.3-2). Core flow distribution tests used the same inlet plenum feature model but effectively blocked off one inlet slot completely. The results from this test, summarized in Reference Q241.72-3, conclude that the flow maldistributions throughout the core is typically less than 2% and randomly distributed. Additional information on cleanliness requirements, precautionary operations and sodium coolant purity requirements that assist in the prevention of blockages to the fuel and radial blanket assemblies are given in PSAR Sections 15.4.1.3.1 and 15.4.3.3.1.
6. A complete description of the discrimination systems that assure accurate location in the core of the fuel rods and fuel, radial blanket, control and removable radial shield assemblies is given in PSAR Section 4.2.1.2.3.

In view of the above, none of these items require resolution in topical report form.

References

- Q241.72-1 I.E. Idel'Chik, "Handbook of Hydraulic Resistance", AEC-TR-6630, Clearinghouse for Federal Scientific and Technical Information.
- Q241.72-2 HEDL-TME-75-94, P.M. McConnel, J. Spalek, S.J. Mech, "Inlet Plenum Feature Model Flow Test of the CRBR: Initial Results", November, 1975.
- Q241.72-3 HEDL-TME-76-33, P.M. McConnel, "IPFM Flow Test of CRBRP: Addendum V" March, 1976.

Question 241.73 (4.2.1.1)

Features said to minimize flow induced vibration and the potential for fretting and wear include: (1) an axial pitch of 11.9 inches with a backup 6-inch axial pitch for the fuel rod wire wrap; and (2) minimization of radial porosity between the fuel rod bundle and duct by means of selective assembly techniques (CRBRP Amendment 15, page 4.2-13a). The adequacy of these features in controlling fuel rod cladding fretting and wear is reportedly being evaluated in the prototypic EBR-II experimental subassemblies P13, P14, and P14A. Please describe these subassemblies and tests, including program scope, schedule, objectives, methods, expected results, and application of findings to the CRBRP cladding fretting and wear design features above.

Response:

The information requested is provided in revised PSAR section 4.2.1.1.3.4.

Question 241.74 (4.2.1.1)

The discussion of potential differences in environmental effects in the radial blanket versus the fuel is not quantitative enough for PSAR. Even though existing data may be insufficient for a finalized analysis, the PSAR should contain quantitative estimates of the environmental effects in the radial blanket founded on the existing data, (and/or assumptions, if necessary) along with discussion of uncertainties and R&D programs which will generate new information in this area.

Response:

51 | The response to this question has been expanded to discuss the radial and inner blanket assemblies. The radial and inner blanket assembly types have been analyzed in the same detail as the fuel assembly and the important radial and inner blanket performance analyses have been presented in the comparable detail in the PSAR. The differences between the operating environments of the two designs were pointed out in the PSAR to indicate that the differences between the designs were considered. The differences in operating conditions are inherent in the nuclear and the thermal data as they are presented in the PSAR. The effect of the environmental differences on the blanket performance have been stressed in Section 4.2.1.1 of the PSAR. It is indicated that several important environmental effects are less severe for the blanket rod than they are for a fuel rod:

51 | • The fuel cladding chemical interaction in the radial and inner blanket is less than in the fuel rod.

• Fuel-sodium reaction in a failed radial and inner blanket rod results in less relative fuel expansion than in a failed fuel rod.

51 | Also, due to lower sodium flow velocities in the radial blanket assemblies with long residence times, the corrosion rate will be lower for the radial blanket rod cladding than that for the fuel rod cladding.

The effect of the environmental parameters on the radial and inner blanket performance was calculated in the PSAR by estimating the effect of environmental conditions on the blanket using performance models that were calibrated on fuel rod data.

51 | The basic data and the analytical models used to predict the effect of the environmental conditions on the radial and inner blanket are being generated in the fuel development programs. The development tests, the technical information obtained from these tests and its utilization in design are identified in PSAR Section 4.2.1.3. The information generated for fuel design covers a parameter range which generally envelops the environmental conditions of the radial and inner blanket and therefore includes the general technical information required for the radial and inner blanket design.

51 | Table Q241.74-1 lists this technical information which will be available from fuel rod and fuel assembly experiments or analysis. Table Q241-74-1 also indicates which data are supplemented by specific blanket tests to confirm the applicability of the fuel design data to blanket design. Additional experiments are identified to test those blanket features which are unique and are not tested in the fuel development program. Such features include the effect of larger rod sizes, the large power gradients, assembly configuration and power history. Although the testing program was initially planned to verify critical features of the radial blanket assembly, this testing program generally envelopes the inner blanket assembly conditions. The testing parameters in these programs were expanded to envelope inner blanket assembly conditions, which deviate significantly from the radial blanket conditions, such as the larger flux in the inner blanket assemblies. All these test programs do not eliminate the uncertainty associated with the long goal operating time of ~ 21,000 hours for radial blanket which requires extrapolation of the available data. Confirmation of the validity of the extrapolation will be obtained from irradiation of WBA-40 and WBA-41 in FFTF which will test operation of the CRBRP blanket.

The radial blanket test program plans, and the rationale for obtaining data to support the radial blanket design were discussed at the "CRBRP Fuel Meeting" with NRC on October 13 and 14, 1976 in Bethesda, Maryland. (Additional details are contained in the handout from that meeting, entitled "Radial Blanket Rod Test", H. D. Garkisch.)

TABLE Q241.74-1 (Cont.)

Blanket Development*

51

Area of Technical Uncertainty	Technical Information Required	Required Experiment or Analysis	Utilization of Results
2. Fuel Behavior During Steady State & Transient	Fission Gas Release	Determine Release Fraction in WBA-20 WBA-21 Develop a F.G. Release Model in LIFE to Accommodate Radial and Inner Blanket Parameters	Final Design Verification. Design Release for Fabrication
	Fuel Swelling	Verify Release Fraction in WBA-20 WBA-21 Determine Fuel Swelling from WBA-21 Develop Fuel Swelling Model Based on Fuel Assembly Data and WBA-20	Reactor Operation Final Design Verification Final Design Verification
	Fuel Densification	Verify Fuel Swelling with WBA-21 Fuel Assembly Data Verify Densification in WBA-20	Reactor Operation FSAR Submittal
	Fuel-Cladding Interactions (Steady State)	WBA-20, Develop a Fuel-Cladding Interaction Model in LIFE to Accommodate the Radial and Inner Blanket Parameters	Final Design Verification Reactor Operation
	Fuel-Cladding Interactions During Transients	WBA-20 (Power Jump)	FSAR Submittal
	Assessment of CRBRP RBCB Capabilities	Analyze Data, Tests are being planned.	Reactor Operation Design Release for Fabrication
	Assessment of CRBRP Radial and Inner Blanket Rod Performance	Radial and Inner Blanket Rod Analyses	FSAR Submittal

51

51

51

Q241.74-4

Amend. 51
Sept. 1979

51

*Only approved planned and ongoing tests are listed.

**WBA-20, WBA-21, WBA-40, WBA-41, WBA-45/46 are designators for Irradiation Tests which Testing Objectives were presented at the CRBRP Fuel Meeting with NRC, October 13 and 14, 1976 in Bethesda, Maryland.

TABLE Q241.74-1 (Cont.)

Blanket Development*

51

Area of Technical Uncertainty	Technical Information Required	Required Experiment or Analysis	Utilization of Results
3. Cladding Integrity During Transient Operation	Cladding Material Properties at Transient Temperatures and Strain Rates Fuel-Cladding Interactions Transient Cladding Performance Code	Fuel Assembly Data See Item 2 Fuel Assembly Data	Design Release for Fabrication
4. Internal/External Cladding Degradation	Fretting Wear Sodium Corrosion Fuel-Cladding Chemical Attack Carbon and Nitrogen Depletion Develop a Cladding Wastage Model Develop a Carbon/Nitrogen Depletion Model	Rod Bundle Compaction Test Wire Wrap Cladding Wear Test Flow and Vibration Test in Water Fuel Assembly Data WBA-20 Post Irradiation Examination Fuel Assembly Data Analyze Data and Issue Topical Confirmation from WBA-20 Analyze Data and Issue Topical	Design Verification Design Verification Design Verification Design Verification FSAR Submittal FSAR Submittal FSAR Submittal
5. Wire Wrap Integrity	Wire Material Properties Wire External Degradation Wire Wrap Performance Code	Use Cladding Material Properties Use Sodium Corrosion and Fretting Wear from Cladding. See Item 4 and Fuel Assembly Data Fuel Assembly Data	

51

Q241.74-5

Amend. 51
Sept. 1979

*Only approved planned and ongoing tests are listed.

**WBA-20, WBA-21, WBA-40 are designators for Irradiation Tests which Testing Objectives were presented at the CRBRP Fuel Meeting with NRC, October 13 and 14, 1976 in Bethesda, Maryland.

TABLE Q241.74-1 (Cont.)

Blanket Development*

51

Area of Technical Uncertainty	Technical Information Required	Required Experiment or Analysis	Utilization of Results
51 6. Blanket Assembly Thermal Behavior 51 51	Performance of CRBRP Radial and Inner Blanket Assembly Wire Wrap	Wire Wrap Analysis with WRAPUP	Final Design
	Power-to-Melt	Experimental Data for Limiting Power-to-Melt During Blanket Rod Lifetime, WBA-46 Experiment will supply data.	FSAR Submittal
	Hot Channel Uncertainty Factors	Update Hot Channel Factors and substantiate	Input to T&H Design Final Design Verification
	Assembly Temperature Distribution	Develop Rigorous Steady State and Transient Subchannel Analysis Codes; Experimental Determination of Coolant Temperature Through Prototype Blanket Heat Transfer Test	Input to T&H Design Input to T&H Design Input to T&H Design
	Rod Temperature Profile	Develop Method of Calculating 3-D Rod Temperature Profile and verify	Input to T&H Design
	Assemblies Orificing	Develop Criteria and Methodology for Orificing Core Assemblies (OCTOPUS Code) Flow Orificing Test	Input to T&H Design Complete Final Design Verification
	Materials Properties and Behavior	Characterize Thermal Properties of Materials; Perform Irradiation Tests Analytical Modeling of Fuel Behavior (Fuel Rod Performance Code Development)	Input to T&H Design Final Design Verification Input to T&H Design

Q241.74-6

Amend. 51
Sept. 1979

*Only approved planned and ongoing tests are listed.

51

*WBA-20, WBA-21, WBA-40, WBA-41, WBA-45/46 are designators for Irradiation Tests which Testing Objectives were presented at the CRBRP Fuel Meeting with NRC, October 13 and 14, 1976 in Bethesda, Maryland.

TABLE Q241.74-1 (Cont.)

Blanket Development*

51

Area of Technical Uncertainty	Technical Information Required	Required Experiment or Analysis	Utilization of Results
7. Assembly Hydraulic Behavior	3-D Duct Temperature Profile	Development of Analytical Code (TRITON) to Calculate Duct Temps. in CRBR Core Including Inter-Assembly Heat Transfer	Final Design Review
	Core Natural Circulation Capability Verification	Blanket inter-assembly Heat Transfer Testing Blanket low flow Heat Transfer and ΔP Testing	Design Verification
	Rod T&H Performance Code	Continue Development of Analytical Code for Blanket Rod T&H Design and Performance Under Steady State and Transient Conditions	Input to T&H Design
	Blanket Assembly and Rod T&H Design and Performance	Perform T&H Design and Performance Evaluation of CRBRP Blanket Assemblies	Final Design Review
	Pressure Drops through the Following Components: A. Inlet Nozzle B. Trimming Orifice C. Shield D. Rod Bundle E. Outlet Nozzle	Blanket Assembly Flow and Vibration Test in Water Blanket Component Pressure Drop Test	Design Verification Design Verification
	Flow Induced Rod and Assembly Vibrations	Blanket Assembly Flow and Vibration Test	Design Verification
	Core Exit Instrumentation Uncertainties	Assembly Outlet Nozzle Instrumentation Test	Design Verification
	Flow Distributions in Rod Bundles During Transients and Low Flows	CØBRA-IV Loss of Flow Event Transient Analysis Blanket Assembly Heat Transfer Test Whole Core T&H Code Development Flow Distribution in Rod Air Flow Testing	Transient Analysis Transient Analysis Design Verification Design Verification

Q241.74-7

51

Amend. 51
Sept. 1979

51

*Only approved planned and ongoing tests are listed.

51 | **WBA-20, WBA-21, WBA-40, WBA-41, WBA-45/46 are designators for Irradiation Tests which Testing Objectives were presented at the CRBRP Fuel Meeting with NRC, October 13 and 14, 1976 in Bethesda, Maryland.

TABLE Q241.74-1 (Cont.)

Blanket Development*

51 |

Area of Technical Uncertainty	Technical Information Required	Required Experiment or Analysis	Utilization of Results
8. Rod Bundle-Duct Interaction		Blanket Assembly Flow and Vibration Test in Water	Transient Analysis
	Rod Bowing and Duct Bowing	Analyses of Rod and Duct Bow Verification with WBA-40, WBA-41	Design Verification CRBRP Operation
	Duct Dilatation Due to Irradiation Effects	Analyses of Duct Dilatation Verification with WBA-40, WBA-41	Design Verification CRBRP Operation
	Rod-to-Rod Forces Caused by Bundle-Duct Differential Growth	Rod Bundle Compaction Test Analyses of Rod Bundle-Duct Interaction Forces	Final Design Review Complete
		Verification with WBA-40, WBA-41	CRBRP Operation

Q241.74-8

51 |

51 |

51 |

51 |

Amend. 51
Sept. 1979

*Only approved planned and ongoing tests are listed.

51 |

**WBA-20, WBA-21, WBA-40, WBA-41, WBA-45/46 are designators for Irradiation Tests which Testing Objectives were presented at the CRBRP Fuel Meeting with NRC, October 13 and 14, 1976 in Bethesda, Maryland.

Question 241.75 (4.2.1.1)

- a) The extent of a cesium reaction with the axial blanket in the CRBRP fuel rods should be discussed in quantitative terms; i.e. provide a quantitative estimate of the extent of the reaction along with the applicable data base and estimate of uncertainty in the data.
- b) Describe the planned irradiation tests in prototypic FFTF irradiations which will provide additional information on cesium migration and associated cladding reaction and interaction effects.

Response:

The response to this question is provided in amended PSAR Section 4.2.1.1.3.7, 4.2.1.1.3.8 and 4.2.1.3.1.1.

Question 241.76 (4.2.1.1)

The current discussion in the PSAR of the development of a limit to sodium exposure by failed fuel is vague. Please provide a more detailed description of the program which will result in "the development of appropriate technology which will assure the benign nature of operation with limited fuel-sodium contact." Include scope and schedule in your discussion of the program.

The applicant should make a commitment to remove all defected rods having sodium contact at each refueling until sufficient data are available to show that such fuel can be operated with predictable and safe results. Outline the proposed run-beyond-failure irradiation testing fuel program to be conducted in EBR-II. When would the results of these tests be available?

Response:

Section 4.2.1.1.3.8, presents a summary of the state of the art for operation of failed fuel in contact with sodium. It identifies the lack of sufficient data to predict local swelling under non-uniform reaction conditions as the major difficulty from the standpoint of steady-state operation with breached cladding. Task C - Run Beyond-Cladding-Breach (RBCB) of the Reference Fuel Steady State Irradiation Program Plan (Reference Q241.76-1) is intended to provide this data as well as assure the benign nature of operation with limited fuel-sodium contact.

A brief description of the RBCB task may be found in Section 4.2.1.3.1.3 of the PSAR and a more detailed description is given in Reference Q241.76-1. The EBR-II phase of the program will provide: 1) reactor operational experience with breached fuel rods, 2) confirmation of the capability of reactor instrumentation to monitor fuel and fission product release from a breached fuel rod, 3) verification of the capability to detect a new cladding breach with a previously breached fuel rod residing in the core, 4) data on the growth of the cladding fissure after breach, 5) information on the potential for fuel washout, and 6) the effect of failed fuel rods on neighboring fuel rods.

Subassemblies for the RBCB test include P-23A, P-23B, P-23C, P-13, and P-14. Naturally occurring failures are anticipated for these assemblies and the failures are expected to occur at high burnups (in excess of 80,000 MWD/MTM). Irradiation of some of the rods will continue beyond Na-fuel contact as indicated by continuous delayed neutron signals up to EBR-II operational limits. It is anticipated that initial irradiation testing of the run-beyond-cladding breach subassemblies in EBR-II will be completed by late 1978. This will allow time to complete the postirradiation examination, analyze the test results and prepare a Topical report for submittal to NRC about the same time as FSAR submittal.

| 31

Q241.76-1

Amend. 31
Nov. 1976

The applicant has committed to remove all known defected fuel rods having fuel-sodium contact at each refueling until sufficient data are available to show that such fuel can be operated with predictable and safe results. This commitment is contained in Section 4.2.1.1.4 revised as a result of the applicant's response to Q241.79.

The RBCB program is scheduled to continue in the FFTF once FFTF operation is initiated. The scope and schedule are given in Reference Q241.76-1. Final confirmation of the benign nature of operation with limited fuel-sodium contact is expected to come from the EBR-II phase of the Task. As a fallback position, data from the FFTF phase of the Task or a combination of the EBR-II phase and limited surveillance type CRBRP operation as given in answer to Question 241.78, will be utilized.

131

All known defected fuel rods having fuel-sodium contact will be removed at each refueling until sufficient data are available to show that such fuel can be operated with predictable and safe results.

REFERENCE

Q241.76-1, TC-573, Revision 1, "Reference Fuel Steady State Irradiation Program Plan, Revision 1", March, 1976.

Q241.76-2

Amend. 31
Nov. 1976

Question 241.77 (4.2.1.1)

Please present a detailed explanation of the statement that "... fuel assemblies charged into the initial reactor loading should be well characterized and identified relative to fabrication attributes." In particular, define the term "well characterized" and specify the fabrication "attributes" alluded to on CRBRP page 4.2-24.

Response:

The response to this question is contained in revised PSAR Section 4.2.1.1.4.1.

Question 241.78 (4.2.1.1)

Please explain the selection of the proposed surveillance schedule (on page 4.2-25 of the PSAR). The statement that "surveillance assemblies which are run to failure may be left in reactor after the initial demonstration phase of the operation" also requires additional clarification and justification.

Response:

The response to this question is located in amended PSAR Sections 4.2.1.1.4, 4.2.1.1.4.1 and 4.2.1.1.4.3.

Q241.78-1

Amend. 29
Oct. 1976

Question 241.79 (4.2.1.1)

A strong surveillance program is essential for CRBR and will be required. The extent of the surveillance will be established during the FSAR review and will depend, in part, on the availability of useful results from EBR-II and FFTF. The lack of such adequate results could necessitate special reactor shutdowns or fuel handling activities to provide the verification that is needed.

Response:

The response to this question is located in amended PSAR Section 4.2.1.1.4, 4.2.1.1.4.1, and 4.2.1.1.4.3.

Question 241.80 (4.2.1.1)

Please list the hydraulic and gravity forces and the net hold force acting to keep the fuel assembly seated in the receptacle. Discuss in more detail how the hydraulic holddown is to be sustained even if the fuel assembly is lifted to contact the upper internals structure.

Response:

The requested information is provided in amended Section 4.2.1.2.1

Question 241.81 (4.2.1.2)

Describe the stress analyses and/or tests which have been performed which support the assertion that the load pads are capable of (1) transmitting the radial core restraint loads, and (2) restraining an assembly from irradiation and thermally induced twist and bow. (3) What are the magnitudes of the stresses associated with these phenomena and with local pressure pulses, from which the hexagonal ducts are said to be capable of absorbing damage?

Response:

The response to this question is divided into three parts. The first of these consists of minor changes to PSAR Section 4.2.1.2.1. The purposes of these changes are to improve clarity of the text and to delete any reference to irradiation and thermally induced twist of core assembly duct structures since the current refined analysis status does not indicate existence of this kind of loading condition. The latter two are discussed in the following paragraphs.

Minor torsional duct loads could originate from manufacturing tolerances. Recent calculations show a maximum expected shear stress due to this loading condition of about 2200 PSI. This stress is combined, using a MOHR'S circle approach, with operational and seismic stresses several times greater in magnitude. Consequently, the effect of duct twisting stresses upon the overall net design margin is negligible. Deletion of the reference in the PSAR to irradiation and thermally induced bow is justified, since that effect is reflected in the magnitude of radial core restraint loads.

A comprehensive structural analysis of the worst loaded core duct was recently completed. The analysis focused on the above core load pad which preliminary screening work showed to be most severely stressed. The analysis considered two loading cases. The first of these combined operational core restraint loads with seismic loads and produces the lowest margins of safety in an evaluation of primary stresses. The second loading case combined operational core restraint loads with thermal steady-state and transient loading condition. That load combination provides a check against long-term evaluation criteria such as the combined effects of creep and fatigue damage. The latter analysis does not consider irradiation creep effects, since the end-of-life fluence level at the area considered is low ($\sim 1.3 \times 10^{22}$ n/cm², E>0.1Mev). However, irradiation effects upon material properties were considered as appropriate. Table 241.82-1 provides a summary of the analysis results. It shows a minimum margin of safety of 0.31.

These results were derived from a three dimensional finite element model of the above core load pad. The model uses the ANSYS finite element computer program.

The computer model is optimized for mechanical loading conditions and allows a practically arbitrary lateral and axial load distribution at or about the ACLP region. However, to achieve this load versatility, numerous finite elements were required. As a consequence, the computer time required per run is considerable. Therefore, the model has been used under elastic conditions of analysis only and the stresses predicted do not reflect possible stress reductions due to local yielding. However, an elastic/plastic analysis is not expected to result in a significant reduction of critical stresses.

Time-dependent effects, i.e., creep damage, were assessed by applying a conservative relaxation procedure, (same as used in comparable FFTF analyses) to the elastically calculated stresses.

Amend. 31
Nov. 1976

No detailed structural analysis has been conducted on the effect upon the hexagonal duct by local pressure pulses from escaping fission gas. However, an assesment of that loading situation is presented in the response to another PSAR Question, Reference PSAR Q241.96.

The foregoing information is interim in nature. Existing applicable PSAR information will be updated as appropriate.

Table 241.81-1
 REVIEW OF MINIMUM MARGINS OF SAFETY AND DAMAGE FACTORS
 FOR CORE ASSEMBLY DUCT STRUCTURE

Nature of Governing Loading Condition	Critical Load Combinations and Evaluation Objectives	Environment Temp. (°F)	Fluence (n/cm ²) (EOL) E > .1 MEV	Stress Category	Condition of Evaluation Criteria	Structural Area Considered	Max. Equip. Stress (PSI) or Strain (in/in)*	Allowable Stress (PSI) or Strain (in/in) Ref. Table T5-3	Margin of Safety or EOL Damage Factor		
Seismic	Seismic and Core Restraint Under Primary BOL Stress Limits, Ref.	935	N/A	(P _L +P _b)	Normal/Upset	Worst Duct Corner at ACLP	OBE	31882	54500	.71	
					Failed		SSE	45563	63200	.38	
	Seismic and Core Restraint Under Primary EOL Stress Limits, Ref.	980	1.3x10 ²²	(P _L +P _b)	Normal/Upset	Worst Duct Corner at ACLP	OBE	31882	62000	.31	
					Failed		SSE	45563	60000	.32	
	Seismic and Core Restraint Under EOL Strain Limits Ref.	980	1.3x10 ²²	N/A	Normal/Upset	Worst Duct Corner at ACLP	OBE	.00172	SBR = 0.0:1	.0175	9.1
					Failed		SSE	.00227	SBR = 0.0:1	.0175	6.7
Operational Steady State	Core Restraint Plus Thermal Steady-State Under BOL Secondary Stress Limits	935	N/A	(P _L +P _b +Q)	Normal/Upset	Any Duct Corner at ACLP Region Under Worst Combination of Stresses.		27220	109000	3.00	
	Core Restraint Plus Thermal Steady-State Under EOL Stress Limits	980	1.3x10 ²²	(P _L +P _b +Q)	Normal/Upset			19410	60000	2.09	
	Core Restraint Plus Thermal Steady-State Under Stress Rupture Limits	980	1.3x10 ²²	(P _L +P _b +Q)	Creep Damage (Stress Rupture)			28700	Ref. Fig. F6-15	.502 .70(Est)**	
Thermal Transients	Core Restraint Plus Thermal Steady-State Plus Thermal Transient Under EOL Strain Limits	980	1.3x10 ²²	N/A	Normal/Upset	Any Inside Duct Corner at ACLP Region		.00130	.0125	8.6	
	Thermal Transients Fatigue Damage Evaluation Ref.	1200 Max. 900 Min. Ref. Table T6-7, T6-8	1.3x10 ²²	(P _L +P _b +Q+F)	Fatigue Damage			.00143**	.0070**	3.9**	
								<.001 (range)	Based on Total EOL Cycles 121	<.10	
							<.001 (range)**	61**	<.10**		
Stress Rupture	EOL Cumulative Creep/Fatigue Damage Factor	--	1.3x10 ²²	N/A	Cumulative Damage Function		--	--	0.51		
							--	--	.60(Est)**		

BOL = Begin-of-Life
 EOL = End-of-life
 SBR = Stress Biaxiality Ratio
 P_L - Primary general plus local membrane stress
 P_b - Primary bending stress
 Q - Secondary stress
 F - Peak stress

* = Greater of Von Mises or Maximum Pos. Principal Strain
 ** = Applies for Worst Fuel Assembly

241.81-3

Amend. 31
 Nov. 1976

Question 241.82 (4.2.1.2)

The mating surfaces of the inlet nozzle are said to be chrome plated (and the load pads on the duct and outlet nozzle are chrome-plated) "to minimize the potential for damage, galling, and wear". Please describe the tests which have been performed on these components to demonstrate their resistance to damage, galling, and wear.

Response

The information requested is provided in revised PSAR Section 4.2.1.2.1.

Question 241.83 (4.2.1.3)

Please provide more detail on the analysis and modeling of pellet-cladding mechanical interaction (PCMI). Specifically, which codes are used to analyze what aspects of this phenomenon? Please provide a topical report on this subject. The report should include a description of (1) the phenomena associated with PCMI, (2) the codes used to analyze and model it, (3) the physical and mechanical properties used as input to the codes, (4) the results of the analyses, and (5) tests used to verify the code results. Descriptions of any planned tests on PCMI should also be provided.

Response:

Pellet-Cladding Mechanical Interaction (PCMI) is addressed in the user's manual for the LIFE III provided in response to Item #1 of PSAR question/response section "Responses to 10/6/75 letter." The manual addresses the analysis code and the mechanical properties input to the code. PCMI analyses will be reported in the FSAR. Tests to determine the effects of PCMI are described in the Reference Fuel Steady-State Irradiation Program Plan and in the plan for the National LMFBR Mixed Oxide Fuel Transient Performance Program, TC-705, Rev. 1 previously submitted to NRC.

Q241.83-1

Amend. 71
Sept. 1982

Question 241.84 (4.2.1.3)

- A. Please show some examples where using upper material property design limits is conservative (as indicated on PSAR page 4.2-38).
- B. In the discussion of fuel rod steady state analyses, please provide a description of test results which support the contention that "steady state operation to 411 full power days can be achieved within the constraints of the design requirements for steady state cladding damage."
- C. Are "design requirements" intended to mean "design limits" here?
- D. Please list the specific "design requirements" or "design limits" for this section and show how the test results indicate that they will not be exceeded.

Response:

- A. The conservatism of using upper material property design limits is discussed in revised PSAR Section 4.2.1.3.1.1.
- B. Revised Table 4.2-B in the PSAR demonstrates how EBR-II experiments support the fuel rod lifetime of 411 full power days. As noted in Section 4.2.1.1, 411 full power days corresponds to 80,000 MWD/T peak burnup.
- C. Yes.
- D. The design requirements and limits for the fuel rods are presented in Section 4.2.1.1.2.2 of the PSAR. These requirements and limits are evaluated by utilizing analytical models. The requirements, limits and models are evaluated against test results to verify their adequacy as described in Section 4.2.1.1. Section 4.2.1.3 provides the evaluation of the CRBRP fuel rod design using these requirements, limits and models.

Question 241.85 (4.2.1.3 and 4.2.2.1)

Certain test data make the bases for fuel rod failure criteria and design limits unclear. Examples are given below:

- (A) With respect to steady state limits (e.g., 0.2% strain) stress-rupture tests on irradiated cold worked cladding, at low fluences, show failures near or below the 0.2% strain limit (see HEDL-TME-75-4, V.1, p. A-22). In addition, HEDL-TME-75-48, p. VD-3 ff shows fuel rod diametral change data with 0.2% $\Delta D/D$ at very low burnups and fluence.
- (B) Regarding transient limits (0.1% additional strain) FCTT tests (HEDL-TME-75-28) show failure strains as low as 0.03% $\Delta D/D$ at $\phi(t) < 1 \times 10^{22}$, and further analysis (BNWL-2041) indicates a zero $\Delta D/D$ 95% confidence limit (in plot of $\Delta D/D$ versus midwall irradiation temperature).
- (C) In regard to the 1450^oF (upset) and 1600^oF (emergency) cladding temperature limits (associated with PPS trip settings), FCTT tests (HEDL-TME-75-28) indicate that most fuel failures occur below these temperatures. TREAT tests (GE, ANL, R&E series) on irradiated rods also show failures occurring well below these values.
- (D) With respect to the CDF limit (≤ 1.0), residual strength, values obtained from FCTT data fall below those utilized in evaluating the CDF approach as an analysis method which can ensure rod integrity. For example, a CDF of 0.725 to 0.864 is quoted in the CRBRP PSAR (Table 15-1.2-5) whereas a 95% confidence limit of 0.3 to 0.5 was obtained in FCTT tests in which 10^oF/Sec heating rate was used (See plot of percent of unirradiated load bearing capability versus mid-wall irradiation temperature for fueled specimens (Fig. 3 BNL-2041)).

The above data examples, used in the comparisons with design limits, may also not reflect worst case values since they represent (1) irradiations at less than goal CRBRP burnup (80,000 MWD/T), (2) less severe cladding fluence to burnup ratio than planned for CRBR, and (3) potentially less severe fuel/cladding chemical attack (PCCI), due to the burning of U²³⁵ in EBR-II, as compared to Pu²³⁹ in CRBR.

In view of the above findings, which appear to provide reason to challenge the CRBRP fuel design limits and failure criteria, please restate the bases for these limits and criteria. Respond to the above comparisons and challenges point-by-point in your discussion. Provide further substantiation for the presently proposed PPS system set points and emergency conditions. Please distinguish between design "limits" and design "guidelines" and provide explanations of the choices of term and its use for each specific case in which it is applied. List the relevant experimental data, models and codes with which one can assess (1) the adequacy of the value used for design "limit" and "guideline" as well as (2) the adequacy of the arguments used to justify the choice of terminology.

Q241.85-1

Amend. 30
Nov. 1976

Response:

Point-by-point responses to the specific items presented by NRC and Reference Q241.85-1 are given below. However, prior to considering these detailed phases of the response, the general issues given above will be discussed.

First, it is recognized that the currently available data base does not encompass the entire range of CRBRP parameters with respect to burn-up, fluence, etc. However, the design limits and criteria will be periodically evaluated and updated as more relevant data become available (e.g., see the response to Question 241.134). These data will derive from numerous sources, viz., (a) the Reference Fuel Steady State Irradiation Program, (b) the Transient Testing Program, and (c) various elements of the Reference Cladding and Duct Program; these programs are described in the responses to Questions 241.15, 001.284 and 241.56, respectively.

Next, the current codes that might be used for various phases of the assessment of the CRBRP limits include: FORE-II, FRST, FURFAN and LIFE. These codes are described in PSAR Appendix A.

Finally, with respect to the terminology "design limit" and "design guideline", the following definitions are offered:

- (a) Design Limit - a value of some parameter which cannot be exceeded during the design lifetime of the component, on the basis of prior agreement or physical impossibility.
- (b) Design Guideline - a policy, rule or practice to be followed as a matter of course when a component is being designed or when its potential operating conditions are being considered; this policy, rule or practice is voidable so long as the restrictions set forth by any relevant design limit are upheld.

I. Temperature Limits (see Item C and Question 241.71)

With respect to cladding temperature, it should be recognized that the "1450⁰F (upset) and 1600⁰F (emergency)" temperatures referred to in this question and in Reference 241.85-1 are not limits. CRBRP does not employ single valued temperature limits for the fuel pin. Rather, the design procedures are such that the cladding temperature limits for an emergency event are time dependent functions of (a) the prevailing steady state conditions, (b) the fuel pin's prior history, and (c) the nature of the emergency event itself. This is the underlying concept of the Transient Limit Curve (TLC) which is discussed in considerable detail in PSAR pages 15.1-59 to 15.1-61 and in Reference Q241.85-2.

The source of the misconception regarding the 1450⁰F and 1600⁰F values may well derive from PSAR Figures 4.2-19 and 4.2-20 which define the umbrella conditions for the analysis of upset and emergency events, respectively.

In simulating these events, the temperature changes shown by these curves (rather than the absolute values of temperature) are applied to the prevailing steady state clad temperature; this aspect of the simulation is discussed on PSAR page 4.2-42 and is graphically illustrated in PSAR Figure 4.2-21. Since the steady state temperature decreases with time, the peak transient temperatures will follow accordingly. On this basis, if the quoted 1450^oF and 1600^oF temperatures were ever achieved by a fuel pin, it would be only at start of life.

Figure 4.2-21 (as well as Figure 4.2-22) also illustrates the time dependence of the temperature limit as defined by the TLC. As shown, the TLC yields a limit which decreases with time, reflecting the effects of the fuel pin's prior history and the prevailing steady state condition. Importantly, the TLC's shown are applicable only for the fuel-pin and axial location in question; as stated in response to NRC question 241.92. TLC's for other fuel-pins and at other axial locations will be provided.

In addition to the erroneous interpretation of the CRBRP temperature limits, the Reference Q241.85-1 interpretation of the FCTT data is inaccurate; specifically, Reference Q241.85-1 ignores stress as a parameter in these rupture tests. Indeed, when the stress levels of the tests are considered, the results show the ability of the CRBRP fuel pin to withstand undercooling emergency events.

The FCTT failures referred to in Reference Q241.85-1 were achieved at temperature-stress combinations that are well beyond those expected in the CRBRP fuel-pins, even at design lifetime (i.e., 411 Effective Full Power Days, EFPD). To illustrate this point, a conservative estimate of the tangential stress at 411 EFPD, as derived from gas pressure during a transient, is compared to the FCTT data in Figure Q241.85-1; these data are from Reference Q241.85-3. The line showing the CRBRP condition was computed assuming an initial (steady state) plenum temperature of 1200^oF and a pressure of 1000 psi. The pressure, and hence the stress, was taken to increase with plenum temperature, as might be the case during an undercooling event. As shown in Figure Q241.85-1, at comparable temperatures, the anticipated CRBRP condition is well below the FCTT failure condition. This figure also shows that for cladding stress below 20 ksi, failure temperatures much higher than 1600^oF have been recorded.

II. Residual Strength as Defined by the CDF Procedure (see Item D)

The procedures for computing the residual strength of the cladding have been discussed in considerable detail in PSAR Section 15.1 and in Reference Q241.85-2. However, two salient features of the procedure should be emphasized.

First, for design computations, the relative strength factors are applied to the irradiated tensile strength at its lower 99% confidence band; thus, the irradiated tensile strength is assumed to prevail even at start of life.

Secondly, the relative residual strength at any time is defined by the product of two independent factors, viz., R_1 which defines the effect of interstitial loss and R_2 which defines the effect of the accrued CDF. Both R_1 and R_2 are functions of time, depending on the prior operating history; for example, for operation at $\sim 1200^\circ\text{F}$, R_1 rapidly equilibrates at ~ 0.7 . Furthermore, the product $R = R_1 R_2$ will often vary from ~ 0.7 to ~ 0.4 during the major period of operation, ultimately tending toward zero as the steady state failure point is approached, e.g., see Section VI, in Reference Q241.85-2.

With these key features in mind, the merit of the Reference Q241.85-1 conclusions can now be evaluated. First, Reference Q241.85-1 computes the FCTT residual strengths of irradiated material on the basis of unirradiated properties. Clearly, this is inconsistent with the CDF procedure which utilizes, as its base, the irradiated properties at their lower levels of uncertainty.

Next, Reference Q241.85-1 uses as its basis for conclusion, totally unrelated values for residual strength, i.e., "0.735 to 0.864" from Table 15.1.2-5*. This table defines the parameters used in the Section 15.5 validation study of the CDF. Specifically, the 0.864 value was the nominal relative residual strength (R_1) of unirradiated material held at 37.5 ksi and at 1200°F for 40 hours; the 0.735 value was for material held at these conditions for 80 hours. Beyond this special application, these values have no meaning and they certainly are not universal.

Assuming for a moment that the above relative strength values are more general than they actually are, it is instructive to follow the Reference Q241.85-1 logic to its rightful conclusion. As explained above, the Table 15.1.2-5 values were for unirradiated material subjected only to prior creep. On the other hand, the relative strengths from the FCTT test as computed in Reference Q241.85-1, result from not only prior creep but also from irradiation. Thus, the Reference Q241.85-1 is predicated on a comparison of the effects of prior creep alone to the combined effects of prior creep and irradiation. Obviously, such a comparison has no merit.

The FCTT data reported in Reference Q241.85-3 are with cladding specimens which had been sectioned from fuel pins irradiated in EBR-II, viz., fuel pins from NUMEC F, PNL-10 and PNL-11. These data show a significant difference in the behavior between those sections adjacent to fuel and those from above or below to fuel column; specifically, the fuel-adjacent sections exhibit a marked reduction in FCTT strength.

*Table 15.1.2-5 has since been deleted from the PSAR by Amendment 2.

Although the cause of the fuel-adjacency effect is as yet not clearly understood, one potential cause is that the fuel-adjacent sections had accrued a substantial CDF during their irradiation period; furthermore, they may also have suffered a loss of interstitial elements, although this has not yet been detected. On the basis of this hypothesis, it would follow that the fuel-adjacent sections entered the FCTT test with $R_{\sigma} R_I < 1$.

The actual values for R_{σ} and R_I for the FCTT specimens are unknown. However, it is noteworthy that the CRBRP procedures regarding the relative strength can adequately explain the data by utilizing reasonable values for the project $R_{\sigma} R_I$; this is illustrated in Figure Q241.85-2.

The first curve in Figure Q241.85-2 defines the design level (i.e., lower 99% confidence) strength taken to exist at start of life (i.e., $R = R_{\sigma} R_I = 1.0$). As shown, this curve encompasses (or would have limited) $\sim 77\%$ of the failures, including all the non-adjacent sections. As the relative strength decreases ($R = 0.9, 0.5$ and 0.3) the strength curves collapse through the remainder of the data so that when $R = 0.5$, 94% of the data are explained.

As mentioned earlier, a relative strength of 0.5 (computed at the design level) is not unusual; this corresponds to a steady state design level CDF of ~ 0.7 . Thus, the residual strengths (relative to the design level properties) inferred from the FCTT data are not unreasonable and are certainly within the realm of calculation by current CRBRP procedures.

The above analysis is, of course, qualitative and does not prove the concept of residual strength as employed by the CDF technique. On the other hand, the analysis does show that the concept can indeed explain the observed FCTT results.

III. Strain Limits (see Items A and B)

The procedures related to the CRBRP strain criteria were initially set forth in FCF-213 (Ref. Q241.85-4) and have been adopted by the CRBRP project; this reference prescribes the methods and mechanical properties to be employed by the procedure.

In CRBRP design applications, the fuel pin cladding strain computed according to the FCF-213 methods, must be less than the limiting values (i.e., 0.2% for steady state and 0.1% additional for upset and emergency transients).

There are two salient features of the FCF-213 methodology that should be emphasized. First, the mechanical properties utilized in the procedure are for unirradiated, solution annealed 316, in no way related to those of the actual cladding, e.g., see Tables A.2.1, A.2.2 and A.1.1 in Reference Q241.85-4. Second, the FCF-213 transient limit, although nominally a strain limit, is in fact a stress limit (e.g., see PSAR Section 15.1.2.2, page 15.1-65) and the computed transient strain is only a measure of the proximity to the stress limit. Therefore, the strain values computed via the FCF-213 procedures bear no relationship to actual physical displacements that might be measured experimentally, regardless of the data source.

In view of the above, a comparison of the CRBRP strain limits to experimental deformations is moot. Indeed, the key issue is whether the FCF-213 methodology coupled with the CRBRP limits can preclude failure; this can only be gauged in terms of the computed time (or condition) to achieve the specified limit vs. the actual failure time (or condition).

The steady state aspects of the FCF-213 procedure coupled with the 0.2% strain limit are examined in Figure Q241.85-3. The data in Figure Q241.85-3 are stress-rupture data on irradiated material from Reference Q241.85-5; the curves were computed using the FCF-213 creep rates and define the time at which the 0.2% limit would be achieved. As shown, these limits would have precluded all of the experimental failures. Clearly, with the limits of these data, the results shown in Figure Q241.85-3 confirm the steady state FCF-213 procedure as combined with the 0.2% strain limit.

The applicability of the FCF-213 methods with respect to transient behavior are examined against the FCTT data in Figure Q241.85-4. The curve shown in Figure Q241.85-4 corresponds to the tangential stress in a pressurized tube that would achieve the design limit; nominally 0.1% incremental strain but, in reality, the ultimate strength.

As shown, the FCF-213 limit encompasses (or would have precluded) ~83% of the FCTT failures which is somewhat comparable to the results obtained in the previous section when the relative residual strength was taken to be 1.0, i.e., see Figure Q241.85-2. Interestingly however, the limit curve encompasses 100% of the 200⁰F/sec points including those adjacent to fuel.

Figure 241.85-5 compares the 200⁰F/sec Fuel Cladding Transient Test (FCTT) data to the Fuel Cladding Mechanical Interaction (FCMI) related stresses developed during a rapid reactivity insertion. These stresses were computed in a study simulating a characteristic rapid reactivity insertion with a 0.5 second duration. The stresses shown in the figure are the maximum achieved at each axial location throughout the life of the fuel-pin and correspond to the point in time at which the steady state FCMI is maximum. As shown in Figure 241.85-5, the stress-temperature cladding conditions developed during the rapid reactivity insertion are well below the FCTT failure conditions.

38

Amend. 38
April 1977

References

- Q241.85-1 J.W. Wald and I.S. Levy, "LMFBR Fuel Pin Cladding Transient Performance Capabilities - An analysis of FCTT Data", BNWL-2041.
- Q241.85-2 D. C. Jacobs, "The Development and Application of a Cumulative Mechanical Damage Function for Fuel-Pin Failure Analysis in LMFBR Systems", CRBRP-ARD-0115, May, 1976.
- Q241.85-3 C.W. Hunter, G.D. Johnson and R.L. Fish, "Mechanical Properties During Simulated Overpower Transients of Fast Reactor Cladding Irradiated from 700-1000^oF", HEDL-TME-75-28, June, 1975.
- Q241.85-4 R. Sim and A. Veca, "FFTF Fuel-Pin Final Design Support Document", FCF-213, December, 1971; revised February, 1972.
- Q241.85-5 "HEDL Quarterly Technical Report - April, May, June, 1973", HEDL TME-73-4, Volume 1, August, 1973, page A-22.

Amend. 38
April 1977

Q241.85-6a

7683-212

Q241.85-7

Amend. 30
NOV. 1976

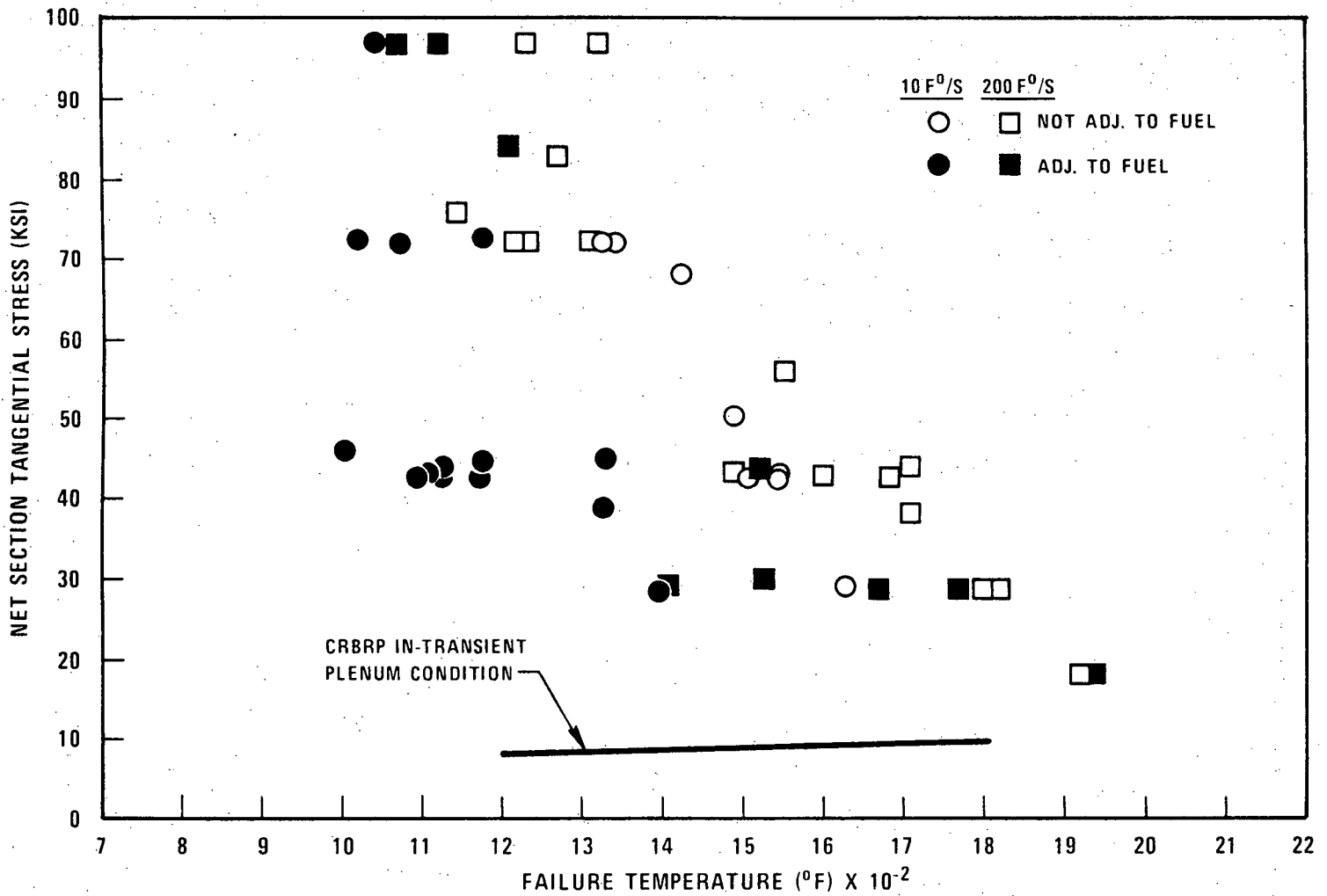


Figure Q241.85-1. FCTT Test Results with Clad Sections from Irradiated Fuel-Pins as Compared to In-Transient Plenum Condition for CRBRP Fuel-Pins

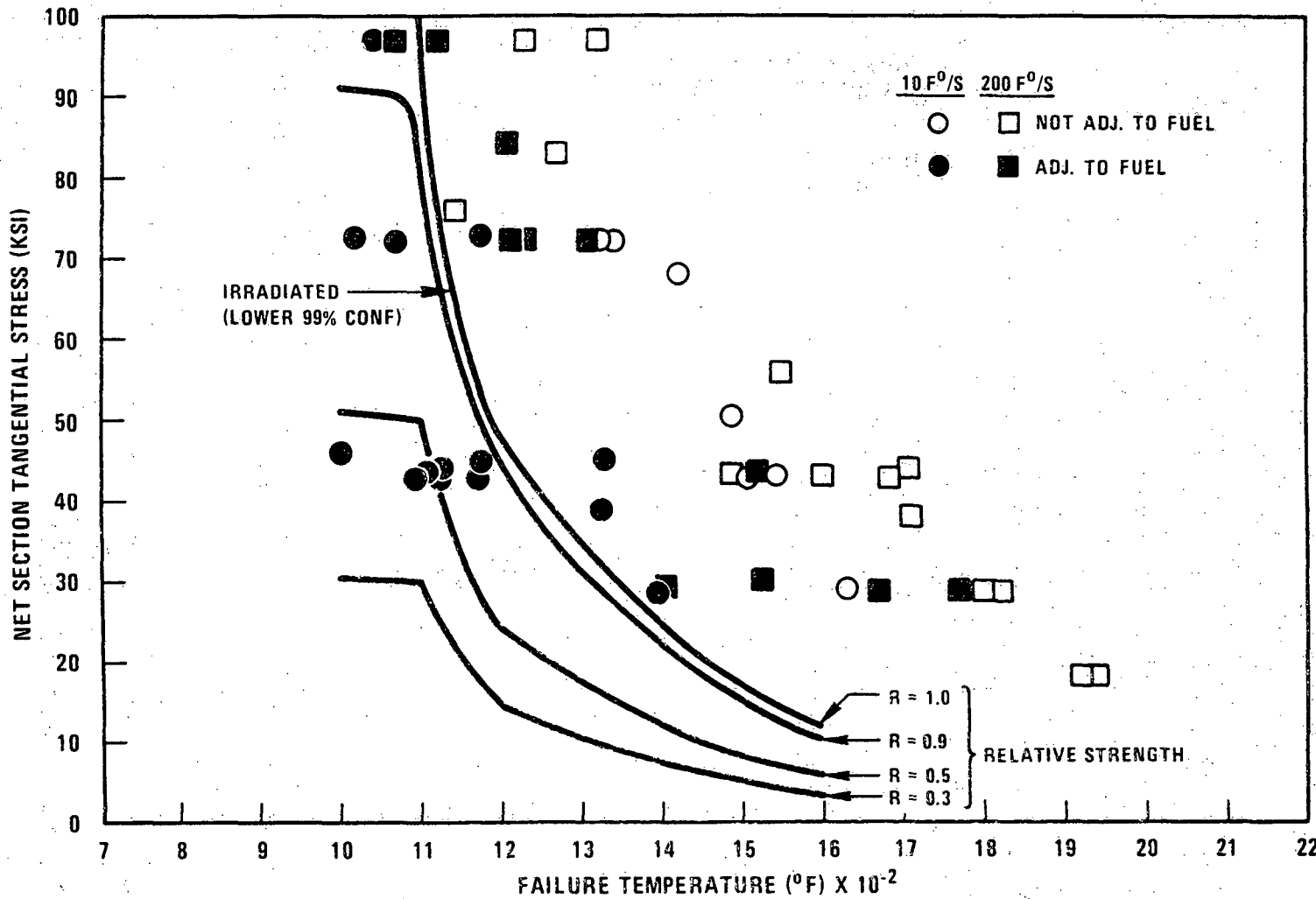


Figure 241.85-2. FCTT Test Results with Clad Sections from Irradiated Fuel-Pins as Compared to CDF (FURFAN) Residual Strength at N-Lot Design Level

7683-214

0241.85-9

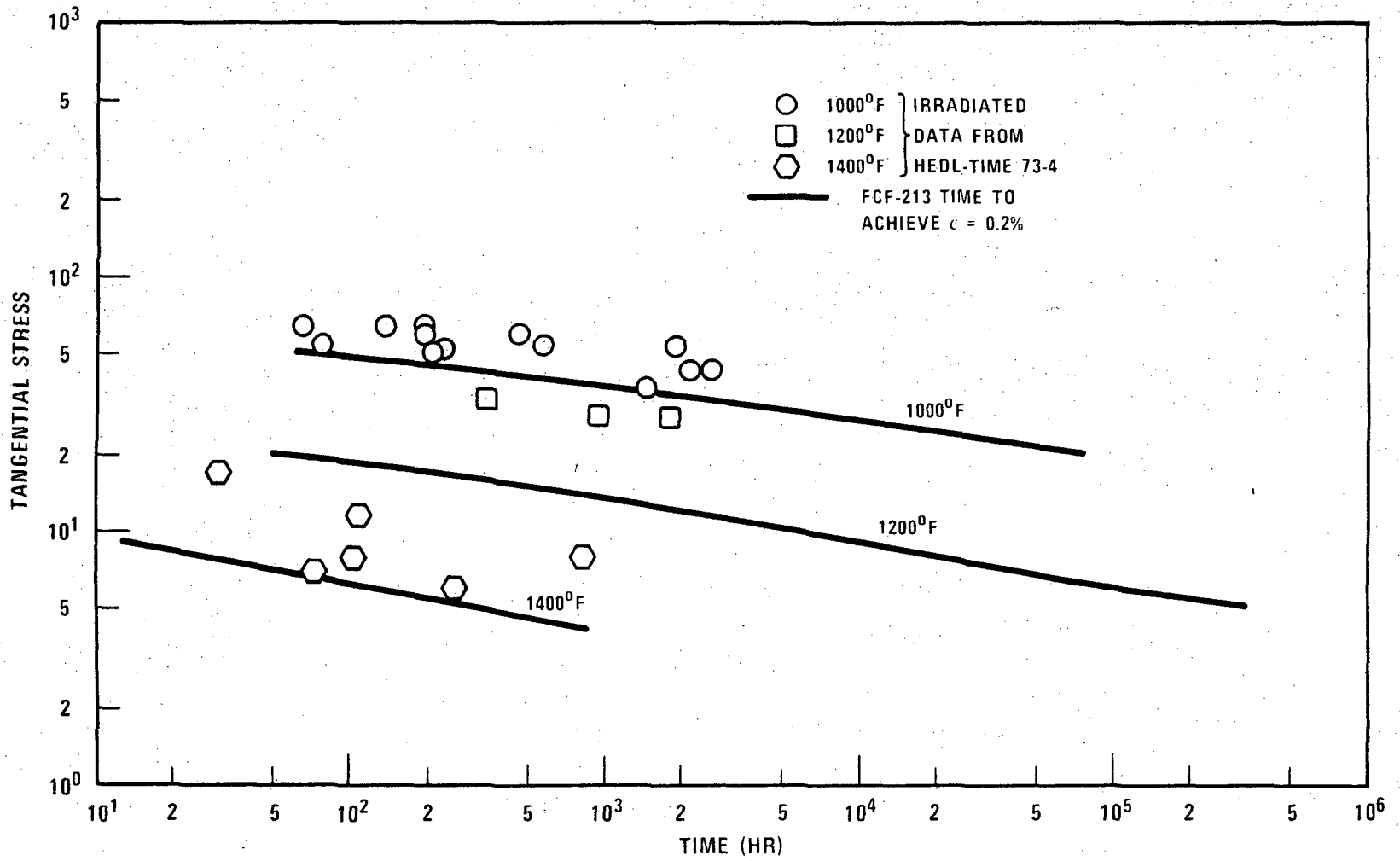


Figure 241.85-3. Comparison of the FCF-213 Steady State Design Limit and Stress Rupture Data

Amend. 30
Nov. 1976

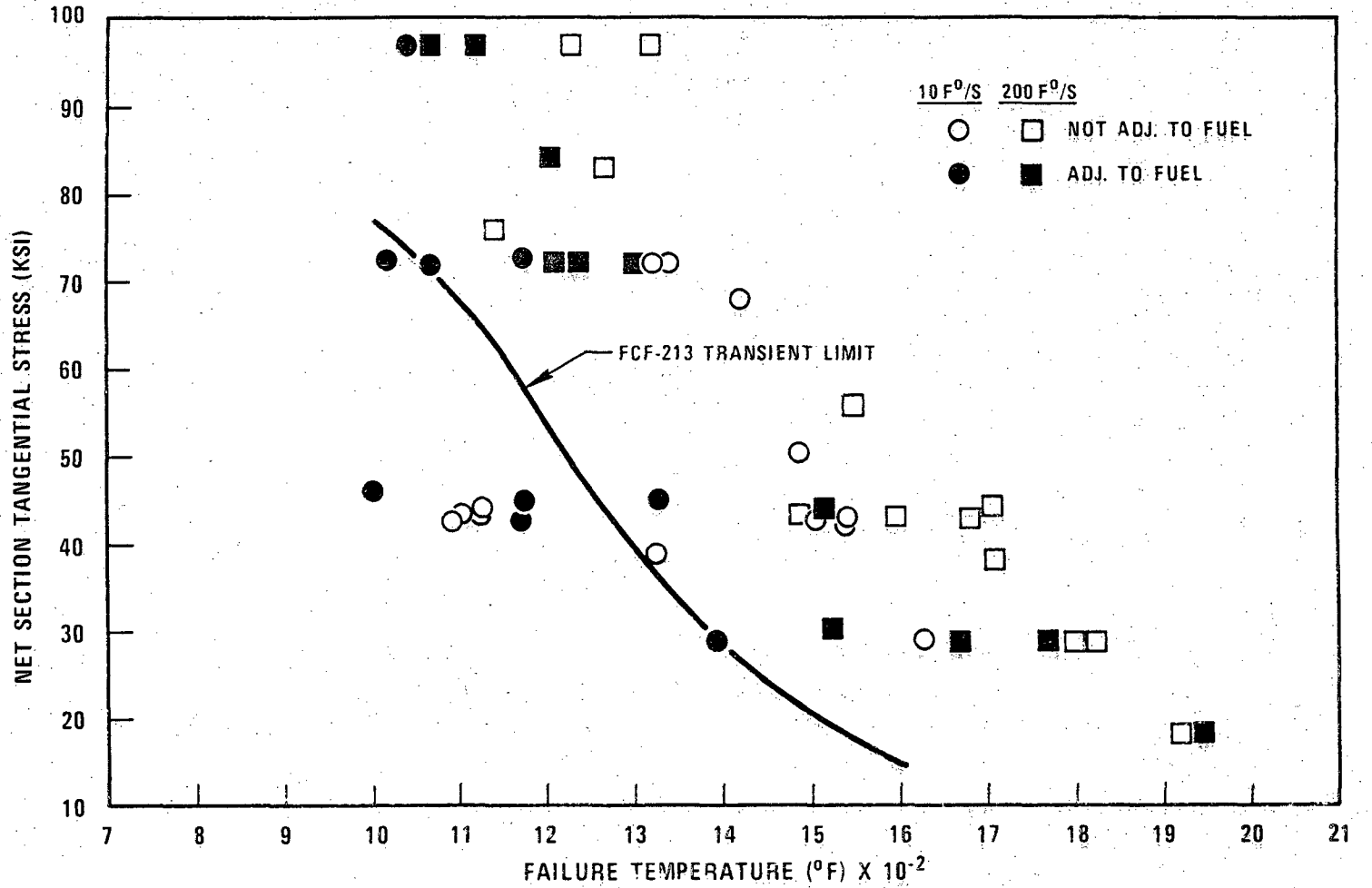
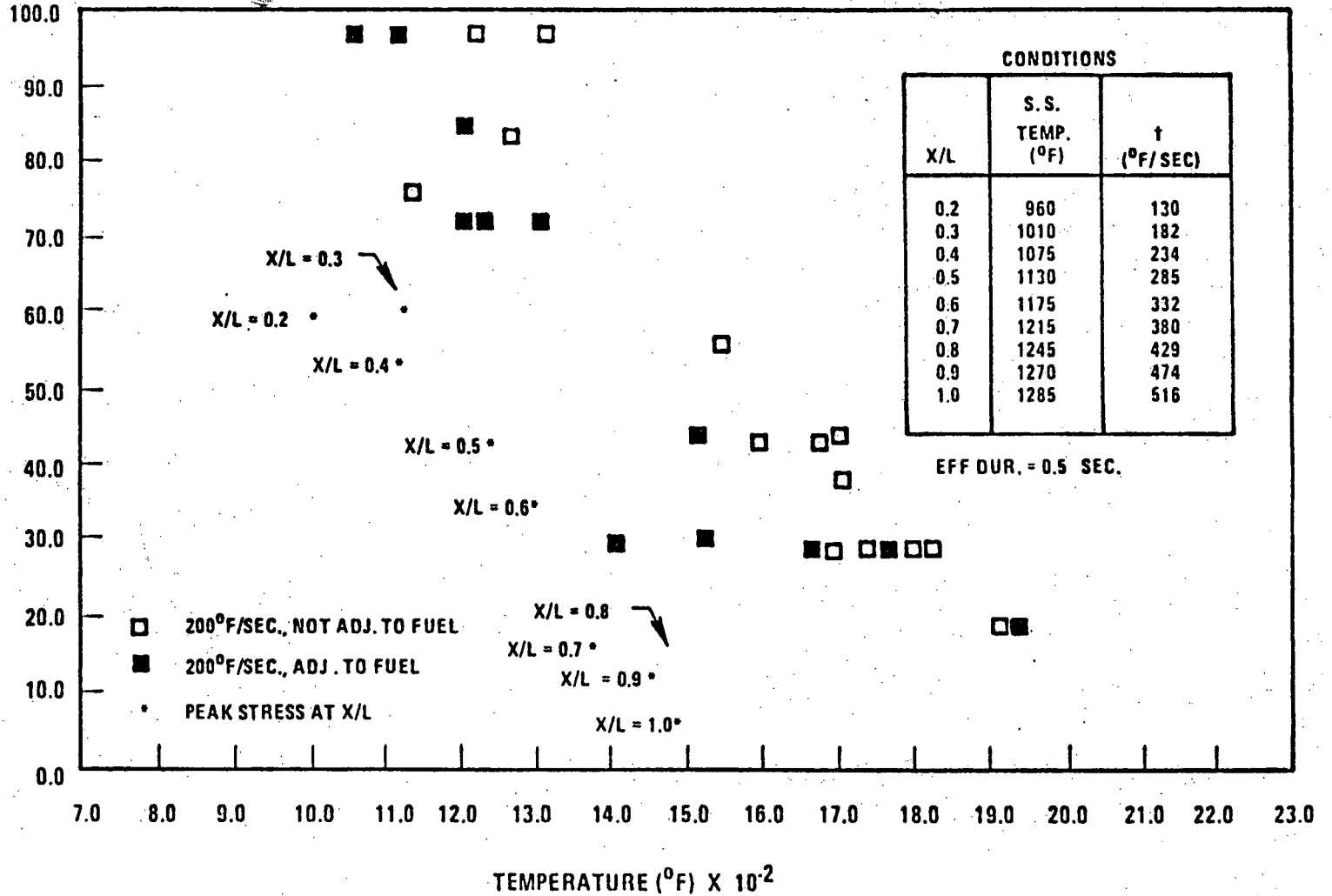


Figure 241.85-4. FCTT Test Results with Clad Sections from Irradiated Fuel-Pins as Compared to the FCF-213 Limit

NET SECTION TANGENTIAL
STRESS (KSI)



Q241.85-11

Amend. 38
April 1977

Figure 241.85-5 Comparison of 200°F/sec FCTT Test Results With CRBRP Conditions During a Characteristic Rapid Reactivity Insertion

Question 241.86 (4.2.1.3 and 4.2.2.1)

The translation, in Amendment 15, of strain limits into predictions of the time required to reach the strain limits (steady-state burnup or transient time of failure) and the applicant's comparison of these predictions with experimental values are of concern for two reasons:

- (1) the predictions use models of rod performance that, in themselves, are the subject of questions as to their validity; for example, while the codes do not predict fuel rod failures under upset and emergency transient conditions to occur at temperatures less than 1600°F, experimental data suggest failures will occur at 1600°F.
- (2) experimental data, though limited, do exist (see previous question) against which the design criteria might be assessed, but there are no design limits in the PSAR as to time to preclude failure, especially not for transients.

Is time to be considered a fuel rod design limit along with strain and temperature? Points 1 and 2 above, should be addressed as part of the explanation provided in response to this question. If time is to be considered a design limit or design "guideline", please provide the relevant experimental data, models and codes with which to judge the adequacy of the values chosen.

Response:

Time is not an independent fuel rod design limit. Time is explicitly included as a parameter in the CDF evaluation of fuel lifetime. Further discussion of design limits, design guidelines, and their relationship to experimental data is given in response to Question 241.85.

Question 241.87 (4.2.1.3)

What fretting results from fuel pin broken wire wraps, and how is it accounted for in the fuel design?

Response:

No additional fretting wear is assumed to occur due to broken wire wraps. Wire rupture is considered highly unlikely based on the conclusions presented in the response to NRC Question 241.106.

Even if wire rupture would occur, it would only result in a loose wire. Fuel rods with loose wires have been operated without obvious additional rod wear, as noted in the response to NRC Question 241.88.

Finally, assuming increased fretting wear did occur due to loose wires, this wear would at worst result in a stochastic pin hole cladding failure. These have no serious safety consequences, as described in PSAR Section 15.4.

Question 241.88 (4.2.1.3)

The section on fuel rod wire wrap interaction includes the statement that "calculations based on varying cold work levels and swelling equation confidence limits indicate that loads present in the wire wrap never cause the design limits to be exceeded during steady state operation." These calculations should be discussed in greater detail than currently presented in the PSAR. In particular, the calculation methods, codes, margins, and values used for cold work levels and swelling equation confidence limits should be described. Discuss how the EBR-II PNL-17 irradiation test results relate to the alleged acceptability of a value of 0.025% maximum wire slackening.

Response:

The information requested is contained in the Topical Report No. 6, WARD-D-0149 "Wire Wrap Cladding Interaction in LMFBR Fuel Rods." This report discusses the calculation methods, codes, margins, cold work values, swelling equation confidence limits, and EBR-II test data used to evaluate the fuel rod wire wrap performance. Briefly, fuel rods in the PNL-17 test assembly experienced wire slackening in excess of 0.025% due to solution annealed 316 SS wire being applied to 20% cold worked 316 SS cladding. Despite this, no increased fretting wear or rod failures due to this wire slackening were observed in this assembly, WARD-D-0149 was provided to NRC in September, 1976.

Question 241.89 (4.2.1.3)

The treatment of fuel rod bowing is inadequate. Results of test programs should be given in specific terms and comparisons instead of generalities such as "based on FFTF analyses, the above mentioned design requirement is expected to be satisfied and no limit on fuel pin performance imposed." The details of these FFTF analyses should be presented and related to CRBR. The details of the analysis and prototypic irradiation tests which are intended to confirm the above conclusion should also be presented.

Response:

The details of the FFTF analysis techniques and the details of the analytical and test results to date, which show no adverse fuel rod bowing effects, are discussed in Appendix A and Section 3.0 of the Topical Report No. 4, WARD-D-0150 "Fuel Rod Bowing". WARD-D-0150 was provided to NRC in November 1976.

| 31

Question 241.90 (4.2.1.3)

With respect to fuel rod vibration and fatigue, why are water flow tests and irradiation tests required to verify that "no problems are expected in these areas" if FFTF water and sodium flow tests already indicated that? Why are the FFTF tests inadequate? Present a schedule for the reporting of the results on the 37 pin assemblies fretting and wear tests.

Response:

The requested discussion is provided in revised PSAR Section 4.2.1.3.1.1. Also, see revised PSAR Section 4.2.1.1.3.4.

Question 241.91 (4.2.1.3)

The discussion of CDF due to steady state operation and the combined upset events show that at the design level for assembly 6 failure would occur at 540 full power days. Using the same type of analysis and assumptions, viz., maximum uncertainty in properties, 2σ plant, etc., as used for the assembly 6 analysis, how many assemblies would be shown to fail before their goal lifetimes for equilibrium operation?

Response:

If the same conservative CRBRP first core material properties, environments, and failure criteria are applied to determine the fuel and blanket rod lifetimes during equilibrium cycle operation with steady state and worst upset transient loads (as simulated by cycle 3-4 conditions), it is found that:

- a) At least 70% of the 156 fuel assemblies achieve the 550 day (2 equilibrium cycle) lifetime goal with a worst rod cladding hot spot CDF less than 1.0. However, only 5% of the rods in a typical fuel assembly bundle experience cladding temperatures similar to those for the worst rod. Furthermore, a cladding CDF equal to one implies a survival probability of at least 80 to 90 percent for equilibrium cycle cladding hotspot temperatures. Thus, it is anticipated that future refinements in orificing, environmental uncertainties, material properties and design criteria for precluding cladding failure will result in 100% fuel assembly lifetime goal achievement for equilibrium cycles.
- b) All inner blanket assemblies currently achieve the 550 day lifetime goal with all rods having hotspot cladding CDF's less than 1.0.
- c) Insufficient environmental information is available to predict radial blanket performance over 4 to 5 year equilibrium cycle operation. However, all radial blanket assemblies achieve their first core life-goals (878 full power days for cycles 1 through 4) as noted in PSAR Section 4.2.

It should also be noted that the homogeneous CRBRP core assembly designation numbers indicated in this question have been changed to heterogeneous core assembly numbering scheme shown in Figure 4.2-10B.

Question 241.92 (4.2.1.3)

The transient limit curves (TLC's) shown in Figure 4.2-22 are for a reactivity insertion of ≤ 1 second duration. What is the justification for the 1 second cut-off? Provide a matrix of additional TLC studies for assemblies and axial conditions other than those discussed on PSAR page 4.2-45. These studies should be conducted and reported prior to submittal of the FSAR.

Response:

The 1 second cut-off referred to in Figure 4.2-22 is the limiting time envelope for which the TLC's are valid, e.g., see PSAR Section 15.1 2.1. As it relates to rapid reactivity insertion, this time envelope is the duration over which the temperatures of the fuel and clad are increasing. On this basis, the above 1 second envelope was chosen to encompass this effective duration for the various rapid reactivity events to be considered; e.g., see Figures 15.2-83 and 15.2-84.

Consistent with FSAR submittal, a complete performance analysis, which will include TLC's or their equivalent, will be conducted for at least the hot fuel pins in the highest burnup assembly and the assemblies representing the five orificing zones; currently assemblies: 6, 8, 29, 30, and 31. These analyses will be done at 10 axial locations along each fuel pin; specifically, at $X/L = 0.1, 0.2, 0.3, \dots, 1.0$.

Amend. 29
Oct. 1976

Question 241.93 (4.2.1.3.1.2)

This section requires greater specificity concerning the FFTF fuel assembly structural analyses. Describe or reference these analyses and show how they are related to the CRBR structural analysis.

In particular, show how the FFTF analyses led to the selection of the 3 duct locations considered to be limiting areas on page 4.2-47 of the PSAR.

For these 3 cases, for which the calculated stresses, margin of safety, and fatigue damage are summarized in Table 4.2-8, please discuss how "it can be concluded that the duct will probably meet the desired design lifetime" when the safety margin for some of the stress categories are as low as 0.06 and 0.11.

Discuss in detail the planned additional analysis to consider the effects of irradiation damage and sodium exposure, including brittle fracture modes.

Response:

Under the revised sub-section numbering in the PSAR, the stress analysis of the core assembly structural components is addressed in Section 4.2.1.3.2.3. This section has been updated to reflect the most current analyses methods, structural criteria and design margins in the CRBRP core assemblies. The concerns raised in Question 241.93 have been resolved by using the state-of-the-art analyses procedures which go beyond the scope and the depth of analyses used previously. The results from the new analyses, as described in Section 4.2.1.3.2.3, confirm the structural adequacy of the CRBRP core assembly structural components.

A number of design verification tests are planned for CRBRP and these are summarized in Tables 4.2-19 and 4.2-20 of the PSAR.

Question 241.94 (4.2.1.3)

It is stated on page 4.2-49 of the PSAR that fuel rod failure is not expected to occur by bundle-to-duct interaction, even though preliminary analyses indicate interferences between 0.045 and 0.100 inches at the end of design life, because irradiation induced creep has not been considered in either the preliminary deformation analysis or derivation of the allowable interference.

Outline the future detailed analyses which will incorporate those effects as indicated, based on "available LMFBR technology". Specifically, what available LMFBR technology is expected and on what schedule? Describe the R&D program which will provide verification of the analyses. Include scope and schedule. Verification of the contention that no design life limitation is expected due to bundle-to-duct interaction should be provided consistent with the submittal to the CRBRP FSAR.

Response:

Both completed and planned fuel rod bowing analyses, including the effects of irradiation creep, are discussed in Sections 3.0 and 4.0 of the Topical Report No. 4, WARD-D-0150, "Fuel Rod Bowing" WARD-D-0150 was submitted to NRC in November 1976. | 31

Task A.VI of the National Reference Fuel Steady-State Irradiation Program (Reference Q241.94-1) contains tests to verify the fuel rod bowing analyses in general, including the assessment of rod bundle-duct interaction effects. Subassemblies involved in these tests include PNL-9, PNL-10, NUMEC E, P-E/F, P-13, P-14 and P-14A. These subassemblies are described in Tables A-1 and B-1 of Reference Q241.94-1. Schedules of these tests are given in Figure A-2 of Reference Q241.94-1.

Reference

Q241.94-1 TC-573, "Reference Fuel Steady-State Irradiation Program Plan, Revision 1", March, 1976.

Question 241.95 (4.2.1.3)

(a) Did the uncertainty factors used in the fuel bundle/duct interaction calculations take into account the potential increase in coolant temperature from differential coolant channel closing due to swelling and creep? If not, please explain the rationale for ignoring this phenomenon and list the value of the contributions to the uncertainty factors when this phenomenon is considered.

(b) For the interferences discussed on page 4.2-49, (0.045-0.100 inches), what is the end-of-design life?

(c) For the interferences discussed and the bending from thermal stresses, is it possible to have contact between adjacent fuel element cladding surfaces in fuel column regions (i.e., no spacer wire between them)? Can this result in inadequate heat transfer and loss of cladding integrity? Please provide a quantitative answer to this question; i.e., a response which includes a description of the analyses or tests which provide the basis for the response.

Response:

(a), (c) The thermal effects of coolant channel closing, the configuration of the bowed fuel rods under various conditions, and the application of these considerations to completed and planned fuel rod bowing calculations are discussed in Sections 3.1.2 and 4.0 of the Topical Report No. 4, WARD-D-0150, "Fuel Rod Bowing" WARD-D-0150 was submitted to NRC in November 1976.

(b) For the interferences discussed on page 4.2-49, the end-of-design life is 411 equivalent full power days.

Question 241.96 (4.2.1.3)

Is the stored mechanical energy in the reference CRBR fuel element at terminal burnups of 80,000 and 150,000 MWD/MT large enough to distort or fracture the duct via pressure pulses associated with the loss of cladding integrity? Is there an experimental program in effect that evaluates the effect of pressure pulses? If so, provide the details, including objectives, scope, and schedule. If no program exists or is planned, please explain why one is not needed.

Response:

The stored mechanical energy in the reference fuel elements would not distort or fracture the duct if a loss of fuel pin cladding integrity were to occur. A discussion of the mechanical effects of a loss of cladding integrity is provided in Section 15.4.1.1.4. This section discusses the pressure that would be applied to the duct in the event of a stochastic fuel pin cladding failure and defines the strength of the duct. In summary, this section shows the following:

1. For the lower burnup (80,000 MWD/MT peak) initial core operated at a maximum duct temperature of 1100°F, the peak pressure applied to the duct would be about 180 psi and the duct strength would be sufficient to withstand a pressure greater than 300 psi and,
2. For the higher burnup (150,000 MWD/MT peak) equilibrium core operated at a maximum duct temperature below 1000°F, the peak applied pressure would be about 300 psi and the duct strength would be sufficient to withstand a pressure of about 525 psi.

In conclusion, duct fracture or distortion that could interfere with adjacent ducts would not occur (See Section 15.4.1.1.4 for details). Consequently an experimental program to evaluate the effect of pressure pulses on a duct as a result of fission gas release is not considered necessary to support CRBRP.

Section 15.4.1.1.4 has been modified to address duct deformation resulting from a fission gas pressure pulse.

| 31

Question 241.97 (4.2.1.3)

Please discuss how the EBR-II tests underway at 900°F, which are representative of earlier FFTF rod designs and are thus no longer prototypic of current design CRBR, are used in the formulation of fuel rod performance models. Discuss the schedule for the PIE of GE-HEDL, EBR-II mixed oxide rods, referred to on page 4.2-50 of the PSAR. What is the schedule for reporting the LASL PIE results? Discuss the HEDL run-to-failure tests. Include scope and schedule in your discussion.

Describe the capsule irradiation program for FFTF driver fuel rods. Describe the planned irradiation program for vendor produced fuel pellets in EBR-II.

In addition to scope and schedule for these tests, show precisely how the scientific information to be obtained from each test is to be applied to the CRBR fuel design and the design verification.

Outline the features of the fuel rod characterizations which are carried out in the U.S. irradiation program which provide greater performance predictability in the U.S. programs than is obtained by the larger statistics of the foreign programs (as contended on PSAR page 4.2-51).

Response:

The information requested is provided in revised PSAR Section 4.2.1.3.1.3.

Question 241.98 (4.2.1.3)

Other than the data of HEDL-TME-75-48, how has the adequacy of the current design fuel-cladding chemical interaction wastage allowance of 2 mils been demonstrated for terminal burnups in CRBR? The concerns here are the following:

1. The CRBRP wastage allowance requires extrapolation beyond the maximum burnup (43,800 MWD/MT) for the data base of TME-75-48.
2. Cladding fluences/fuel burnup ratios are vastly different for CRBR when compared to EBR-II irradiations.
3. Fuel-cladding chemical interaction is expected to be larger for CRBR fuels (natural uranium-enriched plutonia) than EBR-II experimental, enriched, uranium-plutonia fuels (ANL-75-53).

Response:

1. The fuel-cladding chemical interaction wastage allowance is based on a conservative correlation developed using data at peak rod burnups up to 48,100 MWD/T (43,800 MWD/T average burnup). At the time that the correlation was developed, the data base did not extend beyond this burnup. At the present time many experimental EBR-II rods have exceeded this burnup, but the resultant fuel-cladding chemical interaction has not yet been quantified. Experimental rods which achieved a peak fuel burnup of 80,000 MWD/T and which were irradiated at CRBRP temperatures are currently awaiting hot cell examination. The forthcoming data will be used to either justify the current correlation or to develop a new correlation.
2. Fluence to fuel burnup ratio has no known relevance to fuel-cladding chemical interaction.
3. ANL-75-53 reports that natural uranium-enriched plutonia fuel would be expected to have higher fuel-cladding chemical interactions than enriched uranium-plutonia fuel due to the lower affinity of its fission products for oxygen. The report further concludes that a lower initial O/M ratio would cause less fuel-cladding chemical interaction than a fuel with a high initial O/M ratio. This was observed in the P-23B experiment where the low O/M rods showed substantially less reaction than the high O/M rods. (See Figure 4.2-8 in the PSAR for a comparison of the O/M ratio history for both natural and enriched uranium fuel). Figure Q241.98-1 also demonstrates that fuel cladding chemical interaction for high O/M fuel is significantly higher than for low O/M fuel. For the CRBRP cladding wastage analysis the correlation based on an O/M ratio of 1.985 was used. The CRBRP fuel initially has an O/M ratio of 1.955 (nominal), which should counteract the effect of a higher reaction for natural uranium-enriched plutonia. In addition, HEDL experiment P-15, which contains natural uranium-enriched plutonia, is currently being irradiated in EBR-II and is scheduled for several interim examinations and a final examination at 26,000 MWD/T. This test will supply experimental data on reactions between natural uranium-enriched plutonia fuel and cladding prior to FSAR submittal.

33

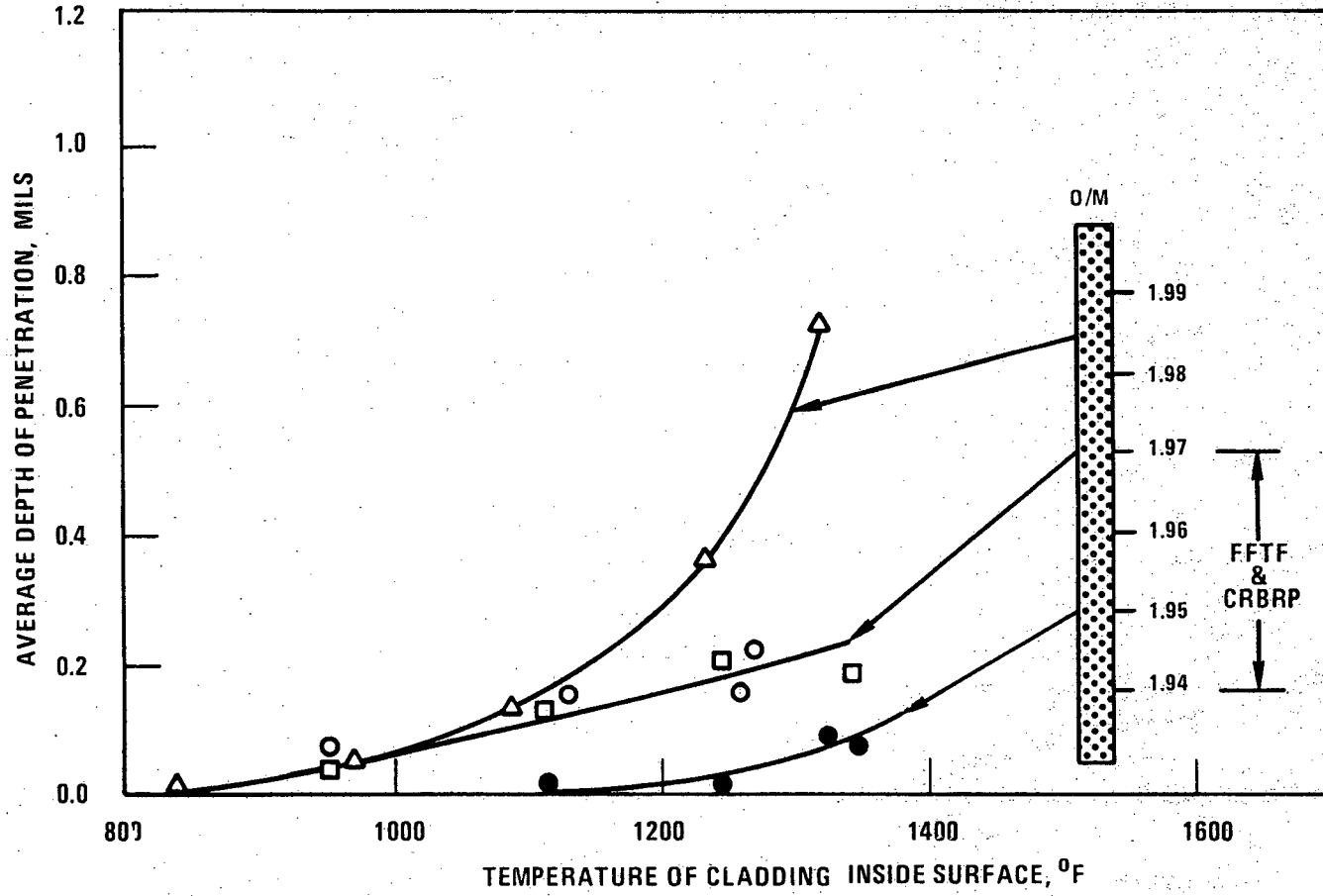


Figure Q241.98-1. Measurements Of Fuel Cladding Reaction At 22.0 Mwd-/kgM

Question 241.99 (4.2.1.3)

Will there be any operating restrictions placed on the rate of power increase during startup or during power changes to avoid PCMI failures? If so, provide the basis for these restrictions or discuss test programs to evaluate these effects.

Response:

If necessary, operating restrictions will be placed on the rate of power increase during startup and power changes to avoid PCMI (Pellet Clad Mechanical Interaction) failures and/or minimize its effect on subsequent operation. The LIFE code (see response to NRC Question 241.83) will be used in conjunction with FURFAN and FRST to analyze the effects of power change rates on PCMI in fuel and radial blanket rods. The power change rates utilized in the EBR-II reactor which are being applied in the reference fuel tests will initially be considered. EBR-II power change rates are typically between 0.4%/min. to 0.6%/min., with an administrative limit of about 1.1%/min.. These results will be reported consistent with the schedule for submittal of the FSAR.

Question 241.100 (4.2.1.3)

Present a detailed discussion of the calculation reported performed with the LIFE II computer code to assess the possibility of fuel cladding mechanical interaction in the radial blanket fuel rods. List the assumptions used, justify their use, and discuss any sensitivity studies performed to determine the assumptions impact on the results of the calculation.

Response:

The response to this question is provided in amended PSAR Section 4.2.1.3.2.1.

Q241.100-1

Amend. 29
Oct. 1976

Question 241.101 (4.2.1.3)

If the residence time of the radial blanket fuel rods is 6 years, how are the calculations, which showed that the hot rod of radial blanket A has a 5.29 year service lifetime, to be employed?

Response:

The lifetime of the outer row radial blanket assemblies is 5 years, the inner row of radial blanket assemblies have a 4 year lifetime, while the inner blanket assemblies have a 2 year lifetime. Preliminary analyses indicate that all blanket assembly types meet these lifetime objectives.

Question 241.102 (4.2.1.3)

How is the fact that the CDF analysis of radial blanket rods resulted in a CDF >1.0 to be utilized in CRBRP fuel design or operation?

Response:

For final design, the radial blanket rod CDF at end of life is expected to be <1.0. This is explained in detail in the response to Question 241,101.

Question 241.103 (4.2.1.3)

An explanation should be provided for the neglect of stress effects on irradiation swelling and swelling effects on irradiation creep in the ANSYS calculation of rod-rod contact forces.

Response:

The response to this question is found in amended PSAR Section 4.2.1.3.2, 1.3.

Question 241.104 (4.2.1.3)

The details of the ANSYS code calculation of the primary, secondary, and bending components of the stresses at critical duct locations should be provided.

The margin of safety for the duct ACLP primary and secondary stresses is less than one (0.439). What constitutes an adequate safety margin?

Please explain the statement "the design criteria for the duct and the associated stress limit magnitudes are currently being revised".

Response:

The response to this question is found in amended PSAR Section 4.2.1.3.2.2.1 and Table 4.2-13.

Question 241.105 (4.2.1.3)

The fact that a bundle/duct interaction is predicted to occur when stress affected swelling and swelling enhanced creep are included in the calculation of clearances is cause for concern. A commitment to the determination of an allowable compressive limit for a radial blanket assembly must be made, including a schedule consistent with submittal of an FSAR. In the interim, design alternatives should be presented and the effects of these alternatives on performance should be analyzed. Ultimately, experimental verification of the analyses must be provided.

Response

A discussion of radial blanket bundle/duct interaction, including analysis, testing and limits, is provided in revised PSAR Section 4.2.1.3.2.1.3.

Q241.105-1

Amend. 32
Dec. 1976

Question 241.106 (4.2.1.3)

The maximum wire stress of 21,000 psi at EOL for the hot rod in radial blanket assembly A is said to be within the design limit with a margin of safety of 0.03. Is this considered to be an adequate margin? Explain.

In view of the fact that transient temperature increases and temperature gradient effects on the wire stress were neglected in the analysis, it appears likely that wire rupture may occur, particularly since the safety margin not including these effects was already near zero. Please present, therefore, a detailed analyses of the potential effects of wire rupture, particularly simultaneous rupture during a transient.

Response:

A discussion of the margins of safety, steady state stress and transient effects with respect to the wire wrap is provided in revised PSAR Section 4.2.1.3.2.2.4.

Q241.106-1

Amend. 29
Oct. 1976

Question 241.107 (4.2.1.3)

Please present a detailed description of the scoping studies asserted to show that a six face duct loading during seismic events results in acceptably low ACLP stresses. Describe the current additional investigation of the load distribution during seismic events.

Response:

The response to this question is found in amended PSAR Section 4.2.1.3.

Question 241.108 (4.2.1.3)

Please describe in detail the "1970-initiated" experiments on mixed oxide fuel rods which provided irradiation experience asserted to be applicable to radial blanket rods. Show how the results are applied to the cladding design.

Provide a reference for the rod radial blanket test initiated in EBR-II in 1974.

Response:

The requested discussion and references are provided in revised PSAR Section 4.2.1.3.2.4.

Question 241.109 (4.2.1.4)

Please provide a precise definition of the term "final design release". Is it intended to be synonymous with FSAR?

Response:

The design process for CRBRP fuel and radial blanket assemblies proceeds through a series of phases. The discussion below defines "final design release" relative to the overall design process. It should be noted that it is not synonymous with FSAR input or submittal.

- **Conceptual Design**

During this phase the component design requirements and the documents which control interfaces with mating equipment and/or systems are developed, reviewed, approved and released to the CRBRP Project. One or several conceptual layout drawings are developed for designs which analyses indicate satisfy the basic requirements.

- **Preliminary Design**

During this design phase engineering studies of the conceptual designs are pursued. The end product is a design layout drawing which identifies the engineering parameters and component design features including critical dimensions, tolerances and fits, and associated materials and processes. This drawing along with the supporting analyses and proposed testing program form the basis for formal design reviews and approvals of the equipment designs. Upon approval, the preliminary design layout drawings are released and procurement activities for long lead material are initiated.

- **Final Design**

During this phase of the design process, the component detail drawings and equipment assembly drawings are prepared consistent with the released design layout drawing. The associated manufacturing requirements, including material, process, fabrication and inspection requirements, are also developed. Detailed specifications for testing are written; performer test plans and drawings are reviewed and approved. Near term tests are completed and evaluated. The drawings, requirements, test results and supporting technical analyses (nuclear, thermal-hydraulic, structural) to demonstrate design adequacy are formally reviewed and approved. The final design drawings and manufacturing requirements are released (final design release) to the CRBRP Project and become the basis for subsequent procurement. | 31

- **Design Verification**

Long term test results are being evaluated and resolution of areas of technical uncertainty are being documented through topical reports which are reviewed, approved and released. Technical analyses supporting design

adequacy are also updated where necessary to incorporate the most recent information. Concurrently, the released design and manufacturing requirements are the basis for preparation of "request for fabrication quotes", vendor negotiations, purchase order placement and vendor manufacturing qualification. Culmination of these efforts is the approved fabrication release for manufacture of the actual CRBRP equipment.

- FSAR Input

The design requirements, design description and technical analyses and testing results which support design adequacy are described. This input to the FSAR is based upon the current information available including as-fabricated manufacturing data, very long term tests data (primarily from high exposure irradiation tests) and all applicable experience to date. This information is included in the derivation of plant technical specification limits.

Relative to the above activity descriptions, two key points should be emphasized:

1. Subsequent to release of a given design document, that document is subject to formal change control procedures. The released design and manufacturing requirements may be changed at any time prior to release for fabrication. Thereafter, any changes in design margins are accommodated by adjusting performance and operational requirements (e.g., increased power, temperature, or burnup).
2. Technical analyses supporting design adequacy are performed during each design phase. In the current evolutionary state of LMFBR fuel technology, each set of analyses may be an improvement over previous analyses. Environmental predictions, irradiated material properties, basic behavioral models and design limits may be updated during each design phase to incorporate the latest CRBRP design supporting test results or results from the ongoing LMFBR base technology programs.

The above discussion defines the "final design release" relative to the overall design process. It should be noted that it is not synonymous with FSAR input or submittal.

Question 241.110 (4.2.3.1)

In the original version of the PSAR (Table 4.3-1, page 4.3-52) B₄C diametral pellet dimensions were 0.470 inches with a 0.013 inch nominal diametral pellet-clad gap for the primary control rods. In subsequent Amendment 14 (March 1976, Page 4.2-272a) these dimensions have been changed to 0.459 inches for the pellet diameter and 0.024 inch for the nominal diametral gap. Provide the revised B₄C operating temperatures for the primary control rods resulting from the pellet-clad gap increase from 0.013 to 0.024 inches. Also explain why the diametral dimensions were not increased for the secondary control rods. Supply maximum diametral swelling values for these two control rod types to substantiate their gap sizes.

Response:

The current primary control rod dimensions are provided in revised Table 4.2-42a and Table 4.3-1. Nominal pellet diameter is 0.459 inch, and nominal pellet/clad gap is 0.023 inch.

Also Table 4.2-46 has been revised to provide new primary control rod operating parameters, including maximum B₄C temperatures.

Information on minimum primary control rod pellet/clad gap as a function of time in operating cycle, as well as the maximum pellet swelling is referenced in revised PSAR Section 4.2.3.3.1.5 and shown in Figure 4.2-111a.

Maximum diametral swelling value for the secondary control rod pellets is included in revised Table 4.2-36. The secondary control rod diametral dimensions were not increased (or decrease) at the same time the primary control rods were, since the swelling data base changes that warranted the increase in the primary had no impact on the secondary control rods.

Question 241.111 (4.2.3.15)

Provide an axial burnup profile for primary and secondary control rods.

Reponse

The calculated axial distribution of neutron captures in the peak absorber pin of the Secondary Control Assembly has been incorporated into a new Figure 4.2-93a.

Figure 4.2-111b provides the axial burnup profiles for the four typical primary control rod locations in an equilibrium cycle.

Q241.111-1

Amend. 28
Oct. 1976

Question 241.112 (4.4.2.6)

Question 241.32 is not completely answered. Tables 4.4.14 through 4.4.19 show that there are hot gaps of less than 2 mils and that the gap conductance changes with burnup (or power) when the gap is closed. How was the gap conductance calculated for hot gaps less than 2 mils?

Response:

Question 241.32 was: "Equation (4.4.2.6-6) is stated to be valid only in the range of 2-7 mils. How is the gap conductance of smaller hot gaps calculated?"

The answer to Question 241.32 was given within the frame work of the empirical model adopted during 1973 and 1974 for preliminary analysis included in the originally submitted PSAR. As stated in that version of the PSAR, Section 4.4.2.6.5, the model is strictly valid for beginning-of-life conditions because the HEDL P-19 test, upon which the model was based, was performed under beginning-of-life conditions. For these conditions, calculations with the empirical model yield hot gaps which are larger than 2 mils (diametral) for the P-19 fuel pins and CRBR fuel rods. These results formed the basis for answering Question 241.32.

However, an earlier question, 001.45 requested gap characteristics as a function of burnup at rated power and overpower conditions. The empirical model referred to above does not provide this detail. Thus, Question 001.45 was answered using the most updated, detailed model available at that time (July 1975), namely the LIFE-III code. (This detailed model has undergone and will continue to undergo further update).

The hot gaps of less than 2 mils and the gap conductances referred to in the current Question (241.112) and shown in Tables 4.4-14 through 4.4-19 were calculated with the LIFE-III code in response to Question 001.45.

Note that the hot gaps shown in the Tables at the beginning-of-life are greater than 2 mils diametral (the Tables give radial gaps) and thus fall within the range of validity established for equation 4.4.2.6-6.

With regard to the above the following should be noted: 1) Additional discussion of the methodology used in employing and deriving the empirical model will be given under Questions 241.119 and 241.122. 2) The LIFE-III code and detailed models based on and correlated with the LIFE-III code will be used for final design and preparation of the FSAR. Additional information in this area is provided under Question 241.120.

Question 241.113 (4.4.2.6)

The answer given to question 241.35 is not the desired response. According to statistical theory, the correlation coefficient, requested in question 241.35 is defined as a measure of the amount of relation between variables or the portion of the sum of squares deviation which has been removed by correlation.

The prediction interval also has a statistical definition. It is the confidence range of any single predicted value of the dependent variable. It will be wider than the confidence range of a value estimated from the correlation by a measure of the confidence of the correlation itself.

Using these terms with their exact statistical definitions, please answer question 241.35 again .

Response:

Equation 4.4.2.6-6 describes the preliminary correlation between gap conductance and gap size based on P-19 data as discussed in response to question 241.112. Figure Q241.113-1 shows equation 4.4.2.6-6 and the six data points from which it was developed. These points represent the relationship between gap conductance, as inferred by metallographic examination of P-19 fuel, and calculated gap size based on a simple thermal expansion model of the fuel pellet.

Subsequent evaluation of the P-19 data, using improved powers as re-calculated from ANL (Ref. Q241.113-1) has shown that the preliminary correlation adopted in PSAR analysis was conservative; i.e., a larger hot gap size corresponded to a given gap conductance, or for a given hot gap size, the gap conductance was larger than predicted by PSAR equation 4.4.2.6-6.

The best fit (minimum absolute variance) hyperbolic curve for the revised set of P-19 gap sizes is given by:

$$hg = -75.2 + \frac{8047}{\text{hot gap}} \quad (1)$$

where the units are the same as for equation 4.4.2.6-6.

Another hyperbolic curve may be fit to these data such that the relative variance (*) is minimized. This correlation, equation 2 below, gives a better fit with regard to the points corresponding to lower values of gap conductance.

$$hg = -117.1 + \frac{7649}{\text{hot gap}} \quad (2)$$

(*) The relative variance is defined as:

$$\sum \left(\frac{hg (\text{measured}) - hg (\text{calculated})}{hg (\text{measured})} \right)^2$$

Figure Q241.113-2 shows a comparison of PSAR equation 4.4.2.6-6 against the revised data points as well as their best fits, i.e., equations (1) and (2) reported above.

The conservatism of the nominal gap conductance correlation adopted in PSAR is evident and is very clearly shown from a different point of view in Figure Q241.113-3: all the points considered in determining the gap conductance design correlation used in PSAR lay on the conservative side of the 45° regression line. The reevaluated data points are shown for comparison, along with the lower confidence limits (90th and 95th percentiles) on individual gap conductance. The prediction interval for the re-evaluated data points is symmetric about the 45° line shown in Figure Q241.113-3. As an example Figure Q241.113-3 demonstrates the conservative portion of the 95% confidence prediction interval for the case of a calculated gap conductance of 1400 BTU/hr-ft²-°F. Note that when applied to the data used in the PSAR, it represents a conservative estimate, as discussed previously.

The correlation coefficient was calculated to be 0.907.

No attempt was made to update equation 4.4.2.6-6 and fuel temperature calculations reported in PSAR since: a) the conservatism of the adopted correlation, as discussed before; and b) future analyses will adopt, rather than an empirical fit, a phenomenological gap conductance model, based on LIFE-III, as discussed in detail in response to questions 241.117 and 241.120.

Reference

- Q241.113-1. L. B. Miller, et al., "Characterization of the Power in an Experimental Irradiation Subassembly of Mixed Oxide Fuel in EBR-II", ANL/EBR-047, September, 1971.

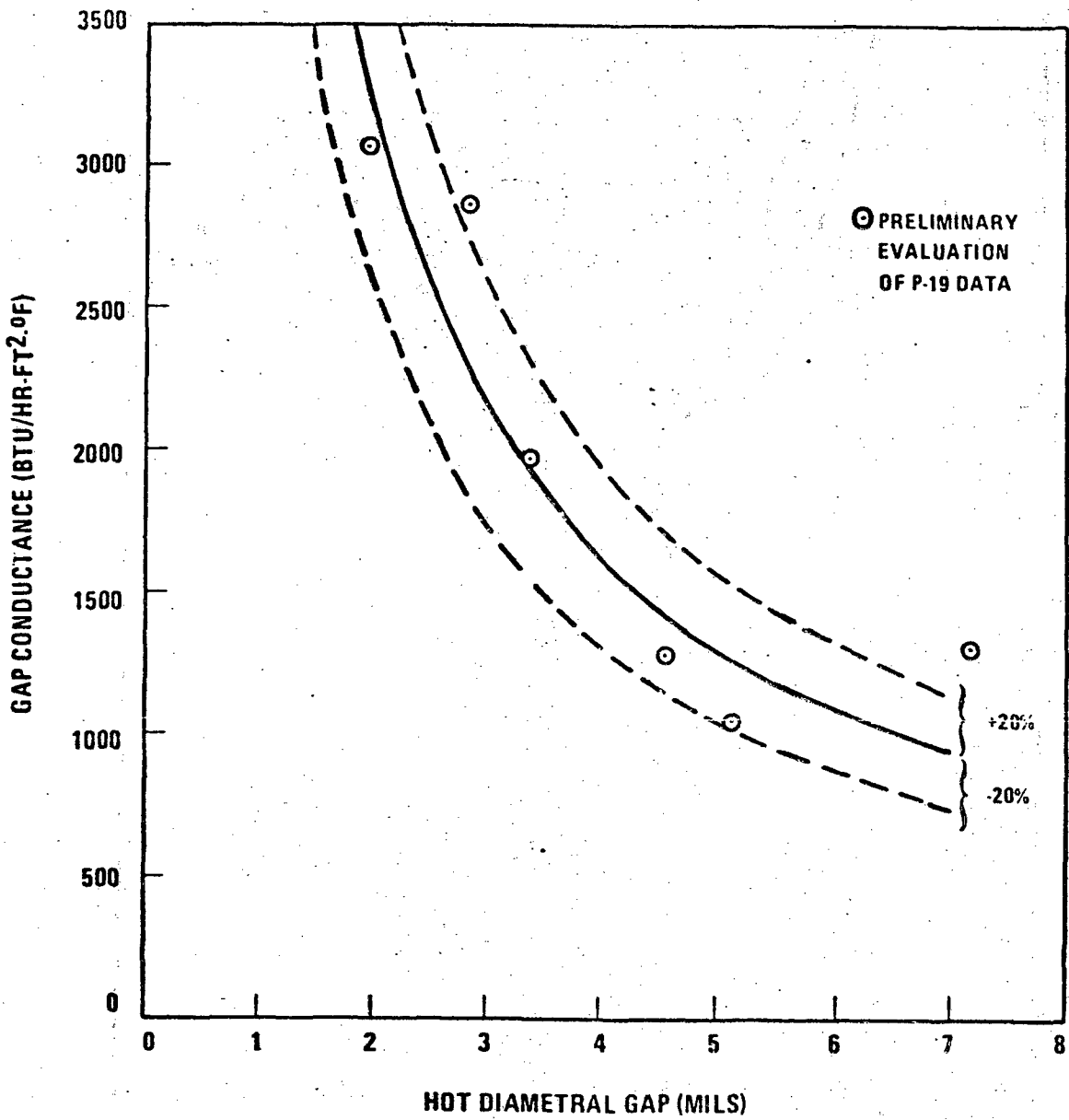


Figure Q 241.113-1. GAP Conductance/Hot Gap Relationship Adopted In PSAR Analysis

7683-233

Q241.113-3

Amend. 33
Jan. 1977

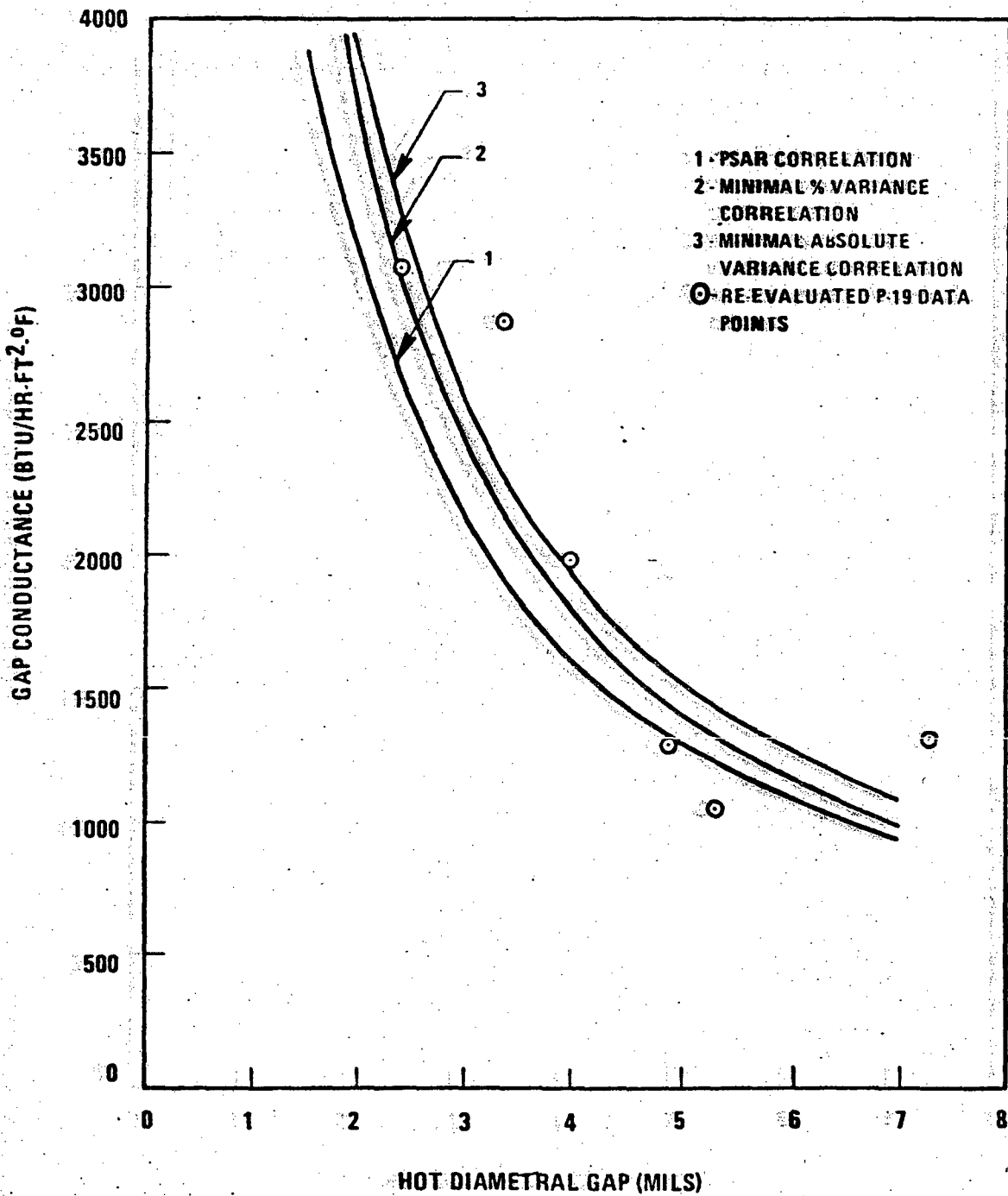


Figure Q 241.113-2. GAP Conductance/Hot Gap Size Relationships

7683-234

Q241.113-4

Amend. 33
Jan. 1977

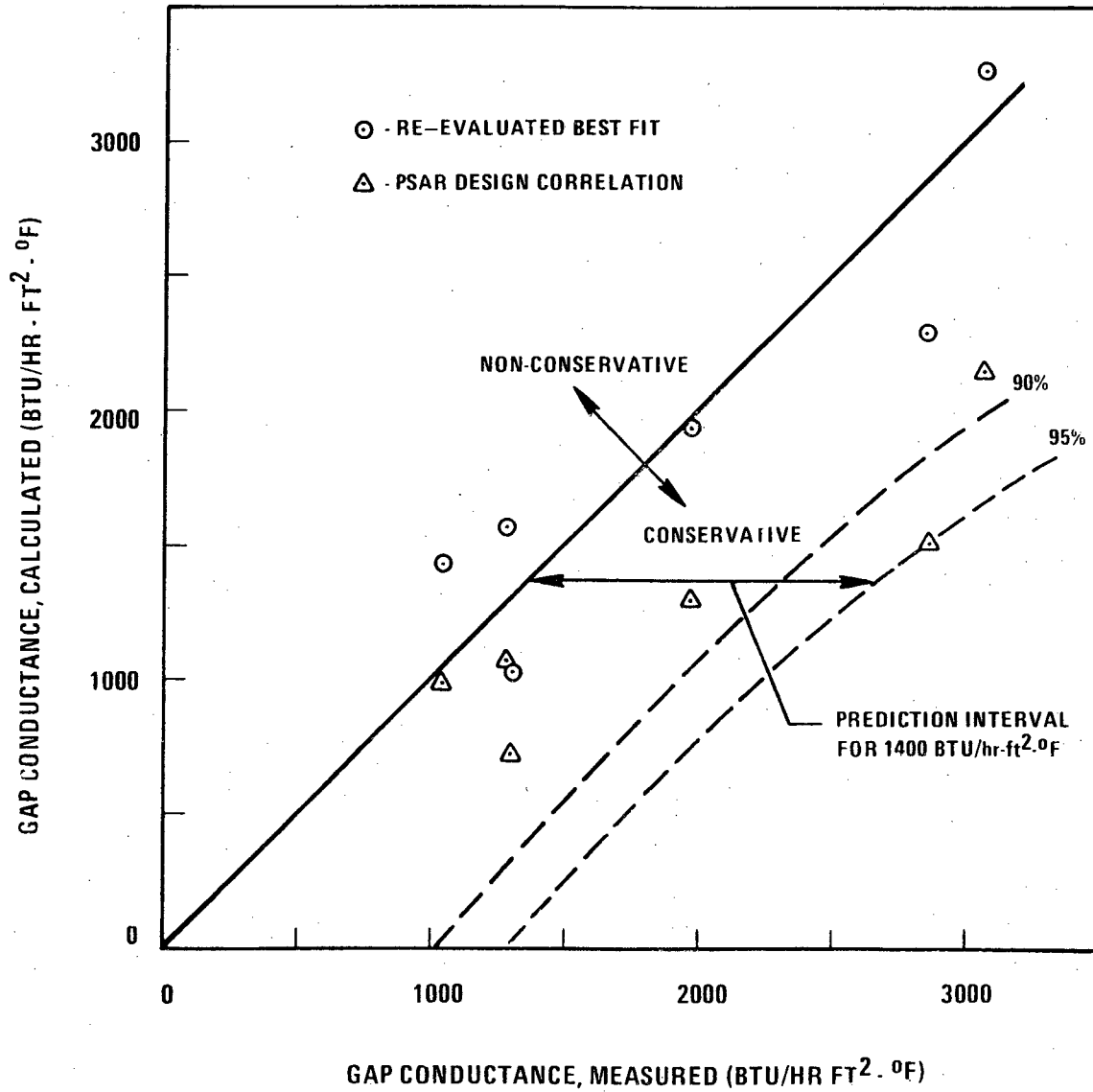


Figure Q 241.113-3 Correlation of GAP Conductances. Comparison Of Calculated Values With P-19 Test Results

7683-235a

Q241.113-5

Question 241.114 (4.4.2.6)

Provide a derivation of the equation for HCE_g given in Section 4.4.2.6.5 and explain how h_1 , h_2 and h_3 are calculated.

Response:

The response to this question is provided in amended PSAR Section 4.4.2.6.5 and new Figure 4.4-55.

Q241.114

Amend. 29
Oct. 1976

Question 241.115 (4.4.2.6)

The answer to Question 241.62 did not give the desired response. In the context of this question, fuel relocation is the cracking of the fuel pellet due to thermal stresses, and the subsequent movement of the cracked pieces towards the cladding.

Please answer PSAR question 241.62 again .

Response:

Cracking of the fuel pellet due to thermal stresses is a highly anisotropic and localized phenomenon. Movement of the cracked pellets towards the cladding results in reducing the gap, thus effectively reducing the fuel center temperature. The simplified thermal analysis procedure given in section 4.4.2.6 does not explicitly account for this type of relocation. However, cracking and relocation is indirectly accounted for, since the correlation was directly based on P-19 experimental results.

The LIFE-III code will be used for FSAR analysis. This code includes an isotropic fuel cracking model which simulates the effects of fuel cracking on the fuel mechanical and thermal behavior. In order to assess, on a comparative basis, the effect of accounting for fuel cracking, the peak pin in fuel assembly #6 (i.e., the pin with highest fuel temperature) was analyzed for beginning-of-life conditions using the LIFE-III code. Two conditions were examined: a) adopting the code fuel cracking model; and b) assuming that no fuel cracking occurs. The fuel centerline temperature predicted by LIFE was higher in the second case, as expected, since accounting for fuel cracking will actually enhance the gap heat transfer characteristics. Therefore, the one-dimensional PSAR analysis which does not explicitly account for fuel cracking, is conservative.

Question 241.116 (4.4.2.6)

The hot channel factors used for calculating fuel temperatures should account for uncertainties in such a way that the resulting temperature calculated by this method are conservative. Please explain how, if the hot channel factors have been properly obtained and applied, this procedure results in "very good agreement . . . between predicted fuel center-line temperature and the P-19 data," as stated in Section 4.4.3.2?

Response :

The response to this question is provided in amended PSAR Section 4.4.3.2.

Question 241.117 (4.4.2.6.)

Describe experiments or calculations planned to update the gap conductance correlation used in the NICER code as discussed in Section 4.4.2.6.5

Response:

Work is in progress to substitute in empirical gap conductance equation with a comprehensive modeling of gap behavior in the fuel rod thermofluids desing code NICER. Specifically, the following three models are being added:

- 1) The complete gap conductance model used in the LIFE-III code;
- 2) A fuel-cladding gap closure model based on the LIFE-III code;
- 3) A fuel-cladding contact pressure model based on the LIFE-III code.

Each of these models are briefly described below.

1. The Gap Conductance Model

The overall gap conductance defining the heat transfer across the fuel-cladding gap is given by:

$$H = H_g + H_s + H_r \quad (1)$$

where H_g = the conductance due to conductive heat transfer through the gas bond and at the gas-solid interface;

H_s = the conductance due to conductive heat transfer across points of fuel-cladding contact;

H_r = the conductance due to radiant heat transfer.

Equation (1) is used solely to compute the fuel surface temperature, T_s , from the cladding I.D. temperature, T_{ci} , the cladding inner radius, R_{ci} , and the linear power, Q , using the relationship

$$T_s - T_{ci} = Q / (2\pi R_{ci} H) \quad (2)$$

Since this model is exactly the same as in LIFE-III, the expressions describing each heat transfer mechanism and the detailed derivations will be available in the LIFE-III code documentation. This gap conductance model has been calibrated and verified against the P-19, P-20, and F-20 experimental fuel pins.

2. Fuel-Cladding Gap Closure Model

The NICER code does not perform structural/mechanical analyses and does not compute the time-variation in fuel cladding gap during gap closure occurring early in life. The LIFE-III gap conductance model, however, requires a value for the gap width as a function of time since this is an important factor in determining the gap conductance. Thus, an expression for gap closure was developed and fit to gap size histories calculated by the LIFE-III code over a wide range of operating conditions. The equation takes into account the following parameters:

- thermal expansion of the cladding;
- thermal expansion (and cracking) of the fuel;
- swelling of the fuel.

It is not necessary to account for swelling of the cladding, since gap closure typically takes place over less than a few hundred hours which is not enough time for significant cladding swelling to occur. Also, the gap-closure equation accounts for variations in:

- cladding I.D. temperature, T_{ci} ;
- linear power, Q ;
- initial cold gap, G_0 ;
- fuel surface temperature, T_s ;
- as-fabricated fuel density, ρ .

The basic equation for the fuel-cladding gap is given by:

$$G = R_{ci} - R_{fo} = G_0 + \Delta R_{ci} - \Delta R_{fo1} - \Delta R_{fo2} \quad (3)$$

- where
- G_0 = gap initial (cold) value;
 - R_{ci} = cladding inner radius;
 - R_{fo} = fuel outer radius;
 - ΔR_{fo1} = increase in fuel outer radius due to thermal expansion and cracking;
 - ΔR_{fo2} = increase in fuel outer radius due to fuel swelling;
 - ΔR_{ci} = increase in cladding inner radius due to thermal expansion.

The constants in the gap-closure model were chosen to produce gap widths varying with burnup, power, fuel density, cladding temperature and fuel surface temperature in essentially the same way as those computed by the calibrated LIFE-III code.

The details of this gap-closure model will be available in the NICER code documentation.

3. Fuel-Cladding Contact Pressure Model

The LIFE-III gap conductance model included in the NICER code also requires evaluation of the fuel-cladding contact pressure since one component of the gap conductance is that due to solid-solid contact. A simple theoretical model was developed to calculate fuel-cladding contact pressure as a function of parameters available in the NICER code. The model takes into consideration such variables as:

- fission gas release;
- cladding swelling and thermal expansion;
- smear density;
- power rating;
- burnup;
- solid fission product swelling;
- fuel thermal expansion and fission-gas swelling.

Basically, the fuel-cladding contact pressure arises due to fuel swelling which in turn is due to fission gases and solid fission products. Pertinent LIFE-III models were combined to develop a simplified model for NICER. The predictions from the simplified model were compared with the LIFE-III predictions and were observed to be in reasonably good agreement. The details of this model also will be available in the NICER code documentation.

Thermal performance fuel pin tests currently available, P-19, P-20, F-20, were used to calibrate and verify the LIFE-III code models as indicated above.

Question 241.118 (4.4.2.6).

The 3σ uncertainty value of -20% for equation 4.4.2.6-6 seems unrealistically low. This uncertainty includes only the statistical scatter of the data points and not any uncertainty in the data points themselves or in the calculation of the hot gap. Such effects as the uncertainty in the power generation, variations in density, etc., were apparently not considered (see Question 241.33).

Also, is it not true that the fuel rods for the test from which these data were obtained (P-19) were fabricated so that there was less variation in fuel rod dimensions than would be the case for standard CRBRP fuel rods? What allowance was made for this in developing the uncertainty in the correlation? How are uncertainties in power included in application of this correlation?

Equation 4.4.2.6-6 applies only to Beginning-of-Life conditions. The uncertainty should be high as burnup increases due to increasing amounts of relocation, fission gas release, fission product redistribution and fuel restructuring. Justify keeping the uncertainty constant at the Beginning-of-Life value .

Response:

The 3σ interval of +20% for equation 4.4.2.6-6 is a conservative estimate of the uncertainty attributable to the use of the correlation itself. In fact, the major contributor to the statistical scatter of the data points shown in Figures 1, 2 and 3 of the response to question 241.113 is not the uncertainty in the correlation (equation 4.4.2.6-6) but rather the combined uncertainties of such effects as local power generation, local coolant temperature, fuel solidus temperature, fuel pellet conductivity, cladding conductivity, film coefficient, etc. On a basis of the best estimate of each of these contributing uncertainties, for the EBR-II reactor and P-19 test conditions, their combined effect is approximately 70% of the total uncertainty which is manifested as statistical scatter of the data points of the above mentioned figures. The uncertainty of 20% in the gap conductance correlation above (which is part of the gap hot spot factor, see response to Question 241.114) is therefore conservative; moreover, the conservatism in the derivation of equation 4.4.2.6-6 was discussed in detail in response to Question 241.113. An objective of the P-19 tests was to minimize the uncertainty in the evaluation through the use of controlled cell gap sizes in the range of 4 to 10 mils. The actual gap sizes are tabulated in the response to Question 241.119.

Uncertainties in power generation and variations in fissile density are accounted for through the heat flux factor (see, for example, Table 4.4-2) which is considered together with the gap conductance hot spot factor in calculating the gap temperature drop. As regards the second and third parts of the question, the preliminary status of the gap conductance empirical model adopted in PSAR, since it was the only one available at that time, has been discussed in detail in response to questions 241.117 and 241.120. In particular, the response to Question 241.117 gives an outline of the comprehensive modeling of gap behavior which is derived from LIFE-III and will be adopted in final design analyses and FSAR preparation. As specifically stated in response to question 241.120, a reassessment of uncertainties will be performed, including proper consideration of burnup effects, to assure that all design criteria are met during the fuel rod lifetime (accounting for 3σ uncertainties and 15% overpower).

Question 241.119(4.4.2.6)

The answer to question 241.34 is incomplete. What was the analytical procedure used to calculate the hot gap conductance correlation (equation 4.4.2.6-6)? Is fuel relocation (fuel cracking and subsequent movement of the fragments towards the cladding) included in this calculation?

In deriving the correlation of equation 4.4.2.6-6 what values were assumed for fuel thermal conductivity and fuel melting temperature?

Describe the model used to calculate the thermal expansion of the fuel pellet.

Response:

The requested information is provided in amended Section 4.4.2.6.5.

Question 241.120 (4.4.2.6)

List the analyses for which equation 4.4.2.6-6 is used.

Response:

The response to this question is found in amended PSAR Section 4.4.2.6.5.

Question 241.121 (4.4.2.6)

Provide the rationale for using the P-19 irradiation results in the thermal analysis of the radial blanket in view of the fact that whereas the fuel in the P-19 pins restructured before the high power operation the radial blanket fuel will see a different power history with essentially no restructuring during early life. (Recall the 3.5 mil gap P-20 pin that melted at high power, most likely due to little early-in-life restructuring). Also provide the quantitative relations that equate power-to-melt of 0.230 and 0.250 inch pins with the power-to-melt of 0.520 inch pins. Explain when and why thermal over or under predictions are conservative. See PSAR page 4.4-16 as an example of the use of "conservative".

Response:

The detailed prediction of fuel temperatures requires an integrated set of models for gap conductance, fuel thermal conductivity, thermal expansion, cracking, pore migration, hot pressing and fuel stress-strain behavior.

However, in the case of fuel rods, the beginning-of-life melting powers were determined from P-19 test results because the test was designed to be nearly prototypic. A simplified but adequate model based on P-19 results was used as given in Section 4.4.2.6.5. Radial blanket rods have a larger diameter and a different power history than fuel rods. Hence, the simplified model based on the P-19 results could not be used for thermal analysis of the radial blanket rods.

In order to perform the thermal analysis of blanket rods, the CYGRØ-F code was used. In this code, the material properties and behavior models indicated above were formulated using basic data and fundamental formulations as far as possible. The uncertainties in models were resolved by calibrating the code against selected fuel pin experimental results and making appropriate modifications to the behavioral models. The code then provides a detailed rigorous thermo-mechanical analysis system which is sensitive to variations in power, temperature, state of the fuel and the reactor environment.

Specifically, the CYGRØ-F code was statistically normalized to the P-19 midplane section data to predict the melt radius, central voids and grain structure. The code was then verified using the P-19 incipient melt section data, and the GE-F1 and WSA-1 and -2 experimental data (see References Q241.121-1 and 2). These analyses confirmed the suitability of the fundamental models in the code for design studies. The fundamental nature of the behavioral models allows the use of the code for conditions different than in fuel rods such as radial blanket rods. No quantitative relations were used to equate the power-to-melt of 0.230 and 0.250 inch pins with the power-to-melt of 0.520 inch pins. The differences in dimension, power history and restructuring characteristics were accounted for by the behavioral models in the code. In the analysis, the thermal conductivity values of mixed oxide fuel were used. The mixed oxide thermal conductivity values are 5 to 15% lower than that for UO_2 , and hence, the results of the analysis are considered to be conservative.

For preliminary analysis, the CYGRØ-F code was considered to be adequate. The FSAR analysis, however, will use the LIFE-III code, which has improved models specific for radial blanket and has been verified more thoroughly.

References

- Q241.121-1 S. A. Rabin, W. W. Kendall, W. F. Bailey, "Short-Term Fast Flux (EBR-II) Irradiation of PuO₂-UO₂ Fuel Pins," GEAP-5570, October 1967.
- Q241.121-2 U. P. Nayak, et. al., "Post Irradiation Examination Results of WSA-1 & WSA-2 Fuel Pins (Interim Discharge)," WARD-OX-00045-25, To Be Published by January 1977.

Question 241.122 (4.4.2.6)

Provide the detailed analysis for the derivation from the P-19 test of equation 4.4.2.6-6 which states $hg = 27 + 6385/\text{hot gap}$. Also show how the -3σ confidence level was determined to be -20% . Your analysis should show how the hot gap was calculated using thermal expansion, cold gap pin power and cladding temperatures. Give an actual example, using a P-19 pin, of the analytic procedure .

Response:

As described in the response to Q241.113, equation 4.4.2.6-6 represents a preliminary correlation between equation 4.4.2.6-6 and the six data points from which it was developed. This response also presents a new equation, $hg = -75.2 + 8047/\text{hot gap}$, which is the best fit hyperbolic curve for a revised set of P-19 gap sizes.

A discussion of the 3σ interval of $\pm 20\%$ is contained in the response to Q241.118.

An analysis showing how the hot gap was calculated is contained in the response to Q241.119. This response also provides an actual example of the analytic procedure using pin 10-19-2.

Question 241.123 (4.4.2.6)

- a) Since the fuel is not at isothermal conditions, please explain how the fuel radial and axial thermal expansions are determined.
- b) What data are used to provide values for fuel thermal emissivity?
- c) What is the density of liquid fuel at its various liquidus temperatures?
- d) Provide the data based on the thermal properties of liquid fuel needed for safety analysis (e.g., heat capacity, thermal conductivity, etc.).

Response:

- a) Fuel radial and axial thermal expansions were explicitly accounted for in PSAR mechanical, but not in fuel thermal analyses. However, fuel radial expansion was considered in calculating the amount of gap closure, in order to obtain the correlation between cold and hot gap; this will be discussed in more detail in response to Question 241.122.

As shown in Ref. Q241.123-1 the fuel thermal expansion coefficient used in the above calculation was:

$$\alpha = 6.689 \times 10^{-6} T + 3.244 \times 10^{-9} T^2$$

where α is in $^{\circ}\text{C}^{-1}$ and T in $^{\circ}\text{C}$.

Explicit consideration of fuel thermal expansion will be included in future analyses conducted using the LIFE code, chiefly in preparation of the FSAR (see discussion in response to question 241.120).

- b) Fuel thermal emissivity per se was not considered. Again, the P-19 data were the basis for calculation of beginning-of-life fuel temperatures. Since the gap conductance correlation was merely an empirical fit of experimental data, it included all phenomena affecting the heat transfer across the gap, thence fuel emissivity among the others.

The radiation component in the fuel thermal conductivity is included in the recommended correlation.

- c) and d) Liquid fuel is beyond the scope of the analyses pertaining to Section 4.4. It is a design limit and constraint that the fuel stays below the solidus line during steady state operation (to which Section 4.4 addresses itself) even for sustained operation at 115% of rated power, including uncertainty factors at the 3 σ level of confidence. However the information requested can be found in Table B-1 of Ref. Q241.123-2 and the Fuel section of Ref. Q241.123-3.

References

- Q241.123-1 GEAP 5748, "Heat Transfer Coefficients Between Fuel and Cladding in Oxide Rods", G. N. Craig, et al, January 1969.
- Q241.123-2 ANL/RAS 74-29, "Ex-Vessel Considerations in Post-Accident Heat Removal", Kumar, L., et al, October, 1971.
- Q241.123-3 ANL-CEN-RSD-76-1, "Properties for LMFBR Safety Analyses", March, 1976.

Question 241.124 (4.4.2.6)

What effect does pore size, shape and distribution (fabrication process and feed material dependence) have on fuel thermal performance-mainly fuel thermal conductivity? Will additional P19, P20 type of tests be conducted with actual CRBR fuel? If no such tests are planned, please explain why they are not needed even though the P19, P20 test fuel was not fabricated by the same vendor as CRBR fuel.

Response:

The response to the first part of this question is found in amended PSAR Section 4.4.2.6.7.

Additional P-19 and P-20 type tests are not specifically planned for the CRBRP fuel. The justification for this position is based on the following:

1. The P-19 fuel was fabricated using a high pressure preslug, low pressure compaction fabrication process. This process resulted in fuel pellets with laminar porosity and microcracks of the type which show a decrease in thermal conductivity compared to fuels with isometric, uniformly distributed porosity. The PSAR fuel pin design analysis was based on power-to-melt values determined from the P-19 experiment, and therefore, the possible effects of pore morphology which cause lower thermal conductivity are already conservatively included. When CRBRP fuel characteristics are available, a comparison with experimental fuel (such as P-19, P-20, and F-20) characteristics will form the basis for a reassessment. Note that the current analysis of the P-19 and P-20 results indicate substantial margin between CRBRP maximum linear heating rate and power-to-melt as discussed in the PSAR and in response to Questions 241.116 and 241.127.
2. The CRBRP fuel is expected to be fabricated by similar processes as that used for FFTF fuel. HEDL is performing comparative power-to-melt experiments with the two FFTF vendor fuels and HEDL fuel manufactured to the same fuel specifications in the GETR reactor. (References Q241.124-1 and PSAR Reference 4.2-164). These GETR tests will provide a comparison of irradiation performance of vendor fuel and HEDL type fuel and indicate if any unanticipated performance characteristics were introduced by the vendor's process. These tests are completed and the results will be available prior to FSAR preparation.

References

- Q241.124- 1 HEDL-TME-75-48, HEDL Steady-State Irradiation Testing Program
- Status Report - February, 1975.

Amend. 34
Feb. 1977

Q241.124-1

Question 241.125 (4.4.2.6)

How is the + 10% thermal conductivity hot channel factor determined? Are variations in density, stoichiometry, etc. included in this number? Is the porosity correction included in this number? List all the factors considered and their values.

Response:

The requested information is provided in amended Section 4.4.3.3.1 and is discussed below:

Effects of Variations in Density:

The + 10% uncertainty in the thermal conductivity does not explicitly account for the variations in the density from the specified nominal value. The CRBRP fuel specification specifies fuel pellet weight per unit length, with nominal fuel density as a percent of theoretical density. This specification in combination with the dimensional specification results in a density requirement of 91.3% + 1.61% TD. This narrow band of density variation will result in an uncertainty of + 5.5% in thermal conductivity. As previously stated, this out-of-reactor difference will be reduced due to in-reactor effects such as restructuring. The adopted 10% hot spot factor was an overall estimate to be used in conjunction with the empirical model based on P-19 data; its adequacy for preliminary analysis was verified by analytically reproducing the P-19 data as discussed in detail in revised Section 4.4.3.2. As mentioned in revised Section 4.4.2.6.5, phenomenological models developed for the LIFE-III code are being incorporated in the fuel thermal analysis and will be used in final design and FSAR preparation. Following incorporation of these models and the availability of final fuel specifications, the uncertainties including the effects of density variation will be re-assessed.

30

Effects of Stoichiometry

Under in-pile conditions, variations in stoichiometry occur across the diameter of the fuel as a result of temperature gradients. Based on the analysis of Rand and Markin (Ref. Q241.125-1) the oxygen to metal ratio (O/M ratio) in the cooler outer region will increase towards the stoichiometric value resulting in an increase in the thermal conductivity value with a concomitant decrease in the hot region.

The thermal conductivity correlation was formulated to be representative of in-reactor fuel which had an original O/M ratio of ~1.96. The lower temperature regions of the correlation were developed using an O/M ratio of 2.00 and the higher temperature region was based on in-reactor experiments which used fuel with an O/M ratio of 1.96.

The important parameter in the fuel thermal analysis is the $\int KdT$ value. Christensen (Ref. 4.4-53) compared the in-reactor heat-ratings to melting ($\int_{\text{melt}} KdT$) for mixed oxide fuel of O/M ratios 2.00, 1.99 and 1.94. The results showed that the melting heat ratings in this O/M range were nearly identical within experimental error. There was essentially no difference between an O/M ratio of 1.99 and 1.94 (note that CRBRP fuel will range between 1.94 and 1.97). Similar studies by Cantley et al. (Ref. Q241.125-2) at GE showed that the effect of fuel O/M on the integrated conductivity to melting ($\int_{\text{melt}} KdT$) was within experimental error. Based on these results, it was concluded that stoichiometry variations in the range of the CRBRP fuel specifications have a negligible effect on temperature calculations.

Effect of Porosity

The recommended + 10% thermal conductivity hot channel factor includes the uncertainty in the porosity correction correlation. The experimental data existing for various fuel densities were originally normalized to a single density using the porosity correction factor. The uncertainties in the thermal conductivity values were then determined and hence the recommended hot channel factor accounts for the uncertainties in the porosity correction factor.

References:

- Q241.125-1. M. H. Rand and T. L. Markin, AERE-R-5560 (1967).
- Q241.125-2. D. A. Cantley, B. F. Rubin and C. N. Craig, GEAP-13935, January 1973.

Question 241.126 (4.4.2.6)

PSAR Table 4.4-20 indicates that certain fuel data values were obtained from the Nuclear Systems Material Handbook, but we are unable to locate these data in the handbook (actually, the handbook does not appear to contain any ceramic fuel data). Please clarify the reference to Nuclear System Material Handbook data.

Response:

The Nuclear Systems Material Handbook Advisory Committee is currently in the process of compiling, reviewing, and approving the data for ceramic fuels. The data supplied and referred to in Table 4.4-20 is the melting temperature data for the fuel and has been approved by the NSMH Ceramic Fuels Working Group as interim data. These approved interim data were sent to the NSMH Advisory Committee in February, 1976 and publication in the Handbook is expected in the near future.

Question 241.127(4.4.2.6.14)

Explain the derivation of the 3σ value of $\pm .92$ kw/ft. on equation 4.4.2.6-13.

Response:

The response to this question is in amended PSAR Section 4.4.2.6.14 and Figure 4.4-55.

Q241.127-1

Amend. 29
Oct. 1976

Question 241.128 (4.4.2.6)

How is equation 4.4.2.6-14 used in the context of CRBRP? Give values of A_1 , A_2 and A_3 .

Response:

The response to this question is found in amended PSAR Section 4.4.2.6.

Question 241.129 (4.4.2.6.16)

List the additional data fit to Dutt's correlation and show predicted versus measured values for a comparison. Also, what was the standard deviation, ρ , for the new correlation, where the correlation coefficient is:

$$\rho = \sqrt{1 - \frac{S_y^2}{S^2}}$$

and
$$S_y^2 = \frac{n}{\sum_i} (\hat{y}_i - y_i)^2 / (n-p)$$

$$S^2 = \frac{n}{\sum_i} (y_i - \bar{y})^2 / (n-p)$$

where n = number of data points;

y_i = observed value of i th data point;

\hat{y}_i = predicted value of i th data point

\bar{y} = average of observed data;

p = number of parameters in model.

Response:

The response to this question is provided in amendment PSAR Section 4.4.2.6.16.

Amend. 30
Nov. 1976

Question 241.130: (4.4.3.2)

Provide a derivation of the equation for T_E on page 4.4-25. Discuss how the various quantities in the equation are calculated.

Response:

The information requested is provided in revised Section 4.4.3.2.

Question 241.131 (4.4.3.2.)

The response to question 241.43 lacks sufficient detail. The response contains information on the combination of hot channel factors but it is not clear what data or analyses were used to obtain the hot channel factors. For instance, the fuel thermal conductivity hot channel factor does not state which data were used or how the data were manipulated to obtain a hot channel factor of 1.1.

Response:

A detailed discussion of the fuel thermal conductivity hot spot factor was reported in response to question 241.125.

As regards the first part of the question, i.e., "what data or analyses were used to obtain the hot channel factors", they were discussed in topical report WARD-D-0050. This information is again summarized in the following for all the hot spot factors listed in Table 4.4.2. Before going into the point-by-point discussion, it should be mentioned that these hot spot factors are preliminary and are continually being refined.

1) Power Level Measurement and Control System Dead Band

This factor accounts for the specified power measurement error plus the set dead band. The value reported in PSAR is currently being updated for Plant Expected Conditions, following detailed Monte Carlo type analyses.

2) Inlet Flow Maldistribution

This factor is an engineering estimate based on FFTF experience. The same value was used in PWR early analyses and was found to be overly-conservative (present PWR's FSARs have an inlet flow maldistribution hot channel factor equal to 1.01). Data from CRBR hydraulic tests and additional detailed analyses have become available since PSAR preparation, thus, this value is currently being re-evaluated.

3) Assembly Flow Maldistribution Calculational Uncertainties

This factor is a conservative engineering estimate based on analytical evaluation of numerous rod bundle tests. Since PSAR preparation, a very systematic, detailed statistical study has been completed by comparing and calibrating the code CØTEC against experimental data. The data examined included: 217-pin HEDL water test, ANL 91-pin salt and hot water tests, 19-rod bundle sodium test in FFM, the very recent 11:1 air flow test conducted at Westinghouse Research Laboratories, MIT 61-pin test, etc. Following this study, an optimized set of empirical parameters to be used in CØTEC analyses for CRBR was recommended along with uncertainties affecting CØTEC predictions. Typical CØTEC calculations were also compared against parallel CØBRA, THI-3D and ENERGY predictions. The value reported in the PSAR is therefore being reassessed.

4) Physics Calculational Methods and Control Rod Effects

Discussions are provided in PSAR Section 4.3.2.2. These uncertainties are currently being updated.

5) Cladding Circumferential Temperature Variation

This was calculated employing the FATHØM-II code. FATHØM-II calculations showed excellent agreement (Reference 25, PSAR Section 4.4) with published results of similar studies (References 21 and 22, PSAR Section 4.4). Since PSAR preparation, the more advanced FATHØM-360 code was developed and made operational. Re-evaluation of this factor is therefore in progress.

6) Inlet Temperature Variation

See Item 1. It should be noted that this hot channel factor applies only to Plant Expected Conditions and is not used in safety and transient analyses, which are based on Plant T&H Conditions.

7) Reactor ΔT Variation

See Item 6.

8) Nuclear Data

See Item 4.

9) Fissile Fuel Maldistribution

See Item 4. Current CRBR fuel manufacturing specifications confirmed that this factor was under-estimated for the coolant enthalpy rise factor (see discussion in WARD-D-0050). A value of 1.03 is being used in present analyses.

10) Wire Wrap Orientation

Value based on analyses performed with the CØTEC code for all combinations of wire wrap orientations. The quoted value, even though small, is conservative, since CØTEC slightly over-predicts the peripheral flow component.

11) Subchannel Flow Area

Value based on analyses performed with the CØBRA code accounting for bowing and worst stackup of tolerances leading to maximum channel closing. Re-evaluation and updating of this factor is in progress.

12) Film Heat Transfer Coefficient

Value based on analysis reported in WARD-D-0034.

13) Pellet-Cladding Eccentricity

Value based on Reference Q241.131-1 analyses. The factor is currently being reassessed following availability of the LIFE-III code for calculation of gap size and conductance.

14) Cladding Thickness and Conductivity

Value calculated from uncertainty on published data combined with tolerances effect.

15) Gap Conductance

Discussed in detail in response to several NRC questions (see, for example, 241.114).

16) Fuel Thermal Conductivity

Based on published data uncertainty, as discussed in response to PSAR question 241.125.

17) Coolant Properties

Uncertainty on adopted sodium properties (Reference 2, PSAR Section 4.4).

References

- Q241.131-1 R. Nijssing, "Temperature and Heat Flux Distribution in Nuclear Fuel Element Rods", Nucl. Eng. and Design, 4, pp. 1-20, 1966.

Question 241.132 (4.4.3.2.)

It is a staff position that the values of the hot channel factors cannot be accepted until the computer codes used to obtain these factors and the experimental data and fabrication data used to obtain these factors have been reviewed and approved by the staff. This can be done during the review of the CRBRP FSAR.

Response:

The preliminary bases for hot channel factors philosophy, method of combination and quantitative value are discussed in topical report WARD-D-0050 referenced in the PSAR. Hot channel factors evaluation is continually updated following availability of new experimental data, development of new analytical techniques or improvement of existing ones, better characterization of plant operating parameters, finalization of fabrication process, etc. Therefore, periodic revisions of the topical report will be issued to reflect updating of the hot channel factors.

Question 241.133(4.4.3.3)

In topical report WARD-D-0054, page 17 (Reference 16, Section 4.4 of the PSAR), the amount of γ energy deposited in structure and coolant is considered in the calculated power-to-melt. Was this taken into account in determining the power in P-19 and P-20 experiments? If so, what value was used for the heat generation in materials other than the fuel? How was this number determined for the P-19 and P-20 experiments? How is the number calculated in the design? Does the number change with burnup? Is the change with burnup accounted for? When monitored in the plant for comparison with the limit, what value will be monitored, the total or the fuel power?

Response:

The distinction is made in topical report WARD-D-0054 between pellet linear power rating (which accounts for only the power produced in the fuel pellet by either fission or γ -production) and rod linear power rating (which also includes γ -energy deposited in structure and coolant). Assessment of the margin between maximum operating conditions and limiting power-to-melt should be based on the pellet power rating, as recommended in WARD-D-0054. Most importantly, however, both operating conditions and limiting power-to-melt shall be calculated on the same basis; for this reason, PSAR Section 4.4 and WARD-D-0054 report the core mapping of the maximum (3σ plus over-power) linear power rating for both pellet and rod.

P-19 powers were adopted by HEDL on the basis of calculations performed by ANL/EBR-II (Ref. Q241.133-1). In ANL calculations, the distinction was made between fission and γ -heating; however, γ -heating occurs in the fuel as well as in the structure and coolant and no distinction in this respect was made. P-20 powers were normalized on P-19 powers (Ref. Q241.133-2). Therefore, P-19 and P-20 powers were calculated from the total assembly power and thus, represent rod, rather than pellet, limiting power-to-melting. In conclusion, calculated rod linear power ratings shall be compared against P-19 (and P-20) experimental power-to-melt; since the amount of γ -heating outside the fuel pellet is only of the order of 3%, a substantial positive margin exists as discussed in the PSAR and in response to question 241.127.

The gamma and fission heating distributions in CRBRP are determined using two-dimensional diffusion theory techniques with coupled neutron-gamma cross sections. These techniques are verified by comparison against measurements in the ZPPR critical as described in PSAR Section 4.3.2.2 for the power (fission) distributions. In the core, the gamma and fission heat deposited external to the fuel pellet (in the cladding, wire wrap, coolant and duct) ranges from 2-3% of the total power, as previously mentioned. The fraction of power generated within the fuel pellets is therefore 97-98% of the total power; the change of this value with burnup is within the specified range.

In CRBR operation, total power will be monitored; assembly exit instrumentation (thermocouples) will indirectly monitor the total power in individual assemblies, while neutron flux monitors will verify the total reactor power.

References

- Q241.133- 1. L.B. Miller, et al., "Characterization of the Power in an Experimental Irradiation Subassembly of Mixed-Oxide Fuel in EBR-II", ANL/EBR-047, September, 1971.
- Q241.133- 2. R.B. Baker, R.D. Leggett and D.S. Dutt, "Interim Report: Effect of Burnup on Heat-Rating-to-Incipient Fuel Melting -- HEDL P-20", HEDL-TME-75-63, 1975.

Question 241.134 (15.1.2)

"Validation" of the CDF technique and its ability to preclude fuel-pin failures is discussed on page 15.1-64, Section 15.1.2.1 (Amendment 2). Please present more detail on how the EBR-II and TREAT irradiation results will be used. Be more specific regarding scope and schedule; i.e., relate the schedule to the CRBR licensing schedule. Discuss fall-back positions should the CDF technique prove non-verifiable.

Response:

As they relate to the validation of the CDF technique, the EBR-II and TREAT test data will be utilized in the manner described on PSAR pages 15.1-63 and 15.1-64. The schedules for these tests and their relations to submittal of the FSAR are given in References Q241.134-1 and 2.

If, on the basis of the EBR-II and TREAT data, the CDF technique proves to be non-verifiable, the following fallback positions, in order of preference, are available:

1. Develop a new analytical technique based on a statistical approach consistent with the requirements outlined in PSAR Table 15.1.2-1;
2. Reduce the allowable CDF value downward from unity;
3. Adopt completely the strain limit criterion.
4. Develop a new design criterion.

References:

- Q241.134-1. TC-573, "Reference Fuel Steady-State Irradiation Program Plan, Revision 1", March, 1976.
- Q241.134-2. "Summary of CRBRP Transient Testing Portion of the Plan for the National LMFBR Mixed Oxide Fuel Transient Performance Program", April, 1976.

Q241.134-1

Amend. 29
Oct. 1976

Question 241.135 (15.1.2)

It is stated on PSAR page 15.1-55 that "the fuel, blanket and absorber rods must operate under expected steady state conditions, must be capable of sustaining all anticipated transients (operational incidents), must be capable of surviving one minor incident (emergency event) without loss of cladding integrity, and must be capable of surviving one major incident without loss of core coolability." Disregarding the clad strain limit arguments, are there data to support no loss of cladding integrity up to maximum emergency event cladding temperature of 1600°F?

Response:

This question is addressed in Part I of the response to Question 241.85; in particular, see Figure Q241.85-1 in that response. This figure clearly shows that the conservatively estimated CRBRP fuel pin cladding stress during a design basis undercooling emergency event at 411 EFPD is well below FCTT failure data obtained with clad sections from fuel pins from NUMEC F, PNL-10 and PNL-11.

Amend. 30
Nov. 1976

Question 310.1 (3.5)

The set of tornado missiles and corresponding impact velocities in Table 3.3-1 do not conform with the spectrum of missiles currently used by the staff and described in WASH-1361.

An acceptable degree of protection against tornado missiles will be attained by designing the Clinch River plant to withstand the impact of the following missiles.

A - Wood plank	4" x 12" x 12'	200 lb	420 fps
B - Steel pipe	3" ϕ , 10' long, schedule 40	78 lb	210 fps
C - Steel rod	1" ϕ x 3' long	8 lb	310 fps
D - Steel pipe	6" ϕ , 15' long, schedule 40	285 lb	210 fps
E - Steel pipe	12" ϕ , 15' long, schedule 40	743 lb	210 fps
F - Utility pole	13.5" ϕ x 35' long	1490 lb	210 fps
G - Automobile	20 ft ² frontal area	4000 lb	100 fps

These missiles are to be considered as striking in all directions. Missiles A, B, C, D, and E are to be considered at all elevations and Missiles F and G at elevations up to 30 feet above all grade levels within 1/2-mile of the facility structures.

Alternatively, we have found, based on an interim review of TVA's Topical Report TVA-TR74-1, that the use of their no-tumbling horizontal velocities in addition to a 4000-lb automobile at 70 mph forms an adequately conservative design basis. Vertical velocities equal to 80% of the TVA no-tumbling horizontal velocities will also be acceptable. These velocities are summarized in Table 1.

It is also stated in the PSAR that ~~separation~~ of redundant components is used as a method of protection against tornado missiles. The staff, however, does not consider this an acceptable method of protection. Provide a list of the systems or components that fall under this category and indicate new means of protection.

TABLE 1
 TORNADO MISSILE VELOCITIES ACCEPTED IN PRELIMINARY
 EVALUATION OF TVA-TR74-1

			<u>Horizontal Velocity</u>	<u>Vertical Velocity</u>
A - Wood plank	4" x 12" x 12'	200 lb	368 fps	294 fps
B - Steel pipe	3" ϕ , 15' long, schedule 40	115 lb	268 fps	214 fps
C - Steel rod	1" ϕ x 3' long	8 lb	259 fps	207 fps
D - Steel pipe	6" ϕ , 15' long, schedule 40	300 lb	230 fps	184 fps
E - Steel pipe	12" ϕ , 30' long, schedule 40	1500 lb	205 fps	164 fps
F - Utility Pole	14" ϕ x 35' long	1500 lb	241 fps	193 fps
G - Automobile	20 ft ² frontal area	4000 lb	100 fps	80 fps

Missiles A, B, C, D, E, and F are to be considered at all elevations and missile G at elevations less than 30 feet above all grade levels within 1/2 mile of the facility structures.

Response:

Table 3.3-1 has been revised to indicate that CRBRP will be designed to withstand the impact of the tornado missiles listed in WASH 1361.

In response to the second part of the question, there is no statement in the PSAR such that "separation of redundant components is used as a method of protection against tornado missiles", as stated in the Question. Nor does CRBRP presently have any safety-related redundant components relying upon "separation" alone for protection against tornado missiles.

It appears that what gave rise to this second part of the question could be an interpretation of the "Protection Method" No. 3 of the seven methods delineated under Design Basis 3, Section 3.5 of the PSAR (page 3.5-1). The description of this protection method is recapitulated below:

- "3. Separation - Sufficient separation of redundant systems or complete train separation of components in a safety network so that a potential missile cannot damage both redundant systems and prevent safe shutdown of the reactor plant."

As stated immediately below Design Basis 3, "Method of Protection", on p. 3.5-1 of the PSAR,

"Protection against a potential missile may be provided by, but not necessarily be limited to, any one or combination of the following methods".

Of the seven protection methods identified (PSAR pages 3.5-1 and 3.5-2), it is not intended that Method No. 3 alone will be used for protection of redundant components against tornado missiles, although it may be proper and adequate for protection against certain other types of missiles, such as "internal" missiles.

Question 310.2 (3.5)

Given (a) a design overspeed turbine failure, and (b) a destructive overspeed failure, provide an analysis which evaluates the overall probability of a high trajectory turbine missile (from LP stages) strike with respect to the plant vital systems. Vital system targets should include all plant structures and equipment whose damage could lead to significant radiological consequences. This should include direct effects (e.g., damage to vital systems, spent fuel, etc.) and indirect effects (e.g., control room).

List in tabular form the following information:

- a. Vital system target name (e.g., control room, diesel generators, etc.).
- b. Horizontal target area - in the case of a control room or containment this would correspond to the roof area. For vital systems and components within the building subcompartments, an area smaller than the total roof may be appropriate.
- c. Horizontal barrier thickness - itemized list of one or more horizontal barriers protecting vital systems in terms of thicknesses and material properties (e.g., 18 inches of 5000 psi concrete, 1/4" steel plate, etc.).
- d. Separation distance - where vital system targets are redundant, the physical separation between the systems should be indicated.
- e. Turbine missile characteristics in terms of size, shape, and turbine exit speed ranges for design and destructive overspeed.
- f. Strike probabilities with respect to each vital system target roof area for design and destructive overspeed missiles.
- g. Penetration probability of each vital roof area for design and destructive overspeed missiles (provide and justify the penetration formulas used.).

Response:

The response to this question is provided in revised PSAR Section 10.2.3.

Question 310.3 (6.4)

Describe the physical location of the outside air intakes for the control room ventilation system. Indicate the locations on plant layout drawings (plan and elevation views).

Response:

49 | The interim response to this question stated that the need for a second
59 | Control Room air intake would be evaluated based upon the radiological
dose rates, Control Room leakage rate, plant effluent release point locations
and site meteorological conditions. To insure Control Room habitability
following extremely low probability accidents which are beyond the design
basis, two widely separated intakes are provided. One Control Room
air intake will be located at the SW corner of the Control Building roof
at approximately elevation 880' and the other one will be located at the
NE corner of the Steam Generator Building Auxiliary Bay wall at approximately
elevation 858'. The selected air intake locations are based on the following:

- 59 |
- (1) Control Room Filter Units
 - (a) 500 CFM outside air intake through charcoal/HEPA filter train for 1/4 inch W.G. Control Room pressurization.
 - (b) 8,500 CFM Control Room air recirculation through same charcoal/HEPA filter train, as (a) above.
 - (c) Redundant charcoal/HEPA filter trains with 95% charcoal and 99.97% HEPA filter efficiencies.
 - (2) Two door vestibules for all Control Room exits/entrances.
 - (3) 3 CFM unfiltered air infiltration based on Item 2 above.

The following new and revised sections, tables and figures indicate revisions to the design basis of the Habitability System, the addition of redundant toxic chemical and smoke detectors in the Control Room air intake duct, the increase in size of the Control Room filter trains, the deletion of water sprays for the charcoal filter banks, and the conformance to Regulatory Position 4d of Regulatory Guide 1.52:

- (a) Revised Section 6.3.1.1
- (b) Revised Section 6.3.1.2
- (c) Revised Section 6.3.1.3
- (d) Revised Section 6.3.1.5
- (e) Revised Table 6.3-1
- (f) Revised Section 9.6.1.2

- (g) Revised Section 9.6.1.3.1.
- (h) Revised Section 9.6.1.3.4.
- (i) Revised Table 9.6-1
- (j) Revised General Arrangement Drawing 1.2-72.

22 | 50

Question 310.4 (6.4)

Identify all toxic materials that may be stored on or in the vicinity of the site, as well as those that may be transported in significant quantities on nearby roads, waterways, rails, or pipelines. Apply Regulatory Guides 1.78 and 1.95 in evaluating the severity of accidents involving toxic gas releases and the steps taken to mitigate their consequences with respect to control room operators.

Response:

Information concerning the storage of toxic chemicals in the vicinity of the site, the evaluation of the severity of accidents involving toxic gas releases and the steps taken to mitigate the consequences of such accidents to control room operators is provided in Section 6.3.1.6.2 and Table 6.3-3.

25

Question 310.5 (6.5)

The discussion in Section 6.3.1.2 on the emergency operation of the control room ventilation system does not identify explicitly the mode of system actuation. It is our position that the Control Room emergency ventilation mode should be initiated automatically by appropriate accident signals including signals from redundant radiation detectors in the outside air intakes. Clarify this matter and also indicate the physical location of the radiation detectors, as well as their location on a schematic, such as Figure 9.6-20.

Response:

49 | The initiation of the Control Room HVAC System emergency operation is described in the revised Section 9.6.1.2.1. The locations of the radiation detectors are identified on revised Figure 9.6-1. The updated Section 12.2.4 describes the airborne radioactivity monitoring. Figures 12.1-1 through 12.1-19C illustrate the location of the airborne radiation monitors for the plant. The Control Room radiation monitoring is described in Section 11.4.2.2.

Question 310.6 (6.3)

Provide an estimate of the free air space volume serviced by the control room emergency ventilation system.

Response:

The response to this question is provided in Section 6.3, Table 6.3-2, "Free Air Space Volume Serviced by the Control Room Emergency Ventilation System".

Question 310.7 (3.5)

The "Observation Room Plan Above El. 831'-0" shown in Figure 1.2-37 is insufficient for evaluating the control room layout. Provide plan and elevation views of the control room. Indicate all doorways, stairs, elevators and other major openings which are on the boundary of the control room emergency ventilation system. Indicate the placement of major control room items, such as control consoles.

Response:

A plan view identifying the control room layout is provided on new Figure 1.2-43, Control Building General Arrangement Plan Elevation 794'-0" and 816'-0". An elevation view of the control room is provided on new Figure 1.2-44, Control Building Section A-A and Section B-B.

Question 310.8 (3.5)

Provide ingress/egress dose and supporting analyses with respect to control room operations when changing shifts under accident conditions. The analysis should include source terms as the direct radiation source from the distribution of noble gases, halogens, fission products, and activated sodium.

Response:

Section 6.3.1.3 has been expanded to incorporate the requested information.

| 25

Question 310.9 (6.3)

In Section 6.3.1.1, the radiation source for control room dose analysis is described in terms of "100% noble gases and 1% of all other fission products." However, later in the same section, reference is made to the "Control Room Design Source" of Section 12.1.3, which is described as consisting of noble gases, halogens, volatile solids, and remaining fission products. It is not apparent that the two source descriptions are consistent. Furthermore, it is not evident whether Na^{24} has been included in the accident dose calculations for the control room operators. Provide additional discussion clarifying the above including a tabulation of the nuclide quantities in each source term.

Response:

For the Reference Design, the Control Room shielding design radioactive source term is a third level design requirement; provided to extend the plant capability beyond that necessary to accommodate the Extremely Unlikely Faults included in the Reference Design.

Although the wording used in various sections of the PSAR to describe the Control Room shielding design source term is slightly different, the intent of the requirement has been applied consistently. To clarify the requirement, elaboration is provided in expanded Section 6.3.1.1.

25

Question 310.10 (6.4)

Given a significant sodium release (e.g., the rupture and spill of a sodium storage tank) describe the effectiveness of the control room habitability systems in protecting the control room operators against the direct and indirect effects of the sodium (e.g., sodium fire, sodium aerosol, sodium-concrete reactions). Also, consider the case of tank ruptures caused by external missiles (tornado or turbine missiles) which may breach barriers as well as cause tank failures.

Response:

Information concerning the effectiveness of the control room habitability systems in protecting the control room operators against the direct and indirect effects of sodium is provided in Section 6.3.1.6.1.

25

Q310.10-1

Amend. 25
Aug. 1976

Question 310.11 (15.1)

Present the radiological consequences of all transients and accidents producing a turbine trip with and without the assumption of a loss of offsite power.

Response:

The data requested is provided in revised Sections 15.3.1.5.2 and 15.3.1.5.3.

25

Question 310.12 (15.1)

The method used for calculating the radiological consequences of sodium spills (15.6) is not acceptable. It should include a tabulation of the fission products released to the containment volume. If it is assumed that any of these fission product isotopes are partially retained in the liquid sodium, finite partition coefficients should be stated and justified for each element. For spills outside the primary containment, all assumptions concerning the isolation, ventilation, or leakage of the receiving building must be stated and justified.

Response

For the analysis of sodium spills in Section 15.6 of the PSAR, it was assumed that all of the airborne activity in a cell from the spill is due to the sodium oxide aerosol produced from sodium burning. The radioisotopic activities ($\mu\text{Ci/gm}$ sodium) in the aerosol are assumed equal to the activities in the liquid sodium pool. It is implied in the analysis that the fission product release from the bulk sodium pool is negligible compared with the release from the airborne sodium oxide aerosols.

The bulk of experimental work on fission product release from sodium during a sodium fire is being done at Atomics International (AI). Recent experimental results at AI for burning of 1000^oF sodium containing I-131 in a one cubic meter test cell are as follows: the ratio of

$$\frac{\mu\text{Ci I-131}}{\text{gm Na in air}} \text{ to } \frac{\mu\text{Ci I-131}}{\text{gm Na in pool}} \text{ is } 2.6 \text{ (Reference Q310.12-1)}$$

Independently, S. Kitani measured the release of I-131 and sodium from pool fires in air in a one cubic meter chamber and obtained similar results. (Reference Q310.12-2) For uranium release, experimental work at AI has indicated negligible release fractions of uranium for burning of 10 gms of sodium containing 0.1 gm uranate and a uranium release fraction of 0.1% for burning of 20 gms of sodium containing 0.2 gm uranate. The release fraction of sodium in these experiments was 5%. (Reference Q310.12-1). More recent experiments at AI have shown that the plutonium release from burning sodium is very small; nine experiments resulted in an average plutonium release fraction from burning sodium of 1×10^{-5} (Reference Q310.12-3).

The assumption of equal concentrations of the isotopes in the aerosol and the bulk pool should be conservative when applied to non-volatiles which do not tend to concentrate at the gas liquid interface as the volatiles do. (Reference Q310.12-4) In fact, if the non-volatiles behave as uranium, then their aerosol concentrations will be well below the assumed value.

From the results of the aforementioned AI experiments, it is possible that the activity concentration of iodine and volatile fission products (cesium) may be higher in the aerosol than in the sodium pool. However, in the response to Q310.50, the current methodology for evaluating sodium fires used in the PSAR (equal aerosol and liquid concentration) is shown to provide ample margin for such potential preferential releases of iodine and cesium.

The other source of activity release from sodium fires other than from aerosol formation is from the partitioning of each of the radionuclides between the bulk sodium and air. It has been shown experimentally by Hart and Nelson (Reference Q310.12-5) that release of volatile fission products from a sodium pool at 1500°F to an inert cover gas is small. Release fractions were on the order of 10^{-4} for Cs and Rb, 10^{-6} for I, and 10^{-7} for Sr and Ba. In-pile experimental results from Kunkel, Elliott, and Gibson give release fractions on the order of 10^{-5} for I, and 10^{-4} for Cs, Ba, La.. (Reference Q310.12-6) The release fractions for non-volatiles from sodium based on the above would be so small that the pool release would not add significantly to the aerosol component. However, as the response to Q310-50 shows, these measured release fractions are based on equilibrium-vaporization experiments not directly applicable to the evaluation of sodium fires, and, in any event, the measurement of activity releases in the burning-release experiments reflect the total (aerosol transport and vapor partitioning) release associated with pool burning conditions.

The total release of radionuclides to the containing cell for each accident in 15.6 is given below. These numbers are based on the assumption of equal aerosol-liquid concentrations, which is shown to provide a conservative radiological assessment in the response to Q310.50.

Accident 15.6.1.1: Primary Sodium In-Containment Storage Tank Failure During Maintenance

<u>Nuclide</u>	<u>Release to Cell (curies)</u>	<u>Nuclide</u>	<u>Release to Cell (curies)</u>
Na 24	7.68	Ru 106	0.828
Na 22	26.8	Rh 106	0.828
Cs 137	1221.	Ba 140	0.550
Cs 136	178.2	La 140	0.550
Cs 134	33.1	Ce 141	0.924
Sb 125	7.09	Ce 143	0.481
I 131	327.	Ce 144	0.654
Te 132	5.83	Pr 144	0.654
I 132	58.3	Pr 143	0.482
Te 129m	8.66	Nd 147	0.201
Te 129	8.66	Pm 147	0.375
Sr 89	1.40	Pu 238	0.231
Sr 90	0.995	Pu 239	0.064

<u>Nuclide</u>	<u>Release to Cell (curies)</u>	<u>Nuclide</u>	<u>Release To Cell (curies)</u>
Y 90	0.995	Pu 240	0.083
Y 91	0.407	Pu 241	7.00
Zr 95	0.768	Pu 242	1.77-4*
Nb 95	0.768	H-3	33.1
Ru 103	1.07	Co 60	4.08-2
		Co 58	7.64-2
		Mn 54	0.302

*1.77-4 = 1.77×10^{-4}

Accident 15.6.1.2: Failure of the Ex-Vessel Storage Tank Sodium Cooling System During Operation

<u>Nuclide</u>	<u>Release to Cell (curies)</u>	<u>Nuclide</u>	<u>Release to Cell (curies)</u>
Na 24	0.100	Pu 238	5.38-5
Na 22	4.42-3*	Pu 239	1.43-5
Cs 137	0.260	Pu 240	1.84-5
Cs 136	4.08-3	Pu 241	1.25-3
Cs 134	2.59-3	Pu 242	4.02-8
I 131	9.13-3	H 3	5.20

* 4.42-3 = 4.42×10^{-3}

Accident 15.6.1.3: Failure of Ex-Containment Primary Sodium Storage Tank

<u>Nuclide</u>	<u>Release to Cell (curies)</u>	<u>Nuclide</u>	<u>Release to Cell (curies)</u>
Na 124	1.06-2*	Ru 106	1.15-3
Na 22	3.73-2	Rh 106	1.15-3
Cs 137	1.70	Ba 140	7.66-4

* 1.06-2 = 1.06×10^{-2}

<u>Nuclide</u>	<u>Release to Cell (curies)</u>	<u>Nuclide</u>	<u>Release to Cell (curies)</u>
Cs 136	0.248	La 140	7.66-4
Cs 134	4.60-2	Ce 141	1.28-3
Sb 125	9.86-3	Ce 143	6.70-4
I 131	0.455	Ce 144	9.10-4
Te 132	8.11-3	Pr 144	9.10-4
I 132	8.11-2	Pr 143	6.70-4
Te 129m	1.20-2	Nd 147	2.79-4
Te 129	1.20-2	Pm 147	5.22-4
Sr 89	1.95-3	Pu 238	3.21-4
Sr 90	1.38-3	Pu 239	8.90-5
Y 90	1.38-3	Pu 240	1.16-4
Y 91	5.66-4	Pu 241	9.74-3
Zr 95	1.06-3	Pu 242	2.47-7
Nb 95	1.06-3	H 3	4.60-2
Ru 103	1.48-3	Co 60	5.68-5
		Co 58	1.06-4
		Mn 54	4.20-4

* $1.06-2 = 1.06 \times 10^{-2}$

Accident 15.6.1.4: Primary Heat Transport System Piping Leaks

<u>Nuclide</u>	<u>Release to Cell (curies)</u>	<u>Nuclide</u>	<u>Release to Cell (curies)</u>
Na 24	1.26+3*	Ru 106	2.04-3
Na 22	6.52-2	Rh 106	2.04-3
Cs 137	2.95	Ba 140	2.32-3
Cs 136	0.713	La 140	2.32-3
Cs 134	8.06-2	Ce 141	2.74-3
Sb 125	1.72-2	Ce 143	1.93-3
I 131	1.87	Ce 144	1.61-3

* $1.26 + 3 = 1.26 \times 10^{+3}$

<u>Nuclide</u>	<u>Release to Cell (curies)</u>	<u>Nuclide</u>	<u>Release to Cell (curies)</u>
Te 132	0.119	Pr 144	1.61-3
I 132	1.19	Pr 143	1.93-3
Te 129m	2.56-2	Nd 147	9.05-4
Te 129	2.56-2	Pm 147	9.14-4
Sr 89	3.86-3	Pu 238	5.58-4
Sr 90	2.40-3	Pu 239	1.54-4
Y 90	2.40-3	Pu 240	2.02-4
Y 91	1.10-3	Pu 241	1.69-2
Zr 95	2.06-3	Pu 242	4.29-7
Nb 95	2.06-3	H 3	7.97-2
Ru 103	3.06-3	Co 60	9.87-5
		Co 58	1.84-4
		Mn 54	7.29-4

* $1.26 \times 10^{-3} = 1.26 \times 10^{-3}$

Accident 15.6.1.5: Intermediate Heat Transport System Leak

<u>Nuclide</u>	<u>Release to Cell (curies)</u>	<u>Nuclide</u>	<u>Release to Cell (curies)</u>
Na 24	1.18	Ru 106	1.90-6
Na 22	6.08-5*	Rh 106	1.90-6
Cs 137	2.75-3	Ba 140	2.16-6
Cs 136	6.65-4	La 140	2.16-6
Cs 134	7.52-5	Ce 141	2.56-6
Sb 125	1.64-5	Ce 143	1.80-6
I 131	1.75-3	Ce 144	1.51-6
Te 132	1.11-4	Pr 144	1.51-6
I 132	1.11-4	Pr 143	1.80-6
Te 129m	2.39-5	Nd 147	8.44-7

* $6.08 \times 10^{-5} = 6.05 \times 10^{-5}$

<u>Nuclide</u>	<u>Release to Cell (curies)</u>	<u>Nuclide</u>	<u>Release to Cell (curies)</u>
Te 129	2.39-5	Pm 147	8.52-7
Sr 89	3.60-6	Pu 238	5.20-7
Sr 90	2.24-6	Pu 239	1.44-7
Y 90	2.24-6	Pu 240	1.88-7
Y 91	1.03-6	Pu 241	1.58-5
Zr 95	1.92-6	Pu 242	4.00-10
Nb 95	1.92-6	H3	7.44-5
Ru 103	2.86-6	Co 60	9.20-8
		Co 58	1.72-7
		Mn 54	6.80-7

* $1.02-4 = 1.02 \times 10^{-4}$

With regard to spills outside containment, three events fall in the category of spills outside the primary containment. These are:

- (1) Failure of ex-vessel sodium cooling system during operation (Section 15.6.1.2),
- (2) Failure of ex-containment primary sodium storage tank (Section 15.6.1.3), and
- (3) Intermediate Heat Transport System (IHTS) piping leak (Section 15.6.1.5).

The receiving building for the first case is the Reactor Service Building (RSB). For the second and third cases the receiving building is the Intermediate Bay of the Steam Generator Building (SGB/IB).

In all three cases no credit for retention, plate-out, or settling of the aerosol was taken. It was conservatively assumed that all the aerosol generated during combustion was released directly to the atmosphere.

For the third case, operator action to turn off the ventilation fans after five minutes is assumed. Building venting during this initial five minutes was simulated in the SOFIRE-II analysis; however, the ventilation rate (1000 CFM) is relatively small and has little influence on the amount of oxygen available for combustion. The burning rate for this spill falls off very rapidly due to the large ratio of spill area to cell volume which results in a rapid consumption of available oxygen. The SOFIRE-II analysis shows the cell pressure decreases to atmospheric

pressure after eight minutes and terminates any further release from the building. However, all the combustion products from the first eight minutes are assumed to be released directly to the atmosphere with no clean-up action by the ventilating system.

Because the ventilation rate has little influence on the extent of sodium combustion and since no credit for depletion of the sodium aerosol in the ventilation system is taken in the analysis, the predicted consequences of this event, as presented for the PSAR, are judged to be conservative.

References

- Q310.12-1. R. L. Koontz and D. Toppen, "Radionuclide Release From Burning Sodium" presented at the Safety Technology Meeting on Radiological Assessment, July 30-31, 1975.
- Q310.12-2. LMFBR Japanese and American Information Exchange Meeting on LMFBR Safety. Held at Beverly Hilton Hotel in Los Angeles, April 1, 1974.
- Q310.12-3. AI-ERDA-13166, "Quarterly Technical Progress Report: Nuclear Safety, Characterization of Sodium Fires and Fast Reactor Fission Products, October-December 1975", Feb. 15, 1976.
- Q310.12-4. A. W. Castleman, Jr., "LMFBR Safety, I. Fission Product Behavior in Sodium", Nuclear Safety 11, 379, 1970.
- Q310.12-5. R. S. Hart and C. T. Nelson, "Introduction of Cesium, Strontium and Iodine into Sodium", in W. P. Kunkel, "Fission Product Retention in Sodium - A Summary of Analytical and Experimental Studies at Atomics International", NAA-SR-11766, 1966, pp. 11-13.
- Q310.12-6. W. Kunkel, D. Elliott, and A. Gibson, "High Temperature Sodium Studies in KEWB" in W. P. Kunkel, "Fission Product Retention in Sodium - A Summary of Analytical and Experimental Studies at Atomics International", NAA-SR-11766, 1966, pp. 45-46.

Question 310.13 (15.1)

The list of primary coolant activities should include the plutonium concentration expected from the design basis (1%) failed fuel operation. This activity should be taken into consideration for all accidents involving primary coolant release.

Response:

Response to this question is provided in the revised introduction of PSAR Section 15.6. Based on limited data, conservative calculations indicate that for 1% failed fuel a maximum reactor coolant plutonium concentration of 1 PPM was calculated. However, the project has accepted a commitment to limit the plutonium concentration in the reactor coolant to 100ppb.

Question 310.14 (15.1)

The analysis of water-to-sodium leaks in the steam generators (Section 15.3.2.3) should include leak rates up to and including the design basis leak rate from seven failed tubes (which is stated to be the design basis condition in Section 5.5.1). Include the maximum permissible intermediate-to-primary sodium loop leak rate in the analysis of the radiological consequences of this accident. Specify the design basis and technical specification requirements for closure times and leak rates of all isolation valves used for the mitigation of the consequences of this accident.

Response:

Table 5.5-11 presents the calculational results for a number of different steam generator tube failure sequences. Revised Sections 15.3.2.3 and 15.3.3.3 discuss the potential release of radioactive sodium as a result of water-to-sodium leaks.

Isolation valve leak rates are given in Table 5.5-12. The leak rates given in the Table are not technical specifications, but design criteria and are easily met in the types of valves specified for the systems.

Question 310.15 (15.1)

Table 11.1-9 lists the radioisotope inventory in the primary cold traps after 15 years operation. It is noted that no uranium isotopes are included. Please elucidate, in view of Section 3.2, Sodium Cooled Reactors, page 721 of "The Technology of Nuclear Reactor Safety", Vol. 2, which indicates that cold traps remove essentially all of the uranium. Indicate the frequency and method of replacement of the cold trap.

Provide a design basis accident analysis which assumes that this primary coolant cold trap is suddenly ruptured and ignited in air during removal releasing all of the activity to the cell in which the trap is located. Based on the design leak rate of the containment, provide an analysis of the site boundary and low population zone doses.

Response:

The question has been responded to in the following manner:

- (a) Uranium source term for cold traps - response provided in revised PSAR Table 11.1-9.
- (b) Frequency and method of replacement of cold traps - response addressed with response to Q011.7 and provided in revised PSAR Section 11.5.3.
- (c) Design basis accidents for cold traps.
As concluded in the response to NRC ER Question 001.12 (Section 7.1.2.4), which is discussed in ER Amendment II pages 28 through 32, cold trap fires in non-inerted environment cannot occur. Also, PSAR Section 15.7.2.7.2 has been revised to incorporate this discussion.

25

Question 310.16 (9.7)

Section 9.7, Page 9.7-1, indicates that Dowtherm J is used as a coolant in the airconditioning systems located in the containment building and the reactor service building.

- 1) Describe any possible paths for this material to leak into a sodium system.
- 2) Indicate the effects of this compound on sodium and/or heat transfer surfaces within the primary containment system.
- 3) Indicate the effects of high level radiation from the core if this material should enter the primary sodium cooling loop.
- 4) Indicate the effect of this material on the primary cold trap.
- 5) Also discuss the effect of a post-accident high radiation source term on this fluid.

Response:

Since the time that this question was originally asked, chilled water has replaced Dowtherm J as the coolant in the air conditioning systems located in the Reactor Containment Building (RCB) and the Reactor Service Building (RSB) (Amendment 15, April 1976). Dowtherm J is still utilized in certain applications where the requirements of Section 9.7.3 cannot be met for water. These are the service to the fuel handling cell commercial coolers in the RSB and to the primary Na cold trap NaK cooler in the RCB. Section 9.7.4 should be consulted for details.

Individual responses are provided below:

- 1) For a discussion of possible water leak paths into a sodium system, see Section 9.7.3. For Dowtherm J, see Section 9.7.4.
- 2) See Section 9.7.4.
- 3) See Section 9.7.4.
- 4) See Section 9.7.4.
- 5) See Section 9.7.4.

Question 310.17 (15.1)

Table 9.7-4 describes the principal properties of Dowtherm J to have a flash point of 145⁰F and a fire point of 155⁰F. Indicate the location of the coolers within the primary containment and the total quantity of this fluid within the cooling units in this area. In the event of an electrical fire in a containment cooling unit, provide an analysis of the combustion of this material on the safe operation of the nuclear reactor. Indicate the distance from the fan coolers to the large 48-inch diameter containment isolation valves. Evaluate the effects of a Dowtherm J fire on the gasketing material used on these valves and other sealed openings such as personnel and equipment hatches.

Indicate the pressure in the Dowtherm J lines inside the primary containment. Assume that a leak inside primary containment causes a vapor cloud to form. Discuss the effects of a deflagration or of a detonation on the integrity of the containment and safety-related equipment.

Response:

The only Dowtherm J located in the Reactor Containment Building is contained in the secondary coolant loop serving the Primary Cold Trap NaK heat exchanger. The secondary coolant loop components are contained in cell 168 at elevation 752' - 8" (Figure 1.2-10) and serve the primary cold trap NaK heat exchanger in cell 131 at elevation 780' - 0" (Figure 1.2-8). The location of the Dowtherm J containing cells assure that a Dowtherm J fire will not affect the integrity or operation of the containment and other safety related equipment due to their location below the operating floor and remoteness from containment penetrations.

Further design information and parameters are contained in the PSAR Section 9.7.4. The possibility of a vapor cloud and the potential for deflagration or a detonation are discussed in Section 9.7.4. It should also be noted that Table 9.7-4 has been redesignated as Table 9.7-6.

The HVAC system unit cooler and air conditioning motors are mounted external to the metal cabinet housing the coils and fans. The motors are totally enclosed and the wiring is in metal conduit. Leak detectors are provided in each unit to actuate isolation valves to limit the spill to a minor amount and to stop the fan to prevent the spread of Dowtherm J to the surrounding area. The quality and conservative design of the piping together with the location of the electrical equipment and highly sensitive leak detectors precludes any credible Dowtherm J fire resulting from the electrical equipment.

The Recirculating Gas Cooling System (RGCS) cooler motors are totally enclosed and the wiring is enclosed in metal conduit. Any electrical fire would be contained within the motor housing and metal conduit which precludes having a Dowtherm J fire resulting from an electrical fire in the cooler. Additional safety features are:

1. The Dowtherm J heat exchanger is fabricated from 1" continuous tubing which has no joints inside the cooler casing. All joints are made outside the casing thus precluding any credible leak of Dowtherm J in the cooler.
2. Except for the Head Access Area (HAA) cooler, all units serve inerted cells, which, due to lack of oxygen, precludes any fire in these cells.
3. The recirculating atmosphere of all cells (including the HAA) is continuously monitored for Dowtherm J leakage. Upon detection of a Dowtherm J leak, an alarm is sounded and the isolation valves for that cooler actuate to limit the Dowtherm J spill to a minor amount.
4. All inerted cells served by the RGCS are monitored for oxygen content. Presence of oxygen will be alarmed well below the threshold of combustion so that appropriate protective action can be taken.
5. The RGCS system cooler motors are separated from the cooling coils by a metal barrier thus preventing direct impingement on hot motor surfaces in case of a leak.

Even though the HAA unit does not benefit from the added fire protection afforded by the inerted atmosphere, there is still sufficient fire protection redundancy combined with the high quality, conservative design and highly sensitive leak detection to preclude a credible electrical fire in this unit.

In summary all units served by ACFS are adequately protected from an internal electrical fire thus precluding any affect on the operation of the nuclear reactor.

The closest cooler is 26 ft. from the 48" isolation valve. As stated above, quick leak detection and isolation will limit any leak to a minor amount and will be contained. If the leaking Dowtherm J cannot be contained and if the resulting uncontrolled Dowtherm J leak were to be ignited, the extent of the resulting fire would be limited to a small area due to the minor amount of Dowtherm J spilled.

The small area affected by the fire coupled with the distance from the fire to the containment isolation valves and the personnel and equipment hatches ensures that their seals and gaskets will not be affected by the heat generated by the fire. The gaskets will be selected to be compatible with Dowtherm J and its products of combustion.

Question 310.18 (15.1)

Radiological consequences of any accident resulting in releases from the containment should consider the delay time required and the mechanism employed to isolate the containment ventilation system and achieve containment isolation. Provide an analysis of the potential radiological consequences of each accident prior to containment isolation.

Response:

As discussed in the technical specifications, containment isolation will be initiated if sensors in the head access area or H&V ducts indicate activity levels at a to-be-determined fraction of 10CFR20. As indicated in Section 7.3 of the PSAR, the requirement for containment isolation is a delay time of 4 seconds with a 3 second or less detection time. As mentioned in response 310.45, the air transport time between the exhaust sensors and isolation valve is 10 seconds or more. Hence, the volume of air initiating the isolating signal will not be released to the atmosphere.

PSAR accident analysis has taken credit for containment isolation in Section 15.6.1.1 and 15.6.1.4. In either case, as indicated above, the potential consequences of releases will result in conformance to 10CFR20 requirements and are decades below the requirements of 10CFR100.

Question 310.19 (15.1)

Radiological releases resulting from sodium fires in any portion of the containment should be considered as release directly to the environment until containment isolation is assured, and directly to the containment when it is isolated, unless the particular cell to which the release is made has a design leak rate, which is presented in the Technical Specification, and which is tested periodically. Justification for any dilution in the containment atmosphere before release should be presented.

Response:

The containment design basis accident is examined in detail in Chapter 15. A spectrum of postulated in-containment sodium fires has been analyzed. Table 6.2-1 summarizes the results of the analysis for the most limiting fire investigated, which is the Primary Sodium In-Containment Storage Tank Failure during maintenance.

This postulated failure results in the maximum postulated spill of liquid primary sodium in any de-inerted in-containment cell, and thus represents the most limiting fire condition with respect to containment integrity. In this analysis, no dilution is assumed, and the sodium aerosol is released directly to containment. Section 7.3.2.1. of the PSAR indicates that the main exhaust and inlet valves will close in less than 4 seconds after a signal is received. Since the air transport time from the exhaust detector to the valve will be 10 seconds or more and the detection time is three seconds or less, the valves will be closed before the aerosol reaches them. As shown in Table 6.2-1, reproduced on the following page, the potential site boundary doses confirm the ability of the containment isolation system to mitigate the external consequences of this accident.

30

Question 310.20 (15.5)

(Section 15.5.2.4) Release of reactor cover gas from an open floor valve should be assumed to be directly to the environment unless containment integrity and isolation can be assured.

Response:

49 | The response to this questions has been incorporated into amended
Section 15.5.2.4.

TABLE Q310.20-2

OFF-SITE DOSES FROM COVER GAS
RELEASE DURING REFUELING

(Based on on-site Meteorological Tower X/Q's)

	Dose (Rem)	
	SB (2-hr.) (0.42 mi.)	LPZ (30 days) (5.0 miles)
Case 1 - Extremely Unlikely (Release 3 hrs. after shutdown)		
DB (Skin)	1.33	0.085
D _γ (Whole Body)	1.46	0.094
10CFR100	25	
Case 2 - Unlikely (Release 30 hrs. after shutdown)		
DB (Skin)	2.5×10^{-4}	1.6×10^{-5}
D _γ (Whole Body)	1.6×10^{-4}	1.0×10^{-5}
10CFR20	0.5	

Question

310.21
(15.0)

For design basis accident dose calculations, a containment leak rate of less than 0.1% per day at peak accident pressure is not considered acceptable because of the difficulty of establishing lower leak rates by test with sufficient confidence. Provide analyses of all accidents using a containment leak rate of not less than 0.1% per day.

Response

There are two design basis accidents evaluated in the PSAR for which credit for containment isolation and subsequent controlled leakage are taken, namely:

Accident 15.6.1.1, "Primary Sodium In-Containment Storage Tank Failure During Maintenance".

Accident 15.6.1.4, "Primary Heat Transport System Piping Leaks".

For Accident 15.6.1.1, leakage from the RCB to the environment was computed based on the pressure/time history in containment resulting from the postulated sodium fire, and the relationship that leakage is proportional to $\sqrt{\Delta P}$.

For Accident 15.6.1.4, no direct means of containment pressurization is evident. As a conservative allowance for possible variations in atmospheric pressure outside the containment and some heatup of the building atmosphere following shutdown of the ventilation system and containment isolation, a RCB overpressure of 0.5 psig was assumed to exist for the duration of the accident. Using the relationship that leakage is proportional to $\sqrt{\Delta P}$, and the RCB design leak rate, 0.1%/day @ 10 psig, a leak rate of 0.022%/day was computed and used in the analysis.

The potential radiological consequences of each of these events have been re-evaluated assuming containment leakage at its design rate, 0.1%/day, for the duration of the events. Other accident conditions and assumptions pertinent to the analysis are identical to those used in the PSAR.

ACCIDENT 15.6.1.1 - With the assumption of RCB leakage at its design rate, radioactive sodium aerosol release to the environment during specific time intervals is as follows:

<u>Time (hr.)</u>	<u>Mass Na Released (gm)</u>
0 - 2	21
0 - 8	147
8 - 24	292
24 - 96	1014
96 - 720	2070

Aerosol leakage beyond 30 days (720 hrs.) is not expected. Sodium combustion, the source of aerosol, is over at approximately 21 days because of RCB oxygen depletion. The suspended aerosol concentration in containment at 30 days is 3.7×10^{-4} ug/cc; this corresponds to approximately 30 grams of radioactive sodium suspended in containment. To insure the conservatism of the analysis, this remaining 30 grams of sodium was assumed released instantly at the end of 30 days, and added to the 96-720 hour release value of 2070 grams.

The potential 2-hour, site boundary and accident duration low population zone whole body and organ doses resulting from the radioactive sodium release are itemized in Table I. A large margin (greater than a factor of 10^5) exists between each of the potential doses and the applicable guideline limits.

ACCIDENT 15.6.1.4 - With the assumption of RCB leakage at its design rate, radioactive sodium aerosol release to the environment during specific time intervals is as follows:

<u>Time (hr.)</u>	<u>Mass Na Released (gm)</u>
0 - 2	2.4
0 - 8	14
8 - 24	19
24 - 96	12
96 - 720	2.3

The suspended aerosol concentration in containment at 30 days (720 hours) is 3.9×10^{-5} ug/cc; this corresponds to approximately 3 grams of radioactive sodium suspended in containment. To insure the conservatism of this analysis, this remaining 3 grams of sodium was assumed released instantly at the end of 30 days, and added to the 96-720 hour release value of 2.3 grams.

The potential 2-hour, site boundary and accident duration low population zone doses are itemized in Table II. A large margin (greater than a factor of 10^4) exists between each of the potential doses and the applicable guideline limits.

TABLE I

Potential Off-Site Doses Following
 Failure of In-Containment Na Storage Tank
 •RCB Leakage at Design Rate, 0.1%/day, for Accident Duration

Organ	Dose (Rem)*		
	10CFR100	SB (0.42 mi.) 2-hour	LPZ (5.0 mi.) Accident Duration
Skin (Beta)	-	1.05E - 7	6.84E - 8
Whole Body**	25	4.33E - 5	2.82E - 5
Thyroid	300	2.33E - 4	1.52E - 4
Bone	150 ⁺	1.18E - 3	7.68E - 4
Lung	75 ⁺	2.45E - 4	1.59E - 4

* Based on site measured atmospheric dilution factors (X/Q's) per Supplement 1 to Chapter 2 of the PSAR.

** Includes both inhalation and external gamma exposure.

+ Not covered in 10CFR100; used as guideline values.
 E - 7 = 10⁻⁷

TABLE II

Potential Off-Site Doses Following
 Design Basis Primary Heat Transport System Piping Leak
 ●RCB Leakage at Design Rate, 0.1%/day, for Accident Duration

Organ	Dose (Rem)*		
	10CFR100	SB (0.42 mi.)+ 2-hour	LPZ (5.0 mi.) Accident Duration
Skin (Beta)	-	6.51E - 6	2.65E - 6
Whole Body**	25	9.54E - 5	3.88E - 5
Thyroid	300	6.43E - 5	2.62E - 5
Bone	150 ⁺	1.35E - 4	5.49E - 5
Lung	75 ⁺	7.91E - 4	3.22E - 4

* Based on site measured atmospheric dilution factors (X/Q's) per Supplement 1 to Chapter 2 of the PSAR.

** Includes both inhalation and external gamma exposure.

+ Not covered in 10CFR100; used as guideline values.
 E - 6 = 10⁻⁶

Question 310.22 (15.5.2.3)

Releases from the dropped fuel assembly should be assumed as direct to the environment, or direct to the containment if it is isolated, unless a technical specification limit and appropriate testing are planned for leakage from the EVTM (ex-vessel transfer machine).

Response

The release of fission gas for the accident described in Section 15.5.2.3 takes credit for low leakage through the EVTM seals. This small leakage will be assured by a technical specification limit and appropriate leak testing requirement. The technical specification, Section 16.3.10, has been revised.

Question 310.23 (15.7)

(Section 15.7.2.4) Rupture of the RAPS Surge Vessel should assume an instantaneous release of its contents to the atmosphere with no mixing in the cell volume unless technical specifications and appropriate testing procedures are provided for the cell leak rate. The assumption of "50 vol. %/day" is not acceptable for a design basis calculation.

Response:

Credit was taken for cell leakage following a RAPS surge vessel rupture, since a technical specification and testing provision are included as discussed in Section 16.5.8, "Pressure and Leakage Rate Test of RAPS Surge Tank Cell".

Question 310.24 (15.7)

(Section 15.7.3.2). The results of a realistic analysis for an environmental report are not appropriate in preparing a safety analysis of a design basis event. Provide this analysis using conservative assumptions for parameters such as decay time, gap inventory, and number of failed pins. Justify that each assumption represents a reasonable upper bound for the accident in question.

Response:

A conservative analysis is presented in revised PSAR Section 15.7.3.2 for the purpose of demonstrating the inherent safety margins of the spent fuel shipping cask (SFSC) design for the accident in question.

A drop of the SFSC from the maximum handling height in the RSB to the bottom of the cask handling shaft is considered a hypothetical event as discussed in Section 15.7.3.2 of the attached accident description. The postulated SFSC drop height has been assumed as 72 ft.-an assumption containing safety margin relative to the vertical distance from the operating floor of the RSB to the bottom of the SFSC handling shaft (67 ft.)

Calculations have shown that the impact energy of a 72-ft. free fall of the SFSC is limited by the crush strength of concrete. The peak cask deceleration would be about 92 g as compared to the 123 g deceleration (Reference Q310.24-1) the cask would experience impacting an unyielding surface after a 30-ft free drop.

The gap activity is defined in Regulatory Guide 4.2 as 1% of the total activity in the fuel rods. However, for this analysis, it is conservatively assumed that the entire fission gas activity of all fuel rods in the SFSC is released into the cask containment following a hypothetical cask drop. The SFSC for the CRBRP is the same as the one used in the FFTF and has two leak-checked containments. The space between both containments is at a lower than ambient pressure. Both containments are designed to maintain their integrity following the hypothetical 30-ft. drop accident condition. Following cask loading below the FHC, the SFSC is closed and is handled only in the closed-up condition.

The assumptions and results of the analysis are presented in the attachment.

The major assumptions postulate conservatively that:

- (a) The SFSC drops 72 ft. onto a surfade which causes a break of the outer cask containment.
- (b) All volatile fission products from the fuel rods of all fuel assemblies in the cask are released into the inner cask containment, and
- (c) volatile fission products leave the inner cask containment at the maximum allowable leak rate of the inner containment seals, specified in Reference Q310.24-1.

The analysis of radioactivity release from the SFSC is consistent with the corresponding analysis for the EVM as shown in Section 15.5.1.2 as supplemented by the response to question 001.212.

Reference:

Q310.24-1 Safety Analysis Report for LMFBR Spent Fuel Shipping Cask Model I-(182)-1. Aerojet/AMCO Report AMCO-02-R-107, Revision 2, March 1975.

Question 310.25 (15.0)

Provide justification for use of continuous containment purge through large purge lines considering the radiological impact of early releases following a design basis accident (particularly sodium fires) prior to containment isolation.

Response:

As indicated in response to NRC questions 310.18 and 310.19, the integrated system design (air transport time, isolation valve closure time, and sensor location) of the Reactor Containment Building Isolation System insures containment isolation prior to activity releases approaching 10CFR20 guidelines. Sections 7.3 and 6.2.4 of the PSAR present the description and functional design requirements of the Containment Isolation System.

PSAR accident analyses have taken credit for containment isolation in Sections 15.6.1.1 (Primary Sodium In-Containment Storage Tank Failure During Maintenance) and 15.6.1.4 (Primary Heat Transport System Piping Leaks). In either case, as indicated above, the potential consequences of releases will conform to 10CFR20 requirements and are decades below the requirements of 10CFR100. Therefore, use of a continuous containment purge, during normal reactor operation, does not lead to unacceptable consequences to the health and safety of the public even in the event of design basis sodium fire accidents.

Question 310.26 (6.5.3)

Section 9.6.2 indicates that a 48-inch diameter, 50,000 cfm continuous purge is used to cool the reactor containment building during normal operation and to maintain the radioactive gas concentrations at an acceptable level for routine occupancy. It is further indicated that four (butterfly-type) isolation valves (one on each side of the two containment building penetrations), are used for isolation. Indicate the gasketing material for these valves and list its qualifications to withstand thermally hot or burning sodium which might be ejected into the upper area of the containment building.

Response

The supply duct isolation valve inside the Reactor Containment Building is located approximately 40° CCW to the N-S axis of the building at Elevation 858'-0". The exhaust duct isolation valve inside the Reactor Containment building is located approximately 60° CW to the N-S axis of the building at Elevation 847'-6".

No event resulting in postulated ejection of burning sodium onto the operating floor has been identified. However, even if this were to be postulated, it could not reach the isolation valves because of their location.

The Containment isolation valves gasketing material will be based on an assumed conservative temperature of 400°F and on its ability to withstand any chemical reaction with the combustion products of burning sodium.

Question 310.27 (15.1)

Page 15.1-23 indicates that the Control Room shielding design is based on the release of 100% of the noble gases, 1% of the halogens and 1% of other fission products. Describe the basis of the 1% halogen source term. Indicate the maximum quantity of radioactive sodium and list the curie inventory of each radio-nuclide which could be in the containment building following a design basis accident. Provide a plot of gamma radiation level vs. distance from the outer surface of the steel containment building. Describe the basis for not including a concrete building around the steel liner to provide both shielding and protection against external missiles.

Response:

This information has been incorporated in revised Section 15.1.1.3.4.

25

Q310.27-1

Amend. 25
August 1976

Question 310.28 (15.1)

Page 15.6-46 indicates that in the event of a large leak in the IHTS piping, pressure buildup in the cell could be accommodated by strengthening the cell walls or by venting at 700,000 cfm.

Indicate all accidents for the LMFBR where venting is to be used to prevent overpressurization of a cell or structure. Describe the type of filters to be used to reduce the exposure to the outside population. Accident doses resulting from incidents which could be expected to happen with moderate frequency should be shown to result in only small fractions of the 10CFR Part 100 siting guideline exposures.

Response:

As stated in the PSAR (15.6.1.5.3), a large leak in the IHTS piping equivalent to the complete severance of the pipe is not considered to be appropriate as a design basis event. Work is currently in progress to establish a design basis leak for the IHTS system. This effort is expected to result in a conservatively established leak rate which is much smaller than that caused by the complete severance of the pipe. Additionally, the venting rate of 700,000 CFM cited above is based upon a very conservative analysis of the maximum postulated spray rate. The venting rate and cell pressures calculated by this analysis are overly conservative. Once the design basis leak has been established, cell pressures, and venting rates if venting is necessary, will be determined.

As indicated on PSAR Table 15.6-1, the off-site doses resulting from the worst case IHTS spill are all less than 3 percent of the 10CFR100 guidelines.

Question 310.29 (2.1)

Table 1.3-3 compares the 975 Mwt CRBR plant with the 400 Mwt FFTF. Compare the exclusion distance and the low population zone distance for these two plants. Provide a table showing the comparison of CRBR design parameters with the 714 Mwt Monju reactor which more closely compares with the CRBR power level.

Response:

- (a) Comparison with FFTF of the boundaries for dose calculations is provided in revised PSAR Section 2.1.2.2.
- (b) Comparison of the CRBR plant with the 714 Mwt Monju reactor is provided in revised PSAR Table 1.3-3.

Question 310.30 (6.5)

Page 6.2.3 indicates that, as presently envisioned, there is no requirement for a containment atmosphere cleanup system following a fire with sodium (which is radioactive after reactor operation). Provide the basis for determining that such a system is not required.

Response

The most limiting in-containment radioactive sodium fires result from 1) the postulated failure of the Primary Sodium Storage Tank during maintenance, and 2) a postulated Primary Heat Transport System piping leak during operation. A containment atmosphere cleanup system, or some other accident mitigating device, would be necessary if leakage of radioactive sodium aerosol to the environment, resulting from either of these postulated fires, resulted in unacceptable off-site exposures.

The potential consequences of these events have been analyzed in detail and are reported in Section 15.6.1 of the PSAR. The PSAR analyses computed aerosol leakage to the environment as a function of containment over-pressurization. In response to NRC Question 310.21, aerosol leakage to the environment has been re-evaluated based on continuous leakage at the RCB design leak rate. Both of these analyses indicate clearly that the total integrated offsite exposure from the released radioactive aerosol results in potential doses well within (greater than a factor of 10^4) the guideline values of 10CFR100. Since the RCB design leakage rate provides adequate protection to the health and safety of the public, a containment atmosphere cleanup system is not required.

Question 310.31 (15.1)

All assumptions in Appendix D9 concerning the retention of fission products in intact fuel, molten fuel, and sodium must be adequately supported. Reference to experiments simulating LWR LOCA conditions does not constitute adequate justification of arbitrary fission product release fractions. Provide justification for the conservatism of the fission product release and transport assumptions using as a data base those experiments which can be shown to be applicable to the LMFBR accident conditions. Note that the Contamination/Decontamination experiment results are not applied directly to LWR release fraction computations as they are not adequately representative even of LWR meltdown conditions.

Response:

Appendix D has been deleted from the PSAR. Analyses of hypothetical accidents involving significant molten fuel are discussed in CRBRP-3, Volume 2 (Reference 10b of PSAR Section 1.6). Section 4 of that document provides results of a range of radio-nuclide release scenarios that address the concern reflected in this question.

Question 310.32 (6.4 Yellow)

In reference to the question 310.10 response regarding the evaluation of sodium fire effects on control room habitability, the expressed intent of providing the requested information for the PSAR is not acceptable for the purpose of evaluating the PSAR. Review question 310.10 and provide the requested information.

Response:

Information concerning the release of sodium or NaK caused by sodium/NaK tank or pipe rupture by external missiles, or by transportation accidents and the subsequent operation of the control room HVAC system upon detection of the release, is discussed in the response to Question 310.10.

The release of sodium and subsequent sodium fires resulting in the release of sodium combustion products to the atmosphere is described in Section 7.2.1.1 of the Environmental Report. A preliminary analysis was conducted to determine the effect of the release of these products to the atmosphere on the habitability of the Control Room in accordance with Regulatory Guide 1.78. The analysis was based on the following assumptions:

- 59 | a. At the time of the sodium release and start of the fire, any one of the following sensors, which are located in non-inerted cells containing sodium, will initiate an alarm in the Control Room.
- 59 | o sodium leak detectors
 - 59 | o cell temperature detectors
 - 59 | o cell pressure detectors

In addition, sodium combustion product detectors are also provided in the Control Room air intakes and will activate the emergency operating mode of the Control Room HVAC System.

- 59 | b. Upon detection of sodium smoke, the control room HVAC system emergency operating mode functions as follows:
- 59 | • The outside air intake where smoke is detected is isolated
 - 59 | • The control room is pressurized to 1/4" positive pressure
 - 59 | • The air required for the control room pressurization is supplied from the redundant air intake
 - 59 | • A portion of the control room atmosphere is continuously recirculated through one of the two redundant Safety Class 3, 99.97% efficient HEPA filter units at an 8500 CFM rate
 - 59 | • The air required for the Control Room pressurization is also filtered by one of two redundant, Safety Class 3, 99.97% efficient HEPA filter units
 - 59 | • The control room atmosphere is also recirculated through the 85% efficient HVAC system filters contained in the air conditioning units at a 51500 CFM rate.
- 59 | 49 |

- c. The Control Room is provided with double doors. The unfiltered infiltration is estimated to be 3 CFM.

The findings of the preliminary analysis are as follows:

- a. The time required to isolate the normal control room air intake and initiate operation of the emergency control room HVAC system is significantly less than the time between the initiating signal at the source and the time required for the sodium plume to reach the control room intakes.
- b. During the first two minutes after the initiation of the sodium release alarm in the control room the toxicity level in the control room will not exceed the $2\text{mg}/\text{m}^3$ toxicity limit, which is identified in Regulatory Guide 1.78. However, this limit may be exceeded during the course of the accident.

Since the sodium or NaK combustion product concentration may exceed the permissible concentration during the early phase of the accident, but not within the first two minutes, the operability of the control room will be assured by requiring the Control Room operators to use breathing apparatus and protective clothing upon the initiation of the sodium or NaK combustion product alarm in the Control Room. Each operator will be taught to use the breathing apparatus and protective clothing. Practice drills will be conducted to ensure that personnel can don breathing apparatus within two (2) minutes. The time period during which the toxicity limit would be exceeded is anticipated to be relatively short, so that long term operation of the Control Room following the accident can be performed without masks.

The analysis of the sodium fire effect on the control room habitability is continuing as part of the design process and the information presented above will be updated if future results will require a change.

Question 310.33 (App. F)

The following events are postulated in the PSAR for the purpose of evaluating the reactor cavity (RC) radiation source terms:

1. A melt through of the reactor vessel and guard vessel occurs wherein 100% of the core is deposited in the ex-vessel core catcher (EVCC).
2. The molten fuel in the EVCC is covered with the primary sodium that drains out of the reactor vessel and associated primary sodium piping.
3. With the exception of the noble gases (all which are assumed to be released to the sealed head access area), the fission products in the molten fuel are released to and mixed with the primary sodium.
4. The resulting fission product inventory in the RC atmosphere above the sodium is determined on the basis of equilibrium concentration relationships.

It is not clear if the above sequence of events results in the most severe RC source term that can be expected with respect to radiological consequences. For example, if reactor vessel and guard vessel melt through can be postulated to occur with only a fraction of the core fuel participating in the melting, then subsequent drainage of the primary sodium into the RC would leave the remainder of the core in a "dry configuration." Subsequent melting of the "dry" fuel could release fission products directly to the RC atmosphere, bypassing the attenuating effect of the primary sodium.

Re-assess your evaluation and provide a response to address this concern.

Response:

A radiological source term appropriate for the sequence of events leading to a "dry" core, suggested in this question, has been conservatively developed. This response is provided in the context of the thermal margin beyond the design base (TMBDB) design features, since the scenario represented in the question is not within the spectrum of design base accidents. While the analyses referenced herein were performed for the homogeneous core arrangement, the conclusions reached are equally valid for the heterogeneous core arrangement. It is also noted that the EVCC and the sealed head access area are not part of the CRBRP design, and thus were not assumed to exist for the analysis.

The principal release mechanism for this "dry" fuel case would be vaporization of the more volatile fission products as the fuel heats to its melting temperature. An analysis was conducted to determine the rate at which fuel melting would proceed given that the core was left in a "dry" configuration. The analysis assumed complete drainage of the reactor vessel at 1000 seconds (the minimum calculated vessel melt-through time), end of equilibrium cycle decay heating rates, and adiabatic conditions in-vessel after sodium drainage. Under these conditions, the range of times involved in melting assemblies under their own decay power was determined. The average inner core assembly would melt in 8 minutes, the average outer core assembly in 10 minutes, the highest power radial blanket assembly in 32 minutes and the lowest power radial blanket assembly in 90 minutes. The fuel is supported by stainless steel (either the cladding or surface within the vessel on which the fuel

debris has collected). Penetration of the steel would occur at temperatures in the range of the steel melting temperature ($\sim 2500^{\circ}$ F).

The alternative to this continuous downward slumping is eventual solidification of the fuel-clad mixture postulated by assuming sufficient mixing with structural steel such that the mean temperature of the mixture is below the steel melting point. In either instance, the time during which "dry" fuel could be releasing materials in the reactor vessel is limited.

The fission product release from the fuel during the meltdown phase was treated conservatively. Based on the compilation of experimental data on meltdown release fractions presented in Reference Q310.33-1, it was conservatively assumed that 100% of the noble gas, halogen, and volatile (Cs, Rb, Te, Sb, Se) fission products and 1% of the solid fission products were released from the "dry" molten fuel immediately. Because of the extremely low vapor pressure of fuel at temperatures in the range of the melting temperature of steel, the amount of fuel released as a vapor would be insignificant. Thus the source term would not contain fuel.

It was assumed that this source term immediately enters the Reactor Containment Building (RCB). Except for the noble gases, the airborne fission products in the RCB atmosphere would be reduced by plate out and deposition on internal surfaces. The rate of aerosol depletion in the RCB was calculated by the HAA-3B computer code.

During the period from zero to twenty-four hours, reactor containment integrity would be maintained as indicated in Table Q310.33-1 (based on CACECO results). It is noted that the containment conditions would be less severe for this "dry" fuel case than for the "wet" fuel case in which all fuel and fission products are released to the reactor cavity at the time of reactor vessel and guard vessel melt-through. This results since the release of heat producing fission products to the Reactor Containment Building reduces the heat in the sodium pool and, consequently, delays the onset of sodium boiling and the rate of sodium vapor generation.

Leakage of the source term from the RCB to the environment would be by way of the Annulus Recirculation and Filter System. The leakage rate of the source term to the annulus was calculated by the CACECO code. Unfiltered bypass leakage was also considered. The potential radiological consequences of off-site exposure resulting from the dry fuel scenario are compared with the corresponding consequences of the wet fuel case in Table Q310.33-2. Atmospheric dispersion factors used were the fiftieth percentile x/Q values based on site measured data. Although the doses for the "dry" case are higher than for the wet fuel case, the conclusion that the doses are acceptably low is not changed.

References

Q310.33-1 WASH-1400, Appendix VII, "Release of Radioactivity in Reactor Accidents" (Draft August 1974).

TABLE Q310.33-1

Comparison of RCB Atmosphere Conditions at 24 Hours
for "Wet" Fuel Case and "Dry" Fuel Case

	<u>"Wet" Fuel Case</u>	<u>"Dry" Fuel Case</u>
Temperature (°F)	495	310
Pressure (psig)	16	8
% H ₂	1	0

TABLE Q310.33-2

COMPARISON OF POTENTIAL OFF-SITE EXPOSURES
for "Wet" Fuel Case and "Dry" Fuel Case

		<u>Doses in REM</u>	
		<u>"Wet" Fuel Case</u>	<u>"Dry" Fuel Case</u>
2 Hour E. B.	<u>Organ</u>		
	Bone	0.027	0.029
	Lung	0.0029	0.109
	Thyroid	0.0017	5.75
	Whole Body*	0.16	0.26
24 Hour LPZ	Bone	0.020	0.028
	Lung	0.0024	0.11
	Thyroid	0.0059	5.33
	Whole Body*	0.099	0.16

* Includes: Inhalation, external gamma cloud, and direct gamma shine

Question 310.34 (2.2.3)

The Oak Ridge Reservation Land Use Plan (ORO-748, August 1975) indicates possible uses of land near the CRBRP site not presently identified in the PSAR.

Examples of new facilities being considered for location in the vicinity of the CRBRP site are found on the following pages of the aforementioned report:

Page 20	Gas-Centrifuge Plant
Page 22	Fusion-Research Type Experimental Power Reactor
Page 23	Hydrogen-Protection Process Development Plant
Page 23	Demonstration Plant for Bioconversion of Wastes to Fuel Gases
Page 39	Spent Fuel Reprocessing Plant
Page 39	Pipeline Corridor
Page 41	Airstrip

The considerations that should be addressed in the PSAR in describing new facility/land use requirements are as identified in Sections 2.2.1 through 2.2.3 of NUREG-75/087, (Standard Review Plan).

Describe in the PSAR the requirements that have or will be established to assure that potential new activities on ERDA controlled land will not pose an undue risk to the continued safe operation of the CRBRP.

Response:

New Facility/Land Use Section 2.2.3 has been added to Section 2.2 in response to this question.

Question 310.35 (2.1)

On the basis of the information presently in the PSAR, we find that U.S. Government ownership and TVA custodianship of the site constitutes adequate control over all activities as required by 10 CFR Part 100. However, to complete our evaluation, provide a clarification in the PSAR of the distinction, if any, between the site area and the exclusion area. Provide a suitability scaled map which indicates the boundaries of each if they are not identical. Indicate the relationship of the Clinch River Consolidated Industrial Park (CRCIP) to each of these areas; also indicate for each of the 16 sectors of the compass, the minimum distance from the plant to the exclusion boundary.

Response:

Section 2.1.2 of the PSAR has been revised to more clearly define the Clinch River Site and the exclusion area. The Site is the peninsula containing 1364 land acres bordered on the north by the ERDA Oak Ridge Reservation and the south by the Clinch River. The Clinch River Site includes the Clinch River Consolidated Industrial Park containing approximately 112 acres located at the north boundary of the Site between Bear Creek Road and Grassey Creek (see Figure 2.1-4).

The exclusion area is shown on Figure 2.1-5. It includes the Clinch River Site (except the CRCIP) and the river adjacent to the Site. Below are listed the distance in feet from the center of the containment/confinement building to the nearest point on the exclusion boundary in each of the 16 sectors of the compass.

<u>Sector</u>	<u>Minimum Distance to Exclusion Boundary (feet)</u>
N	7100
NNE	8150
NE	2870
ENE	2670
E	2685
ESE	3190
SE	3990
SSE	2700
S	2280
SSW	2200
SW	2200
WSW	2290
W	2490
WNW	2290
NW	2700
NNW	3160

Question 310.36 (RSP) (2.2)

Your response to item 310.34 does not provide the necessary assurance that potential industrial developments in the Clinch River Consolidated Industrial Park (CRCIP) will not pose an undue risk to the safe operation of the CRBRP. It is our position that you should provide a commitment that you will remain informed and will also inform the NRC of the nature of proposed industrial developments in this area, and that you will provide an analysis of the impact of any development upon the safe operation of the CRBRP. In this regard, provide an expanded discussion and analysis of the impact of the activities of the U.S. Nuclear, Inc. and Nuclear Environmental Engineering, Inc. on the CRBRP.

Response:

The CRBRP Project will remain informed of industrial developments in the CRCIP and will determine their potential effects, if any, on the safe operation of the CRBRP. NRC will be informed and provided an evaluation of a new industrial development in the CRCIP when such a development is certain and if there is any potential impact on the CRBRP. Assurance that the CRBRP will be compatible with all activities in the CRCIP is described below.

The CRCIP is presently U.S. Government property in the custody of TVA. TVA has given the City of Oak Ridge a permanent industrial easement to four (4) parcels within the CRCIP. The City of Oak Ridge subsequently conveyed three (3) of them to Nuclear Environmental Engineering, Inc. (five acres), and U.S. Nuclear, Inc. (33 acres) (see PSAR Section 2.2.1.1 and Figure 2.2-2).

Additionally, easements for a small sewage treatment plant, sewage treatment plant access road and sewer lines have been conveyed by TVA to the City of Oak Ridge. Conveyance of any TVA land including the CRCIP is made only after a thorough assessment has been made by TVA. Upon receipt of a request for conveyance of TVA land, all TVA offices and divisions having a program interest in the land make a formal review and determine whether the proposed use is compatible with and furthers TVA's program objectives, is in the public interest, and will not be adverse to the interests of the United States.

TVA applies controls and procedures in its disposal of real property which protect its financial interests and which safeguard public benefits and obligations. When it conveys or transfers property, it includes in the transfer documents such covenants, reservations, and restrictions as it considers to be necessary in carrying out the provisions and objectives of the TVA Act.

When TVA receives a request for land near any of its nuclear facilities, a review is initiated to determine the compatibility of the proposed use of the inquiring industry with the nuclear project (including assurance that the industry can comply with the emergency plans of the TVA facility). TVA requires that prospective industries submit, in writing, details of their planned operation. The above will assure that potential developments in the CRCIP will not pose an undue risk to the safe operation of the CRBRP.

Section 2.2.1.1 and 2.2.2 of the PSAR have been revised to provide an expanded discussion and evaluation of the impact of activities of U.S. Nuclear, Inc. Section 2.2.1.1, concerning Nuclear Environmental Engineering, Inc. has been revised to indicate their proposed plans, and the Project will determine the impact of their facility, if any, on the safe operation of the CRBRP at the time construction is initiated.

Question 310.37 (2.2)

Your response to item 310.4 asserts that transportation accidents involving barge traffic on the Clinch River are not postulated, since the frequency of traffic is extremely low and does not involve toxic materials. However, the only data presented to support this (Table 2.1-5) shows only the total tonnage through the river and are insufficient for us to make a conclusion. Provide additional data on the frequency or average weight of barges passing the site. Indicate how much of the traffic is associated with explosive, toxic or hazardous materials. Provide data on barge accidents, if any, on the Clinch River.

Response:

The response to this question is provided in revised Section 2.2.1.3.3.

Question 310.38 (2.2)

With regard to the proposed Exxon reprocessing facility, provide an evaluation of the possible effects on the Clinch River plant of an accidental release of potentially hazardous materials which may be stored at the Exxon site. State all your assumptions. Provide a revised Figure 2.2-1 which indicates the location of the Exxon facility. We will require that the CRBRP be designed to safely withstand the consequences of any design basis event at the Exxon facility.

Response:

The proposed Exxon reprocessing facility will be required to obtain a construction permit and operating license from the NRC and the requirement for demonstrating the environmental acceptability of the proposed site and plant safety will be the responsibility of Exxon. Compliance with NRC licensing requirements should insure accidents from the Exxon facility will not impact the safe operation of the CRBRP. The CRBRP Project will, however, evaluate the possible effects on the CRBRP from accidents occurring at the Exxon facility when Exxon has received a construction permit from the NRC. Until that time the CRBRP will continue to follow the activities of the Exxon facility.

Figure 2.2-1 has been revised to indicate the 2500 acre site on the Oak Ridge Reservation which Exxon has requested from ERDA for the proposed Exxon facility.

Question 310.39 (RSP) (6.4)

Verify that the Control Room air intakes will be provided with hydrogen fluoride detectors and that the ammonia storage vessels on-site will be provided with leak detectors and that the Control Room will be automatically isolated upon a signal from these detectors. It is our position that these instruments should meet the performance criteria for monitoring instrumentation as given by Regulatory Guide 1.78, and should have detection sensitivities such that the toxic vapor concentrations inside the Control Room shall not exceed the respective toxicity limits of hydrogen fluoride and ammonia. In this regard, indicate what action you plan to take.

Response:

The response to this question is contained in Section 6.3.1.6 and revised Section 9.6.1.2. The intent of Regulatory Guide 1.78 will be met.

Question 310.40 (10.2.3)

We have reviewed the proposed plant design with respect to turbine missile hazards and find that it meets the general intent of our position on turbine missile protection requirements as outlined in Standard Review Plan Section 3.5.3 and Regulatory Guide 1.115. However, there are some specific aspects of the turbine missile analysis (General Electric Report "Hypothetical Turbine Missile Data and Probability of Occurrence for 3600-RPM TC6F-23 Inch LSB Unit for Use with Liquid Metal-Cooled Fast Breeder Reactor," submitted on April 9, 1976) that need clarification. Accordingly, provide additional information in response to the following questions:

1. Scaled cross sectional drawings of the turbogenerator should be provided. The drawings should illustrate the principal configuration features of the turbine rotor and the stationary turbine internals.
2. Provide the basis for each of the following statements or information indicated in Reference 1:
 - a. "...energy stored in the hypothetical fragments is of the same order as the energy absorbing capability of the stationary parts." (Page 3, Paragraph 4).
 - b. "Only one rotor failing...is assumed..." (Page 3, Paragraph 2).
 - c. "...we assume that the high pressure rotor sections...will not eject missiles." (Page 4, Paragraph 4).
 - d. "...the ensuing damage would preclude further speed rise of other rotors..." (Page 9, Paragraph 5).
 - e. "...we suggest a uniform probability distribution to be assigned to the impact orientation angle." (Page 18, Paragraph 3).
 - f. The zero energy and velocity entries in Table III for the minimum energy and velocity of high speed burst missiles.
3. The statement on Page 6, Paragraph 2 of Reference 1 that it takes a combination of stuck valves and electronic faults to lead to destructive overspeeds does not appear to be justifiable. For example, a common mode failure of the turbine steam valves would lead to a destructive overspeed in a loss of load incident, even though the speed sensing and tripping portions of the overspeed protection system were fully operational. A clarification of this aspect of overspeed protection should be provided.

Response:

1. The actual cut-away drawing for the CRBRP Turbine is scheduled to be developed by G.E. in April 1979. A similar drawing is shown in Figure Q310.40.1 except the double flow intermediate pressure section will be deleted, the high pressure exhaust will come off the top into the crossover pipe to the low pressure turbine and one low pressure section will be added in the case of the CRBRP. The nomenclature and the relative size and location of the various parts in Figure Q310.40-1 are applicable to the CRBRP Turbine design.

- 2a. The initial energy of a hypothetical rotor fragment produced by an L.P. rotor and the energy absorption capability of its casings are of the same order of magnitude. A complete treatment of calculating initial energies of rotor fragments and energy losses due to collision and penetration of stationary sections is provided in Reference 19 of the report and is included as Appendix A to this response.

- 2b. In order to account for the worst possible (most destructive) missiles, a high speed or runaway failure mode is included in our analysis. We do not believe that a rotor burst is the inevitable result of an overspeed excursion, but to account for the possibility, we make the assumption that a rotor will burst prior to or at its highest possible (see section V of report) overspeed. It's at this highest speed that the kinetic energy of each missile is calculated as the maximum.

Since the material properties and inherent physical characteristics of rotors vary between forgings, in any given group of rotors there will be one rotor which is more susceptible to failure than the others. So we assume that no two rotors in the same power train will burst simultaneously. Furthermore, at the instant that a rotor does burst, additional damage would occur throughout the system which would preclude further speed rise of those rotors still intact and force them to decelerate (steam path opened to atmosphere, bucket shedding, rubbing, bearings seize, etc.). Therefore, if the first rotor to burst does so at less than the maximum possible overspeed, the other rotors would not continue to accelerate and hence, would not burst.

- 2c. Calculations show that the relatively low energies of the missile which would be postulated for a high pressure rotor burst would easily be contained within their heavy cast-steel shells. This was stated in the referenced report on page 2, paragraph 4 and page 4, paragraph 4. This is due primarily to the fact that our high pressure rotors are encased by two low alloy steel shells, each with a minimum thickness of three inches.

- 2d. See response to b.

Amend 39
May 1977

- 2e. The calculation of missile penetration of given targets was not within the scope of the report. We do, however, review our assumptions in relation to how they would eventually be applied. Of particular concern was how the group 1 and 2 missiles would be treated in making penetration estimates. Their geometries are such that the difference between using the minimum projected area and the maximum projected area would result in large deviations in their penetration capabilities. We believe that use of the minimum projected area would be unduly conservative since it seems reasonable to us that if a target is substantially distant from the missile source, any impact orientation is possible. Therefore, the recommendation was made that a uniform probability distribution be used.
- 2f. To account for the variations inherent in the calculation of a multitude of rotor fragments penetrating the surrounding mass of metal (web, ring, casing and hood), a range of exit energies is provided for in each of the postulated missile groups. Thus, depending on a fragment's orientation, size, angle of ejection, etc., it is possible that a fragment from a particular group would either be contained or else exit the hood at some calculated maximum value. Thus, the zero value entry for missile groups 1, 2 and 4 indicates that the fragments could be contained. Calculations for the group 3 fragments indicate that total containment is unlikely. Group 5 and 6 missile fragments are explained on page 18, paragraph 1 of the report. In any case, the midpoint value supplied in Table III can be used to represent the characteristic energy and velocity values of any fragment possible within a group. Further discussion of how the range of values are determined can be found on Page 4 of reference 19, (Appendix A to this response).
3. In response to the request for clarification of the aspect of overspeed protection described in Page 6, Paragraph 2 of Reference 1, i.e., that it takes a combination of stuck valves and electronic faults to lead to destructive overspeeds, the following information is provided to clarify and replace Page 6, Paragraph 2 of Memo Report, Hypothetical Turbine Missile Data and Probability of Occurrence for 3600 RPM TC6F - 23" inch LSB Unit for Use with the Liquid Metal Cooled Fast Breeder Reactor dated August 29, 1975 (Reference 1).

In order for steam flow through the main steam valves to lead to a destructive overspeed during a loss of load incident, at least one stop valve and associated control valve must fail to close. For this situation to arise, one of the following failure combinations must occur:

- (1) steam stop valve and associated steam control valve mechanically stuck.
- (2) hydraulic system component failure to relieve emergency trip system pressure under the steam stop and associated steam control valve pistons.
- (3) electronic component failures and failure of the mechanical overspeed trip mechanism.

- (4) hydraulic and electronic component failures.
- (5) hydraulic component failures and control valve mechanically stuck
- (6) electronic failures and failure of the mechanical overspeed trip mechanism and control valve mechanically stuck.
- (7) hydraulic and electronic component failures and failure of the mechanical overspeed trip mechanism.

For the case where the turbine is not carrying loads, for a destructive overspeed to occur, either of the following failure combinations must occur:

- (1) electronic component failures and failure of the mechanical overspeed trip mechanism.
- (2) hydraulic and electronic component failures.

NOMENCLATURE LIST

1. STANDARD AND CAP, TURBINE SIDE
2. BEARING JOURNAL T-1
3. OIL DEFLECTOR T-1
4. STEAM PACKING N-1
5. EXHAUST, HIGH PRESSURE TO REHEATER
6. NOZZLE DIAPHRAGMS, HIGH PRESSURE
7. BUCKET BLADES, HIGH PRESSURE
8. SHELL, HIGH PRESSURE, INNER
9. SHELL, HIGH PRESSURE, OUTER
10. MIDSPAN BALANCE ACCESS
11. NOZZLE, FIRST STAGE, HIGH PRESSURE
12. STEAM INLET, HIGH PRESSURE
13. STEAM PACKING N-2
14. OIL DEFLECTOR T-2, TURBINE SIDE
15. BEARING JOURNAL T-2
16. STANDARD AND CAP, MIDDLE
17. ROTOR, HIGH PRESSURE
18. REHEAT ROTOR, DOUBLE-FLOW
19. THRUST BEARING, WEAR DETECTOR
20. THRUST BEARING
21. BEARING JOURNAL T-3
22. OIL DEFLECTOR T-3, GENERATOR SIDE
23. CROSSOVER PIPE
24. STEAM PACKING N-3
25. REHEAT INLET
26. REHEAT INNER SHELL, TURBINE SIDE
27. REHEAT DOUBLE-FLOW NOZZLE
28. REHEAT INNER SHELL, GENERATOR SIDE
29. OUTER REHEAT SHELL
30. STEAM PACKING N-4
31. OIL DEFLECTOR T-4, TURBINE SIDE
32. BEARING JOURNAL T-4
33. ROTOR, LOW PRESSURE, "A" SECTION
34. EXHAUST HOOD "A" SECTION
35. BEARING JOURNAL T-5
36. OIL DEFLECTOR T-5, GENERATOR SIDE
37. STEAM PACKING N-5
38. ATMOSPHERIC RELIEF DIAHRAGM
39. NOZZLE, LOW PRESSURE, DOUBLE-FLOW "A" SECTION
40. STEAM PACKING N-6
41. OIL DEFLECTOR, TURBINE SIDE T-6
42. BEARING JOURNAL T-6
43. OIL REFLECTOR, GENERATOR SIDE T-6
44. OIL REFLECTOR T-7, TURBINE SIDE
45. ROTOR, LOW PRESSURE, "B" SECTION
46. EXHAUST HOOD "B" SECTION
47. BEARING JOURNAL T-7
48. OIL DEFLECTOR T-7, GENERATOR SIDE
49. STEAM PACKING N-7
50. STEAM PACKING N-8
51. OIL DEFLECTOR T-8, TURBINE SIDE
52. BEARING JOURNAL T-8
53. TURNING GEAR
54. GENERATOR FIELD
55. OIL DEFLECTOR T-8, GENERATOR SIDE
56. EXHAUST TO CONDENSER
57. EXPANSION JT. SHL. HTG. & BAL. WT. ACCESS

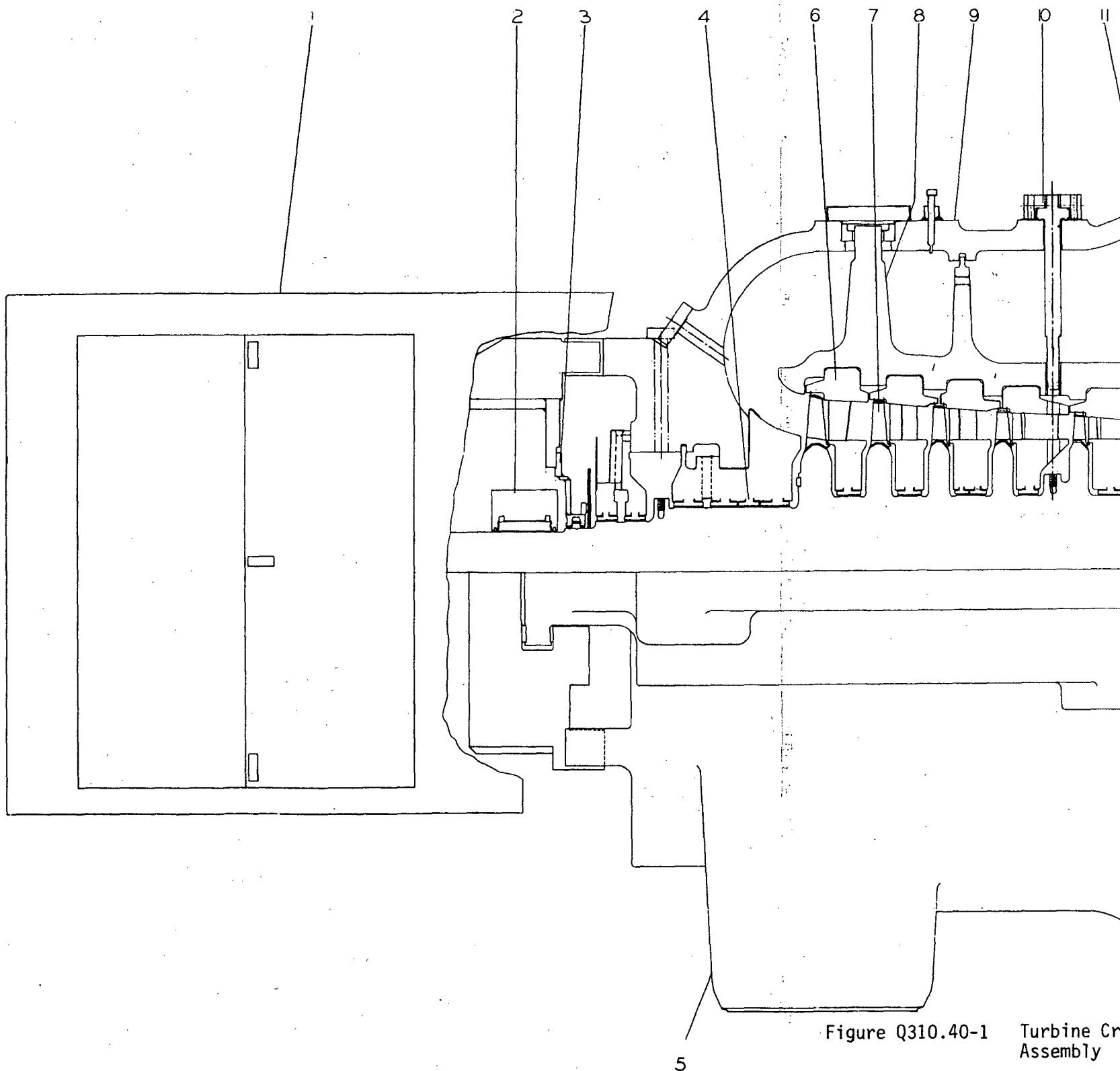
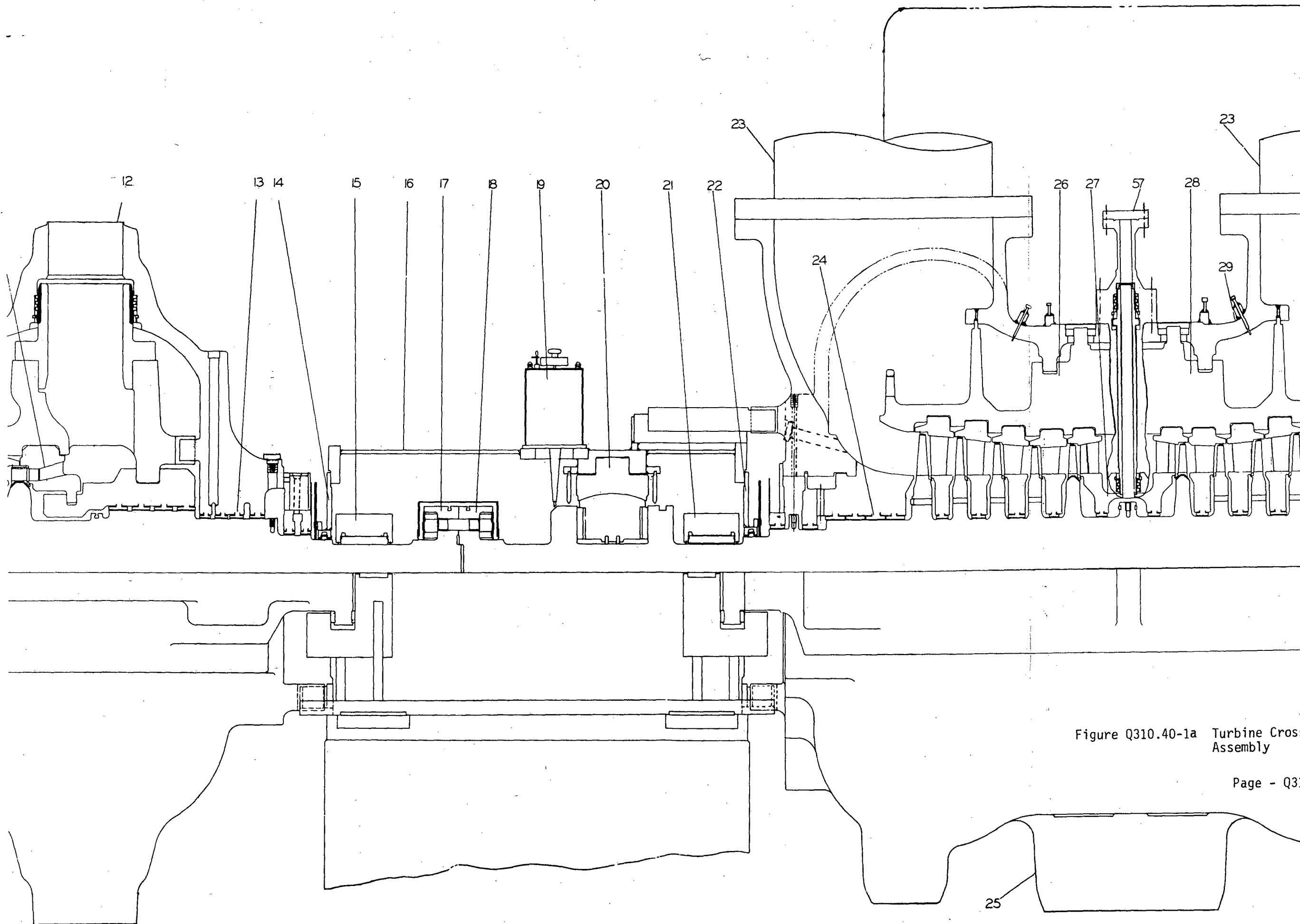


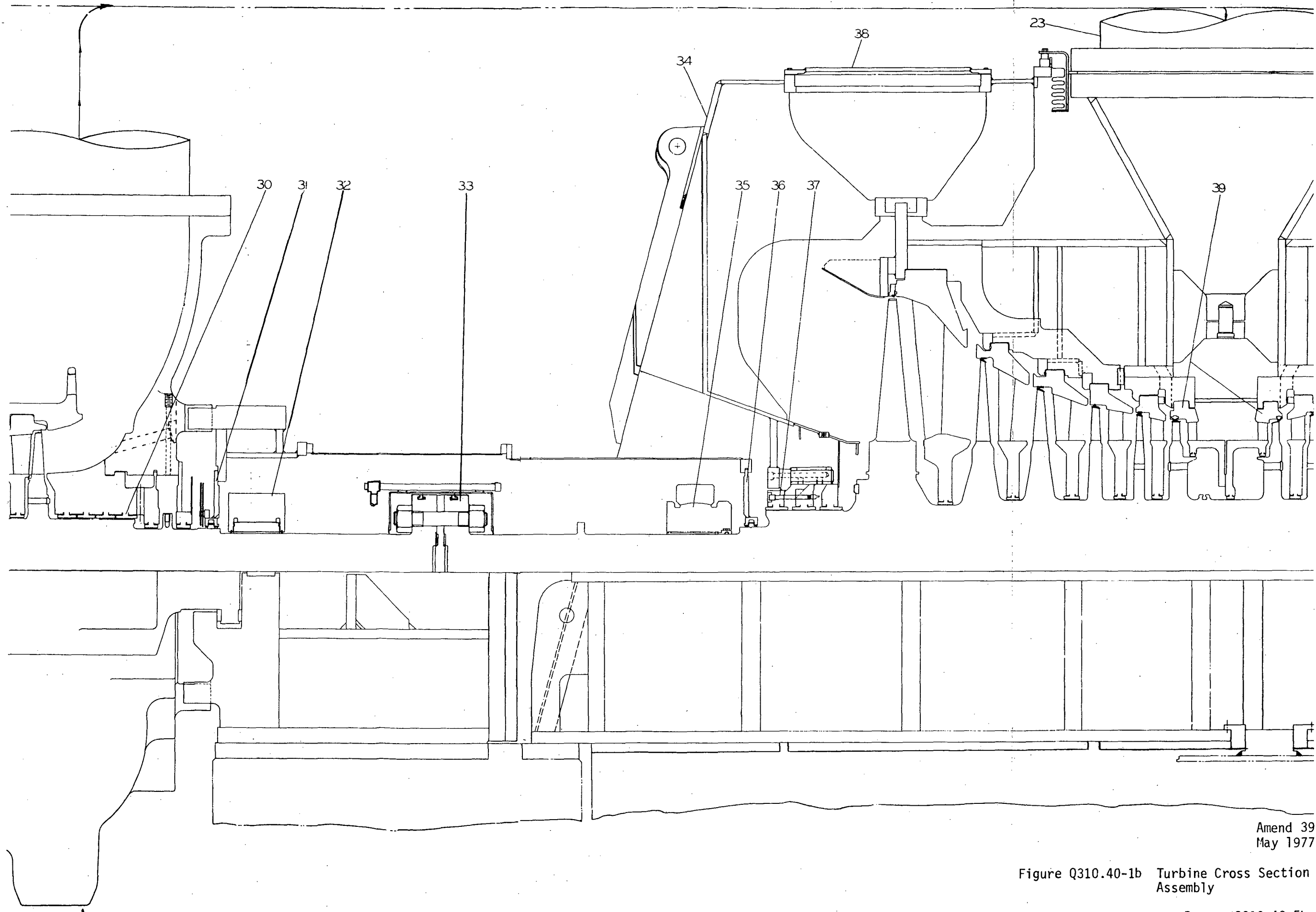
Figure Q310.40-1 Turbine Cross Section Assembly

Amend 39
May 1977



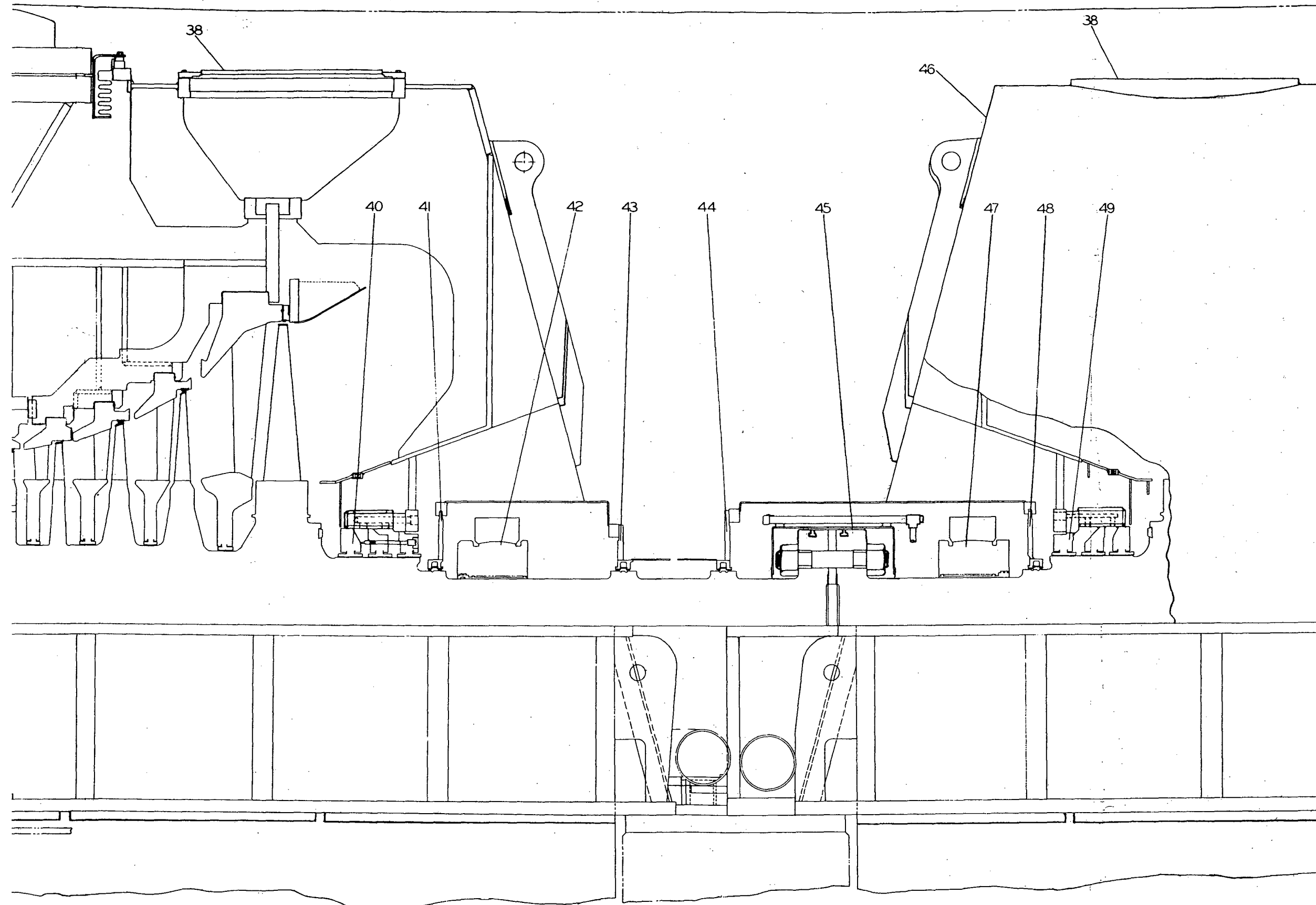
Amend 39
May 1977

Figure Q310.40-1a Turbine Cross Section
Assembly



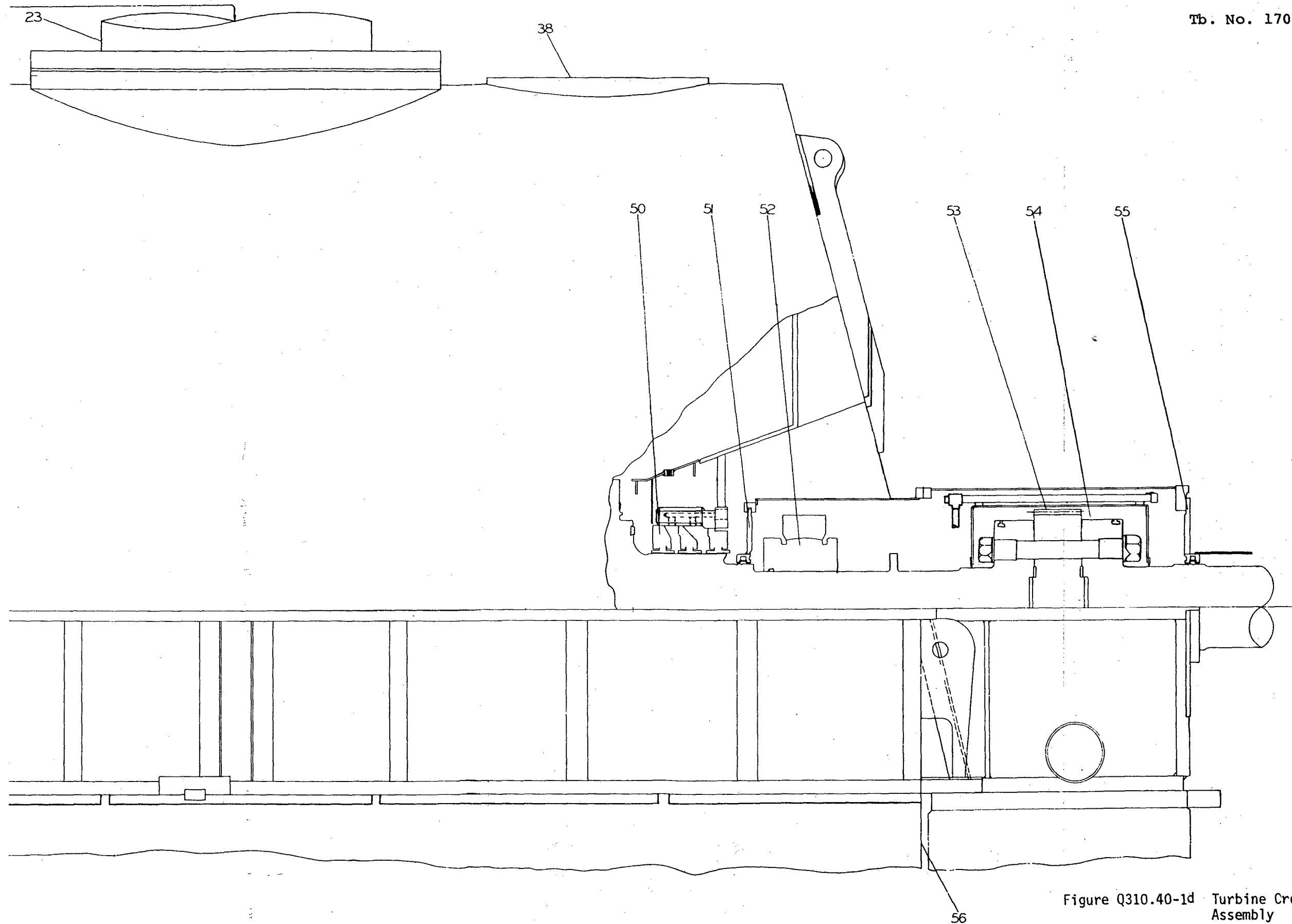
Amend 39
May 1977

Figure Q310.40-1b Turbine Cross Section
Assembly



Amend 39
May 1977

Figure Q310.40-1c Turbine Cross Section
Assembly



Amend 39
May 1977

Figure Q310.40-1d Turbine Cross Section
Assembly

APPENDIX A

AN ANALYSIS OF THE ENERGY OF
HYPOTHETICAL WHEEL MISSILES
ESCAPING FROM TURBINE CASINGS

by

D.C. Gonyea

DF73LS12

February 1973

Q310.40-6

Amend 39
May 1977



TECHNICAL INFORMATION SERIES

Title Page

AUTHOR D.C. Gonyea	SUBJECT Hypothetical Turbine Wheel Missiles	NO. DF73LS12
		DATE Feb. 1973
TITLE An Analysis of the Energy of Hypothetical Wheel Missiles Escaping from Turbine Casings		G.E. CLASS I
		GOVT. CLASS none
REPRODUCIBLE COPY FILED AT Technical Library, Bldg.273-Rm.293		NO. PAGES 29
SUMMARY The exit energy and velocity of hypothetical turbine wheel missiles from the LP section of nuclear turbines have been calculated. All low pressure turbine wheels are assumed candidates for burst in both "low speed" and "high speed" burst modes. Sixteen fragments are postulated to be generated per wheel burst; missiles weighing up to 8000 pounds may be ejected. A new penetration model is employed to determine the energy absorption capability of the stationary structures. The exit energy and velocity ranges for the entire spectrum of postulated missiles are discussed with reference to the 43 inch last stage bucket nuclear unit.		
KEY WORDS turbine missiles, wheel fragments, energy, velocity, penetration		

Amend 39
May 1977

INFORMATION PREPARED FOR Structural Development Engineering

TESTS MADE BY _____

AUTHOR D.C. Gonyea *David C. Gonyea*

COMPONENT Mechanics & Rotor Development

APPROVED R.J. Placek *R.J. Placek 8/3/73*

TG-1013(4/65)

TECHNICAL INFORMATION SERIES
NO. DF73LS12

TABLE OF CONTENTS

	<u>Page</u>
I. Introduction	1
II. Results	2
A. Missile Sizes and Energy	2
B. Model for Energy Calculations	4
III. Technical Discussion	5
A. Wheel Fragments	5
B. Assumed Burst Speeds	7
C. Initial Fragment Energy	8
1. Translational and Rotational Energy	8
2. Effective Translational Energy	9
D. Diaphragm Web and Ring Collisions	11
E. Wrapper and Exhaust Hood Penetration	13
F. Exit Energy and Velocity	15
IV. Conclusions	17
V. Acknowledgement	19
VI. References	20
VII. List of Tables	21
VIII. List of Figures	24

TECHNICAL INFORMATION SERIES

NO. DF73LS12

I. INTRODUCTION

The licensing procedures of the Atomic Energy Commission require the consideration of hypothetical turbine missiles as part of the review of plant safety. The Turbine Department has assisted the utilities in the preparation of their Safety Analysis Reports by providing a description of these hypothetical turbine missiles. This description includes the probability of occurrence as well as the resulting energy and velocity of the missile, should a burst occur.

Earlier work in connection with missile description includes that of Downs [1]* and Zwicky [2]. Zwicky concludes that the most energetic turbine wheel missile is a 120° fragment of a last stage wheel. Downs finds that the probability of generation of such a missile is extremely small.

The Turbine Department has recently reconsidered the missile problem and has issued a series of Memo Reports [3-6] summarizing its findings. This new body of work considers all the wheels of the low pressure turbine and takes into account a spectrum of fragment sizes per wheel burst. The purpose of this report is to describe the technique employed in the evaluation of these fragments.

Prior to obtaining the information contained in References [3] through [6], missile energies were calculated using Zwicky's method of analysis. Many assumptions were made in

*Numbers in brackets refer to the references.

GENERAL ELECTRIC COMPANY
TECHNICAL INFORMATION SERIES
NO. DF73LS12

that analysis, including the manner in which energy is absorbed by the stationary parts. Zwicky assumed that the stationary material surrounding the last stage wheel would be stretched to its ultimate strength. Simple containment tests recently conducted by the Turbine Department have indicated that energy is lost to the containment primarily by local plastic deformation rather than by gross stretching. In light of these findings, a new technique for the calculation of missile energies has been developed.

II. RESULTS

II. A. Missile Sizes and Energy

Turbine missiles are assumed to be generated as a result of a hypothetical burst of a low pressure turbine wheel. Two burst situations are considered: (1) a "low speed" burst near running speed due to material deficiency and (2) a "high speed" burst at 80% overspeed in a runaway condition following a control system failure. These two postulated burst situations are identified in the studies of the probability of wheel burst by Downs [1] and [3].

All wheels of the low pressure turbine are considered as candidates for bursting. The probability of burst of a given wheel is a function of the speed as well as the particular turbine type under consideration.

To simplify calculations, wheels with similar characteristics (e.g., weight, size, energy) are grouped together and the properties of one wheel of the group are used to

TECHNICAL INFORMATION SERIES
NO. DF73LS12

calculate missile properties. For example, the seven wheels of the 43 inch last stage bucket low pressure turbine are divided into three Groups. Group I consists of the first three stages; Group II - the fourth through sixth stages; and Group III - the last stage wheel. Assuming that a burst occurs, it has been found that all wheels are capable of producing missiles external to the turbine in both the low speed and high speed burst situations. However, the analysis contained in Ref.[4] points out that the probability of burst of stages in Groups I and II at low speed is not statistically significant.

For each wheel fragment and assumed burst speed a range of energy is specified. This range results from uncertainties associated with the orientation of the missile fragment as it penetrates the turbine casing as well as the energy absorbing capability of the stationary components. A small fragment, for example, may exit through a hole created in the turbine by a larger missile, or it may be completely contained by the stationary components. In this case, its escape energy can vary between its initial energy (no collision) to zero (containment).

Table 2 is a summary of the exit energy and velocity ranges that have been calculated for the entire spectrum of postulated fragments. Notice that the fragments of the last stage wheel are significantly more energetic than those of all the other wheels. The velocity ranges given in the table are intended for use in trajectory related calculations.

The entire spectrum of fragment sizes, energies, and velocities given in Tables 1 and 2 is required to perform a

Amend 39
May 1977

GENERAL ELECTRIC COMPANY
TECHNICAL INFORMATION SERIES
NO. DF73LS12

detailed analysis of the overall probability of unacceptable consequences due to hypothetical turbine missiles. The need for this information has been prompted by consideration of trajectory related calculations.

II. B. Model for Energy Calculations

A small fragment (chosen less than 45°) could escape the turbine through a hole made by a larger fragment. In this case, its escape energy is equal to its initial energy. On the other hand, a small fragment could be completely contained within the turbine, in which case its exit energy is zero. Then the range of exit energies for small fragments is taken to be between their initial energies and zero.

The larger fragments (45° or larger) cannot escape the turbine casing without loss of energy due to impact with and penetration of various stationary components. The model used in estimating the energy absorption capability of these stationary parts is shown in Figure 1.

The complex nature of the geometry and uncertainties such as the effect of rotation has led to an idealization of the overall problem. Components included in the analysis are the wheel fragment, the web and ring of the diaphragm, the inner casing wrapper, and the exhaust hood.

The behavior of the hypothetical missile is postulated as follows: (1) the wheel bursts into various fragments with no loss of total energy, (2) each major fragment impacts the diaphragm web and creates at least two web fragments, (3) the web

GENERAL ELECTRIC COMPANY

TECHNICAL INFORMATION SERIES

NO. DF73LS12

fragments are accelerated out of the path of the missile,
(4) diaphragm ring fragments are also created and accelerated,
(5) the inner casing is penetrated, and finally (6) penetration
of the exhaust hood occurs.

Figure 2 shows the calculated energy and velocity ranges
as a function of fragment size. Data for the 43 inch last
stage wheel are used for illustration. Note that a wide
variation in velocity exists for the smaller fragments.

III. TECHNICAL DISCUSSION

III. A. Wheel Fragments

Missile studies in the past have been concerned with only
one size fragment; the fragment that possessed the highest
energy external to the turbine. This simplification was justi-
fied since it was further assumed that, given a wheel burst,
the fragment would strike a critical target. The missile with
the highest energy would, therefore, have the highest overall
probability of damaging the critical target.

The introduction of trajectory-related calculations
requires consideration of both the energy and the velocity of
hypothetical missiles. The velocity is required to determine
the strike probability. Downs [6] shows that a missile
with low velocity is important since it has a relatively higher
probability of striking a given target. Furthermore, various
fragment sizes must be considered since the fragment mass in-
fluences the relationship between energy and velocity.

TECHNICAL INFORMATION SERIES

NO. DF73LS12

Two sources of information have been utilized in estimating the number and associated sizes of wheel fragments assumed in this report. One source is the Hinkley Point failure of September 1969 [7]; the other source is an extensive experimental disc-bursting study conducted by the Steam Turbine Department of the General Electric Company.

A review of General Electric burst tests clearly indicates a trend of fewer fragments with increasing excess temperature* (increasing toughness). All tests produced three or four large fragments. In addition, those tests conducted at negative excess temperatures produced many small fragments.

The failure of the Hinkley Point wheels is attributed to their low material toughness, which made them incapable of accommodating small cracks produced by stress corrosion. These wheels, which burst at negative excess temperature, generated between about 5 and 40 fragments.

The following number of fragments and associated sizes have been selected for use in this report after a careful review of many burst tests:

<u>Fragment Group</u> <u>(See Table I)</u>	<u>Number of</u> <u>Fragments</u>
Type a	2
Type b	1
Type c	3
Type d	10

*The excess temperature is defined as the operating temperature minus the fracture appearance transition temperature.

GENERAL ELECTRIC COMPANY
TECHNICAL INFORMATION SERIES
NO. DF73LS12

Because of the high material toughness of wheels used in nuclear turbines built by the author's company, a relatively low number of smaller fragments (Type d) is expected. A number of ten is assumed to admit other potential missiles, such as buckets, to the distribution.

III. B. Assumed Burst Speeds

Two situations are postulated which result in a hypothetical wheel burst. One case is termed a "low speed" burst which is assumed to occur at or near running speed. The specific turbine speed for this situation is taken to be 120% of normal running speed, since it is the maximum rotor speed reached without a complete control system failure. The second case is termed a "high speed" burst during runaway following a complete control system failure.

The "high speed" burst is assumed to occur at the vane shedding speed which is 180% of running speed. It is postulated that the rotational unbalance developed during the loss of the vanes will cause gross mechanical failure, particularly of the bearings, so that higher rotor speed is unlikely.

Thus, the high speed wheel failure is postulated to occur at an upper limit of maximum turbine speed. Even at this speed, it is unlikely that the wheel will fail since the unloading of the wheel caused by the loss of the vanes results in a higher overspeed capability of the wheel.

TECHNICAL INFORMATION SERIES

NO. DF73LS12

III. C. Initial Fragment Energy

C.1. Translational and Rotational Energy

The wheel is assumed to fracture into various fragments with the fracture surfaces occurring in an axial-radial plane. The assumption of conservation of linear and angular momentum leads to the following expressions for the translational and angular velocities of the center of gravity of each fragment.

$$V_{cg} = \omega R_{cg} \quad (1)$$

$$\psi_{cg} = \omega \quad (2)$$

where

V_{cg} = linear velocity at center of gravity of fragment,

ω = angular velocity of shaft at burst,

R_{cg} = radius to center of gravity of fragment measured from shaft centerline, and

ψ_{cg} = angular velocity of fragment.

The translational and rotational energy of the fragment are simply:

$$KE_{tr} = \frac{1}{2} M_f V_{cg}^2 \quad (3)$$

$$KE_{ro} = \frac{1}{2} J_f \psi_{cg}^2 \quad (4)$$

where

KE_{tr} = translational kinetic energy of fragment,

KE_{ro} = rotational kinetic energy of fragment,

M_f = total mass of fragment, and

J_f = polar moment of inertia about c.g. of fragment.

TECHNICAL INFORMATION SERIES

NO. DF73LS12

These formulations of initial fragment motion and energies conservatively assume that there is no loss of energy during the generation of fragments and that there is no transfer of energy between fragments due to collisions subsequent to the burst.

III. C.2. Effective Translational Energy

The rotational energy comprises a significant fraction of the initial total energy of a fragment, and can contribute to the penetrating capability of the fragment. Hence the rotational energy cannot be neglected in estimating the escape energy of the missile fragment. The rotational energy of a 120° fragment, for example, represents approximately 35% of the total energy.

An "Effective Translational Energy" is defined which accounts for the additional penetrating capability of a fragment possessing rotational as well as translational energy. The fragment is visualized as a system of particles, each with a different velocity. A particle having a velocity normal to a stationary component, has greater penetrating capability than another particle with the same velocity magnitude, but impacting the plate at an oblique angle. A particle with a velocity in a direction parallel to the stationary component has no penetrating capability. This model leads to the following definition of the quantity, "Effective Translational Energy":

$$KE_{\text{eff}} \triangleq \frac{1}{2} \int_v v_x^2 \rho dv \quad (5)$$

GENERAL ELECTRIC COMPANY
 TECHNICAL INFORMATION SERIES
 NO. DF73LS12

where

$$\begin{aligned}
 KE_{eff} &= \text{effective translational energy,} \\
 V_{\alpha} &= \text{component of absolute velocity} \\
 &\quad \text{normal to the stationary component,} \\
 \rho &= \text{mass density of fragment, and} \\
 dv &= \text{incremental volume of fragment.}
 \end{aligned}$$

Figure 3 describes the model and the nomenclature which is used to develop Equation 5. The wheel fragment is treated as a sector of a disc and the stationary component as a flat surface. The fragment has both rotational and translational motion.

The integration of Equation 5 leads to the following expression for the Effective Translational Energy of the disc fragment:

$$KE_{eff} = KE_{tr} \left\{ 1 + \frac{9}{16} \left[\left(\frac{\phi/2}{\sin \phi/2} \right)^2 + \cos \frac{\phi}{2} (2 \cos^2 \alpha - 1) \left(\frac{\phi/2}{\sin \frac{\phi}{2}} \right) \right] - \cos^2 \alpha \right\} \quad (6)$$

The important feature of this relationship is that the Effective Translational Energy is a function of the missile size, ϕ , and the orientation of the missile at impact, α . Equation 6 can also be expressed in terms of the translational and rotational energies of the disc sector:

$$KE_{eff} = KE_{tr} + C KE_{ro} \quad (7)$$

TECHNICAL INFORMATION SERIES
NO. DF73LS12

The value of "C" in Equation 7 is a function of the missile size and the orientation at impact. For example, the value of "C" for a 120° segment striking a stationary component in the direction of minimum projected area ($\alpha = 0^\circ$) is 0.25, and in the direction of maximum projected area ($\alpha = 90^\circ$), "C" is 0.75.

A study dealing with the effect of "C" has shown that the hypothetical missile energy external to the turbine is largest when the motion of the fragment is in the direction of minimum projected area ($\alpha = 0$). Although other orientations result in higher initial energies of the missile fragments, the energies external to the turbine are lower because of larger impact areas and greater energy absorption by the stationary components.

Equation 7 is applied to the wheel fragment. The uncertainty concerning the angle of orientation leads to an uncertainty in exit energies and is included in the ranges of hypothetical missile energies.

A number of fragment properties are necessary to compute the initial missile energy. These include the fragment mass, location of center of gravity, and the polar moment of inertia. Because of the irregular shape of the wheel fragment, a numerical technique similar to that described by Zwicky [2] is used to calculate the properties.

III. D. Diaphragm Web and Ring Collisions

The diaphragm is in the path of the wheel fragment and must be accelerated out of the way to permit the escape of the missile. It is assumed that the impact causes the diaphragm

Amend 39
May 1977

TECHNICAL INFORMATION SERIES
NO. DF73LS12

web to fracture in a brittle manner with no loss of energy, so that the only energy absorbed is that required to accelerate the diaphragm web fragments out of the missile path. The energy absorption capability of the diaphragm partitions is assumed to be zero--they are neglected.

The wheel fragment is assumed to accelerate the fragments of the diaphragm web that are directly in its path and transfer energy to them during the collision. A similar collision and energy transfer is assumed to occur between the wheel fragment and the diaphragm ring.

Figure 4 illustrates the model that is used to estimate the energy loss by the missile as a result of the web and ring collisions. Recall from the discussion of the Effective Translational Energy that the wheel fragment is assumed to be oriented in the direction of minimum projected area at the instant of impact (to minimize energy loss in penetration, and thus maximize the escape energy).

The wheel fragment is assumed to accelerate two web fragments in directions approximately 45° from the missile path. The assumed number and directions of the web fragments chosen were based primarily on the shape of the impacting wheel fragment missile. The same model is used for the ring impact.

Conservation of both momentum and energy is assumed in calculating the energy of the wheel fragment after collision:

$$\text{Momentum: } M_f V_{fi} = M_f V_{ff} + 2 \left(\frac{M_w}{2} \right) V_{wf} \cos 45^\circ \quad (8)$$

$$\text{Energy: } M_f V_{fi}^2 = M_f V_{ff}^2 + 2 \left(\frac{M_w}{2} \right) V_{wf}^2 \quad (9)$$

GENERAL ELECTRIC COMPANY
 TECHNICAL INFORMATION SERIES
 NO. DF73LS12

where

- M_f = mass of wheel fragment
- M_w = mass of web fragments,
- V_{fi} = wheel fragment velocity before collision,
- V_{ft} = wheel fragment velocity after collision, and
- V_{wf} = web fragment velocity after collision.

The resulting expression for the energy retained by the wheel fragment is:

$$KE_f = KE_i \left[\frac{2 \frac{M_f}{M_w} - 1}{2 \frac{M_f}{M_w} + 1} \right]^2 \quad (10)$$

where

- KE_f = wheel fragment energy after collision and
- KE_i = wheel fragment energy before collision.

The mass of the web and ring fragments is calculated using the volume of web and ring material which is in the path of the exiting wheel fragment. One web and ring are considered per wheel.

III. E. Wrapper and Exhaust Hood Penetration

The energy lost by the missile during penetration of the inner casing wrapper and the exhaust hood is calculated by use of the empirical relation described by Moore [8] as the "Stanford formula." The Stanford formula applies to missiles having

TECHNICAL INFORMATION SERIES

NO. DF73LS12

a right circular solid shape which impact a flat plate with the axis of the cylinder normal to the plate.

An "equivalent circular diameter" concept is used to account for the irregular shape of the wheel fragment missile. Since the penetration is produced primarily by a shear mode, the perimeter of the projected impact area is used to define the equivalent circular diameter:

$$D_{eg} = \frac{P}{\pi} \quad (11)$$

where

D_{eg} = equivalent circular diameter, and

P = perimeter of projected impact area.

The "window width," which defines the unsupported area of the plate, is conservatively approximated by the equivalent diameter. The modified Stanford formula is thus:

$$E_{loss} = U D_{eg} t (0.344 t + 0.008 D_{eg}) \quad (12)$$

where

E_{loss} = energy loss during penetration (ft.lbs.),

U = ultimate tensile strength of stationary component (psi),

D_{eg} = equivalent circular diameter (in.), and

t = thickness of stationary component (in.).

Defining the thickness and the perimeter to use in connection with the inner casing wrapper penetration calculations requires judgment. Fig. 5 is a cross section of a typical low pressure turbine illustrating the wheels, diaphragm web and ring sections, and the inner casing wrapper. All structures illustrated

GENERAL ELECTRIC COMPANY
TECHNICAL INFORMATION SERIES
NO. DF73LS12

extend the full 360° about the machine axis. The flange, axial ribs, and struts are conservatively neglected in penetration calculations.

Note that the wrapper does not extend axially over the entire last stage wheel. In this situation the perimeter is taken to be one half of the value calculated by the minimum projected area of the fragment (Eq. 11). The thickness is taken to be the minimum value.

The second stage has a large radial section which is directly over the wheel. The wheel fragment is assumed to be deflected slightly by this section with no loss of energy. When two wrapper regions cover a wheel, separate energy absorption calculations are made for each thickness, and the total absorbed energy is taken to be the sum of the two individual energy values. Since the exhaust hood completely encloses all wheels, the energy loss to the hood is found using the full projected perimeter and a thickness of 1-1/4".

Many assumptions and approximations are necessary in evaluating the energy absorbed by the inner casing wrapper and exhaust hood. Consideration is given to these uncertainties in defining the reported range of external energies.

III. F. Exit Energy and Velocity

Figure 2 is a typical plot of exit energy and velocity as a function of missile size. Note that ranges of energy are given. These ranges result from the many uncertainties involved.

GENERAL ELECTRIC COMPANY

TECHNICAL INFORMATION SERIES

NO. DF73LS12

The energy range shown for the larger fragments (greater than 45° in size) is basically due to the uncertainty connected with the absorption capability of the stationary components. The energy range for the smaller fragments (less than 45°) results from the assumption that the small fragments may be ejected through a hole created by a larger fragment or may be slowed down or stopped by the stationary components.

The velocity is calculated by assuming that the energy is all translational energy. This assumption is consistent with the definition of Effective Translational Energy.

$$V = \frac{2E}{M_f} = \frac{64.4 E}{W_f} \quad (13)$$

where

V = velocity of c.g., ft. per sec.;

E = exit energy, ft.lbs.;

M_f = fragment mass, slugs; and

W_f = fragment weight, lbs.

The fragment sizes and associated energy and velocity ranges given in Table 2 assume that the spectrum of fragments described in Section III.A. is generated for each wheel burst.

TECHNICAL INFORMATION SERIES

NO. DF73LS12

IV. CONCLUSIONS

A new method for the calculation of the energy of hypothetical turbine missiles has been developed. The principle difference between this new method and the method of Zwicky [3] is the mode by which energy is absorbed by the stationary turbine components. Simple containment tests recently conducted by the General Electric Company indicate that local shear deformation rather than the gross deformation assumed by Zwicky is the principle mode of energy absorption. The local deformation mode of energy absorption is utilized by the new method. This results in considerably higher exit energies than those predicted by Zwicky.

The introduction of trajectory related calculations has led to the consideration of both large and small wheel fragment missiles. The number and sizes of these fragments is taken from disc bursting tests by the author's company and from Ref. [7].

The larger wheel fragments impact with and transfer energy to the stationary components of the turbine casing. An "Effective Translational Energy" is utilized to account for the rotational energy of the postulated missile fragments. The "Stanford formula" is employed in calculation of energy absorbed by the turbine casing. A range of exit energy is reported which accounts for the uncertainties involved in these calculations.

The smaller fragments are visualized as either escaping through a hole in the turbine casing created by a larger fragment or being slowed down (or stopped) by the stationary turbine components. The reported energy ranges for the smaller fragments thus lie between their initial energy and zero.

Amend 39
May 1977

TECHNICAL INFORMATION SERIES

NO. DF73LS12

Many assumptions and approximations are used in connection with the initial size and number of fragments, the initial burst speeds, the path of the missile, and the energy absorption capability of the stationary components. These assumptions result in conservative limits of the reported energy and velocity ranges.

TECHNICAL INFORMATION SERIES

NO. DF73LS12

V. ACKNOWLEDGEMENT

The development of the approach presented in this report involved the combined efforts of many people. Many of the assumptions and approximations evolved as a result of numerous meetings and discussions. The author would like to express his appreciation to the individuals intimately involved in this project.

GENERAL ELECTRIC COMPANY
TECHNICAL INFORMATION SERIES
NO. DF73LS12

VI. REFERENCES

1. J.E. Downs, "Probability of Turbine-Generator Failure Leading to the Ejection of External Missiles," General Electric Company Memo Report, February 22, 1971.
2. E.E. Zwicky, "An Analysis of Turbine Missiles Resulting from Last-Stage Wheel Failure," TR67SL211, October 3, 1967.
3. J.E. Downs, "Hypothetical Turbine Missiles--Probability of Occurrence," General Electric Company Memo Report, March 14, 1973.
4. J.E. Downs, "Hypothetical Turbine Missile Data - 43-Inch Last Stage Bucket Units," General Electric Company Memo Report, March 15, 1973.
5. J.E. Downs, "Hypothetical Turbine Missile Data - 38-Inch Last Stage Bucket Units," General Electric Company Memo Report, March 16, 1973.
6. J.E. Downs, "Hypothetical Turbine Missiles - Sample Calculation," General Electric Memo Report, March 17, 1973.
7. D. Kalderon, "Steam Turbine Failure at Hinkley Point 'A'," Proc. Instn. Mech. Engrs., Vol. 186, 31, 1972.
8. C.V. Moore, "The Design of Barricades for Hazardous Pressure Systems," Nuclear Eng. and Design, Vol. 5, No. 1, 1967.

TECHNICAL INFORMATION SERIES
NO. DF73LS12

VII. LIST OF TABLES

1. Description of Postulated Wheel Fragments.
2. Energy and Velocity of Hypothetical Wheel Fragment Missiles External to the Turbine.

Q310.40-29

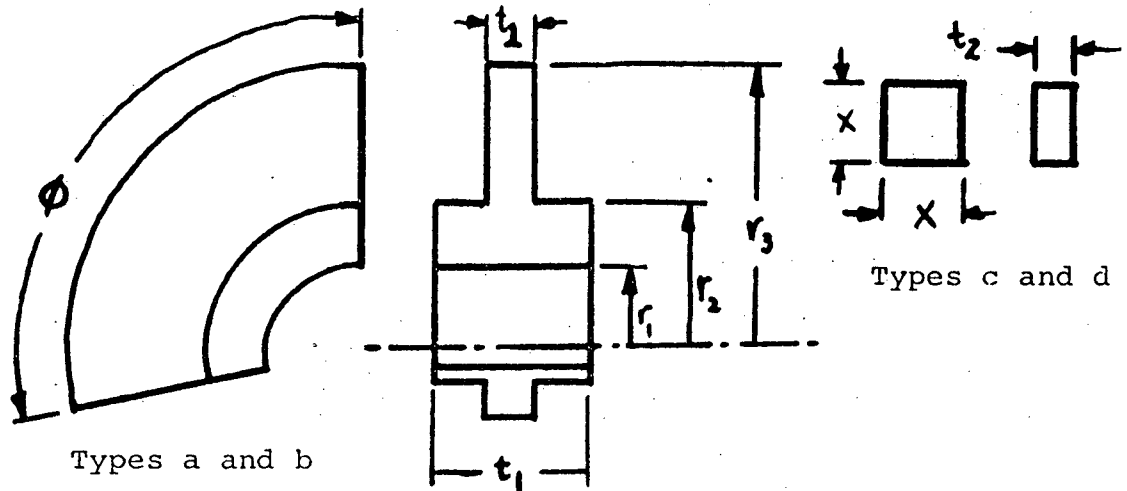
Amend 39
May 1977

TECHNICAL INFORMATION SERIES

NO. DF73LS12

TABLE 1

Simplified Geometry of Hypothetical Wheel Missiles



Type a: wheel shape, $\phi = 120^\circ$

Type b: wheel shape, $\phi = 60^\circ$

Type c: x_1 , square, t_2 thick

Type d: x_2 , square, t_2 thick

Wheel	r_1	r_2	r_3	t_1	t_2	x_1	x_2
43" LSW	17	28	45	27	12	20	8
L-2	18	27	47	12	5	20	10
L-5	20	27	48	9	3	19	11

Note: All dimensions in inches

TECHNICAL INFORMATION SERIES

NO. DF73LS12

TABLE 2

Hypothetical Missile Energy and Velocities
 For All Wheel Groups and Fragment Types
 Of a 43" Last-Stage Bucket Unit

Number of Fragments	Quantity in Table	1st to 3rd Wheel Group	4th to 6th Wheel Group	Last Stage Wheel
2 (Type a)	Weight	2000 (1)	4000	8200
	Energy	0-8 0-3 (2)	0-17 0-7	26-53 10-22
	Velocity	0-510 0-320	0-520 0-340	450-650 280-420
1 (Type b)	Weight	1000	2000	4100
	Energy	0-8 0-3	0-16 0-6	0-38 0-18
	Velocity	0-720 0-440	0-720 0-440	0-770 0-530
3 (Type c)	Weight	300	600	1400
	Energy	0-5 0-2	0-8 0-4	0-16 0-8
	Velocity	0-1000 0-660	0-930 0-660	0-860 0-610
10 (Type d)	Weight	100	150	200
	Energy	0-2 0-1	0-2 0-1	0-3 0-2
	Velocity	0-1100 0-800	0-930 0-660	0-980 0-800

Note: (1) weight is given in lbs ; energy in 10^6 ft lbs ; velocity in ft /sec.

(2) the upper range of values of energy and velocity are calculated for a high speed burst at 180% running speed; lower values - low speed burst at 120% running speed.

GENERAL ELECTRIC COMPANY
TECHNICAL INFORMATION SERIES
NO. DF73LS12

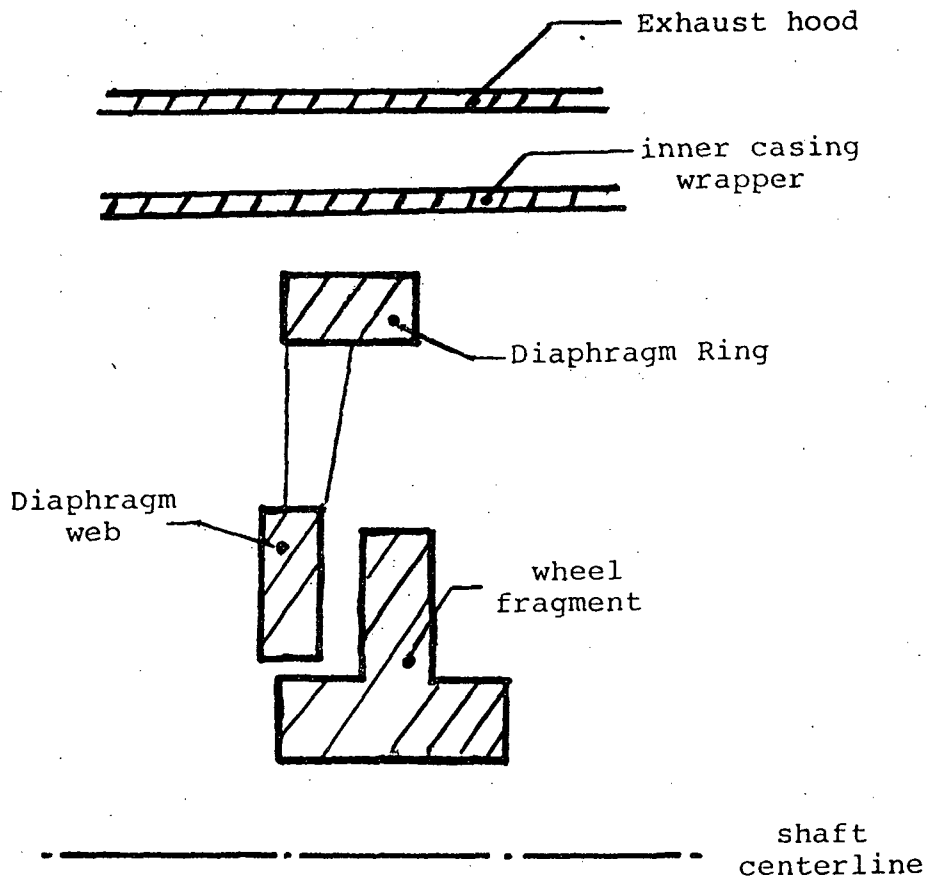
VIII. LIST OF FIGURES

1. Sketch of Wheel Region Illustrating Components Included in Penetration Model.
2. Distribution of Hypothetical Missile Energy and Velocity as a Function of Missile Size.
3. Model Employed to Evaluate the Effective Translational Energy
4. Collision Model for Web and Ring Impacts.
5. Cross Section of Typical Low Pressure Turbine.

TECHNICAL INFORMATION SERIES
NO. DF73LS12

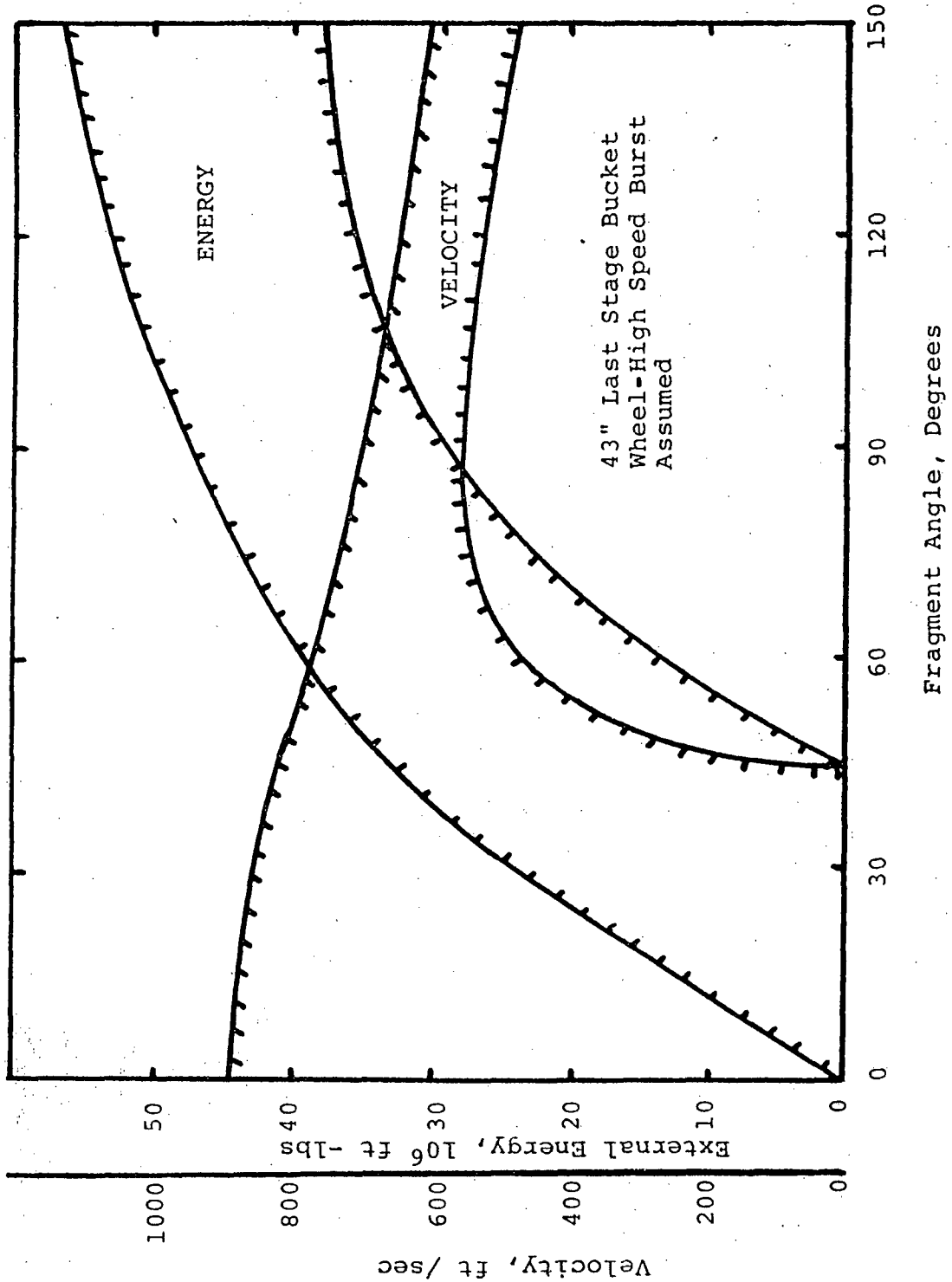
FIGURE 1

Sketch of Wheel Region Illustrating Components
Included in Penetration Model



GENERAL ELECTRIC COMPANY
TECHNICAL INFORMATION SERIES
NO. DF73LS12

Figure 2
Distribution of Hypothetical Missile Energy
And Velocity as a Function of Missile Size



GENERAL ELECTRIC COMPANY Page 27 of 29
TECHNICAL INFORMATION SERIES
NO. DF73LS12

FIGURE 3
Model Employed to Evaluate the
Effective Translational Energy

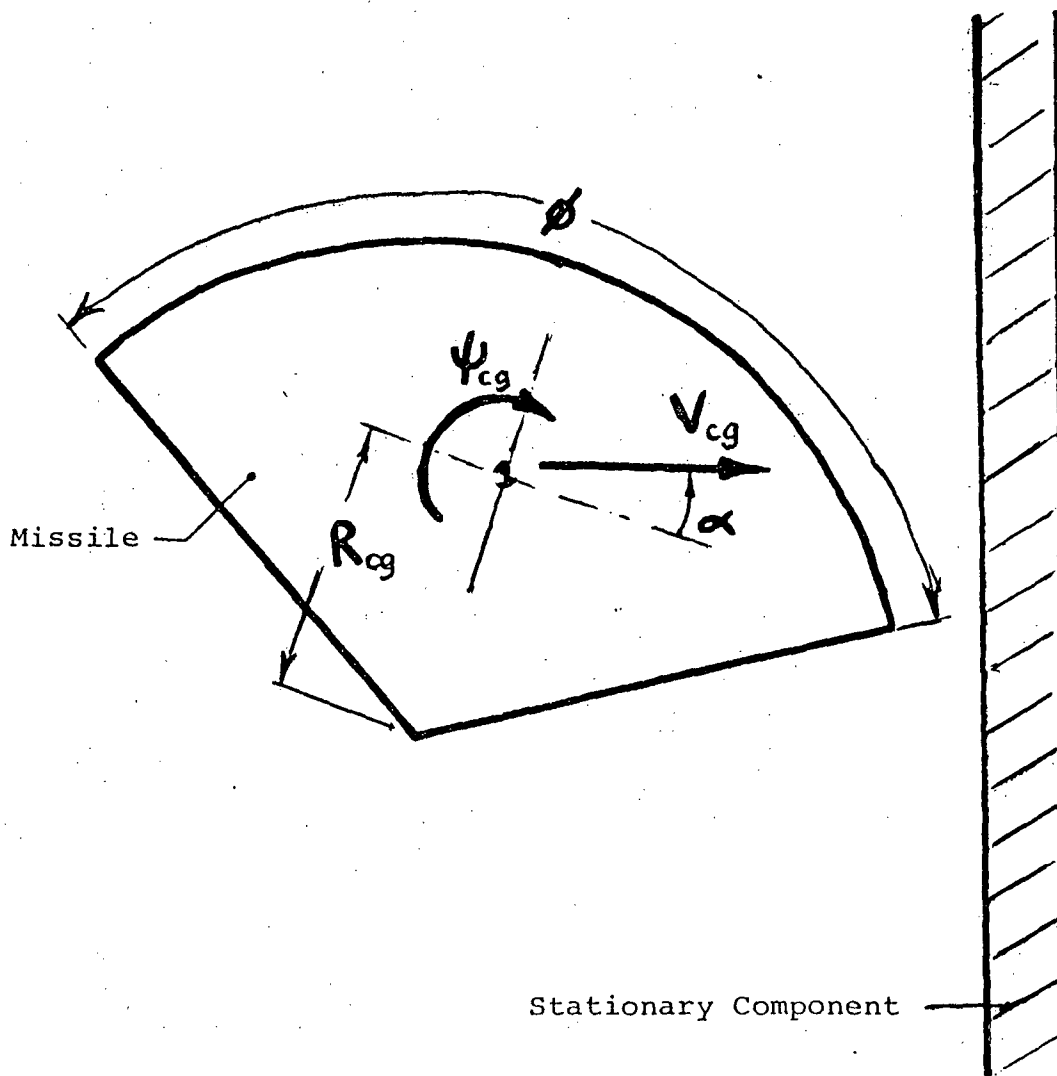
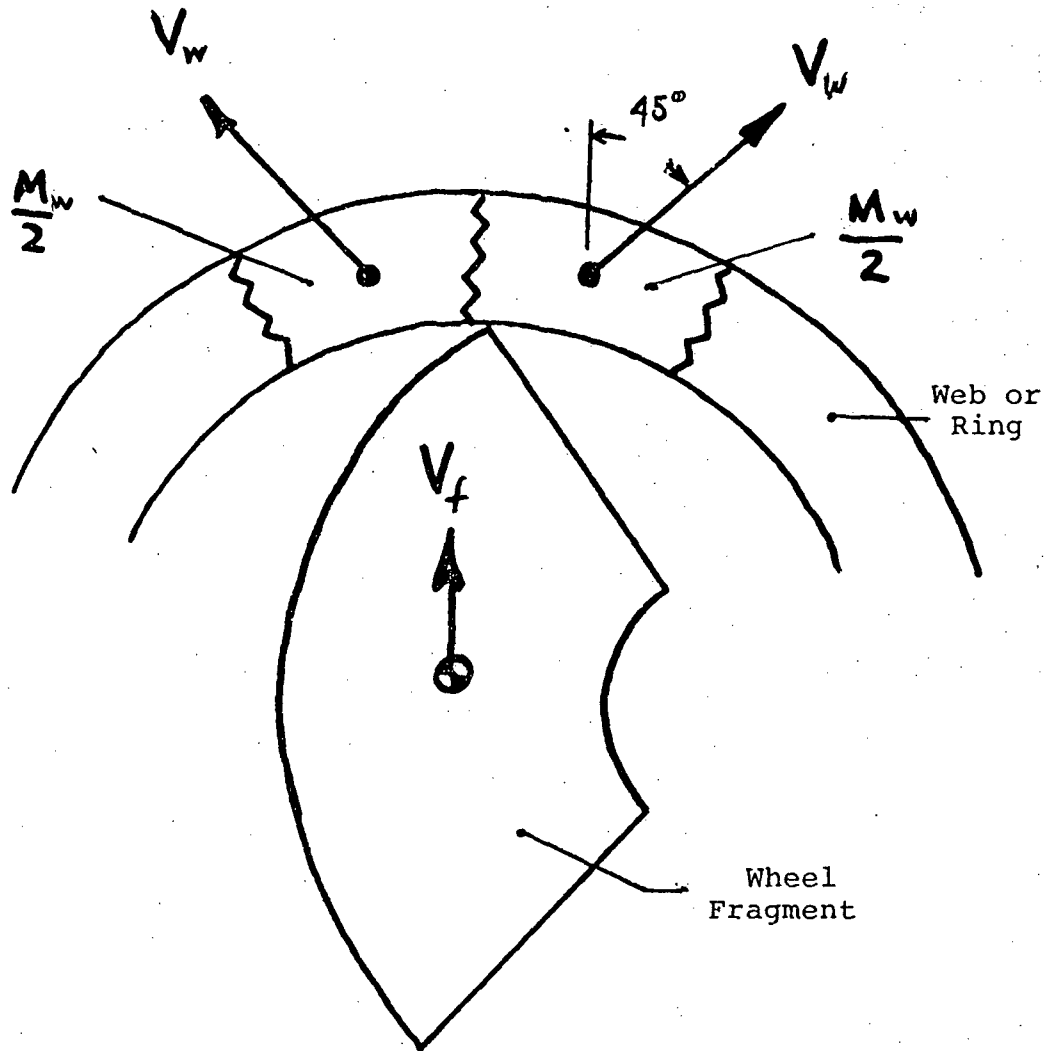


FIGURE 4

Collision Model for Web and Ring Impacts

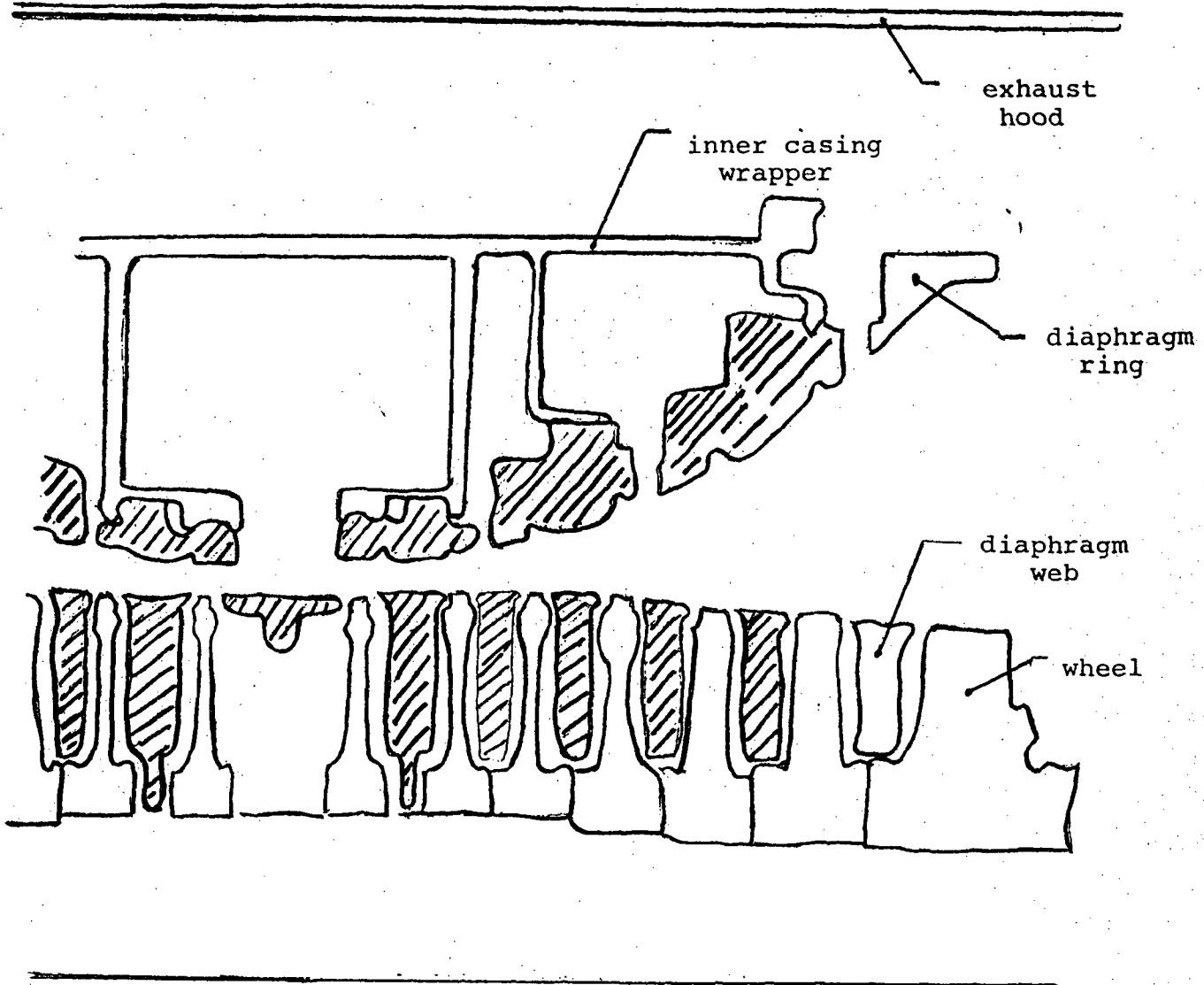


TECHNICAL INFORMATION SERIES

NO. DF73LS12

FIGURE 5

Cross-section of Typical Low Pressure Turbine
Illustrating Major Structural Components



Question 310.41 (15.3)

Indicate whether there are any small lines, such as instrument lines or sample lines, that are connected to the primary coolant boundary and whose failure could result in a release of primary coolant outside of the containment. If so, provide an analysis of the radiological consequences of such a failure.

Response:

In the CRBRP design, there are no small lines, such as instrument lines or sample lines, that are connected to the primary Coolant boundary and whose failure could result in a release of primary coolant outside of the containment.

Question 310.42 (15.3)

The design basis steam generator tube failure accident is stated to be a double-ended failure of a steam generator tube which results in the failure of six additional tubes. By definition, the consequences of a design basis event must be demonstrated to be acceptable in order to determine the adequacy of the design and its protective features. However, this design basis event has not been included in the analysis of steam generator tube failure accidents in Section 15.3.3, in spite of specific requests (e.g. item 310.14). It is our position that the consequences of this design basis steam generator tube failure accident must be analyzed, including its radiological consequences. Your analysis should include:

- a) a single failure anywhere in the system or its support system. Include the possibility of a failure to reseal of a SWRPRS relief valve in your consideration of the worst single failure.
- b) the effects of the initial pressure pulse on the integrity of the primary heat exchanger, particularly in view of the possibility of undetected deterioration of the primary barrier during normal operation. Provide the primary to intermediate loop leak rate following the depressurization of the intermediate sodium loop.
- c) technical specification leak rate for all valves. The use of best-estimate or expected values for valve leak rates is not acceptable for design basis accident calculations. If technical specifications cannot be provided at this time, indicate the maximum acceptable leak rates required to control the consequences of this event to acceptable levels.

Response:

An amendment to 15.3.3.3.1 is provided to clarify and better identify the Design Basis Leak (DBL) information which has been provided in the PSAR and in response to previous NRC questions. Also an amendment is provided to 15.3.3.3.2 to summarize the potential effects of release of radioactive sodium and radioactive water/steam.

Part (a) of this question requests consideration of the consequences of failure of a SWRPRS relief valve to reseal during a sodium-water reaction incident. Relief valves are not used in the SWRPRS to provide overpressure protection to the IHTS. Main rupture disc assemblies are located on the IHTS piping adjacent to the sodium inlet nozzle of the superheater module and adjacent to the sodium outlet nozzles in the evaporator modules to provide the overpressure protection for the IHTS from large sodium-water reaction incidents.

When overpressure protection against large sodium-water reactions is provided by the large rupture discs, the IHTS will blowdown into the SWRPRS and will vent until the pressure in the IHTS has been reduced to essentially ambient pressure. This is the normal manner in which the system functions and analyses of the events related to activation of SWRPRS following a sodium-water incident are based upon this. The limiting type analysis discussed in 15.3.3.3.2 encompasses the effects of postulated single failures.

The response to part (b) regarding IHX integrity is provided in PSAR Sections 5.3.3.1.5 and 5.3.3.5. Briefly, the IHX is designed to withstand conservatively determined pressure flow, temperature transients for the design basis SWR within the emergency limits of the ASME Code (Section III, Class 1 with Code Case 1592). Long term degradation effects (e.g. corrosion) have been accommodated in tube thickness allowances. Primary to intermediate sodium leakage is considered in analysis of the radiological consequences of a SWR as discussed in Section 15.3.3.3.2.

Part (c) requests information on valve leakages. The only valves associated with SWRPRS operation are the steam/water pressure relief valves, the evaporator water dump valves and the module isolation valves. Valve leakage across the isolation valve seat during a large SWR is of interest. Valve water leakage does not contribute to either the maximum pressures experienced during the event, nor does it contribute significantly to the maximum expected exposures at the site boundary. Site boundary dose for this event is far below acceptable limits.

The maximum valve leakages given in Table 5.5-12 are only for establishing the limiting leakage from the system during SGAHRS operation to establish the minimum auxiliary feedwater supply required. Technical specification values for valve leakage have not yet been established, but will be developed as part of continuing design evolution. Technical Specifications will be provided in the FSAR.

Question 310.43 (15.3.3.4)

Although we have not completed our analysis, our preliminary calculations of the off-site dose consequences as a result of postulating the NRC staff site suitability source term indicate that the off-site doses and in particular the bone dose will be in excess of the dose guidelines given in our position of May 6, 1976 from R. P. Denise to L. W. Caffey and that they are, therefore, unacceptable. The staff evaluation model assumed a dual containment having a primary containment design leak rate of 0.1% per day where the releases are treated via filters having a removal efficiency of 99% for all forms of iodines, solid fission products and plutonium and where no more than 1% of the primary containment leak rate bypasses the filters and is released directly to the atmosphere. Staff values of atmospheric dispersion factors appropriate to the site were used. In addition, our calculation model assumed that the secondary containment annulus region is maintained at a negative pressure of at least 1/4" WG so that there is no positive pressure transient during the accident. Furthermore, our calculation assumed that no other pathways to the atmosphere such as the containment purge lines, were open.

It is our position that you should provide a design for the CRBRP that incorporates sufficient Engineered Safety Features, that will bring the off-site doses within the limits of acceptability with respect to the exposure dose guidelines as given in our position letter of May 6, 1976. Based on our LWR reviews, improvements in the annulus filtration system could achieve the necessary dose reductions. Sequoyah, OPS, WPPS 3&5, and Black Fox employ annulus air recirculation, which is one way of achieving further dose reduction beyond that proposed in the current CRBRP design. Indicate what action you plan to take in this regard.

Response:

An annulus air recirculating filter system has been incorporated into CRBRP design, as committed in Reference Q310.43-1. This system is described in revised PSAR Sections 6.2.5 and 9.6.2.

References:

Q310.43-1- S:L:1805, A. R. Buhl (ERDA) to R. S. Boyd (NRC), "Resolution of CRBRP Site Suitability Source Term" dated November 2, 1976.

Question 310.44 (15.5)

Your response to Item 310.20 indicates that the radiological consequences of a reactor cover gas release are unacceptably high. We believe the acceptable off-site dose consequences should be limited to no more than a small fraction of the Part 100 limits. It is our position that, in order to mitigate the consequence of this event, you should either assure that containment is isolated before this event can occur, or provide venting through an ESF system which is effective in absorbing and delaying noble gas release, such as a refrigerated charcoal system, and which delays their release to the atmosphere sufficiently so that the doses will be reduced. In this regard, indicate what action you plan to take.

Response:

49 | The analyses originally presented were based on very preliminary and intentionally very conservative data regarding refueling times. Since that time, a more thorough study of the operational sequence has been conducted. This has shown that the minimum time after reactor shutdown before cover gas release could occur is 30 hours rather than the 3 hours originally assumed. The analyses have been revised for this new time and appear in amended Section 15.5.2.4.

49 | From the data shown on Table 15.5.2.4-1, the whole body dose at the exclusion boundary is well below the 10 CFR 100 guideline limits. Therefore, the Project does not consider any further action required.

Question 310.45 (15.7)

In your response to items 310.13, 310.19 and 310.25 you make the a priori assumption that the continuous containment purge of the RCB can be terminated, and containment isolation achieved, prior to any significant release of activity to the environs. The statement that activity detectors will be located in the RCB to achieve isolation prior to release implies that all accidents involving activity release from the containment must be analyzed in sufficient detail to permit appropriate design, sensitivity, and location of the detectors. However, no analysis of any of the applicable accidents is provided. In view of the uncertainties involved in the numerous accident analyses requiring exact computation of accident location, sequence of events, release mechanisms, and diffusion and convection paths in the containment, it is our position that it is not appropriate to assume that containment isolation can be achieved in all cases prior to the release of activity via the RCB ventilation system. Therefore, we will require the inclusion of the release prior to isolation in the accident dose calculations. In lieu of appropriately detailed analyses of release paths and mechanisms, the incident source term may be assumed to be instantaneously dispersed in the RCB atmosphere (implying the balancing assumption of instantaneous dilution by the RCB atmosphere, as well as immediate availability in diluted concentrations, for release).

Response:

Design requirements imposed on the containment isolation system are consistent with safety analyses which assume containment isolation before activity release.

As stated in PSAR sections 7.3 and 15.1, one of the design requirements of the CRBRP is to assure that containment isolation will be achieved prior to release of activity via the RCB ventilation system. Specifically, scoping analyses, as mentioned in PSAR section 15.1 have determined that this requirement is achieved. Such a scoping study was done assuming a 50,000 CFM exhaust rate. The current design value of 14,000 CFM implies an added margin for the current design to achieve the desired objective for the air transport time and valve closure time.

The study assumes a 10 second air transport time from the exhaust detector sensing point to the isolation valve. This provides a conservative margin since the instrument response and valve closure can be achieved in 7 seconds or less. A maximum of 3 seconds is required for instrument response from the time levels as low as 10^{-6} $\mu\text{Ci/cc}$ appear at the sampling point in the RCB exhaust duct until the signal is received at the isolation valve, with a maximum of 4 seconds for complete valve closure.

The three second detection time and four second closure time, per discussion with equipment vendors, are achievable with state of the art hardware. The concomitant air transport delay is a design requirement imposed on the design of the RCB exhaust ducting. Additionally, a positive pressure with respect to the containment atmosphere will be maintained at the HVAC inlet duct until containment isolation is achieved.

It is emphasized that the design requirements are imposed on sensors in the exhaust duct i.e. located directly in the pathway to release. Activity in the process of release will be identified by the detectors. Potential locations of accidents, sequence of events, release mechanisms and diffusion and convection paths in containment will possibly impact the time elapsed, after a postulated accident initiation, before activity reaches the exhaust ducting. However, the final design of the exhaust ducting will assure an air transport time of 10 seconds or more between exhaust sensor and isolation valve. The time between sensor action, initiation, and valve closure will be 7 seconds or less. This combination of times will prevent activity release above levels of 10^{-6} $\mu\text{Ci}/\text{cc}$ before isolation of containment. The Project is appropriately taking account of this design requirement in its accident analyses.

Based on the above isolation capabilities, all appropriate criteria are achieved including conformance with 10CFR20 and 10CFR100. The placement of a sensor set in the actual release path assures that the sensors detect activity released. Additionally radiation monitors in the Head Access Area (NSS) will provide early signal for closing the containment isolation valves if the release is from that area.

Section 6.2.4.1 and responses to NRC Questions 310.18, 310.19 and 310.25 have been revised to more clearly identify the requirements discussed above.

Question 310.46 (15.5, 15.7.3)

While we recognize that the reference refueling concept requires an open containment, our review of the postulated accidents during this mode lead us to conclude that the potential consequences of refueling accidents could be unacceptably high. Since the refueling concept is, as yet, unproven in service, we conclude that it is inappropriate to have two EVTMs as the only means for preventing a large uncontrolled release to the environment in the event of EVTMs failures. We therefore believe that additional barriers to release of radioactivity are required. It is our position that refueling operations should be performed either with the containment and RSB isolated, or that venting to the atmosphere should be through ESF filters which fully comply with the positions in Regulatory Guide 1.52, and where the areas served by the filters are maintained at a slight negative pressure to prevent out-leakage. In this regard, indicate what action you plan to take.

Response:

The revised design of the HVAC Systems serving the RSB and the RCB provides capability to mitigate the consequences of the SSST. The changes to the RSB HVAC System have been incorporated into Sections 9.1, 9.1.4.1, and 9.6.3. The Engineered Safety Feature portion of the HVAC System is described in Section 6.2.6.

The General Arrangement Drawings included in Section 1.2 presently are being updated to include the revised RSB HVAC Systems as identified above, and will be supplied in a future PSAR amendment. The figures and tables listed below are being revised also and will be supplied in a future amendment.

Table

Title

3.5-4	Roof and Wall Openings for Ventilation System Air Intakes and Exhausts
8.3-1.A	Diesel Generator "A" Load List
8.3-1B	Diesel Generator "B" Load List
8.3-2A	125V DC System "A" Load List
8.3-2B	125V DC System "B" Load List
8.3-2C	250V DC System Load List
9.6-5	Reactor Service Building HVAC System Equipment List
9.7-3	Components Served by Emergency Chilled Water System
9.13-1	Non-Sodium Fire Protection System Areas of Coverage and Fire Barriers
9.13-3	Non-Sodium Fire Protection System Design Basis/ Features
11.4-1	Process and Effluent Sampling and Monitors

Figure

Title

49 9.6-7 through 9.6-10	Flow Diagrams - Reactor Service Building HVAC System
12.1-8 thru 14	Plant Radiation Protection

Question 310.47 (15.7.3)

The analyses presented are very brief and fail to support the conclusion that fuel handling failures will have small consequences. Specifically we disagree with your conclusions in Section 15.7.3.1.3 that the consequences of core component pot leakage are bounded by the radiological consequences described in 15.5.2.3. Significantly larger fission product releases must be expected for an over-heating fuel assembly than the gap activity release as a result of mechanical failure of the clad. It is our position that the radiological consequences of the CCP leakage must be shown to be well within 10 CFR 100 assuming all gap gases are released and include a conservative estimate of the fission products released from the fuel matrix. Provide a revised analysis in this regard and describe any designs or features proposed to limit the consequences.

Response:

The information requested is provided in revised Section 15.7.3.1

Amend. 29
Oct. 1976

Question 310.48 (15.7.2)

We have performed an evaluation of the radiological consequences of the failure of a RAPS surge vessel assuming credit for the cell being a controlled release environment and using a leak rate of 50% per day (assuming a satisfactory leakage test program in compliance with Appendix J of 10 CFR 50). We calculate that the two-hour dose at the exclusion boundary would be well in excess of the 0.5 rem acceptance criterion given in Standard Review Plan 15.7.1. Since we believe that the radiological consequences of a radioactive waste gas system failure for the CRBRP should not be greater than that for an LWR, it is our position that either the design leak rate of the tank cell should be reduced or else the activity placed in more than one tank such that a failure of any one component will not result in a whole body dose at the nearest exclusion boundary in excess of 0.5 rem. In this regard, indicate what action you plan to take.

Response:

Standard Review Plan Section 15.7.1 "Waste Gas System Failure" was written to guide the review of accidents involving failure of LWR waste gas systems. Specifically, the Plan specifies that offsite doses greater than 0.5 rem, whole body, should not result from single failure of a component of a system "that (complies) with the current staff position on seismic and quality group design requirements". Standard Review Plan Section 11.3 "Gaseous Waste Management Systems", subsection II.3 states that "the seismic and quality group classification of . . . the gaseous waste treatment system . . . should conform to the guidelines of Branch Technical Position (BTP) ETSB 11-1 (Rev. 1)". BTP ETSB 11-1 (Rev. 1) Section II.a states that the system should be designed to industry codes for Quality Group D (non-Safety Class); and Section V.a.(1) requires the system be designed to withstand loadings from the OBE (Seismic Category II). The requirement that a single failure in a non-Safety Class Seismic Category II system result in offsite doses no greater than 0.5 rem is consistent with Regulatory Guide 1.26 "Quality Group Classifications and Standards for Water-, Steam-, and Radioactive-Waste-containing components of Nuclear Power Plants". That Reg. Guide (Section C.2.e) requires that components "whose postulated failure would result in conservatively calculated offsite doses . . . that exceed 0.5 rem to the whole body . . ." should be constructed to Qualify Group C (Safety Class 3) standards.

The CRBRP Radioactive Argon Processing System (RAPS) has been designated a Seismic Category I Safety Class 3 (Quality Group C) system. The PSAR Section 15.7.2.4 provides a conservative analysis of the Safety Class system which shows that accidental offsite doses will be maintained below (2.5 rem wholebody) for failure of such a system.

The RAPS circuit has been relocated with the RAPS surge vessel relocated in the Reactor Containment Building (RCB). Two interconnected vessels are used, but with a total effective volume equal to the original. The RCB has a leak tightness specification of 0.1% per day at a pressure differential of 10 psid, so that the rupture of either of these RAPS surge vessels within the RCB is estimated to result in a maximum 0-2 hr site boundary dose of 0.001 rem. Therefore, this postulated accident is no longer the most serious one in the inert gas receiving and processing system. The appropriate revisions to the PSAR to reflect the relocation of the RAPS circuit will be provided in a future amendment.

The revised RAPS circuit has the cold box located in a Reactor Service Building (RSB) cell adjacent to the RCB. A postulated failure of the process gas boundary within the cold box could result in not only the release of absorbed gases from the cryogenic charcoal beds; but also, part of the surge vessel contents could be released into the cold box cell. As a consequence, this cell must have a leak tightness specification with a test program in compliance with Appendix J of 10 CFR 50. For the postulated accident in the cold box cell, the cell tightness required to limit the site boundary dose to 2.5 rem is 40% per day at 11.0 psid.

Because the postulated rupture of the surge vessel in the RCB does not constitute a site boundary dose hazard, and because the postulated cold box rupture in the RSB is potentially the most serious accident in the inert gas receiving and processing system, Paragraph 15.7.2 is retitled and replaced by a description of the cold box accident.

EVS Sodium Cold Trap

A conservative assessment of the consequence of a postulated EVS cold trap fire has been conducted by assuming a sodium spray and subsequent pool fire. In the scenario which is analyzed herein, it was assumed that a sodium leak occurs in the cold trap cell, causing the cold trap cooling system to fail. The plant operators would be alerted by several sodium leakage, temperature, smoke, radiation and pressure detectors, but it is assumed that they fail to isolate the cold trap circuit with the isolation valves which are located in a separate environment and thus not affected by the fire. The leaked sodium burns all the oxygen available in the cell. It should be noted that a leak in this cell is not expected to release the radioactive contents of the cold trap inventory since this inventory consists of condensed solids in the trap. Nevertheless, it is conservatively assumed that the radionuclide concentration in the leaked sodium is that which would exist if all of the cold trap inventory was redissolved in the EVS sodium. In fact, most of the redissolution would take place long after the available oxygen was consumed.

For a sodium leak, the resultant cell temperature, and thus the cold trap temperature, would not rise to a value above that of the leaked sodium. Analysis for the Primary Cold Trap shows that it takes tens of hours to redissolve the cold trap contents, even if the cold trap temperature rises to 600°F. Similar analysis for the EVS cold trap has not been done, but similar behavior would occur. In actuality, the EVS cold trap release would be expected to be slower since its normal inlet sodium temperature is less than 500°F. The temperature rises to 600°F infrequently, only during operations to remove sodium surface impurity buildup in the EVST.

The decay heat generated in the cold trap is not sufficient to cause a significant temperature rise in the cold trap. If the trap were cut off from both its cooling system and the sodium process stream, the trap temperature would not rise above its normal operating temperature.

The radiological consequences of this event were analyzed as follows:

1. The total inventory of the cold trap is redissolved into the EVS sodium. The radioactivity within the 60,000 gal. of EVS sodium includes the normal inventory plus that from the cold trap. It was obtained from the cold trap inventory as given in Table 12.1-24 and the distributions ratio between the cold trap and the EVS sodium as given in Table 12.1-7. The concentration was assumed uniform throughout the volume.
2. Following failure of the EVS cold trap, 15,250 gal. of sodium spills into the cold trap cell. This is the maximum amount that can spill due to the arrangement of the lines from the EVST. With the conservative assumptions followed, the radiological consequences are insensitive to the total volume of sodium spilled.

3. All of the oxygen within the cold trap cell and the adjoining cells which share a common atmosphere reacts with the sodium. The total volume of these cells is 33000 cubic feet. These cells contain a maximum of 2 w/o oxygen in nitrogen.
4. All of the sodium oxide produced is Na_2O and all of it is airborne as an aerosol.
5. All of the aerosol generated is immediately released to the atmosphere without credit for plate-out or settling within the cold trap cell or the Reactor Service Building (RSB), depletion along the leak paths from the cold trap cell to the RSB or filtration through the RSB exhaust system.
6. The concentration of radioactivity in the aerosol is the same as that in the spilled sodium. The discussion forwarded in response to Question 310.50 reviewed the partitioning of fission products in the aerosol resulting from burning of the spilled sodium. It was shown that the assumption of equal activity in the pool and aerosol sodium was conservative.
7. Radioactivity decay during the accident is neglected.
8. Fallout (cloud depletion) of radioactive material during downwind transport is conservatively neglected.

Using the dose calculational methodology described in Chapter 7 of the ER and 95% X/Q's, potential offsite doses have been determined. Doses at the Exclusion Boundary and the Low Population Zone are itemized in Table Q310.49-2.

Question 310.50 (15.6)

Your response to Q310.12 lists partition factors for iodine and cesium in the range of 10^{-4} to 10^{-7} . Also, observed increases of iodine concentrations in sodium aerosols over bulk sodium are cited. These observations appear to contradict each other, as the most likely mechanism for increased iodine concentration in the aerosol is scavenging of iodine from the vapor phase. It should also be noted that iodine partition factors vary by orders of magnitude depending on the iodine species present. Your response does not address these considerations, nor the applicability of the experimental conditions of Reference 310.12-5 to the postulated accident conditions.

In lieu of applicable data on partitioning of the various forms of volatile fissions products, analysis should be performed with the conservative assumption of immediate volatilization of these species.

Response

Two basic types of experiments were discussed in the response to Q310.12. One type dealt with the release of fission products from essentially static sodium pools in the absence of oxidation, and the other with the release of iodine from sodium pools under burning conditions.

The former (Refs. Q310.12-5 and -6) are basically equilibrium-vaporization studies in which the relative volatility of particular isotopes (solutes) are measured in relationship to sodium (solvent). In these experiments the only mechanism for release of either the solute or solvent to the gas space above the sodium is evaporation - partitioning of the volatile substances between the liquid sodium and the gas phase. Two principal parameters are determined in these types of experiments. One is the "distribution coefficient" and the other is the "release (partition) fraction".

The "distribution coefficient" is defined as the ratio of the mole fraction of solute in the gas phase to its mole fraction in the liquid, and is determined experimentally by relating the specific activity of an isotope in the gas phase to its specific activity in the liquid. For dilute solutions, representative of the fission product concentrations in the sodium coolant, the distribution coefficient is a function of temperature only, and is meaningful only for equilibrium conditions.

Kunkel (Reference Q310.50-1) used the experimental data cited in Q310.12 (Refs Q310.12-5 and -6) to obtain distribution coefficients for iodine and cesium. For iodine/sodium, Kunkel obtained distribution coefficients between 1 and 0.6 for equilibrium temperatures between 925°F and 1000°F. As the temperature increased, the iodine distribution coefficient decreased and for temperatures less than about 925°F the distribution coefficient exceeded unity. Kunkel's experimentally determined iodine distribution coefficients were compared and agreed well with theoretical coefficients developed by Pollock (Reference Q310.50-2). Pollock's model predicts that

the iodine distribution coefficient exceeds unity for temperatures less than 970°F. For cesium/sodium, Kunkel also found that the distribution coefficient decreased with increasing temperature; the measured coefficients ranged from 60-90 for an equilibrium temperature of about 1000°F.

Pollock, Silberberg, and Koontz (Ref. Q310.50-3) have also measured distribution coefficients for iodine and cesium in sodium. Their measured iodine coefficients were 2.5, 1.1, and 0.8 for temperatures of 790°F, 900°F, and 1100°F. These values are in reasonable agreement with Kunkel's and again indicate that the iodine coefficient exceeds unity for temperatures less than about 1000°F. For cesium, the measured coefficients ranged from 37 to 96 for a temperature range of 765°F to 1100°F.

The release fraction is defined as the ratio of the actual isotope activity in the gas space above the sodium pool to that in the sodium pool. The release fraction as opposed to the distribution coefficient depends on temperature as well as system parameters such as cell volume and sodium mass. The release fractions cited for iodine in Q310.12 varied from 2×10^{-4} to 1×10^{-6} . The larger of these release fractions (2×10^{-4} to 4×10^{-5}) were based on in-pile experiments (Reference Q310.12-6) involving fission product releases from partially vaporized uranium fuel; this set of experiments is more typical of hypothetical core events involving molten fuel and subsequent fission product vapor releases to the sodium. The smaller of these release fractions (5×10^{-6} to 1×10^{-6}) were based on out-of-pile static sodium pools containing NaI (Reference Q310.12-5) much more typical of postulated sodium spill conditions. Saroul has also conducted out-of-pile experiments in which iodine release fractions of approximately 10^{-5} were observed (Reference Q310.50-4).

The distribution coefficient alone is insufficient to quantify the amount of a particular isotope (solute) released from a sodium pool. Rather it provides a measure of the release of the isotope to the gas space relative to the release of sodium via evaporation, but this relationship only applies strictly for equilibrium conditions. With regard to sodium fire evaluations, the distribution coefficients are not directly applicable since equilibrium conditions are not attained. However, since the distribution coefficient or relative volatility for iodine exceeds unity for temperatures near or below 1000°F and since the cesium coefficient exceeds unity over the entire temperature range associated with sodium fires, releases via evaporation over the course of a sodium fire could result in the preferential release of iodine and cesium vis-a-vis sodium vapor, leading to increased airborne concentrations for these isotopes. Note, however, that the distribution coefficients are concerned with concentrations and not absolute quantities of activity released. Consequently, release fractions less than unity, as cited in response to Q310.12, do not imply that the concentration of solute in the gas phase is less than that in the liquid phase; thus, release fractions less than unity do not contradict the observation of increased iodine

concentrations in the gas phase for the sodium burning experiments. On the other hand, release fractions considerably less than unity, as consistently found in the cited experiments, demonstrate clearly that iodine and cesium are mainly retained in sodium pools, even for relatively high temperature conditions, and do not experience immediate volatilization. It is in this sense, that the results of the equilibrium-vaporization experiments are directly applicable to the response to Q310.12.

The sodium-iodine burning experiments (References Q310.12-1 and -2) are directly applicable to the evaluation of sodium fires. The mechanisms for release of iodine in these experiments include both evaporation and aerosol transport from the sodium pool, and, consequently, the experimental measurement of the iodine airborne concentration reflects the total release of iodine from the pool under burning conditions.

The burning experiments cited in Q310.12 included sixteen separate sodium-iodine pool burning tests. The initial iodine concentration in the liquid sodium for these tests ranged from 0.08 to 59 ppm. In all these tests, the sodium was completely burned, but the fraction of the sodium combustion product becoming airborne did not exceed 15%. One common and important finding of all these tests was that, even for complete sodium combustion, the iodine was not completely released, i.e., the assumption of immediate volatilization is overly conservative.

While demonstrating that the iodine is not completely volatilized, the burning experiments cited in Q310.12 do show that the specific airborne concentration of iodine exceeds the corresponding pool concentration. For the experiments reported in Reference Q310.12-1, it was found that the airborne concentration of iodine was 2.6 times the liquid concentration. In the Reference Q310.12-2 tests, the average airborne to liquid concentration ratio was approximately 2.

Other sodium-iodine burning tests have also been conducted in which the initial iodine concentration in the liquid was lower, more typical of CRBRP sodium conditions. Specifically, the maximum iodine/sodium concentration expected for CRBRP is about 0.4 ppb. Burning experiments reported in Reference Q310.50-5 involved sodium with a trace amount of iodine (<0.01 ppb) and experiments reported in Reference Q310.50-6 were conducted with an initial iodine liquid concentration of 3 ppb. Again, in these experiments, all the sodium was burned but the iodine was not completely released, confirming that the assumption of immediate volatilization is overly conservative. For these lower initial iodine concentration tests, it was found that the airborne concentration of iodine was the same as its liquid concentration or, in other words, the release fraction of iodine was about equal to the sodium release fraction. Noting that the CRBRP iodine/sodium concentration (0.4 ppb) is much more typical of these lower iodine concentration tests, it is considered conservative to apply a preferential release factor of 3 for iodine compared to sodium, based on the higher iodine/sodium concentration tests.

Equally extensive burning experiments for sodium-cesium are not available. However, a series of small-scale experiments, including more than twenty separate burning tests, are reported in Reference Q310.50-6. In all these tests the initial concentration of cesium in the liquid sodium was 5 ppm, typical of the maximum cesium concentration expected in CRBRP (7ppm). For all the tests, the sodium was completely burned but the cesium was not completely released, i.e., the assumption of immediate cesium volatilization is overly conservative. For each test, the release fractions (ratio of the quantity becoming airborne to the quantity initially in the liquid) of both sodium and cesium were measured. The sodium release fraction was found to decrease with increasing oxygen concentration, increasing humidity and decreasing temperature. Similar findings concerning decreasing sodium releases with increasing oxygen concentration have been reported in Reference Q310.50-7. The maximum sodium release fractions were approximately 15-30% and occurred for high temperature (930°F-1100°F) low oxygen (<10%) concentration conditions. The cesium release fractions varied identically with the sodium fractions as temperature, oxygen, and humidity varied. However, the cesium release fraction was consistently greater than that of the sodium. Except for very high humidity (≥ 2 wt%) and high oxygen (>21%) conditions, for which sodium release was less than 5% and cesium releases less than 40%, the cesium release fraction did not exceed the sodium release fraction by more than a factor of 10. Such a preferential cesium release could be expected based on the large relative volatility of cesium with respect to sodium; however, the assumption of immediate and complete cesium volatilization is refuted by these experiments as well as the equilibrium-vaporization experiments discussed previously.

Considering the experimental data reviewed above, it would be overly conservative to assume the immediate volatilization of iodine and cesium from sodium pools during postulated fires. In fact, the data indicate that a conservative assessment can be made by applying a preferential release factor of three for iodine and ten for cesium compared to sodium.

However, in addressing the potential consequences of postulated sodium fires, it is necessary to consider the total radiological source term associated with such fires. It will now be shown that the overall approach as used in the PSAR (i.e., airborne and liquid concentration assumed equal) contains substantial conservatism that provide margin for any uncertainties associated with the preferential release of the more volatile nuclides (iodine and cesium).

In assessing the potential radiological consequences of sodium fires, the starting point for defining an appropriate source term is the initial radionuclide concentrations in the liquid sodium. Such concentrations have been conservatively defined and presented in the PSAR (Section 12.1.3). The basis for computing these concentrations was conservatively established as continuous plant operation for 30 years with 1% failed fuel and a primary sodium content of 100 ppb. of Pu.

Three distinct types of radioactive sodium were considered in the PSAR sodium fire accident analyses. The first was termed Primary Sodium - 0 days decayed; the radioactive inventory of this sodium consists of fission products, fuel and corrosion products which have become entrained in the primary coolant during 30 years of operation with 1% failed fuel plus the steady state nuclide inventory resulting from activation as the coolant is exposed to the core neutron flux as well as the plant operating limit of 100 ppb plutonium. Postulated accidents involving this type of sodium are necessarily limited to leaks in the primary system during power operation. The second type of sodium considered was termed Primary Sodium - 10 days decayed; the radioactive inventory of this sodium is similar to 0 day decayed - Primary Sodium, except that the inventory of short-lived species is substantially reduced following reactor shutdown. Postulated accidents involving this type of sodium are associated with maintenance activities, which are generally restricted to times at least as long as 10 days after shutdown to permit sufficient decay of the primary sodium. The last type of sodium considered was Ex-Vessel Storage (EVS) sodium; the radioactive inventory of this sodium increases slowly over the life of the plant as small quantities of primary sodium are mixed with the EVS sodium during refueling operations. The radionuclide concentrations of each of these types of sodium are specified in the PSAR (Tables 12.1-6 and 12.1-23).

The radiological hazard associated with each type of sodium can be defined on a unit mass basis. The procedure for developing such a hazard index is as follows: each isotope concentration ($\mu\text{Ci/gm}$) is multiplied by its respective inhalation dose factor (Rem/Ci inhaled) for each critical organ (bone, lung, thyroid, and whole body) considered. These products are summed over each organ to provide a value of Rem per organ per unit mass of sodium inhaled. If the radionuclide concentrations in sodium aerosol are equal to the initial concentrations in the liquid sodium (potential variations in this are addressed later), the Rem per organ per unit mass of sodium values then represent a measure of the doses associated with the inhalation of a unit mass of sodium. This procedure is meaningful in that the principal exposure pathway associated with sodium fires is the dispersion of sodium aerosol, containing radionuclides, to off-site locations and the resultant intake of this aerosol by individuals exposed to the dispersing aerosol cloud.

Summaries of the Rem per organ per unit mass of sodium inhaled values for each type of sodium considered are provided in Tables Q310.50-1, -2, and -3.

Table Q310.50-1 shows that with the assumption of equal aerosol-liquid nuclide concentrations, the most limiting exposure (minimum allowable intake) resulting from inhalation of Primary Sodium - 0 days decayed is the bone dose. The principal contributors to this exposure are Na-24 (36%) and the Pu isotopes (61%). The major volatile isotopes, iodine and cesium, contribute little (~4%) to the total bone exposure. Specifically, the release fraction of iodine would have to be increased by more than two orders of magnitude before its contribution to bone exposure would become comparable to the Pu contribution; likewise, the cesium release fraction would have to increase by approximately a factor of 20. Data already cited in response to question 310.12 and amplified herein indicate that such large increases in the fractional release of iodine and cesium from a sodium pool fire would not occur. A conservative variation based on the experimental data is a factor of 3 for iodine and 10 for cesium. The possibility that increased release of either iodine or cesium would result in an organ other than the bone being limiting has also been considered. Again, examination of Table Q310.50-1 indicates that this will not be the case. Considering each organ in turn, the Lung Rem/gram would have to increase by 27% for lung exposure to be limiting. Such an increase would require the fractional cesium release to increase by more than a factor of 20.

For thyroid exposure to become limiting, the Iodine release fraction would have to increase by more than a factor of 20, and for the whole body exposure to become limiting the cesium release would have to increase by more than a factor of 30. Such large increases are not supported by experimental data.

Although the preceding discussion is based on Primary Sodium-0-days decayed (Table Q310.50-1), identical conclusions would be reached regardless of which type of sodium is considered. This can be verified by comparison of Tables Q310.50-1, -2, and -3. In all cases, at least a factor of 20 increase in iodine or cesium release would be required to cause the bone contribution from that isotope to be comparable to the contribution from plutonium, or to cause any other organ dose to be comparable to the bone dose.

The discussion to this point has shown that the Na-24 and Pu isotopes control the exposure from sodium fires, under the assumption of equal aerosol/liquid concentrations and that only by grossly overestimating the release of the more volatile species could this be reversed.

The assumption of equal aerosol/liquid concentrations for the Pu isotopes is extremely conservative based on applicable sodium burning test data. In Reference Q310.50-8, Chatfield determined that a plutonium release fraction of 2.9×10^{-5} resulted from the burning of sodium containing PuO₂. Recent experiments at Atomics International (Reference Q310.50-9) have further assessed the airborne concentration of plutonium resulting from the combustion of plutonium

contaminated sodium. In these tests, sodium was doped with from 10 to 233 ppm PuO_2 or Na_4PuO_5 and then ignited in air at temperatures of 500 to 550°C. The aerosol released from this burning pool of sodium was collected and analyzed for plutonium content. For the sodium containing PuO_2 , nine experiments resulted in plutonium release fractions ranging from 1×10^{-6} to 3.6×10^{-5} . The average release fraction was 1.1×10^{-5} . For sodium-plutonate, the results indicate the release fractions are several orders of magnitude less than for PuO_2 . The application of these data to the evaluation of sodium fire consequences would essentially eliminate the Pu contribution to exposures and thus significantly reduce predicted consequences. However, to insure a conservative assessment of potential radiological consequences, the PSAR analyses include the Pu contribution by pessimistically assuming equal aerosol/liquid concentrations. This assumption overestimates the Pu exposure contribution by several orders of magnitude and consequently provides conservative doses to the limiting organ (i.e. bone) that contain margins for uncertainties in the fractional releases of more volatile species.

To summarize, the PSAR sodium fire analyses are based on the assumption of equal aerosol/liquid radionuclide concentrations. This assumption leads to an overestimate of several orders of magnitude of the contribution of Pu, which is the controlling nuclide dose contributor. This approach results in a conservative assessment of potential radiological consequences and provides ample margin for any uncertainties associated with the preferential release of volatile isotopes. Alternately, the experimental sodium burning-release data could be directly applied to the PSAR sodium fire evaluations. This would result in essentially the complete elimination of the plutonium source term, a factor of three increase in the iodine source, and a factor of ten increase for cesium. These latter two factors have already been shown to be conservative. The overall result of this approach, as shown in the above discussion, would be a net decrease in the controlling off-site exposures, leading to an assessment which is enveloped by that currently presented in the PSAR.

References

- Q310.50-1 "Fission Product Retention in Sodium - A Summary of Analytical and Experimental Studies at Atomics International", NAA-SR-11766, 1966, pp. 73-79.
- Q310.50-2 Reference Q310.50-1, pp.93-95.
- Q310.50-3 Pollock, B.D., Silberberg, M., and Koontz, R.L., "Vaporization of Fission Products From Sodium", ANL-7520, Part I, 1968, pp. 549-554.
- Q310.50-4 Saroul, J., "Investigation on the Behaviour of Fission Products in Sodium and Argon - PIRANA Experiments", in Proceedings of the International Conference on the Safety of Fast Reactors, Aix-en-Provence, September 19-22, 1967, pp. Vb-1-1-3.
- Q310.50-5 "Summary Report for Laboratory Experiments on Sodium Fires", TR-707-130-007, August 1973, pp. 21-22.
- Q310.50-6 Kawahara, S., et. al., "Behavior of Sodium Oxide and Fission Products Under Sodium Pool Fire", in Engineering of Fast Reactors for Safe and Reliable Operation - International Conference, Karlsruhe, Germany, October 9-12, 1973. Vol III, pp. 1406-1422.
- Q310.50-7 NAA-SR-12296, "Quarterly Technical Progress Report - AEC Unclassified Programs, October - December 1966", pp. 60-61.
- Q310.50-8 E. J. Chatfield, J. Fuel Material, 32, 228 (1969).
- Q310.50-9 AI-ERDA-13166, "Quarterly Technical Progress Report: Nuclear Safety, Characterization of Sodium Fires and Fast Reactor Fission Products, October - December 1975", February 15, 1976.

TABLE Q310.50-1

RADIOACTIVE SODIUM HAZARD INDEX

PRIMARY SODIUM - 0 DAYS DECAYED

Isotope	$\mu\text{Ci/gm Na}$	Rem/Gm Na Inhaled ^a			
		Bone	Lung	Thyroid	Whole Body
Na-22	3.49	4.54-2	4.54-2	4.54-2	4.54-2
Na-24	2.94+4	4.97+1	4.97+1	4.97+1	4.97+1
Total Na		4.97+1	4.97+1	4.97+1	4.97+1
I-131	43.7	1.38-1	-	6.52+1	1.12-1
I-132	27.8	4.04-2	-	1.52	4.04-3
Total I		1.78-1	-	6.67+1	1.12-1
Cs-134	1.88	8.78-2	2.30-2	-	1.71-1
Cs-136	16.6	8.14-2	2.50-2	-	2.32-1
Cs-137	68.7	4.12	6.48-1	-	3.68
Total Cs		4.29	6.96-1	-	4.08
Pu-238	1.30-2	3.50+1	2.28	-	8.66-1
Pu-239	3.60-3	1.09+1	6.02-1	-	2.72-1
Pu-240	4.70-3	1.46+1	8.02-1	-	3.62-1
Pu-241	3.94-1	2.38+1	5.98-2	-	5.08-1
Pu-242	1.00-5	2.90-2	1.59-3	-	7.18-4
Total Pu		8.43+1	3.75	-	2.01
Total Others		5.32-1	4.54-1	8.25-4	1.00-1
Total (Rem/Gm)		139	54.60	117	55.91
Exposure Limit ^b (Rem)		15	7.5	150	20
Allowable Intake ^c (Gm)		0.108	0.137	1.28	0.358

a) $\text{Rem/Gm Inhaled} = (\mu\text{Ci/gm}) (10^{-6} \text{Ci}/\mu\text{Ci})$ (Inhalation Dose Factor Per Regulatory Guide 1.109, Rem/Ci).

b) Exposure Limit based on dose (rem) guidelines appropriate at the construction permit stage.

c) Allowable Intake = Exposure Limit (Rem)/Total(Rem/gm).

TABLE Q310.50-2

RADIOACTIVE SODIUM HAZARD INDEX

PRIMARY SODIUM - 10 DAYS DECAYED

Isotope	$\mu\text{Ci/gm Na}$	Rem/Gm Na Inhaled ^a			
		Bone	Lung	Thyroid	Whole Body
Na-22	3.46	4.50-2	4.50-2	4.50-2	4.50-2
Na-24	4.32-1	7.30-4	7.30-4	7.30-4	7.30-4
Total Na		4.57-2	4.57-2	4.57-2	4.57-2
I-131	1.84+1	5.80-2	-	2.74+1	4.72-2
I-132	3.28	4.76-4	-	1.79-1	4.76-4
Total I		5.85-2	-	2.76+1	4.77-2
Cs-134	1.86	8.68-2	2.26-2	-	1.69-1
Cs-136	1.00+1	4.90-2	1.51-2	-	1.39-1
Cs-137	6.87+1	4.12	6.48-1	-	3.68
Total Cs		4.26	6.86-1	-	3.99
Pu-238	1.30-2	3.50+1	2.28	-	8.66-1
Pu-239	3.60-3	1.09+1	6.02-1	-	2.72-1
Pu-240	4.70-3	1.46+1	8.02-1	-	3.62-1
Pu-241	3.94-1	2.38+1	5.98-2	-	5.08-1
Pu-242	1.00-5	2.90-2	1.59-3	-	7.18-4
Total Pu		8.43+1	3.75	-	2.01
Total Others		5.00-1	3.88-1	4.69-4	3.66-2
Total (Rem/Gm)		89.20	4.87	27.65	6.13
Exposure Limit ^b (Rem)		15	7.5	150	20
Allowable Intake ^c (Gm)		0.168	1.54	5.42	3.26

a) $\text{Rem/Gm Inhaled} = (\mu\text{Ci/gm}) (10^{-6} \text{Ci}/\mu\text{Ci}) (\text{Inhalation Dose Factor Per Regulatory Guide 1.109, Rem/Ci})$.

b) Exposure Limit based on dose (rem) guidelines appropriate at the construction permit stage.

c) Allowable Intake = Exposure Limit (Rem)/Total(Rem/Gm).

TABLE Q310.50-3

RADIOACTIVE SODIUM HAZARD INDEX

EX-VESSEL STORAGE SYSTEM SODIUM

Isotope	$\mu\text{Ci/gm Na}$	Rem/Gm Na Inhaled ^a			
		Bone	Lung	Thyroid	Whole Body
Na-22	6.50-1	8.45-3	8.45-3	8.45-3	8.45-3
Na-24	1.47+1	2.48-2	2.48-2	2.48-2	2.48-2
Total Na		3.33-2	3.33-2	3.33-2	3.33-2
I-131	1.34	4.22-3	-	1.99	3.44-3
I-132	-	-	-	-	-
Total I		4.22-3	-	1.99	3.44-3
Cs-134	3.80-1	1.77-2	4.64-3	-	3.46-2
Cs-136	6.00-1	2.94-3	9.00-4	-	8.34-3
Cs-137	3.82+1	2.28	3.60-1	-	2.04
Total Cs		2.30	3.66-1	-	2.08
Pu-238	7.90-3	2.16+1	1.41	-	5.32-1
Pu-239	2.10-3	6.10	3.34-1	-	1.51-1
Pu-240	2.70-3	8.52	4.68-1	-	2.10-1
Pu-241	1.84-1	1.11+1	2.80-2	-	2.38-1
Pu-242	5.90-6	1.73-2	9.54-4	-	4.30-4
Total Pu		4.74+1	2.24	-	1.13
Total Others		-	1.02-4	1.02-4	1.02-4
Total (Rem/Gm)		49.74	2.64	2.02	3.25
Exposure Limit ^b (Rem)		15	7.5	150	20
Allowable Intake ^c (Gm)		0.302	2.84	74.25	6.15

a) $\text{Rem/Gm Inhaled} = (\mu\text{Ci/gm}) (10^{-6} \text{Ci}/\mu\text{Ci})$ (Inhalation Dose Factor Per Regulatory Guide 1.109, Rem/Ci).

b) Exposure Limit based on dose (rem) guidelines appropriate at the construction permit stage.

c) Allowable Intake = $\text{Exposure Limit(Rem)}/\text{Total(Rem/gm)}$.

Question 310.51 (15.7)

Sodium fires and sodium-water reactions can occur accidentally in several places. The resultant combustion products and/or sodium aerosol will disperse towards the site boundary and low population zone (LPZ). Provide detailed analyses of the non-radiological consequences at the minimum site boundary distance and at the LPZ outer radius of sodium fires or sodium-water reactions on all the cases such as these listed in Section 7.0 of the Environmental Report. Include, in addition, analyses for the cold trap fire and the intermediate heat exchange rupture.

In these analyses, the following data should be provided: the expected total sodium spill or burning rate, duration of the fire, the building leakage rate, the aerosol dispersion factor (\bar{x}/Q), and the aerosol concentration at the control room air intakes, the closest site boundary, and the LPZ. State all your assumptions.

Results of an analysis on cases 3, 5, and 6 are presented in Table 7.2.2 of the Environmental Report. However, there are two versions of this table, and the values do not agree with one another. Please resolve these discrepancies and provide the information in the PSAR.

Response:

Those events evaluated in the response are itemized below and include all events in the Environmental Report resulting in the release of sodium reaction products to the atmosphere:

- ER Accident 4.1 Failure of ex-containment primary sodium drain piping during maintenance.
- ER Accident 4.2 Failure of the ex-vessel storage tank (EVST) sodium cooling system during maintenance.
- ER Accident 5.2 Steam Generator tube rupture.
- ER Accident 8.1 Primary sodium in-containment drain tank failure during maintenance.
- ER Accident 8.2 Large primary coolant sodium spill during operation.
- ER Accident 8.3 Gross failure of ex-containment primary sodium storage tank.
- ER Accident 8.4 Rupture of the ex-vessel storage tank sodium cooling system during operation.
- ER Q000.28 Primary cold trap fire.

PSAR Section IHTS Pipe Leak
15.6.1.5

Amend :
May 19

Table Q310.51-1 provides a summary description of each event and the analysis results pertinent to this Question.

For each event, the average aerosol concentrations, in terms of milligrams of NaOH per cubic meter, at scheduled downwind locations have been determined. These concentrations are provided in Table Q310.51-2. This analysis is based on the assumption that all the Na released to the atmosphere is immediately converted to NaOH. Per unit mass of Na released to the atmosphere 1.74 mass units of NaOH are produced. In determining the downwind aerosol concentrations at the exclusion boundary and the LPZ the 0-8 hour 50th percentile x/Q values were employed. Reference Q310.51-1 was used in developing x/Q values for the Control Room Intakes.

42

The specific values used are as follows:

<u>Location</u>	<u>x/Q (sec/m³)</u>
Control Room Intakes	{ 4.0 x 10 ⁻³ *
	{ 3.7 x 10 ⁻³ **
Exclusion Boundary	2.20 x 10 ⁻⁴
Low Population Zone	0.59 x 10 ⁻⁴

A depletion factor credit of 100 has been applied for sodium hydroxide in its transit from release to arrival at the exclusion boundary and LPZ. As described in response to PSAR question 001.233 this factor conservatively accounts for fallout of the sodium and conversion to carbonate form before reaching the exclusion boundary and LPZ. Also, no credit for the confinement annulus filters or RSB filters was taken for events postulated in the RCB or RSB.

For each event, an average aerosol concentration is defined for each downwind position requested. The average concentration is directly proportional to the total aerosol released over the course of the event and inversely proportional to the duration of the release period.

Table 7.2-2 of the CRBRP Environmental Report as modified by Amendment VIII (February 1977) is consistent with the corresponding information in Table Q310.51-2 except for the X/Q values utilized. See ER Section 7.1.1.1 for the explanation of X/Q values utilized in ER Section 7.0.

* ER Accidents 4.1, 8.3 and the IHTS Pipe leak (PSAR Section 15.6.1.5)

** All other Accidents of Table Q310.51-2.

Reference Q310.51 K. G. Murphy and K. M. Campe, "Nuclear Power Plant Control Room Ventilation System Design for Meeting General Criterion 19", Proc. 13th AEC Air Cleaning Conf., Vol. 1 (pp401-428). Conf. 740807.

Amend. 42
Nov. 1977

TABLE Q310.51-1

SUMMARY OF ENVIRONMENTAL REPORT EVENTS RELEASING SODIUM REACTION PRODUCTS TO THE ATMOSPHERE

PARAMETERS

Sodium Spill (LBS)
Pool Area (FT²)
Location

Max. Burning Rate
(LB/HR-FT²)

Release Pathway
(leakage rate)

Duration of Aerosol
Release to Atmosphere

Total Aerosol Released
to Atmosphere
(kg of Na)

Accident 4.1	Accident 4.2	Accident 5.2	Accident 8.1	Accident 8.2	Accident 8.3	Accident 8.4	Q000.28	PSAR
130 2500 SGB-Open Cell During Maintenance	250 280 RSB-Open Cell During Maintenance	337* N/A Steam Generator Sodium Water Reaction Pressure Relief System	240,000 830 RCB-Open Cell During Maintenance	193,000 1450 RCB-Closed PHTS Cell	600,000 2500 SGB-Closed Cell	57,000 280 RSB-Closed EVST Cell	5,000 285 RCB-Closed Cold Trap Cell	15.6
2.30	2.30	N/A	4.90	0.46	0.20	0.30	0.33	
Direct Release to Atmosphere	Direct Release to Atmosphere	SWRPRS Exhaust direct to Atmosphere	Leakage from RCB to Atmosphere (Calculated** based on 0.1%/ day @10 psig)	Leakage from Cell (Calculation ** based on 100%/day @ 10 psig) to RCB; then leakage from RCB to atmosphere (Calculation ** based on 0.1%/day @ 10 psig)	Leakage from Cell to Atmosphere (Calculated** based on 100%/ day @ 10 psig)	Leakage from Cell to Atmosphere (Calculated** based on 100%/ day @ 10 psig)	Leakage from Cell (Calculation** based on 100%/ day @ 10 psig to RCB; then leakage from RCB to atmosphere. (Calculation ** based on 0.1%/day @ 10 psig)	
2 minutes	30 minutes	15 seconds	145 hours	720 hours	192 hours	96 hours		
16	32	9.2	1.2	0.10	2.23	0.5	720 hours 0.003	

*Accident 5.2 considers rupture of a steam generator tube. The 337 pounds of sodium is the quantity of intermediate sodium that reacts with steam generator water.

**Assume square root pressure-leakage relationship

310.51-3

42

42

TABLE Q310.51-2
DOWNWIND NaOH CONCENTRATIONS

Accident	Milligrams NaOH/Cubic Meter		
	Control Room Air Intake	Exclusion Boundary	LPZ
ER 4.1	9.4×10^2	5.2×10^{-1}	0.14
ER 4.2	1.2×10^2	6.9×10^{-2}	2.0×10^{-2}
ER 5.2	4.0×10^3	2.4	0.63
ER 8.1	1.5×10^{-4}	0.9×10^{-8}	2.4×10^{-6}
ER 8.2	2.6×10^{-4}	1.5×10^{-7}	3.9×10^{-9}
ER 8.3	2.2×10^{-2}	1.3×10^{-5}	3.3×10^{-6}
ER 8.4	9.4×10^{-3}	5.7×10^{-6}	1.5×10^{-6}
ER Q000.28	8.0×10^{-6}	4.5×10^{-9}	1.2×10^{-9}
IHTS Pipe Leak (PSAR Sect. 15.6.1.5)	3.5×10^3	2.4	0.63

42

Amend. 42
Nov. 1977

Question 310.52 (4.1)

To confirm that the requirements of the May 6, 1976 letter are met in relation to comparability with LWRs, we believe it is necessary to consider the spectrum of reasonably likely scenarios leading to core melting and the consequence scenarios that may be postulated thereafter and judge the TLTM design features in the context. The current analyses are based on a very limited number of scenarios and are therefore deficient in this regard.

(a) Provide a preliminary evaluation of dominant accident sequences leading to core melt in the CRBR. This evaluation should include an assessment of those events considered analogous to the dominant accident sequences in WASH-1400 (cf. pp. V-45 through V-54).

(b) Additional consequence scenario beyond that summarized in TLTM Section 4.1 should also be presented. As a minimum, the following additional consequence scenarios should be considered.

1. Same as 4.1.A except portions of the core/blanket remain in the reactor vessel (as may be postulated for events not involving loss of heat sink), from which radioactivity may subsequently volatilize without entrainment in liquid sodium.
2. Same as 4.1.B except the bulk sodium temperature is that associated with a complete loss of heat sink accident.
3. Same as 4.1.A and B except that an initial larger release of radioactivity, as per the 5/6/76 letter assumptions, occurs directly into the reactor containment building.
4. For scenarios which involve failure to recover electrical power, include the effects of loss of effective cooling to the cold trap.

Response:

(a) The information requested will be found in CRBRP-3, Volume 1 (Reference 10a of PSAR Section 1.6), Section 3.0.

(b) 1. A scenario for which the core melt down would occur in a "dry" condition was discussed in the response to NRC Question 310.33. The fission product release for this condition was conservatively assumed to be 100% of the noble gas, halogen, and volatile (Cs, Rb, Te, Sb, Se) fission products and 1% of the solid fission products. Because of the low vapor pressure of the fuel in the range of the melting temperature of steel, the amount of fuel released as a vapor would be insignificant. It was assumed that this activity immediately enters the Reactor Containment Building following meltdown.

The consequences of large initial fission product releases from the core are also discussed in CRBRP-3, Volume 2 (Reference 10b of PSAR Section 1.6), Section 4 and Appendix G.4.

- (b) 2. The effect of higher bulk sodium temperatures, such as would be associated with a loss of heat sink accident, is discussed in Section 3.1.4 of CRBRP-3, Volume 2.
- (b) 3. Pertinent information on large initial releases of radioactivity to the reactor containment building will be found in CRBRP-3, Volume 2, Section 4 and Appendix G.4.
- (b) 4. Loss of radioactivity from the primary system cold trap during a TMBDB event would have no significant effect on the consequences of the event. The amount of activity contained within the cold trap is less than 10^{-4} of that contained within the core. Any releases from the cold trap during the TMBDB scenario would be attenuated by the containment cleanup system, as are the releases from the core.

Failure in the cold trap system during normal operation was discussed in response to NRC Question 310.49. Even in the event that the sodium inventory is lost from the cold trap, the decay heat generated is insufficient to significantly raise the temperature of its contents.

Question 310.53 (4.1)

Discuss the effect of CO_2 reactions with airborne NaOH, as it may effect the behavior and release of airborne radioactivity (including release of previously co-agglomerated fission products).

Response:

The potential for CO_2 reactions with NaOH and its effect on the release of sodium and fission products from the containment cleanup system are discussed in CRBRP-3, Volume 2 (Reference 10b of PSAR Section 1.6), Appendix E.7.

Question 310.54 (4.1)

Provide an analysis of the release of fission products from the core debris subsequent to sodium boil off.

Response:

After the sodium pool in the reactor cavity has evaporated a bare fuel/steel debris bed is left. Most of the fission product release is expected to occur prior to boil off. Potential mechanisms for further release of fission products and plutonium from the debris are:

- 1) Surface vaporization
- 2) Particle levitation, and
- 3) Gas sparging

A detailed description of these mechanisms can be found in CRBRP-3, Volume 2 (Reference 10b of PSAR Section 1.6), Section 4.1 and Appendix E.

Question 310.55 (II.2.1)

Since the RC pressure may exceed 15 psi, indicate any requirements on leakage above that value (e.g., is the leakage rate assumed to increase linearly above 100 v/o per day with pressure).

Response:

The design upon which the information requested was based has been superseded by the present design which vents the Reactor Cavity to the upper portion of the Reactor Containment Building. For details of the RC vent into the containment see Sections 2.1.2.6 and 2.2.6 of CRBRP-3, Volume 2 (Reference 10b of PSAR Section 1.6).

Question 310.56 (II.2.1)

The sodium boiling temperature is a function of pressure. The value of 1650°F appears low in this respect. Justify the proposed 1650°F value.

Response:

The information requested will be found in CRBRP-3, Volume 2 (Reference 10b of PSAR Section 1.6), Section C.1.4.4 which provides the basis for the sodium properties.

Question 310.57 (II.2.1)

Justify the claim that increases in the leak rate beyond two hours can have little effect on the consequence scenarios.

Response:

The information requested is no longer relevant with respect to the current scenario described in CRBRP-3, Volume 2 (Reference 10b of PSAR Section 1.6).

Question 310.58 (III.1.E)

List the elements considered as volatiles and the basis for that classification.

Response:

The list of volatile elements and their volatility factors are discussed in Section 4.1.1 of CRBRP-3, Volume 2 (Reference 10b of PSAR Section 1.6).

Question 310.59 (III.1.E)

Provide a discussion of the basis for assuming that 100% of the volatiles will co-agglomerate with sodium based particulates.

Response:

The bases for assuming that 100% of the volatiles will co-agglomerate with sodium based particulates are discussed in Section 4.1.1 of CRBRP-3, Volume 2 (Reference 10b of PSAR Section 1.6).

Question 310.60 (III.1.E)

Gas sparging has been shown to be a significant means of releasing radioactivity from liquids. Provide an analysis of this effect.

Response:

The information requested will be found Section 4.1.1 and Appendix E to CRBRP-3, Volume 2 (Reference 10b of PSAR Section 1.6).

Gas sparging has been considered as a mechanism for fission product and plutonium release from the molten pool.

Question 310.61 (III.2)

It is not clear what specific assumptions were made in the relative release rates of fission products and sodium. Discuss the assumptions made in the context of Castleman's data on volatilization of fission products from sodium and the phenomenon of entrainment. The percent fission product vaporization as a function of sodium vaporization is temperature dependent. Although the assumption that the concentration of radionuclides in the sodium vapor is the same as in the liquid sodium appears to be conservative, the implied assumption that all of these nuclides remain associated with the sodium reaction products as an aerosol subject to settling is non-conservative and has not been substantiated. The release of fission products by carry-over or by gas-sparging should be analyzed. The experimental or analytical basis for assuming no uncombined airborne fission products should be provided.

Response:

The information requested regarding assumptions made about volatilization of fission products, and fission products released by the gas sparging mechanism are discussed in Section 4.1.1 and Appendix E.6 to CRBRP-3, Volume 2 (Reference 10b of PSAR Section 1.6).

Question 310.62 (II.2)

Describe the instrumentation used to detect and initiate system action to mitigate core melt consequences. Describe the provisions of this instrumentation relative to R. G. 1.97.

Response:

The instrumentation requirements will be found in CRBRP-3, Volume 2 (Reference 10b of PSAR Section 1.6), Section 2.1.2.12. The instrumentation design is described in Section 2.2.12 and the operator actions are described in Section 2.3. In addition, monitors for measuring the radiation level inside containment are being added to the design.

Question 310.63 (II.2.5)

The Annulus Air Cooling System, which forces 400,000 cfm of unfiltered outside air through the confinement building annulus, appears to negate the purpose of that structure, i.e., confinement of radionuclides leaking from the RCB. Justify that this method of cooling the RCB is compatible with the concept of a dual containment system or the need to contain the site suitability source term as discussed in the 5/6/76 letter. (You may wish to coordinate this response with Items 001.662 and 222.91.)

Response:

The response to this question is provided in Section 2.2.10 of the CRBRP-3, Volume 2 (Reference 10b of PSAR Section 1.6).

Question 310.64 (II.2.3)

The concept of the separate liner vent systems may be defeated by a liner failure which involves both upper and lower sections of the reactor cavity wall. The validity of the radiological assessment, therefore, depends on the ability to predict the exact location, timing, and mode of liner failure. In view of the uncertainties involved in such a detailed time-space dependent analysis of this hypothetical accident, additional analyses appear to be required. The accident analysis should include the evaluation of the consequences of venting fission products (from the fuel in contact with the concrete) via the liner vents into the non-inerted cells.

Response:

Section 3.2.1 of CRBRP-3, Volume 2 (Reference 10b of PSAR Section 1.6), describes the liner failure scenario and indicates that there would not be simultaneous failure of upper and lower sections. Section 3.2.2 provides the information on location and time of liner failure and Appendix F.7 discusses the sensitivity of the base scenario to variations in assumed times of liner failures.

Question 310.65 (II.2)

The CDA source term in the RCB is based on the assumption that leakage into the RCB will be limited to a mixture of sodium and fuel until the sodium is boiled off. Hence leakage rates are identified in terms of sodium transport (e.g., on a "per pound of sodium leaked out" basis). This is not necessarily a conservative assumption. As indicated by the staff in Q.310.33 (transmitted to the applicant on 12/30/75), it is possible to postulate portions of the molten core remaining in an uncovered condition within the vessel immediately following a vessel melt-through. This assumption leads to the possibility of leakage of fission products into the RCB without the interaction with, and dispersal throughout, the bulk sodium inventory. The release path of radionuclides to the RCB via the liner vent system should also be included.

Response:

The information requested was provided in response to Question 310.33.

Question 310.66 (II.2.8)

On p. II-31 it is indicated that the guideline exposure value for control room operators is 25 rem. Clarify that the 25 rem refers to whole body dose and provide equivalent organ dose limits (bone, lung, thyroid). Provide the basis for selecting a value of 25 rem versus the 5 rem value in CRBRP Design Criteria 17.

Response:

CRBRP-3, Volume 2 (Reference 10b of PSAR Section 1.6), Section 2.1.2.15 provides the whole body and organ dose limits for the control room operators following a TMBDB condition. This shows that the 25 rem value is indeed a whole body dose. The rationale for its selection is given in the section identified above.

Question 310.67

Credit for dual air intakes (p. V-4) cannot be given with the proposed outside air intake locations as they are too close to the plant structures and to each other. Guidance on the criteria for dual inlet credit are outlined in Reference 7 of Section 6.4 of the Standard Review Plan. Revise the TLTM discussion accordingly.

Response:

Credit for dual control room air intakes is not required for design basis accidents because the control room doses based on a single intake are well below the radiation exposure limit of CRBRP GDC-17. The dual inlets, however, are provided to further reduce the resultant risk following an HCDA which is beyond the design basis.

According to Reference Q310.67-1 there are two kinds of acceptable dual inlet configurations:

- 1) Remotely placed dual intakes
- 2) Dual intakes placed on the main plant structures.

Each configuration utilizes a different approach in estimating the atmospheric dilution factors (X/Q values).

The acceptable intake locations for the second concept above are shown in Figure 1 of Reference Q310.67-1.

The dual control room air intakes are described in Section 2.2.15 of the CRBRP-3, Volume 2 (Reference 10b of PSAR Section 1.6).

The locations of these intakes were selected in accordance with the guidance on the dual inlet criteria given in Reference Q310.67-1.

Reference:

Q310.67-1, K. G. Murphy and L. M. Campe, "Nuclear Power Plant Control Room Ventilation System Design for Meeting Design Criterion 19", 13th AEC Air Cleaning Conference, August 1974.